Applying a Lagrangian trajectory model to investigate and describe the distribution of drifting *Ecklonia maxima* within the Benguela Upwelling System

By Ross Mark Coppin[1]

Supervisors

Professor AJ Smit[1,2]

Dr Christo Rautenbach[3]

[1] Department of Biodiversity and Conservation Biology, University of the Western Cape, Private Bag X17, Bellville 7535, South Africa

[2] South African Environmental Observation Network, Elwandle Coastal Node, Port Elizabeth, South Africa

[3] National Institute of Water and Atmospheric Research, Hamilton: Gate 10 Silverdale Road Hillcrest, 3216

Abstract

Macroalgal morphological variation is determined to a large extent by a combination of environmental factors, with wave exposure and temperature perhaps the main influences, as they are key environmental properties to which a species becomes locally adapted. Macroalgae have shown to exhibit different responses to different magnitudes of exposure to waves, such as reduction in overall size and strength increasing traits. In terms of temperature, warmer environments have been shown to reduce the overall size of resident and transplanted species. However, none of the past studies have identified specific wave and temperature metrics responsible for the morphological adaptation macroalgae exhibit. Past research has often used simple or two-dimensional models of wave exposure, which do not take into account important aspects of the nearshore environment such as wave breaking, refraction and diffraction. Furthermore, past studies have often used satellite-derived datasets as sources for temperature data; however, such data have been shown to have large bias when applied to the nearshore environment. This study used in situ temperature data and wave power metrics calculated from a 3D-numerical model to identify specific temperature and wave metrics responsible for morphological adaptation of the kelp, *Ecklonia maxima* and *Laminaria pallida*. Between temperature and wave exposure, the results identify wave exposure as the main influencer of morphological adaptation while identifying specific wave metrics. Furthermore, the results show differences in wave metrics between species, and between deep and shallow populations. The findings from this chapter were used in the next chapter to investigate the role of hydrodynamic and wind drag on floating kelp trajectory.

Ocean currents act as an essential dispersal mechanism of natural and anthropogenic material on the ocean surface. Macroalgae are one of the essential natural dispersal vectors of marine organisms and are regarded as the 'tumble-weed of the ocean.' Despite many studies on the topic, the relative role of wind and surface currents in influencing the trajectory of macroalgal dispersal is still uncertain. Past studies focused on kelp-rafts, which can vary significantly in size, making it difficult to form a consensus on the relative role of wind versus surface currents. In addition, these studies have not considered surface area in relation to drag characteristics of the macroalgae, both of which have been shown to play a role in the trajectory and accumulation of flotsam. Advances in Lagrangian trajectory modelling have been rapid in recent years and allow the use of numerical experiments to investigate trajectories of flotsam in the ocean. This study aimed to shed light on the relative role of wind versus surface currents and the role of drag in macroalgal trajectory and accumulation. We focused on solitary kelp plants. This was achieved by comparing simulations of virtual kelp 'particles' which incorporate drag with that of purely Lagrangian particles (no drag). Geometric representations for each morphological characteristic were used to calculate the overall

surface area used in the calculation of the relevant drag components (hydrodynamic and wind) for each scenario (submerged and partially submerged) and flow-field combinations (currents only, currents with wind, currents with Stokes drift, currents with wind and Stokes drift). The results showed that the virtual kelp particles follow the ocean currents in general but that the inclusion of drag into the scenarios caused trajectories to differ from purely Lagrangian particles. The insights regarding the transport of floating macroalgae are used in the next chapter to the describe the spatial extent of surface and sink accumulations zones in order to shed light on kelps' potential as an organic subsidy and blue carbon potential offshore.

Kelps can persist in harsh environments due to their ability to adapt; however, individuals are dislodged if the threshold of adaptability is breached. Once dislodged, floating kelp generally follow the ocean currents and become entrained in mesoscale features allowing them to travel vast distances. Kelps will continue to float until air-filled structures become compromised or the epibiont load becomes too great, eventually sinking and settling on the seafloor. The ability of kelp to reach distance offshore and nearshore systems makes them an important dispersal mechanism in the ocean and organic subsidy. Most of the work regarding the rafting potential of dislodged macroalgae has focused on rafts, which form through context-specific conditions, making it challenging to gain deeper insights into the broader ecological role that floating kelp plays. In this study, I used the findings from the previous chapter to numerically describe the spatial distribution of floating *E. maxima* along the South African coastline by applying a site-specific Lagrangian Trajectory model. Simulations also consisted of additional parameters needed to describe surface and seafloor accumulation zones, such as sinking and buoyancy, based on site-specific morphological data. Numerical simulations were executed with the Lagrangian software, OceanParcels, for a period of two years. Results from simulations were categorised into year and season, as well as phase (surface, sinking, sunk, beached, and out of bounds). The results showed that the spatial distribution of floating *E. maxima* is dependent on the underlying oceanographic conditions, more specifically, the Benguela Jet and mesoscale features. There is also a clear seasonal component regarding distribution. The results also show the importance of mesoscale features as a mechanism for kelp accumulation on the surface and seafloor, including acting as potential barriers to transport outside the study domain. The findings from this study provide essential insight into the role of kelp as an organic subsidy and the extent of that organic subsidy. Additionally, findings also present numerical evidence for the role of kelp as a potential carbon sink.

Where Does the Kelp Go?

Extant research focuses on macro algae-rafts but what about solitary floating kelp?

- Individual kelp more common, daily occurrence as opposed to rafts which are associated with storms.
- Gaps still remain regarding kelp as an organic subsidy to nearshore and offshore ecosystems (Blue Carbon contribution).
- Gaps remain in understanding the influencers of floating kelp trajectory.
- Findings applicable for both research (ecological) and applied (management agencies).

Research on both anthropogenic and biological flotsam show that surface area and associated drag components important in deterring trajectory

- Morphological characteristics vary considerably with kelp species
- Morphological characteristics are driven by local wave and temperature environment
- Wave exposure and temperature vary considerable along coastlines

Need to take site-specific approach

Chapter 2

Used quantitate approach to investigate and empirically describe influence of waves and temperature on *E. maxima* and *L. pallida*

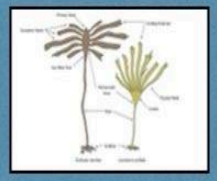

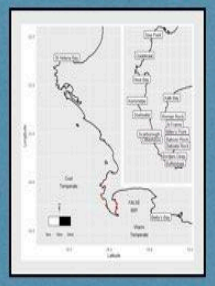

- Use advanced hydrodynamic model.
- Used unbiased nearshore temperature data.
- Comparison between species, and between shallow and deep populations.

- Wave exposure main influencer of morphological characteristics, and temperature to a lesser degree.
- Identified empirical wave and temperature metrics which influence morphological characteristics
- Showed that site-specific morphology may result in the variable effect of drag due to the variation in surface area (morphological characteristics.

Chapter 3

Investigate the role of hydrodynamic and wind drag in trajectory

- Hydrodynamic drag influences trajectory.
- Windage and Stokes drift play little to no direct role.
- Virtual kelp cannot be treated as purely Lagrangian

- Use shape estimates.
- Calculate drag from current and wind based on surface area.
- One site and surface trajectory only

Windage

Hydrodynamic drag

Chapter 4

Numerically characterise dispersal of kelp based on site-specific morphological characteristics

- Use multiple sites (sites from chapter 2)
- Use buoyancy and sink rates calculated from morphological data
- Run at a higher time-step and for longer duration

- Solitary kelp can travel and are deposited far offshore
- Mesoscale features act as accumulation areas and barriers to offshore transport
- Sesaonal component to spatial distribution and beaching patterns

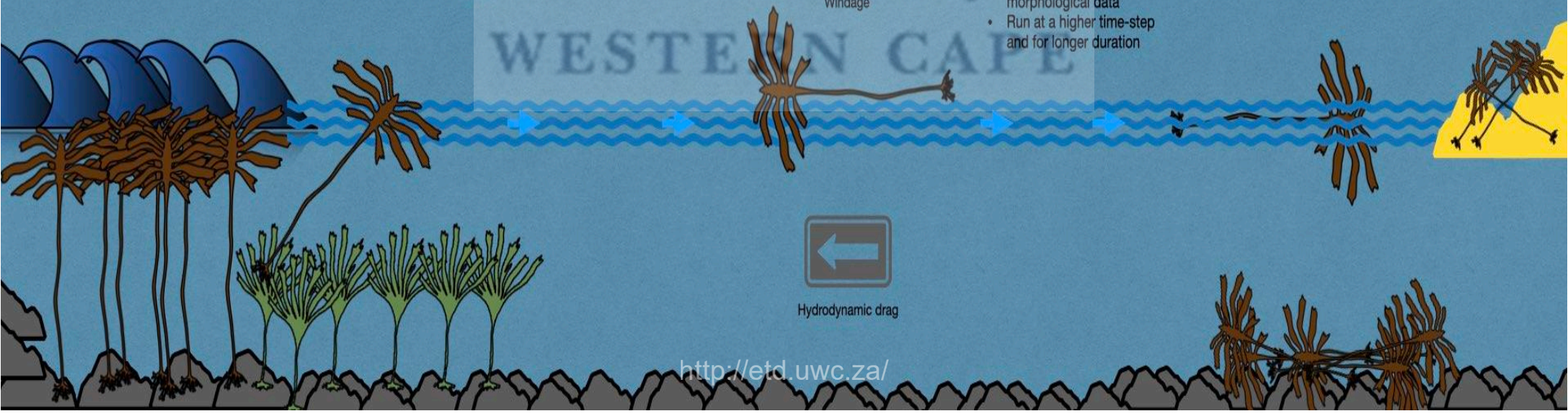

UNIVERSITY of the WESTERN CAPE

Declaration

I declare that 'Applying a Lagrangian trajectory model to investigate and describe the distribution of drifting *Ecklonia maxima* within the Benguela Upwelling System' is my own work, that it has not been submitted before for any degree or examination in any other university, and that all the sources I have used or quoted have been indicated and acknowledged as complete references.

Date: 16th October 2022

Revised: 10th July 2023

Signed: 

Ross Mark Coppin

Student number: 3481215

Primary Email: coppinross@gmail.com

Student Email: 3481215@myuwc.ac.za

Acknowledgements

This project would not have been possible without the financial support I received from the South African National Research Foundation (http://www.nrf.ac.za). Funding number is CSRP170430229220. Aside from funding provided, the funders had no role in the study design, data collection and analysis, decision to publish, or preparation of the manuscript.

I also thank Robert Schlegel and Robert Williamson for their help coordinating the honours class of 2014–2015, in particular Jesse Smith, Janine Greuel, Tevya Lotriet, and Rudy Philander. The work would have not been possible without the dataset from the CSIR report 2014 where the processed data is available at the following DOIs: 10.15493/DEFF.10000004 and 10.15493/DEFF.10000003. I also extent my gratitude to the South African Coastal Temperature Network (SACTN) for access the temperature data used as a part of this dissertation.

To my supervisors – A.J. Smit and C. Rautenbach, thank you for your guidance, patience, and continued support in my endeavour to advance my career. To AJ, thank you for constantly pushing me to do better and expecting nothing but my best. It has been a long time working together; I am truly grateful for the experience. To Christo, thank you for continuing to supervise me even while you had no obligation to. Thank you for making time on weekends, early mornings, and late evenings to talk about the work and for guiding me through the process. Your expertise and help were essential.

I would like to thank Khiara Smith; you have joined me on this journey over the past two years and have supported me every step of the way. Thank you for always being interested in my research and always reminding me of the importance of my work.

Last but not least, To Mom, Dad, and Nikki – I would like to thank you for the unconditional support in helping me complete this endeavour; I am forever grateful. Thank you for always supporting me, even during the really tough times. I could not have done it without you guys.

To all my friends, thank you for your patience and understanding during this time. I will see you all again soon!

The Ph.D. journey has been an incredible, with many ups and downs, that has not only shaped me as a scientist but has also changed me as a person. Thank you to everyone for making this possible.

Table of Contents

List of Figures

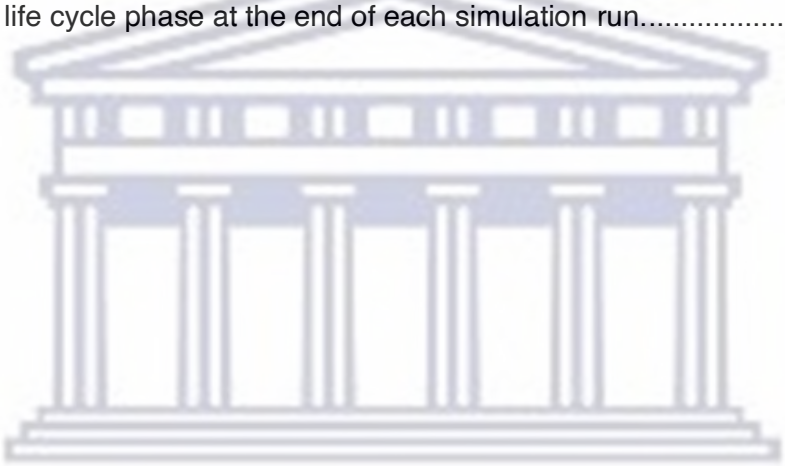

List of Tables

Data Availability Statement

All the script needed to run analyses and associated OceanParcels script are available on GitHub, see link https://github.com/RossCoppin/PhD. Data for Chapter 3 and 4 have not been uploaded, due to the size of the data needed to run the trajectory models and associated analyses. However, this available upon request from the author. The ocean data used to run trajectory simulations was from Copernicus Marine Services. Namely products Global Analysis Forecast PHY_001_030, Global Analysis Forecast WAVE_001_027, and Global Ocean Wind L4_NRT_012_006. All photos used on chapter cover pages were taken by the author

1 : General Introduction

1.1 Background

Marine ecosystems are maintained by a variety of complex interactions between abiotic and biotic variables such as temperature, wave exposure, pH, competition, and processes such as top-down and bottom-up control, predator-prey relationships and phenology (McGowan et al., 1998; Doney et al., 2012; Burrows et al., 2011; Harley et al., 2012). These abiotic and biotic variables, the interactions between them, and the various ecological processes, ultimately determine the community composition and ecological functioning of all ecosystems (Guimaraens and Coutinho, 1996; Dayton et al., 1999; Polovina, 2005; Harley et al., 2006; Jennings and Brander, 2010; Johnson et al., 2011; Poloczanska et al., 2013; Krumhansl et al., 2016). Climate, directly and indirectly, affects the way in which abiotic and biotic variables interact but is often compounded by other impacts such as habitat destruction, pollution, and over-fishing (Blamey and Branch 2012; Blamey et al., 2015). In order to persist and survive within variable and changing environments, organisms must either migrate, adapt, or die.

Seaweeds are sessile organisms that are unable to migrate to new areas when local environmental conditions become unsuitable and therefore are forced to adapt to new conditions to avoid expiration (Dayton, 1985; Tegner et al., 1996). The main form of mortality for seaweeds is through mechanical dislodgement by wave action (Seymour et al., 1989; Graham, 2004; Thomsen et al., 2004; Schiel and Foster, 2006; Cavanaugh et al., 2011; Demes et al., 2013). Seaweeds, particularly brown seaweeds, are able to undergo rapid morphological adaptation to the hydrodynamic environment (Hurd, 2000; Denny and Gaylord, 2002; Thomsen et al., 2004; Fowler-Walker et al., 2005; Wernberg and Thomsen, 2005; Mabin et al., 2013; Bekkby et al., 2014). This allows seaweeds to reduce mortality through mechanical dislodgement by inducing morphology which reduces overall drag. Seaweeds that are unable to avoid mechanical dislodgement either raft out to sea or wash up onto beaches as beach-cast. Not all beach-cast kelp may have originated from a nearby kelp population and may have originated from other sites or regions of the coast (Hobday, 2000a; b; Smith, 2002; Fraser et al., 2011).

Past work investigating macroalgal distribution patterns identified ocean currents and wind as the main influencers of trajectory. Floating macroalgal rafts generally follow the ocean currents, while windage (drag from the wind) influences entrainment patterns (Hobday, 2000b; Thiel and Gutow, 2005; Rothäusler et al., 2011; Fraser et al., 2011). Our understanding of kelp morphological characteristics and trajectory patterns on the ocean surface has been improved through the advances made in the field of hydrodynamic and Lagrangian trajectory modelling (Hill et al., 2010; Sundblad et al., 2014; Brooks et al., 2018, 2019; Putman et al., 2018, 2020; Van Sebille et al., 2018, 2020). All of the past work has focused on kelp rafts, an entanglement of floating individuals, which

can vary greatly in size. Although past work has increased our understanding of macroalgal distribution patterns on the ocean surface, the focus on kelp rafts limits our understanding to those particular scenarios. Furthermore, hydrodynamic drag components relating to the object's surface area have been recognised as an important influencer of other passive flotsam (Beron-Vera et al., 2016; Brach et al., 2018; D'Asaro et al., 2018; Onink et al., 2019), which raises the question of these effects in terms of macroalgae. The inclusion of windage by Putman et al. (2020) and Brooks et al. (2019) is an improvement but is specific to that particular kelp raft and is an *ad-hoc* adjustment based on wind data. All of the past work only considers floating macroalgae but does not attempt to describe patterns once sinking or sunken to the seafloor.

What is needed is an approach which can take the site-specific morphological characteristics of macroalgal species into account while incorporating hydrodynamic and wind drag. Temperature and wave environments can vary vastly along coastlines, as well as the associated macroalgal morphological characteristics. This poses a unique challenge to the site-specific approach proposed, as the local temperature and wave environment, as well as the effects on morphological characteristics, will need to be characterised first. In addition, gaps within our understanding of the physical oceanographic processes and drag parameters regarding macroalgal transport need to be addressed. Once knowledge gaps have been addressed, the site-specific kelp morphological characteristics can be used in conjunction with Lagrangian approaches to numerically describe and investigate macroalgal distribution patterns. The current research will use the advances made in hydrodynamic and Lagrangian trajectory modelling to not only further our understanding of locally driven kelp morphological characteristics in relation to the temperature and wave environment but will also investigate the role of hydrodynamic and wind drag on in the distribution of individuals on the sea surface. Finally, the study will use the site-specific approach to advance our understanding of macroalgal distribution patterns on the ocean surface and seafloor.

1.2 Context of research

Kelp forests are comprised particularly of brown algae of the order Laminariales and dominate nearshore environments along temperate coastlines. These ecosystems are characterised by high levels of productivity that rival or even exceed their terrestrial counterparts (Mann, 1973; Krumhansl et al., 2016; Elliott Smith and Fox, 2022). Many Laminarialian are important habitat-forming species in the nearshore of temperate coastlines (Teagle et al., 2017). Kelp have been shown to alter the wave and light environment (Gerard, 1984; Reed and Foster, 1984; Wing et al., 1993; Monismith et al., 2022), creating a multitude of complex niches for other species to exploit (Hauser et al., 2006; Smale et al., 2013; Teagle et al., 2017; Miller et al., 2018). For example, canopy-forming species limit the amount of light able to reach the seafloor through shading which allows low-light tolerant

species to take advantage of (Duggins et al., 1990; Watanabe et al., 1992; Clark et al., 2004). Highly dense kelp populations are also capable of wave dampening effects, creating areas of lower wave-exposure which are once again exploited by species which cannot tolerate highly wave exposed environments (Mork, 1996; Ma et al., 2013; Monismith et al., 2022). Kelp species do not only support a high species diversity by altering the immediate abiotic environment but also by providing a complex three-dimensional structure on and within which species can inhabit. For example, the holdfast anchors the plant to the substrate by means of finger-like haptera, which in turn creates microhabitats for a range of small invertebrates (Anderson et al., 1997; Anderson 2005), while the fronds and stipes act as a habitat for epiphyte and invertebrate species (Norderhaug et al., 2012; Christie et al., 2003; Coleman et al., 2007; Teagle et al., 2017; Mayombo 2019, 2020), and the stipes by endophytic species (Eggert et al., 2010; Bernard et al., 2019); ultimately this helps drive increased species richness within kelp forests.

1.2.1 Environmental influencers of kelp

Important environmental drivers of kelp individuals and communities include light (Bruhn and Gerard, 1997), nutrients (Jackson, 1977; Field et al., 1980; Fram et al., 2008), temperature (Wernberg et al., 2010; Bolton et al., 2012; Vergés et al., 2014; 2016), and wave exposure (Seymour et al., 1989; Dayton et al., 1992; Utter and Denny, 1996; Kawamata, 2001; Taylor and Schiel, 2003; Fowler-Walker et al., 2006). Although studies have investigated the effects of these important environmental drivers, the roles these factors play is often difficult to evaluate as such factors may never be fully independent of each other, i.e., environmental factors are to some extent dependent on one another. Environmental factors are highly variable on temporal and spatial scales, and their effects may also be dependent on the life stage of the organism, adding a further layer of complexity to investigations. For example, depth does not affect kelp ecosystems directly; however, a change in depth is accompanied by changes in other environmental variables such as water motion, light and temperature. Light is an important factor for kelp survival; however, if light is limited or excessive this may negatively impact kelp survival or growth. An increase in depth can lead to a decrease in sunlight penetration, with some species better adapted for low-light conditions than others, such as *Laminaria pallida* Greville.

Much of the past research on the role of light has focused on the physiological functioning of kelp (Bruhn and Gerard, 1996). For instance, ultraviolet solar radiation has been shown to affect sub-canopy *Ecklonia radiata* (C.Agardh) J.Agardh sporophytes when the canopy of mature *E. radiata* was removed (Wood, 1987). The sub-canopy sporophytes experienced tissue damage, photopigment destruction, reduced growth and decreased survivorship, thus inhibiting their settlement and survival (Wood, 1987). Laboratory experiments revealed that the UV component of radiation, rather than intense radiation itself, was responsible for the effects mentioned above. High

light stress has negative effects, such as photoinhibition and photo-damage on *Ecklonia cava* Kjellman sporophytes. Altamirano et al. (2004) found that *E. cava* is more vulnerable to light stress conditions and less likely to recover under unfavourable conditions. Bolton and Levitt (1985) demonstrated that under sub-saturating irradiances and supra-optimal temperatures, *Ecklonia maxima* (Osbeck) Papenfuss 1940 shows a decrease in reproductive rates and an increase in cell production. An additional finding of this study was that despite the decrease in reproductive rates, the final egg production per female was greater under these conditions. The authors interpreted the response as an ecological adaptation that may increase survival rates under times of stress or non-ideal conditions (Bolton and Levitt, 1985).

The importance of nutrients in the functioning of kelp is well understood (Dayton, 1985; Dayton et al., 1999; Cavanaugh et al., 2011; Gaylord et al., 2012; Gao et al., 2013; Mabin et al., 2013). Dissolved nitrogen, particularly nitrate, are important; however, research has also placed emphasis on phosphate and other trace compounds for the functioning of kelp (Dayton, 1985; Mabin et al., 2013; Supratya et al., 2020). Additionally, some kelp species can store inorganic nitrogen in order to compensate for periods of low nutrient availability, which has been observed for *Laminaria* and *Macrocystis* (Dayton, 1985; Zimmerman and Kremer, 1986; Gaylord et al., 2012; Brzezinski et al., 2013). Nutrient stratification is also an important factor, particularly for canopy type kelp. The concentration of nutrients at the surface is important to the functioning and maintenance of the canopy. For instance, kelp canopies in California often deteriorate in the summer months when surface nitrate levels are low (Jackson, 1977). Temperature has also been closely linked with nutrient concentrations. Nutrients are often in higher concentrations in the water column during low-temperature events. This is often an indication of an upwelling event, which brings cold and nutrient rich waters from the bottom to the surface of the water column (Rouault et al., 2010). Temperature can play a direct role in the uptake of nutrients through effects on algal metabolism; however, this may vary from species to species (Wernberg et al., 2010, 2011; Pedersen et al., 2012).

The majority of kelp species are arctic and temperate in distribution, and the warming of ocean temperature is expected to cause a poleward biogeographical shift of species (Bolton et al., 2012; Krumhansl et al., 2016). There is evidence to suggest that South African kelp forests are expanding due to ocean cooling (Bolton et al., 2012), possibly driven by an intensification and increase in coastal upwelling (Blamey and Branch 2012; Blamey et al., 2015). In South Africa there has been a biogeographical shift eastward along the coast due to a change in inshore temperature regime, making South Africa no exception to changing ocean temperatures (Bolton et al., 2012). Macroalgae, such as kelp, can react to an increase in surface temperatures in one of three ways: they can migrate, adapt and die (Wernberg et al., 2010, 2011; Pedersen et al., 2012). A study by Biskup et al., (2014) investigated the functional response of two kelp species (*Laminaria ochroleuca*

Bachelot Pylaie and *Saccorhiza polyschides* (Lightfoot) Batters) to rising sea temperatures. The functional responses of *S. polyschides* were measured for both the subtidal and intertidal habitats to see what effect non-optimal conditions (intertidal zone) had on the kelp. The study found that *L. ochroleuca* exhibited a poor ability to acclimatise and depended on the kelp's life history traits (Biskup et al., 2014). Therefore, annual kelp species are more likely to survive under non-ideal conditions, and the intertidal *S. polyschides*, compared to the subtidal counterparts, showed higher physiological flexibility to changing conditions (Biskup et al., 2014). This may be because the intertidal zone undergoes far more change than the subtidal, and kelp in the intertidal are forced to adapt to harsher conditions where fluctuations in temperature, sunlight, turbidity, and water motion are common. The effects on temperature have also been investigated by Wernberg et al., (2010). The study looked at the resilience of kelp beds along a latitudinal temperature gradient. Kelp abundance is likely to decline with the predicted warming of ocean waters and although kelp have the ability to acclimatise and adjust their metabolic performance, which in turn allows them to change their physiological performance to mitigate the seasonal fluctuations in temperature. However, this acclimatisation is done at a cost (Wernberg et al., 2010). Other than temperature, wave exposure is also recognised as an important influencer of kelp populations. Wave exposure has been shown to play a role in determining distribution, abundance (Rinde et al., 2014), diversity (Leliaert et al., 2000; Graham, 2004; Norderhaug et al., 2012), composition, growth (Cousens, 1982; Hepburn et al., 2007; Miller et al., 2011) and productivity (Pedersen et al., 2012) of macroalgae communities. The most important direct effect of wave exposure on macroalgal communities is through mechanical dislodgement, which ultimately leads to expiration (Bekkby et al., 2014). Wave exposure is a complex abiotic variable which varies spatially and temporarily in the marine environment (Wernberg and Thomsen, 2005). Nevertheless, macroalgae have been able to persist in often harsh and variable wave environments (Hurd, 2000).

The environmental influencers of kelp are changing in dramatic ways because of climate change effects (Reed et al., 2016, Qiu et al., 2019, Smale. 2020). The warming of the ocean and increasing ocean energy are of particular concern due to their importance to the functioning of kelp and kelp forests and, in turn, the communities that are dependent on kelp (Reed et al., 2016, Qiu et al., 2019, Smale. 2020). Without the effects of human-induced climate change, the marine environment is still a harsh environment that kelp have been persisting under for long before climate change-related effects. This is largely due to their morphological flexibility, which enables them to persist under a range of abiotic conditions (Hurd, 2000).

1.2.2 Kelp morphological adaptations

Macroalgae are sessile organisms and incapable of migrating when local conditions become unsuitable. Therefore, macroalgae must adapt to the local environmental climate in order to persist

and survive and achieve this through morphological adaptation (Hurd, 2000; Bekkby et al., 2014). Warming ocean temperatures and Marine Heat Waves pose a direct threat to kelp populations as warmer temperatures have shown to affect the physiological performance of kelp in terms of photosynthesis and respiration (Zimmerman and Kremer, 1986; Gerard, 1997; Bearham et al., 2013; Gao et al., 2013), causing them to grow thinner and with reduced blade area (Serisawa et al., 2002; Mabin et al., 2013; Supratya et al., 2020). Although kelps persist under a wide temperature range, the compounding effects of reduced physiological performance reduce the ability to adapt to the local hydrodynamic environment, resulting in dislodgment (Supratya et al., 2020).

The morphology of macroalgae are not fixed genetic traits. For example, a study by Koehl et al., (2008) showed that transplanted *Nereocystis luetkeana* (K.Mertens) Postels & Ruprecht from a wave sheltered site to a wave-exposed site changed their morphology to flat blades and narrow laterals that are less prone to drag forces in 4-5 days. Genetic approaches and taxonomy have revealed that species delineation based on morphology has been inaccurate, and organisms that were once considered two separate species are actually one species. For example, Moss (1950) investigated the anatomy chemical composition of *Fucus spiralis* Linnaeus 1753 at three sites that varied in wave exposure (sheltered, medium exposure and exposed). The authors found that individuals in exposed sites showed less branching of thalli as well as a 'crumpling effect' displayed by individuals from exposed sites and, the authors inferred that this strategy may reduce overall drag. Other studies show that macroalgae in wave-exposed environments have morphologies that reduce overall drag, increase strength of attachment, or increase flexibility (Molloy and Bolton, 1996; Hurd, 2000; Denny and Gaylord, 2002; Wernberg et al., 2003; Thomsen et al., 2004; Fowler-Walker et al., 2005; Wernberg and Thomsen, 2005; Bekkby et al., 2014; Rothman et al., 2017).

There is also evidence that morphological adaptation is driven by currents and might be driving the hydrological performance of macroalgae. Duggins et al. (2003) examined the direct and indirect flow effects on population dynamics, morphology, and biomechanics of several understorey macroalgae species. These species included *Costaria costata* (C.Agardh) De A.Saunders, *Agarum fimbriatum* Harvey, *Laminaria complanata* (Setchell & N.L.Gardner) Muenscher and *N. luetkeana*. The authors concluded that although tidal and current velocity did not play a significant role in determining kelp survival, it did play a role in morphological adaptation. This in turn makes those individuals more resilient to dislodgement to wave exposure. Wave exposure is stochastic in nature compared to tidal and ocean currents which are more regular in their frequency and magnitude (Rouault et al., 2010; Veitch et al., 2019). Therefore, the regular forces of tidal and ocean currents may make kelp individuals more resilient to mechanical dislodgement over time (Hurd, 2000; Weisse, 2010).

The morphological adaptations that macroalgae display are driven by site conditions; therefore, individuals must be morphologically flexible to persist in stochastic environments. This may be

achieved through different strategies and are species-specific, which can be directly attributed to the high diversity in morphological characters of algal communities. For example, some algae have fronds, and others have articulated coralline thalli, and therefore these species would need to adapt their morphology differently in order to persist. In general, flat strap-like blades are common in areas that are exposed to high wave energy, while at protected sites, blade morphology is wide and undulated (Wernberg et al., 2003; Wernberg and Thomsen, 2005). However, the specific temperature and wave metrics that influence morphological characteristics have not been established. An empirical understanding of the effects of ocean energy and temperature would help identify the most vital metrics responsible for the morphological adaptability of kelp and how these metrics might change in future climate scenarios.

Although kelps can persist in harsh environments due to their morphological flexibility, they can still be dislodged during times of high wave energy. This results in whole, or clusters of individuals and pieces of kelp being transported offshore or deposited on nearby or distant shorelines. In both cases, the kelp material provides an essential organic subsidy to these ecosystems.

1.2.3 Kelp as an organic subsidy

Kelp-derived organic matter is the primary source of organic input within kelp forests and adjacent and distant marine ecosystems. For example, kelp-derived organic matter supports bottom-up control of intertidal (Bustamante et al., 1995; Tallis, 2009; Elliott Smith et al., 2018), subtidal (Tzetlin et al., 1997; Page et al., 2008; Smale et al., 2021), and deep-offshore communities (Filbee-Dexter and Scheibling, 2014; Filbee-Dexter and Scheibling, 2016; Filbee-Dexter et al., 2018). Due to the high levels of productivity, subtidal ecosystems are often dominated by filter-feeding organisms which feed on particulate organic matter (POM) and phytoplankton communities suspended within the water column. The composition of POM along temperate coastlines largely consists of kelp-derived detritus, although this has been shown to vary during periods of upwelling and downwelling. For example, a study by Dyer et al., (2019) using stable isotopes and C:N ratios of particulate organic carbon (POC) characterised the composition of POM from within a kelp forest to perpendicularly offshore during periods of upwelling and downwelling. The results showed that kelp-derived particulate matter composed most of the POM contribution (>70%) during downwelling periods. Under upwelling periods, phytoplankton communities were found to be the largest contributor to the total POM measured, highlighting the significance of ocean coastal process in regulating the source of POM. The study also showed the contribution to the total POM measured was not limited to within kelp forests themselves but instead extended at least 7.5 km offshore, shedding light on kelp forests' larger contribution to nearby and distant marine ecosystems. Kelp-derived particulate POM, pieces of detrital kelp, and whole kelp can be transported by ocean currents to reach deep, offshore ecosystems. For example, a study by Filbee-Dexter and Scheibling

(2014) investigated the spatial patterns and predictors of algal subsidy in deep subtidal environments along the Nova Scotia coast. Using a combination of towed-video surveys and bathymetry data, the authors were able to create a map of algal drift subsidy to the deep subtidal, providing evidence for the large spatial extent of the subsidy to offshore ecosystems.

In much of the past work investigating the contribution of kelp to nearshore and offshore POM content, the focus was on kelp-derived material and pieces of kelp. However, individuals whose pneumatocyst have not been compromised are able to float at the surface have not been considered. Floating kelp may consist of solitary individuals or a kelp raft, which is an entanglement of individuals (Hobday, 2000b; Tala et al., 2013; Craw and Waters, 2018). Floating kelp and kelp rafts will eventually sink by various interacting abiotic and biotic factors or are deposited on nearby or distant shorelines (Rothäusler et al., 2011; Graiff et al., 2016; Macaya et al., 2016). The transport of kelp and kelp rafts by oceanographic processes has been a focus of research due to both the ecological and socio-economic importance of such processes.

1.2.4 Kelp flotsam

The extant literature focuses on kelp rafts and not solitary individuals; therefore, the studies investigating macroalgae rafts will be the focus of this review. The lack of research on single kelp and focus on kelp rafts with sizes particular to that situation gives further support for my consideration of site-based morphology of the single floating kelp approach, which is the focus of this research.

Dispersal is recognised as an important driver of biodiversity, composition, and structure of ecological systems in the marine environment (Highsmith, 1985; Helmuth et al., 1994; MacArthur and Wilson, 2001; Jackson and Sax, 2010; Bernardes Batista et al., 2018). These processes are largely dependent on currents for dispersal of migrant populations, which ultimately promote the connectivity of marine ecosystems (Mackas et al., 1985; Zakas et al., 2009; Bernardes Batista et al., 2018). This is particularly true for organisms which lack pelagic larvae and are reliant on other modes of transport to reach new habitats through passive modes of dispersal from anthropogenic and natural sources (Thiel and Gutow, 2005). Anthropogenic sources include marine litter and structural debris, while examples of organic sources include pumice and macroalgae in the form of rafts. Macroalgae rafts have been identified as an important mode of passive dispersal of marine organisms, such as invertebrates (Helmuth et al., 1994; Wichmann et al., 2012), epiphytes (Macaya et al., 2016), grazers (Nikula et al., 2010), invasive species (Lewis et al., 2005) and other macroalgae (Macaya et al., 2005) which either make landfall or are transported offshore where they eventually sink. A macroalgal raft consists of an entanglement of macroalgae (one or multiple species) which have been dislodged from the benthic environment through hydrodynamic forces

(mostly storms) and are positively buoyant by means of gas-filled pneumatocyst and/or reproductive organs (Thiel and Gutow, 2005). Macroalgae can float vast distances (Thiel and Gutow, 2005; Fraser et al., 2011) and are considered important dispersal vectors in temperate latitudes, such as the Southern California Bight (Hobday, 2000a; b).

Macroalgal raft abundance has been shown to vary temporally and spatially in the ocean and around coastlines, which is dependent on seasonal growth patterns which ultimately influence the overall biomass of seaweed. For example, studies investigating the dispersal patterns of *Sargassum* in the West Pacific show increased abundance during growth seasons (spring and summer) as more biomass is available to fragment (Deysher and Norton, 1981; Kingsford, 1992). Temporal variability may also be related to seasonal storm frequency, where more storms in a particular season relate to an increase in kelp raft abundance. For example, a study by Kingsford (1995) investigated the contribution of *Macrocystis pyrifera* (Linnaeus) C. Agardh rafts to habitat complexity in pelagic environments. The authors found that the abundance of *M. pyrifera* rafts increased during seasons where storms occurred more frequently.

The trajectory of macroalgal rafts is determined by a combination of oceanographic conditions and biological processes. Since kelp floats, evidence points primarily to wind-driven surface currents as the main driver, although the relative importance of wind versus surface currents is largely unknown. For example, a study by Harrold and Lisin (1989) used radio-trackers on both natural and artificial *M. pyrifera* rafts to investigate seasonal trajectory patterns. The results showed that tracked rafts were mostly deposited near the source population and that seasonal wind direction was the primary driver of trajectory for kelp rafts submerged roughly ~0.5–1 m below the surface Harrold and Lisin (1989). However, the authors did note the influence of surface currents for some of their experiments when winds relaxed, which suggests that surface currents may play a more significant role in determining the trajectory for macroalgal rafts less exposed to wind or when prevailing winds are weak. The field of Lagrangian trajectory modelling has offered new opportunities for investigating the role of wind and surface currents and other oceanographic processes such as Stokes drift in influencing macroalgal trajectory. The advances made in the field of Lagrangian trajectory modelling have allowed for more insight into the influencers of macroalgal rafts, with particular attention to windage/wind drag. Windage, or wind drag, has been recognised as an important influencer of the trajectory of other drifting flotsam (Jutzeler et al., 2020; Olascoaga et al., 2020; Durgadoo et al., 2021).

Depending on the direction of the surface current and wind, the direct effect of wind can manifest differently. If the current direction is in the same direction as the wind, flotsam will experience momentum energy transfer resulting in a further distance travelled and increased velocity. If the wind is in the opposite direction to the current, flotsam will experience wind drag as a result of

frictional forces acting on the surface area above the water line. In both cases, the magnitude of the effect is dependent on the amount of surface area exposed to air and the shape of the object (Allen and Plourde, 1999; Breivik et al., 2011; Cardoso and Caldeira, 2021; Durgadoo et al., 2021). In addition, both manifestations of windage result in changes in velocity, ultimately exposing the floating object to different time-varying flows (Allen and Plourde, 1999; Breivik et al., 2011; Cardoso and Caldeira, 2021; Durgadoo et al., 2021).

The effect of windage are aspects that more recent work has focused on concerning macroalgal rafts. Work by Brooks et al. (2019) used the radial size of *Sargassum* rafts in the calculation of inertia induced by the direct effect of wind. The authors found that the inclusion of inertia increased accuracy of modelled trajectories. Putman et al. (2020) used an *ad-hoc* windage estimate to investigate the role of wind under different magnitudes on macroalgal raft trajectory. An *ad-hoc* windage estimate is usually based on experimental work and generally consists of a percentage of the total wind velocity or an estimate based on current velocity (Bryan et al., 2004). Putman et al., (2020) showed that the inclusion of windage greatly improved the accuracy of modelled to observed trajectories, including better representation of entrainment in mesoscale ocean features. Clearly, the effect of wind is an important aspect that needs to be taken into account for future studies. However, none of the extant research on the subject considers hydrodynamic drag in influencing macroalgal trajectory patterns. In addition, no current research investigates alternative methods which may be able to account for the highly variable morphological characteristics of macroalgae into account with regard to various forms of drag (hydrodynamic and wind).

1.2.5 Kelp in South Africa

The biogeographic distribution of kelp is limited by seawater temperature (Bolton, 2010), where increasing temperature gradients reduce kelp distribution. Due to this limiting factor, the two main species of kelp in southern African waters, *E. maxima* and *L. pallida*, are distributed along a section of the south coast from De Hoop, extending west around the Cape Peninsula, and thriving north into Namibia (Molloy and Bolton, 1996; Stegenga, 1997).

This distribution follows a temperature gradient, where sea temperatures increase as one moves south from Namibia, around Cape Point and towards De Hoop. Although the two species occur together for the majority of the coast, their basic morphologies and resource needs vary to a degree. The larger species, *E. maxima*, is distributed from Lüderitz to Cape Agulhas (Fig. 1) (Bolton and Levitt, 1985; Probyn and McQuaid, 1985; Bolton and Anderson, 1987; Bolton et al., 2012). Characterised by a large distal swollen bulb filled with gas and smooth fronds, this species grows to approximately 10 meters (Bolton and Anderson, 1987). There was, however, a 17-meter specimen collected in 2015 off Cape Point (Smit, unpubl. data). This species of kelp not only dominates the

biomass of the South African nearshore but plays an important ecological role (Bustamante and Branch, 1996). The estimated productivity of *E. maxima* within South Africa varies between 350 and 1500g $Cm^{-2}yr^{-1}$ (Mann 1982).

Across most of the coastline, *L. pallida* remains a subsurface kelp, dominating the kelp biomass at depths greater than 10 meters (Field et al., 1980; Bolton and Anderson, 1987; Molloy and Bolton, 1996). This species is distributed from Danger Point, east of the Cape Peninsula, to Rocky Point in northern Namibia, and reaches depths of greater than 20 meters (Field et al., 1980; Molloy and Bolton, 1996; Stegenga, 1997). Towards the north along the west coast, from around Hondeklipbaai, *L. pallida* replaces *E. maxima* as the dominant kelp species (Velimirov et al., 1977; Stegenga, 1997) and also occupies increasingly shallow subtidal regions. The northern populations also exhibit an increase in stipe hollowness compared to the solid stipe morphs in the species' southern distributions (Molloy and Bolton, 1996). This variation in morphology was thought to represent two distinct species, with the northern populations formerly described as *Laminaria schinzii* Foslie (Molloy and Bolton, 1996). Genetic work has subsequently shown that the two morphs are, in fact, the same species (Rothman et al., 2017b).

Most of the ecological research conducted in recent years has been focused on the impact of harvesting activities on kelp forests. For example, the effect of harvesting on the regrowth of epiphytic species (Anderson et al., 2006), understory algae species (Levitt et al., 2002), population structure and recovery of kelp populations (Rothman et al., 2006), morphological characteristics (Rothman et al., 2017), and regrowth from different harvesting methods (Rothman, 2006). In general, kelp forests on the Atlantic side of the Cape Peninsula have higher recovery and regrowth rates compared to populations within False Bay and the southern coastline. The higher regrowth and recovery rates of Atlantic kelp populations are due to the ideal temperate waters and the frequency and magnitude of upwellings which provide important nutrients to nearshore communities on the Atlantic side. In contrast, False Bay kelp populations are limited by nutrients and a non-ideal temperature environment.

Despite the ecological and economic importance of South African kelp forests in terms of organic subsidy and biomass input into near and distant systems, no research has attempted to describe or investigate the spatial and temporal distribution of floating kelp for the region. The only work investigating the input of kelp into local and adjacent ecosystems is by Dyer et al., (2019). The authors used stable isotopes of chl a C:N ratio, particulate organic carbon, and total suspended solids to characterise the composition of POM from within a kelp forest to perpendicularly offshore during periods of upwelling and downwelling. The results showed that kelp-derived organic matter was the main component of POM, while the opposite was true for upwelling periods. Other work has

shown the reliance of intertidal consumers on kelp-derived organic matter (Bustamante and Branch, 1996) and the extent of the *in-situ* biomass inventory around the coastline (Anderson et al., 2007).

In order to shed light on the role of water motion as an influencer of kelp morphological characteristics, the advances made in hydrodynamic modelling will be used rather than the qualitative measures of wave exposure used in the past. The advances in quantifying wave energy have primarily been through the incorporation of Linear Wave Theory.

1.3 Hydrodynamic modelling

Wave exposure may be modelled through various methods, which range from simple cartographic to more advanced numerical wave models. Traditional ecological measures of wave exposure usually incorporate integrative measures of hydrodynamic conditions at a particular site (Sundblad et al., 2014; Callaghan et al., 2015). Cartographic models can be qualitative or quantitative and are designed to meet the need for wave exposure measures to explain ecological distributions. Cartographic models comprise simple sets of calculations on coastline and wind data, and relatively small input data sets are required (Sundblad et al., 2014). These are regarded as 'fetch-based models,' which measure the length of open water associated with a site along a straight line (Sundblad et al., 2014; Callaghan et al., 2015). The output of such an approach is a simplified estimate of the potential wave energy for a specific set of sites. Advances in cartographical methods using fetch-based approaches allow for wave exposure measurements of larger areas and could be used as a method for predicting macroalgal community structure (Hill et al., 2010; Sundblad et al., 2014). An example of such a model is the 'BioEx model', developed by Rinde et al. (2004) to estimate wave exposure over large regions. BioEx requires frequency, strength and direction of winds, weighted by degree of exposure within various directions. BioEx is calculated as the sum of the index developed at different spatial scales (local, fjord and open) and has been used in mapping marine coastal biodiversity. Lindegarth and Gamfeldt (2005) criticised this approach, arguing that the choice of wave exposure method can influence ecological inference. The authors also highlighted the need for objective, reproducible and quantitative studies comparing exposure indices (Lindegarth and Gamfeldt, 2005).

Other authors, such as Hill et al. (2010), have argued that these simple measures can be improved upon by including bathymetry data which allows the incorporation of diffraction into the calculation. Diffraction is topographically induced variations in wave direction. A model incorporating this complexity was developed by Isaeus (2004) and is known as the 'simplified wave model' (SWM). The SWM model uses measurements of wind strength, fetch, and empirically derived algorithms to mimic diffraction. Advances in numerical modelling have been founded on physical wave theory which describes how a wave 'behaves.' This approach is based on a theoretical perspective rather

than the need to answer ecological questions (Sundblad et al., 2014; Callaghan et al., 2015). Besides diffraction, numerical models incorporate more complexity by including wind forcing, wave-to-wave interactions and energy loss due to friction and wave breaking. Numerical models have a variety of applications and are often incorporated within hydrodynamic general circulation models and are used operationally for forecasting the sea state (Group, 1988; Booij et al., 1999; Smith et al., 2001).

The downside of advanced numerical models is that they are computationally intensive, which creates limitations for large-scale simulations. Therefore, their application along long stretches of variable coastline, inshore environments and ocean-wide simulations are limited due to the poor spatial coverage. However, numerical models can be designed for local or site-specific coverage, provided the correct data is available (Sundblad et al., 2014). Most models have been designed with a specific goal or objective in mind, and so no single model exists that is appropriate for all situations or applications (Hill et al., 2010; Sundblad et al., 2014). Although models are 'situation-specific,' completed models can set the foundation for future models with regard to resolving critical oceanographic processes, identifying gaps, and identifying important tracer coefficients (North et al., 2009).

Hydrodynamic models use the same primitive equations as ocean models, which calculate velocities, turbulence, temperature, salinity, and density (Booij et al., 1999; North et al., 2009). The equations used in hydrodynamic modelling need to be 'discretised,' which means the equations are formulated to be evaluated at discrete temporal and spatial points (Booij et al., 1999; North et al., 2009; Sundblad et al., 2014). Additionally, hydrodynamic models use similar approaches to the grid and coordinate structures. Advances in numerical modelling have gained much traction in recent years and have been applied in a variety of ways with regard to ecological studies.

For example, a study by Wang and Xia (2009) used the Delft3D-Flow model to assess the hydraulic suitability of a stream as a spawning ground for the Chinese Sturgeon (*Acipenser sinensis* Gray, 1835) in the Yangtze River. The authors calculated the mean horizontal velocity, which was used to assess the hydraulic environment of the spawning ground. The flow field state was determined through model simulation and field-measured data used to validate the model. The results were added to existing scientific databases for spawning ground hydraulic environmental protection. Different numerical models can often be integrated to model across ecosystem levels. For example, a study by León et al., (2003) used integrated physical (Delft3D hydrological model), and biochemical (Agricultural Non-point Source model) processes models to investigate the possible impact on the Lake Malawi water quality due to management actions performed on the watershed level.

The investigation of the role of wind and hydrodynamic drag in influencing floating kelp trajectory once dislodged and ultimately using these insights to describe the distribution of kelp on the surface and seafloor within the study region will require the use of ocean models.

1.4 Trajectory modelling

Understanding the distribution of objects floating on the ocean surface has been an area of active study across many disciplines; ranging from finding lost cargo, search and rescue applications, the distribution of plastics (Lebreton et al., 2012; Jalón-Rojas et al., 2019; Li et al., 2020), trajectories of tuna populations (Phillips et al., 2018), marine connectivity (Siegel et al., 2003; Pujolar et al., 2013; Rossi et al., 2014), and volume transport of tracer content (Jönsson et al., 2011; Cheng et al., 2015; Chenillat et al., 2015) as a few examples. In turn, the importance in describing transport patterns of the ocean cuts across disciplines and benefits in both the environmental and socio-economic spheres of society. Both Eulerian and Lagrangian approaches are different sides of the same coin, being two different mathematical based approaches to solve for the flow patterns of the ocean and/or associated tracer content (Bennett, 2006; North et al., 2009; Van Sebille et al., 2018). Both methods have benefits and limitations depending on the situation, and therefore work well in combination as they complement each other (Wong et al., 2021). They can be used in combination as they are both based on the same mathematical framework known as the kinematic framework (Van Sebille et al., 2018).

1.4.1 The kinematic framework

The kinematic framework is the traditional method used to describe fluid motions and is fundamental to how both the Eulerian and Lagrangian methods describe flows in the ocean and/or the associated tracer content (Bennett, 2006; North et al., 2009; Van Sebille et al., 2018). The kinematic framework treats fluid particles as a continuum, in other words, a continuous distribution of mass in spaces, which can be described by Eulerian or Lagrangian methods (Wong et al., 2021). The Eulerian description has space coordinates $x = (x, y, z)$ and time t as the independent variables, and velocity $v(x, y, z, t)$, mass density $p(x, y, z, t)$, and pressure $P(x, y, z, t)$ as dependent variables (Bennett, 2006; Van Sebille et al., 2018; Wong et al., 2021). This is the reason why the Eulerian approach is often described as based on characterising fluid motion within a reference frame that is fixed in space and time since these are independent variables forming the basis of numerical ocean circulation models (Wong et al., 2021). For the Lagrangian description, the independent variables are a set/s of particle labels $a = (a, b, c)$ and time t, while the dependent variables are the coordinates,

$$x(a, b, c, t), y(a, b, c, t), z(a, b, c, t)$$

(1.2)

at the time t of the fluid particle identified by (a, b, c) (Bennett, 2006; Van Sebille et al., 2018; Wong et al., 2021). Unlike the Eulerian description, the particle moves based on the underlying velocity field within a time-dependent variable known as a 'trajectory' (Bennett, 2006; Van Sebille et al., 2018; Wong et al., 2021). The particle set labels are known as the material coordinate that distinguishes a particle from a continuum. The Lagrangian description uses Eulerian described velocity fields for a particular flow field to describe the motion/trajectory of fluid particles. It should be noted that alternatives for an underlying flow-field for Lagrangian trajectory description to the standard Eulerian flow-field do exist and have been used in previous work. For example, there has been application of surface geostrophic velocities derived from satellite altimetry data (Klocker et al., 2012; d'Ovidio et al., 2015) and high frequency (HF) radar (Ullman et al., 2006).

1.4.2 Eulerian and Lagrangian approaches

In both the Eulerian and Lagrangian sense, a fluid particle is described as a microscopically large collection of molecules where the particle velocity is a mass-weighted mean, known as barycentric velocity (Bennett, 2006; Van Sebille et al., 2018). Eulerian and Lagrangian approaches can be coupled together mathematically by equating the particle velocity crossing a point in a fixed space (Eulerian) to the fluid velocity at a particular point in time (Bennett, 2006; Van Sebille et al., 2018; Wong et al., 2021). Considering the different independent and dependent variables between each of the approaches the previous description can be expanded such that,

$$(Dt(a,t)/Dt)_a = v(x,t) \qquad (1.3)$$

where $X(a,t) = x$. It should be noted that the symbol D is used to be able to distinguish the material time derivative (the particle set label described earlier) from the general time derivative which is given by the velocity fields at a particular point in time (Bennett, 2006; Van Sebille et al., 2018; Wong et al., 2021).

$$Dx/Dt = v(x,t) \qquad (1.4)$$

This provided a mathematical basis for Lagrangian fluid analysis (North et al., 2009). In the realm of geophysical fluid dynamics, the trajectories of tracers using a combined approach often consider the underlying flow field as a collection of stream tubes which are only valid for steady-state flows (Döös et al., 2013). The ocean, from a mathematical sense, is composed of time-varying flows, making the use of stream tubes and steady-state flows invalid (Bennett, 2006; Van Sebille et al., 2018). For this reason, ocean models and oceanographers have developed various ways in which to incorporate

time-dependent flows or by introducing separate diffusion equations to account for the turbulence in the ocean (Bennett, 2006; Van Sebille et al., 2018).

These concepts are a focus of pure oceanography and therefore do not fall within the scope of the study. The concept is merely highlighted as it is a fundamental underpinning of Lagrangian trajectory analysis and leads to the two different approaches which can be used (Bennett, 2006; Van Sebille et al., 2018). The particles can be modelled as a volume transport pathway or a tracer transport pathway, the use of which depends on the application or question (Döös et al., 2013).

1.5 Ocean aspects of flotsam dispersion

The trajectory of passively drifting objects on the sea surface is influenced by multiple factors, such as water currents, atmospheric wind, wave motion, wave-induced currents, gravitational force, and buoyancy force. To complicate matters, the previously mentioned factors do not act independently but instead influence one another. Furthermore, the magnitude of forces on the object are determined by the object's shape. Therefore, all these factors need to be taken into account when modelling the trajectory of drifting objects. Given the local wind, surface current, and the shape and buoyancy of the object are known, it is possible to estimate trajectory.

The ocean processes which influence the dispersion and trajectory of flotsam occur over a range of spatial and temporal scales. For example, the spatial extent of ocean eddies is between 50 - 100km across and persists for months or even years, while eddy-associated filaments exist between 1-10km and persist for days to weeks (Fossette et al., 2012; Van Sebille et al., 2020). Therefore, the flow of the ocean is a composite of all the physical ocean processes which overlap spatially and temporally. Ocean currents are defined as the continuous, predictable, directional movement of seawater driven by differences in pressure, water density, and wind. The wind is a result of the combined effects of differential heating of the sea surface from solar radiation and the Coriolis effect from the spinning of the earth (Fossette et al., 2012; Van Sebille et al., 2020). The horizontal flow of the ocean can be divided into two categories, surface currents and deep-water currents, both of which are important transport mechanisms of heat and energy in the ocean. Surface currents, usually limited to 400m depth, are driven by the frictional forces of wind as it blows over the ocean surface (Fossette et al., 2012; Van Sebille et al., 2020). This pushes the upper layers of water along with it in the direction of the wind. Wind-driven surface currents are responsible for large-scale horizontal flow in the ocean, known as Ekman currents.

1.5.1 Ekman currents

Large-scale circulation patterns are driven by a combination of surface wind and the force of the earth's rotation (Coriolis force) which leads to the formation of Ekman transport (Rossby and Montgomery, 1935; Price et al., 1987; Fossette et al., 2012; Van Sebille et al., 2020). Ekman transport is the manifestation of frictional induced mass transport perpendicular to the wind direction and therefore deflects to the right in the Northern Hemisphere and to the left in the Southern Hemisphere (Rossby and Montgomery, 1935; Stommel, 1948; Fossette et al., 2012; Constantin, 2021). The surface deflection flow occurs at approximately 45°, which also generates shear stress on the water layer below and deflecting at a smaller angle than 45° (Fossette et al., 2012; El-Nabulsi, 2019; Van Sebille et al., 2020). This continues vertically down the water column until the direction of the current is in the opposite direction to the surface flow with almost zero velocity, ultimately forming a spiral, as depicted in Figure 1:1 (Price et al., 1987; El-Nabulsi, 2019; Van Sebille et al., 2020; Constantin, 2021). However, this may vary according to the region of study. Recent work by Bressan and Constantin (2019) showed that wave-induced ocean flow in the arctic and low-latitude areas of the ocean deviates from classical Ekman theory and deflects at an angle closer to 30°. The authors attribute the deviation to vertical turbulent mixing of the upper-ocean layers with depth and propose a modified formula for calculating the deflection angle to incorporate the differential vertical mixing (Bressan and Constantin, 2019).

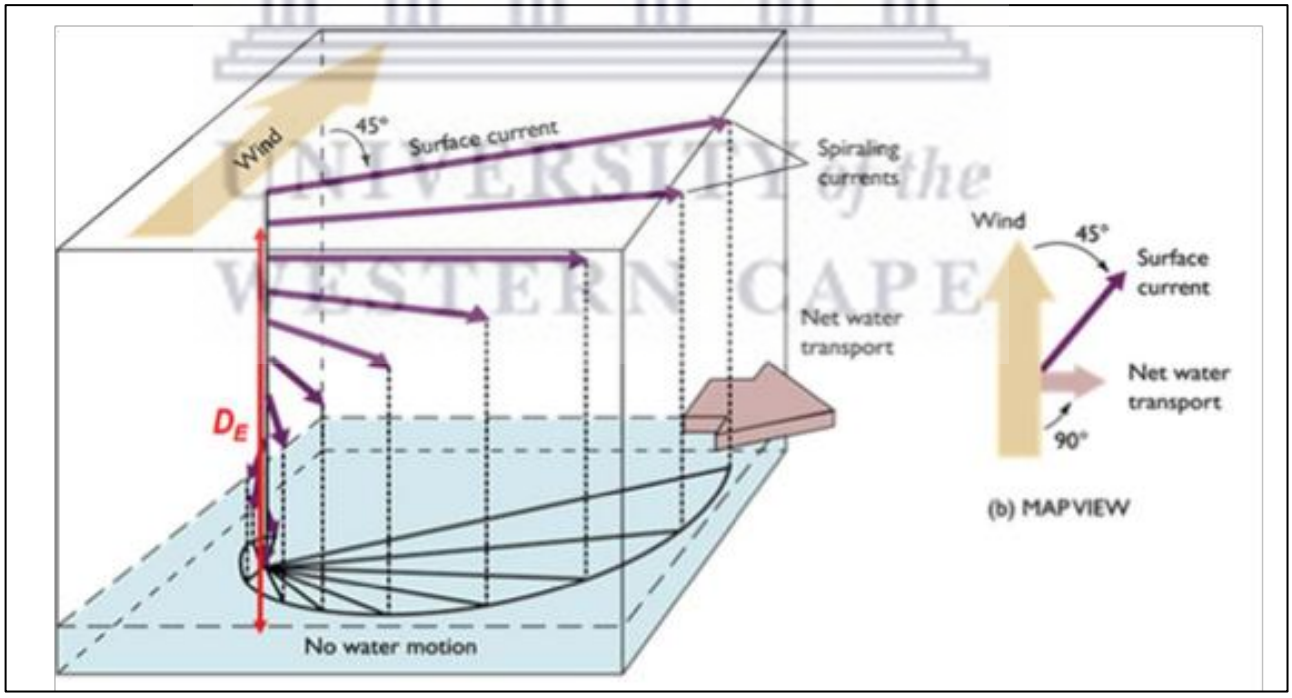

Figure 1:1 A schematic from Wegman (2020) representing the Ekman spiral and the associated Ekman mass transport. The length of the arrows is representative of the magnitude of velocity.

The total Ekman mass transport is calculated by integrating the flow velocities over the depth of the Ekman spiral. Ekman transport, the combined effects of wind and sea surface, creates variations in sea-surface height, consequently developing layers of differential horizontal pressure (Rossby and Montgomery, 1935; Price et al., 1987; Fossette et al., 2012; Constantin, 2021). In turn, the pressure gradient gives rise to geostrophic currents (Fossette et al., 2012; El-Nabulsi, 2019; Van Sebille et al., 2020; Constantin, 2021).

1.5.2 Geostrophic currents

Geostrophic currents are characterised by the balance of forces, namely the pressure gradient force and the Coriolis force (El-Nabulsi, 2019). Pressure gradient forces move water masses from a region of high pressure to a region of low pressure. Therefore, when the pressure gradient force equates to the Coriolis force, the resulting flow moves along lines of equal pressure, known as isobars (El-Nabulsi, 2019; Constantin, 2021). The direction of geostrophic flow is dependent on the hemisphere in which the flow develops (El-Nabulsi, 2019; Constantin, 2021). In the Northern Hemisphere, flow is directed to the right, and in the Southern Hemisphere is directed left. The orientation of geostrophic flow is largely responsible for the clockwise rotational flow in the subtropical gyres, along with the Coriolis effect (El-Nabulsi, 2019; Van Sebille et al., 2020; Constantin, 2021). The geostrophic currents formed across basin-scale areas in the ocean are often slow flowing and in full geostrophic balance. The rate of flow (speed) directly influences the stability of geostrophic flow; if speeds rise above a threshold, geostrophic balance begins to degrade and becomes unstable. Destabilised geostrophic balance through increased flow rate is a characteristic of narrow and fast-flowing Western Boundary Currents (WBCs) (Van Sebille et al., 2020). Examples of WBCs are the Gulf Stream, Kuroshio Current, and the Agulhas Current (Van Sebille et al., 2020). Due to the high flow rate, WBC are only considered to be in approximate geostrophic balance. The instability of WBCs are a large source of mesoscale and submesoscale development. Decaying of geostrophic balance leads to boundary currents becoming unstable, which leads to meandering of the outer boundary flow (El-Nabulsi, 2019). Once the meandering boundary currents accumulate enough kinetic energy, they break away from the overall geostrophic flow patterns in the form of filaments and eddies.

1.5.3 Eddies

Most of the detectable eddies in the ocean form from baroclinic instabilities. The heterogeneous characteristics of the ocean create variation and instabilities in water mass saline and thermodynamic properties, developing open-ocean boundaries between water masses (Holland and Rhines, 1980; Bakun and Nelson, 1991; Bakun, 2006). This, combined with the Coriolis effect and wind, create instabilities along these boundaries, causing vortices of spinning water to develop,

known as eddies (Figure 1:2). The spatial extent of eddies ranges from the mesoscale (10-100km), persisting for months or even years, to the submesoscale (1-10km), persisting for days or weeks (Morrow and Le Traon, 2012; Pegliasco et al., 2015; Van Sebille et al., 2020). The rotation of ocean eddies does not only exist on the surface but also extends vertically through the water column. Ocean eddies also have a 'centre,' which acts as an important surface accumulation zone for flotsam (Brach et al., 2018) as well as the vertical transport of heat, salinity, and nutrients (Jayne and Marotzke, 2002). For example, eddies are considered the main mechanism of transport of heat for the Antarctic Circumpolar Current (ACC) (Karsten et al., 2002a;b). This is due to the upwelling and downwelling characteristics of both cyclonic and anti-cyclonic eddies (Bakun and Nelson, 1991; Bakun, 2006). This is dependent on whether the eddy is "spinning-up" due to frictional forcing from adjacent flow patterns or "spinning-down" when the eddy moves away from the formation source and begins to decay (Bakun, 2006). Along with vertical transport, ocean eddies are also recognised as an important zone of surface accumulation of flotsam (Van Sebille et al., 2020). This is due to the convergent and divergent flow patterns associated with ocean eddies (Jayne and Marotzke, 2002; Bakun, 2006; Morrow and Le Traon, 2012; Pegliasco et al., 2015). For example, an anti-cyclonic eddy that is spinning-up will be characterised by convergent flow patterns on the surface. The surface convergent flow patterns can occasionally develop into convergent

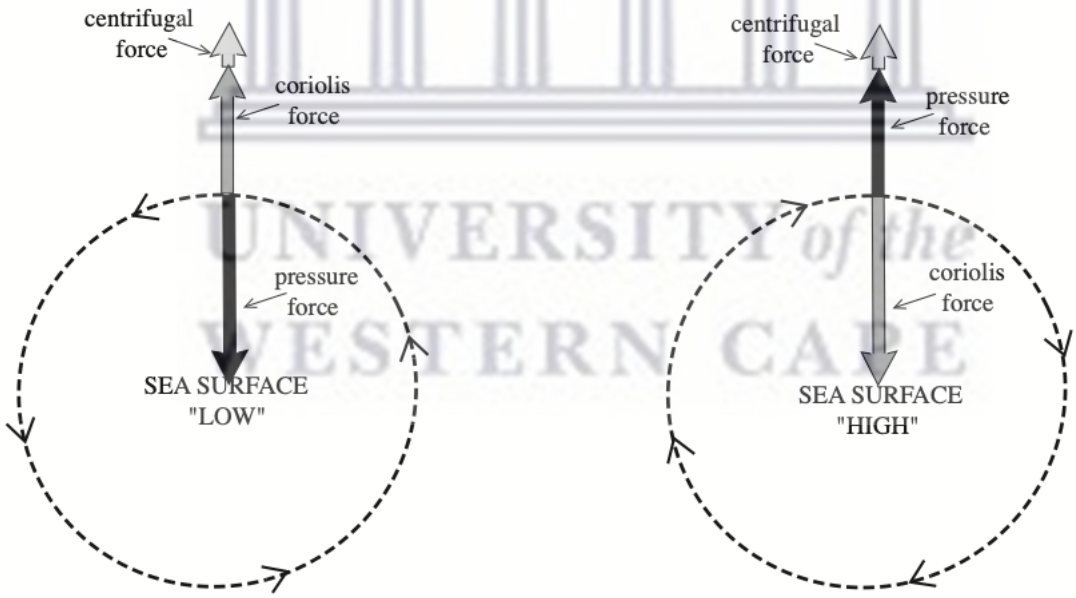

Figure 1:2 The forces that exist within a cyclonic eddy (left) and an anti-cyclonic eddy (right) located in the Northern Hemisphere as depicted by Bakun (2006). Anti-cyclonic eddies spin clockwise in the Southern hemisphere. The length of the arrows depicting the various forces represents the magnitude of the force. The dotted 'L' and 'H' represent 'low' and 'high' sea surface topography. The forces would be identical for an anti-cyclonic eddy but in reverse.

frontal structures, which move within the interior of the eddy (Bakun, 2006; Morrow and Le Traon, 2012). The opposite is true for spinning-up cyclonic eddies, which are characterised by divergent horizontal flow patterns (Spall, 1995; Bakun, 2006). The divergent flow patterns on the surface can

develop into submesoscale eddies and filaments through frictional and shear forces of adjacent flow patterns (Bakun, 2006; Morrow and Le Traon, 2012). Flow patterns and upwelling-downwelling characteristics also differ between the centre and the interior flow patterns (Bakun, 2006; Pegliasco et al., 2015). Ocean eddies which exhibit interiors of upwelling and divergent flow, are associated with convergent flow and downwelling near the edges (Bakun, 2006; Morrow and Le Traon, 2012; Pegliasco et al., 2015). In contrast, eddies with interiors of downwelling and divergent flow are associated with upwelling and convergent flow on the outer edges. The convergent/divergent and upwelling/downwelling dynamics of ocean eddies make them important mechanisms of dispersal and accumulation of flotsam, as well as transport of natural and anthropogenic material and marine organisms (Brach et al., 2018). In areas where large-scale ocean eddies develop, such as in the North Atlantic (Halliwell Jr et al., 1991), boundaries of water masses evolve from the periphery leading to the development of ocean fronts (Spall, 1995).

1.5.4 Ocean fronts

Ocean fronts, also known as surface fronts, are boundaries of water masses with different saline and thermodynamic properties (Saltzman and Tang, 1975; Bakun, 2006). The presence of different types of water masses is commonplace in the ocean. When in close proximity, the water masses interact at the boundaries and mix to form a new intermediate body of water at the interface, which results in the development of convergence zones on the surface and vertical transport of water from the surface (Figure 1:3) (Nardelli et al., 2001; Haine and Williams, 2002; Bakun, 2006). The

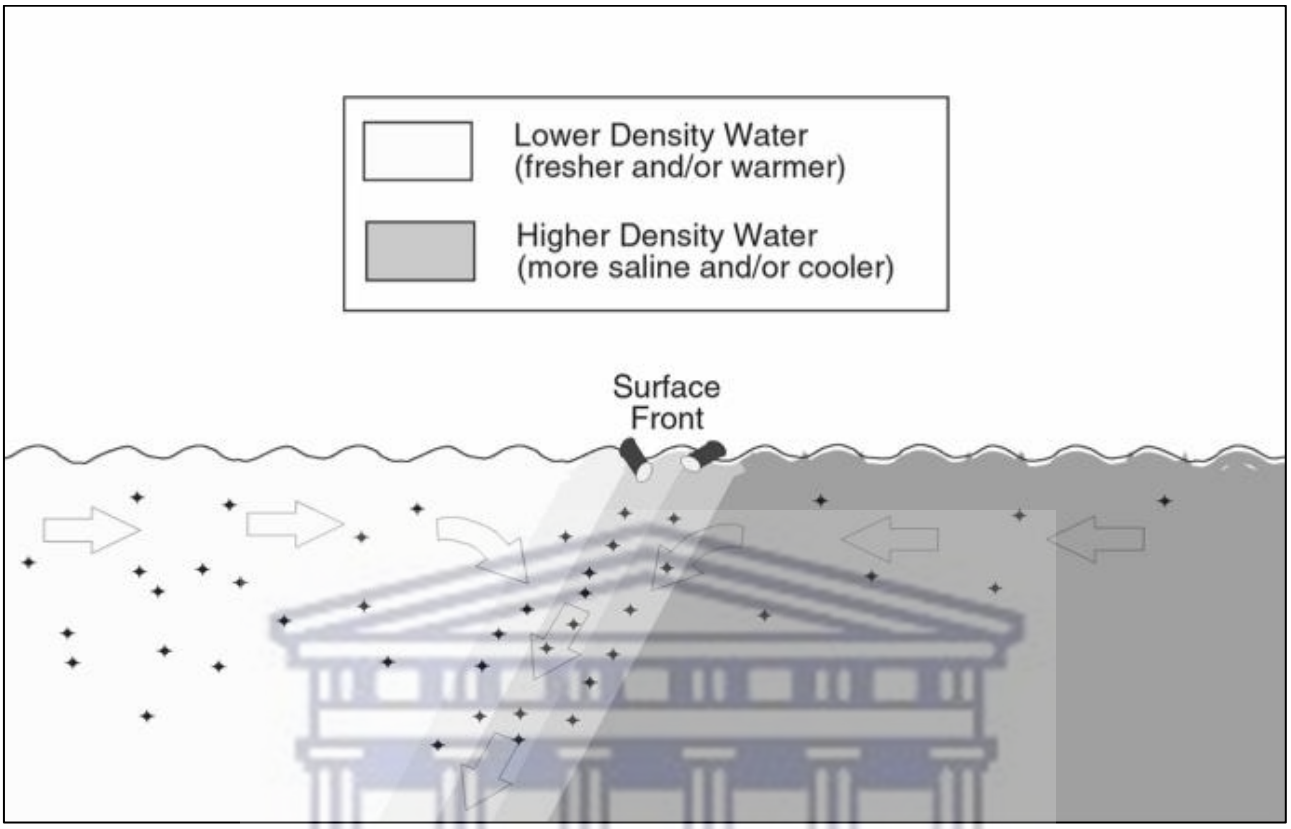

Figure 1:3 Schematic by Bakun (2006) of a front between two different water masses. Arrow symbols represent density-driven flows associated with the formation of a front. The particles in the water represent non-buoyant material and the vertical transport, while the cylinders at the surface represent buoyant flotsam accumulating at the boundaries.

intermediate water mass acts like a boundary, forcing the less dense water masses to flow under denser water masses (Haine and Williams, 2002). The result is the vertical transport of water downwards through the water column while also forming a convergence zone at the interface between the different water masses (Vélez-Belchí and Tintoré 2001; Bakun, 2006; Taylor and Ferrari, 2011). The vertical transport of water that develops at the interaction between ocean fronts plays a significant role in the diurnal cycle of plankton and fish larvae (Lutjeharms et al., 1985; Claustre et al., 1994; Taylor and Ferrari, 2011; Ryan et al., 2014). Non-buoyant particles or organisms, such as microplastics and phytoplankton, will be transported downwards along with the vertical ocean flow (Nardelli et al., 2001; Vélez-Belchí and Tintoré 2001; Bakun, 2006). Buoyant particles, such as macroplastics and kelp, will remain on the surface and accumulate over time at the interface between the different water masses (Lutjeharms et al., 1985; Haine and Williams, 2002; Bakun, 2006). Once the lifespans of the ocean fronts expire, the accumulated material will disperse from the source. For example, A study by D'Asaro et al., (2018) released and tracked an ensemble of satellite-tracked drifters near the site of the 2010 Horizon Oil Spill. At the end of the fieldwork, the authors noted that the drifters accumulated along cyclonic vorticity-associated density fronts. Furthermore, the accumulation of drifters persisted for the lifespan of the fronts, after which the drifters dispersed.

1.5.5 Drag parameters

Drag is a force that has not been considered for macroalgal raft trajectory. However, the role of drag is considered an important aspect of ocean flotsam trajectory and, therefore, is the focus of this review. Drag is the force an object experiences when moving in a fluid due to the rate in change of momentum (Vogel, 2020). The drag around the surface of an object due to the viscosity of the medium is surface drag. The drag induced by a quantity of fluid moving around the object is known as pressure-form/-inertial drag. In general, large objects moving at higher velocities tend to induce larger drag forces; however, this is not always the case. In some instances, the flow around the object changes from laminar to turbulent, which ultimately reduces overall drag. The type of flow, laminar or turbulent, is determined by fluid density *(p)*, flow speed *(U)*, object size *(l)* and fluid viscosity *(v)* (Vogel, 2020). These factors can be used to calculate the Reynolds number, which is used to determine the type of flow. The expression used can be dependent on whether the fluid is Newtonian or non-Newtonian and the object shape (Vogel, 2020).

The drag coefficient is the fluid dynamic drag or is also known as the hydrodynamic drag, but from here on, it will be referred to only as drag. The drag on an object is a combination of skin friction and form drag, the magnitude of which is determined by the characteristics of the object and the medium in which the object is moving (Vogel, 2020). For instance, skin drag is determined by the "roughness" of the object's surface, and the form drag by the shape and size of the object (Salmon, 1998; Vogel, 2020). An object which is moving through a liquid vertically will have multiple forces acting on it, namely the viscosity coefficient of the liquid (F_A), the buoyancy force (BF) and the Drag (F_D); provided the object's density is greater than that of the density of the liquid (Vogel, 2020). The viscosity coefficient is dependent on the characteristics of the medium and the buoyancy force by the mass of the object and the gravitational forces acting on it (Salmon, 1998; Vogel, 2020). For the object in this example to move horizontally, some of the liquid needs to be displaced, which requires force (Vogel, 2020). This force gives the liquid a moment of inertia and is dependent on the shape of the object and, ultimately, the drag force acting on the object as it moves through the liquid. As an example, a short cylinder has less drag than that of a long cylinder as more liquid needs to be displaced for the object to move through the medium (Salmon, 1998; Vogel, 2020). Generally, the initial acceleration is ignored or considered negligible in Lagrangian particle tracking studies because the temporal resolution of the underlying ocean models used does not match the timescales relevant to the relatively rapid acceleration of the object (Allen and Plourde, 1999; Hackett et al., 2006; Breivik et al., 2011).

1.5.6 Sinking parameters

Drifting objects floating on the sea surface are exposed to multiple environmental factors which determine the amount of time objects remain afloat, as shown by experimental work on macroalgae species (Thiel and Gutow, 2005; Rothäusler et al., 2011; Graiff et al., 2016; Macaya et al., 2016). The time that an object remains at the surface before it begins sinking is known as the 'float-time' or 'raft-time.' Deterioration of the object by light, temperature, and biofouling all act to influence object raft-time. Biofouling is the attachment and accumulation of biological organisms on the surface of a submerged object (Ye et al., 1991; Long et al., 2015). Once the buoyancy of the object is overwhelmed, it begins to sink, the rate of which is dependent on the density, size, shape, and texture of the object, as well as fluid density and viscosity, known as the 'sink rate'. In addition, the 'settling velocity' must be calculated, which is an analogous term used for terminal velocity.

The settling velocity, like the sink rate, is determined by the object and fluid medium properties. Most of the earlier work regarding sink rate of natural particles focused on sediments (Corey, 1949; Baba and Komar 1981), while in recent years, the focus has shifted to microplastics (Kooi et al., 2017; Lobelle et al., 2021). Most of the current understanding regarding sink rates and settling velocities is based on work by Dietrich (1982), who used experimental data from previous studies and systematic analysis to develop the method to calculate the sink rates and settling velocities of natural particles. The approach developed by Dietrich (1982) takes into account the size, shape, density, and roundness of natural particles. It should be noted that most of the past and present work has focused on small particles and not larger organisms such as kelp. To effectively calculate the sink rate and settling velocity of smaller particles, viscous drag becomes more important, while for larger objects, this can be ignored (Vogel, 2020). When an object begins to sink in a less dense Newtonian fluid, it will initially accelerate until the forces acting on it are in balance (Dietrich, 1982). The forces acting on a sinking object are dependent on the velocity and acceleration of the object, which are gravitational and resistant forces, i.e. drag forces. In the case of particle tracking studies, the velocity components of the ocean model at a particular time step can be used to calculate and investigate the influence of drag, as particles are often assumed to follow the ocean currents (Furnans et al., 2008; Van Sebille et al., 2020). The force due to the weight of the object/particle can be calculated by

$$Fg = (ps - po)gV \qquad (1.23)$$

where p_s is the density of the object, p_o is the density of the fluid, g is the gravitational acceleration, and V is the volume of the object. The forces are the surface and viscous drag forces acting on the particle. The relative contribution of these is dependent on Reynold's number. The inclusion of

viscous drag forces is applicable to smaller particles, such as sand, sediment, and microplastics, and therefore will not be discussed further. The approach by Dietrich (1982) can be modified to suit a particular application. For example, work by Kooi et al. (2017) adapted the approach to include the effect of biofouling on sinking microplastic. More recently, work by Lobelle et al. (2021) used the 'Kooi-model' to investigate the transport of microplastic in a three-dimensional flow by using a higher resolution of hydrodynamic and biological data. The authors showed that the inclusion of sinking, and particle size were important parameters when describing the dispersion of microplastics on the seafloor.

1.6 Thesis structure and overview

1.6.1 Investigating waves and temperature as drivers of kelp morphology

Macroalgal morphological characteristics have been shown to be influenced by local environmental variables. Although light, turbidity, and nutrients do influence morphological characteristics to a degree, the main influences are considered to be temperature and wave exposure (Hurd, 2000; Denny and Gaylord, 2002; Thomsen et al., 2004; Fowler-Walker et al., 2005; Wernberg and Thomsen, 2005; Mabin et al., 2013; Bekkby et al., 2014). Kelp tends to take on strength-increasing or drag-reducing traits, which reduces the probability of dislodgement during times of high wave energy (Hurd, 2000; Denny and Gaylord, 2002; Thomsen et al., 2004; Fowler-Walker et al., 2005). Temperature affects overall size of the plant by altering the physiological performance, ultimately influencing productivity and growth (Zimmerman and Kremer, 1986; Gerard, 1997; Bearham et al., 2013; Gao et al., 2013). Past research has often used quantitative measures of wave exposure and biased temperature data (Mabin et al., 2013; Smit et al., 2013), not taking advantage of hydrodynamic models and quality unbiased data. Therefore, In Chapter 2, my aims were:

1. Determine how temperature and wave exposure can influence the morphology of sub-canopy and canopy kelp at deep and shallow populations of the same species; and
2. Identify specific temperature and wave metrics which drive kelp morphological characteristics.

This will be achieved through the following Objectives:

1. Develop a climatological temperature and modelled wave dataset to use as predictor for kelp morphology across the study area; and
2. Apply the climatological and modelled data as predictors of the morphological characteristics of *E. maxima* and *L. pallida* using statistical tools.

1.6.2 Numerical experiment investigating the influence of drag on trajectory patterns of floating macroalgae

Ocean currents act as an important dispersal mechanism of material on the ocean surface, both natural and anthropogenic (Edgar, 1987; Norton, 1992; Bushing, 1994; Holmquist, 1994; Helmuth et al., 1994; Smith, 2002; McCormick et al., 2008). Macroalgae are one of the most important natural dispersal vectors of marine organisms and are regarded as the 'tumble-weed of the ocean' (Edgar, 1987; Norton, 1992; Bushing, 1994; Holmquist, 1994; Helmuth et al., 1994; Smith, 2002; McCormick et al., 2008). Despite many studies that exist on the topic (Helmuth et al., 1994; Kingsford, 1995; Hobday, 2000b; Smith, 2002; Macaya et al., 2005; Collins et al., 2010; Wichmann et al., 2012; Saunders, 2014; Graiff et al., 2016; Tala et al., 2013, 2017; Graiff et al., 2016; Batista et al., 2018; Brooks et al., 2018, 2019; Wang et al., 2019; Putman et al., 2018, 2020), the relative role of wind and surface currents in influencing the trajectory of macroalgal dispersal is still unknown. Past studies focussed on kelp rafts (Helmuth et al., 1994; Kingsford, 1995; Hobday, 2000b; Smith, 2002; Macaya et al., 2005; Collins et al., 2010; Wichmann et al., 2012; Saunders, 2014; Graiff et al., 2016; Tala et al., 2013, 2017; Graiff et al., 2016; Batista et al., 2018; Brooks et al., 2018, 2019; Wang et al., 2019; Putman et al., 2018, 2020), which can vary greatly in size making it difficult to form a consensus as to the relative role of wind versus surface currents. In addition, these studies have not considered surface-area in relation to drag characteristics of the macroalgae, both of which have been shown to play a role in the trajectory and accumulation of other flotsam (Brooks et al., 2018, 2019; Putman et al., 2018, 2020). Advances in Lagrangian trajectory modelling have been rapid in recent years and allow the use of numerical experiments to investigate trajectories of flotsam in the ocean (Brooks et al., 2019, Putman et al., 2018, 2020). In this study, I aim to shed light on the relative role of wind versus surface currents and the role of drag in macroalgal trajectory and accumulation. Importantly, I focus on solitary drifting kelp and not kelp rafts. Therefore, in Chapter 3, my aims were to:

1) To understand the direct role of hydrodynamic and wind drag in the transport of floating macroalgae.
2) To identify and shed light on the role of relevant associated physical ocean processes.

This will be achieved through the following Objectives:

1) Use numerical simulations to compare the trajectory of purely Lagrangian particles to that of kelp particles (drag parameters included)
2) Use varying degrees of hydrodynamic and wind drag to investigate the effects of different drag exposures on trajectory, as this relates to buoyancy.

3) Use different combinations of flow-fields to identify key physical ocean processes and features that influence macroalgal trajectory patterns.

1.6.3 Individual-based numerical experiment to describe the distribution of floating kelp within the Southern Benguela Upwelling System

Understanding macroalgal distribution patterns within the nearshore and the open ocean has been given much attention in recent years due to the importance in marine connectivity in both the ecological and socio-economic spheres (Griffiths et al., 1983; Highsmith, 1985; Holmquist, 1994; Kirkman and Kendrick, 1997; Hobday, 2000a; Thiel and Gutow 2005; Troell et al., 2006; Holden et al., 2018; Michaud et al., 2019; Gilson et al., 2021). Macroalgae act as an important source of organic input for coastal, nearshore and offshore ecosystems (Griffiths et al., 1983; Michaud et al., 2019; Gilson et al., 2021). In addition, macroalgae are harvested *in situ* or in the form of beach-cast for a range of economic purposes (Kirkman and Kendrick, 1997; Troell et al., 2006; Holden et al., 2018). Finally, kelps have been shown to act as a Blue Carbon sink due to their ability to sequester carbon dioxide and ultimately help regulate the climate (Bayley et al., 2017, 2021; Smale et al., 2018; Filbee-Dexter and Wernberg, 2020). The ability to describe macroalgal distributions would shed light on the ecological role macroalgae play as an organic subsidy, dispersal vector for other organisms, kelps' contribution to Blue Carbon, and would aid in the management of coastal ecosystems. Therefore, in Chapter 4, I aimed to:

1) Characterise *E. maxima*'s surface and sink distribution with the Southern Benguela Upwelling System.

This will be achieved through the following Objectives:

1) By incorporating a site-specific parameterisation to the relevant drag and physical ocean processes identified in Chapter 3 and using multiple sites of known morphometric *E. maxima* properties to describe distributions on the surface and seafloor within the study domain.
2) Characterise the distribution in terms of underlying physical ocean processes and mesoscale features.
3) Identify any seasonal components to *E. maxima* trajectory patterns due to associated seasonal variation of physical ocean processes and features.

2 : Investigating waves and temperature as drivers of kelp morphology

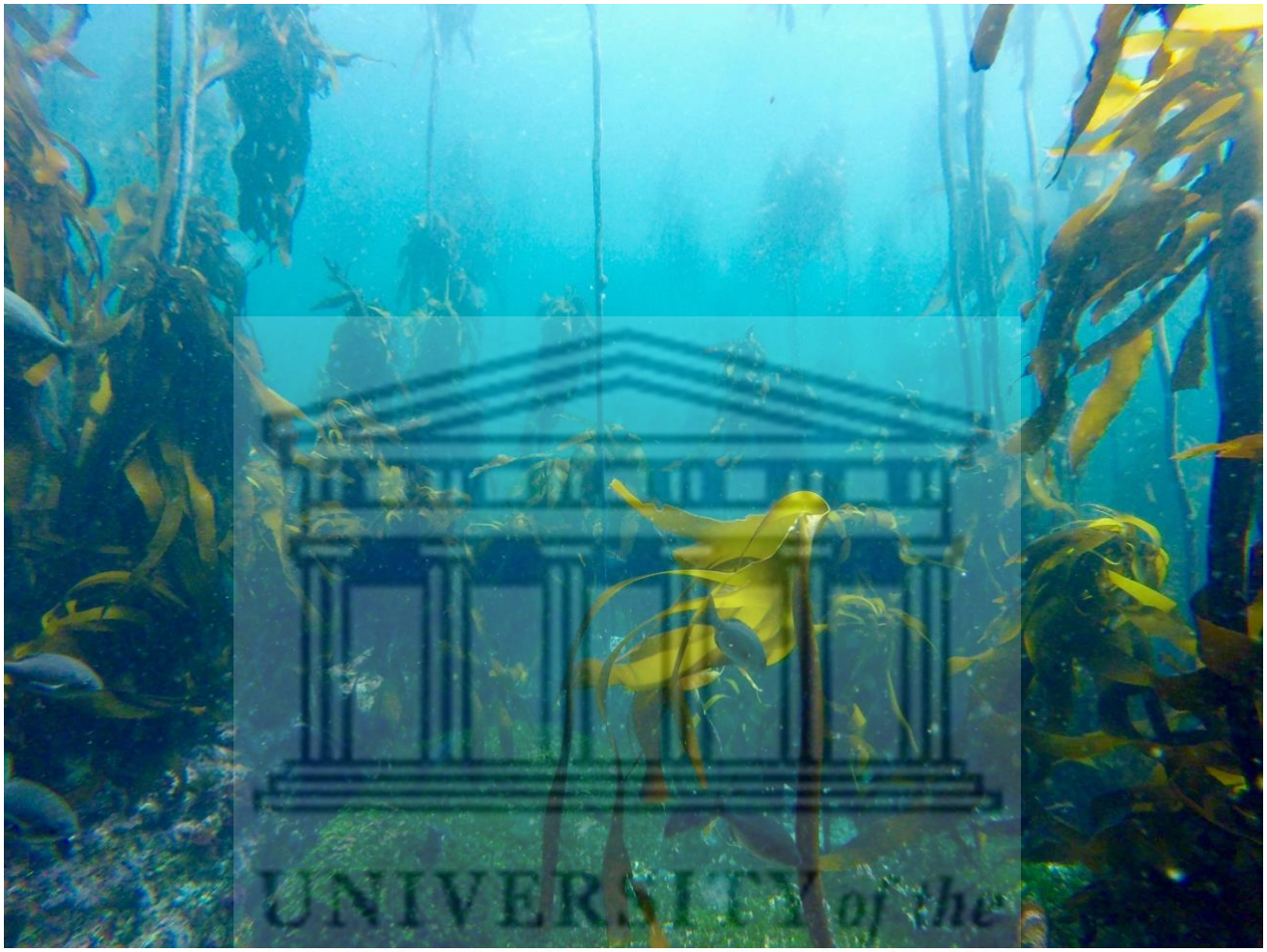

In this chapter, my aim was to understand how temperature and wave exposure can influence the morphology of sub-canopy and canopy kelp, as well as between deep and shallow populations of the same species, and to identify specific temperature and wave metrics which drive kelp morphological characteristics. Once established, this would allow for a site-specific approach to investigate the influence of hydrodynamic and direct windage (wind drag) on floating *E. maxima* in Chapter 3. The main findings from this chapter were:

- Wave variables are the main driver of kelp morphological characteristics in both *E. maxima* and *L. pallida* populations.
- Differences in morphological characteristics between shallow and deep populations of *E. maxima* reflect differences in hydrodynamic and temperature regimes.
- Wave energy thresholds in relation to morphological adaptation were identified.
- When wave exposure is low or insignificant, temperature regime is the main influencer of morphological adaptation.

2.1 Introduction

Kelps are a group of large seaweeds of the order Laminariales (Ochrophyta), which despite their relatively low taxonomic diversity of species in genera (Bolton, 2010), form the basis of one of the most productive ecosystems globally (Mann, 1973; Krumhansl and Scheibling, 2012). Kelps generally have a dependence on cool-temperate and arctic seawater temperatures (Dayton, 1985; Bolton, 2010; Cavanaugh et al., 2011; Mohring et al., 2014) and dominate the nearshore biomass within the rocky shallow coasts in both hemispheres (Steneck et al., 2002). Their size and complex morphology provide a heterogeneous habitat structure (Steneck et al., 2002) that accommodate a multitude of turf and sub-canopy seaweed species, and diverse assemblages of sessile and mobile invertebrates and vertebrates (Mann, 1973; Steneck et al., 2002), each depending on a wide suite of ecological services provided by kelp forests (Dayton, 1985; Gaines and Roughgarden, 1987; Paul and Steneck, 1993; Levin, 1994; Anderson et al., 1997; Willis and Anderson, 2003). Wave exposure and temperature are regarded as important environmental drivers of kelp forests and play a role in their distribution (Gorman et al., 2013), abundance (Dayton et al., 1998; Cavanaugh et al., 2011), diversity (Wing et al., 2007; Wernberg and Goldberg, 2008), composition (Dayton, 1985; Leliaert et al., 2000; Harley et al., 2012; Norderhaug et al., 2012), growth (Cousens, 1982) and productivity (Dayton et al., 1998; Krumhansl and Scheibling, 2012; Pedersen et al., 2012).

Given that kelp are cool-temperate organisms which are vulnerable to dislodgement under high wave exposure scenarios, increases in storm frequency and magnitude, and changes in ocean temperature, pose a direct threat to their survival; which is a concern considering that these variables are known to be affected by climate change (Weisse, 2010; Rose et al., 2012; Rummukainen, 2012; Russo et al., 2014; Reguero et al., 2019). Warmer temperatures reduce the resilience of kelp individuals to storm disturbance (Wernberg et al., 2010), causes fragmentation through weakening tissues (Simonson et al., 2015) and reduces growth and productivity (Zimmerman and Kremer, 1986; Gerard, 1997; Bearham et al., 2013; Gao et al., 2013); while storms and high wave energy dislodge and break kelp (Seymour et al., 1989; Graham, 2004; Byrnes et al., 2011). Despite these threats and disturbances kelp persist across a broad range of environments which is largely due to their morphological plasticity (Fowler-Walker et al., 2006; Wernberg and Vanderklift, 2010). A study by Wernberg et al. (2003) investigated the morphology of *Ecklonia radiata* (C.Agardh) J.Agardh in order to quantify the morphological variation and whether it was dependent on spatial differences along the Australian coast. They found no correlation between spatial distance and morphological similarity; rather the morphology of the kelp was representative of multiple environmental forcings on different morphological characters at different spatial scales (Wernberg et al., 2003). Although multiple environmental factors play a role in kelp morphological adaptation, wave exposure and temperature have been identified as the main influencers across

various kelp species (Hurd, 2000; Denny and Gaylord, 2002; Thomsen et al., 2004; Fowler-Walker et al., 2005; Wernberg and Thomsen, 2005; Mabin et al., 2013; Bekkby et al., 2014). For example, a study by Serisawa et al., (2002) compared the morphology of *Ecklonia cava* Kjellman growing at warmer and cooler sites and showed wrinkling of the blade and reduced size to be a characteristic of higher temperature ranges. Warmer temperature affects important kelp physiological processes such as photosynthesis and respiration, which influences growth and productivity and ultimately leads to a reduction in size (Zimmerman and Kremer, 1986; Gerard, 1997; Bearham et al., 2013; Gao et al., 2013). Past research has shown that in highly wave exposed areas kelp morphology tends to take on characteristics which reduce drag, increase strength and increase flexibility (Hurd, 2000; Denny and Gaylord, 2002; Thomsen et al., 2004; Fowler-Walker et al., 2005). For example, a study by Wernberg and Thomsen (2005) examined the consistency of wave exposure as a driver of *E. radiata* across a broad geographic range and showed trends toward drag- reducing (small size, narrow laterals and blades, low spinosity) and increased strength (large holdfast, thick stipe and thick blades and lamina) at high wave exposure sites. Measures of wave exposure in ecological studies often incorporate integrative measures of hydrodynamic conditions at a particular site which are based on cartographical models of exposure. Cartographical models of wave exposure are "fetch-based-models" which measure the length of open water associated with a particular site in a straight line and are regarded as simple measures of wave exposure. Advances in numerical modelling based on physical/linear wave theory incorporate more complexity (wind forcing, wave-wave interactions, wave breaking, diffraction and variation in wave direction) into the models and allow for a quantitative, reproducible approach for characterizing the hydrodynamic environment. Although Mabin et al. (2013) investigated kelp morphological characteristics using a 2D WAM model, currently no studies investigating macroalgal morphological characteristics in relation to the wave environment have incorporated 3D spectral numerical modelling. Furthermore, no studies have identified specific wave metrics that drive kelp morphological characteristics, which the current work will aim to achieve. Other considerations such as possible differences in morphology between sub-canopy and canopy species, and shallow and deep-water kelp populations have not been considered using advanced numerical and statistical tools. Due to the complex effects of environmental drivers on kelp morphology, one can also expect differences in morphology between deep and shallow water populations of the same species. Deep and shallow water environments may differ in abiotic processes such as the degree of water column mixing (Smit et al., 2013), solar heating (Dunne and Brown, 2001; Dellatorre et al., 2012), and effects of wave dampening (Kobayashi et al., 1993; Dubi and Tørum, 1994; Ma et al., 2013). The kelp *Laminaria pallida* Greville and *Ecklonia maxima* (Osbeck) Papenfuss are important habitat forming seaweeds that exist around the coast of South Africa and offer a unique opportunity to investigate the drivers of macroalgal morphological characteristics between canopy and sub-canopy species, as well as between deep

and shallow water environments. Although both these species exist in the sub-tidal, *L. pallida* dominates deeper waters while *E. maxima* forms dense surface canopies in the shallow sub-littoral. Therefore, *E. maxima* may be exposed to variations in wind driven surface waves, swell waves and temperature, while *L. pallida* is exposed to variations in swell waves, wave exposure and temperature due to differences in depth. Molloy and Bolton (1996) investigated the effect of depth and wave exposure on *L. pallida* and showed that depth had a greater effect than wave exposure when considering all the morphological characteristics; when considering individual characteristics, however, wave exposure had the most significant effect on blade thickness. Another study by Rothman et al., (2017a) investigated the changes in morphology in shallow populations of *L. pallida* and *E. maxima* along the South African coastline and into Namibia; *E. maxima* exhibited no morphological changes along the coast, but the stipes of *L. pallida* become increasingly hollow further north along the coastline. The authors suggested that turbidity in relation to light attenuation was the environmental driver responsible for this change.

My aim in this study is, therefore, to understand how temperature and wave exposure can influence the morphology of sub-canopy and canopy kelp, as well as between deep and shallow populations of the same species. I will also aim to identify specific temperature and wave metrics which drive kelp morphological characteristics. This will be achieved by initially understanding the variation in temperature and waves using a numerical model. The numerical model will then be used as a basis for investigating the consequences for morphological characteristics of *E. maxima* and *L. pallida* using advanced statistical tools.

2.2 Methods

2.2.1 Site selection

Sites were chosen to represent an array of temperature and wave gradients, as indicated in Figure 2:1. St. Helena Bay and Betty's Bay constituted the north-western and south-eastern boundary sites, respectively. These sites are roughly 300 km apart, lie within separate marine provinces (Smit et al., 2017) and span the majority of the south-west coast, in varying thermal and wave energy regimes. The region is dominated by kelp communities that persist in contrasting abiotic environments. The west coast region has been termed cool-temperate, which is defined as a region where mean monthly temperatures are always above 10°C and below 15°C Smit et al., (2013). East of Cape Point marks the beginning of an overlap or transition area, which is also referred to as the Benguela-Agulhas Transition Zone (Smit et al., 2013). The Agulhas Marine Province is characterized by a wide temperature range of up to 7°C difference between mean monthly temperatures between summer and winter and is classified as warm-temperate (Smit et al., 2013).

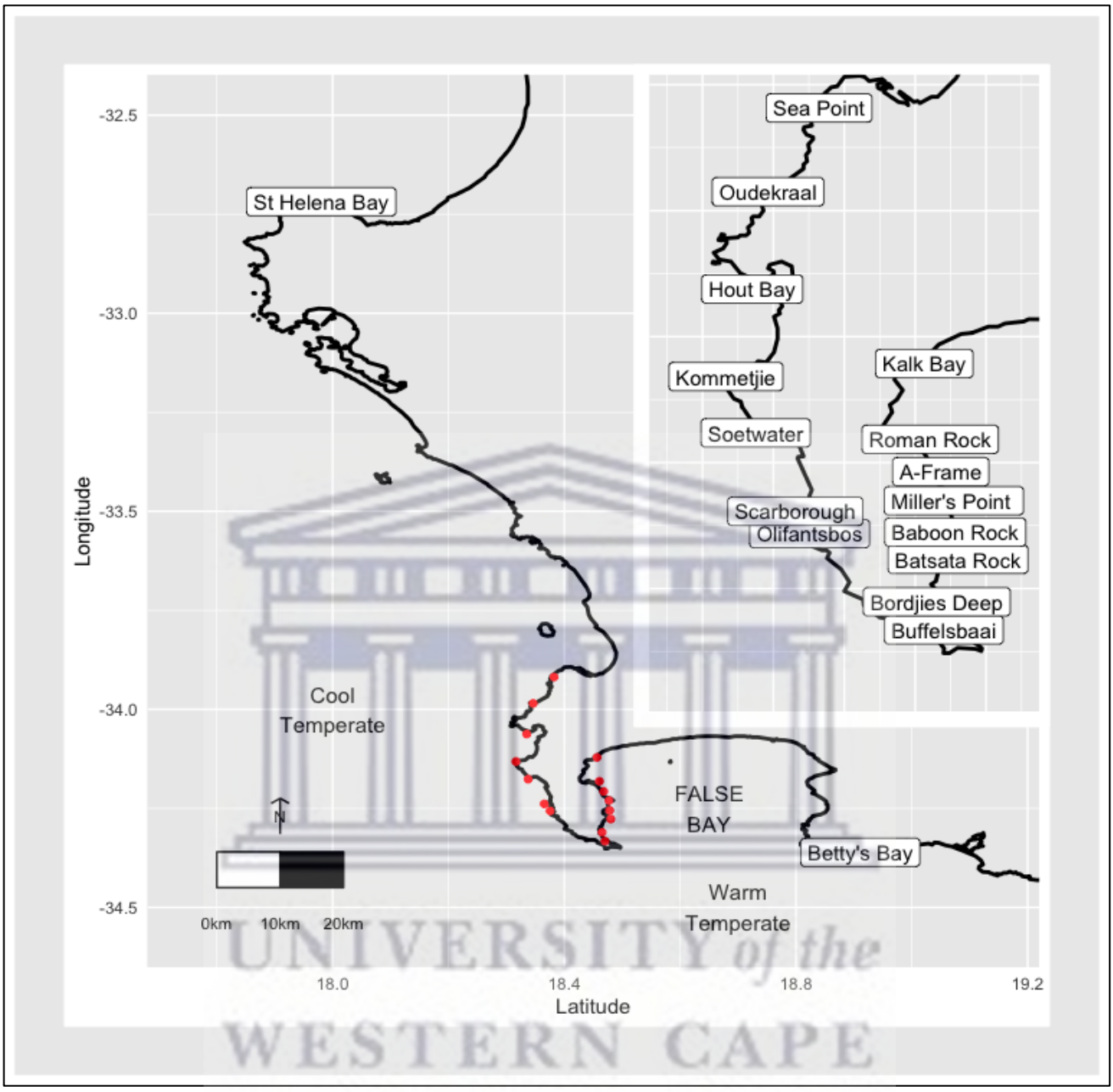

Figure 2:1 Map of the study area and sampling sites. The red dots represent study sites around the Cape Peninsula.

The annual and seasonal patterns in both wind and swell direction influence the thermal regime around the coastline by inducing upwelling. Upwelling brings deep, cool nutrient-rich water to coastal areas which causes a decrease in temperature (Cram, 1970; Gill and Clarke, 1974; Andrews and Hutchings, 1980; Field et al., 1980; Blanke et al., 2002; Rouault et al., 2010). The wind speed and wind direction help drive upwelling in summer on the western side of the Cape Peninsula, where southerly winds blow parallel to the coast and trigger upwelling events (Field et al., 1980; Rouault et al., 2010). This is not the case for False Bay, which is shielded from the dominating wind and swell that the Cape Peninsula is subjected to. In the summer months, upwelling becomes more favourable

in False Bay due to the change in swell and wind direction, causing lower temperatures to dominate during this time (Andrews and Hutchings, 1980; Rouault et al., 2010). Due to the Cape Peninsula temperate latitude, winter months bring an increased frequency of frontal depressions that originate from the Southern Ocean (Reason et al., 2006). These low pressures are joined by large swells with increased wave energy. The nearshore environment, with the accompanied biota, therefore, experiences high wave energy events, with increased frequency in winter (Veitch et al., 2019). The large peninsula acts as an obstruction for large south westerly swells, providing decreased wave energy along the west side of False Bay (Shipley, 1964). Conversely, the west coast of Cape Point is battered by these large swells. Multiple sites, therefore, exist where kelp grow in diverse temperature and wave energy climates, in close proximity and on the same side. The topography and elevation along the Cape Peninsula channel and shield winds along False Bay. This is, however, absent in winter, when strong northerly winds are prevalent from St. Helena Bay to Betty's Bay (Andrews and Hutchings 1980; Field et al., 1980; Jury, 1980; Jury et al., 1985).

2.2.2 Abiotic environment

In order to compare abiotic variables for sites around the coast, large historical databases for temperature, wave energy and wind were accessed.

2.2.2.1 Temperature

Shallow water temperatures were sourced from The South African Coastal Temperature Network (SACTN) website. In terms of nearshore temperature, *in situ* data are preferred over satellite sea surface temperature (SST), which have shown to exhibit large biases (Smit et al., 2013). The underwater temperature recorders (UTRs) are attached to concrete mooring blocks or railway line sections deployed in the shallow at ~3 m depth. The UTRs were comprised of *Starmon Mini* recorders (*Star-Oddi,* Reykjavik, Iceland/*Onset Hobo*® U22-001)) accurate to ±0.2°C. All *in situ* temperature data were reduced to a time-coded, continuous series of monthly means over various timescales (Smit et al., 2013). It was decided that the annual timescale would be used for analysis. Linear interpolated SST were calculated for sites where *in situ* recorders were absent. These data were used to group sites into "Cool temperate" and "Warm temperate" categorizations to investigate the possible effect of thermal regime on kelp morphological characteristics.

2.2.3 Wave environment

Wave model variable data formed part of the South African Coastal Vulnerability Assessment, presented to the Department of Environmental Affairs (DEA) and produced by the Council for Scientific and Industrial Research (CSIR) (Rautenbach, 2015). The South African wave climate was modelled via 20 spectral numerical wave models that simulated the offshore wave climate to the nearshore. The boundary conditions of these models were obtained by using the NOAA Wave

Watch III (WWIII) model output, distributed via the National Centers for Environmental Prediction (NCEP) product (Office of the Director 2000; Environmental Modelling Center/Marine Modeling Branch 2005). The particular hindcast product utilized during the DEA-CSIR study spans 1994–2013 at a 3-hour resolution. These data were then used to model swell propagation into the coastal models while wind waves (seas) were generated via stationary computations in the Simulating Waves in the Nearshore SWAN model (Booij et al., 1997). The assumption of stationary computations is acceptable as the model domains were small enough, so the temporal variation of the model boundary was slower than the time it takes for that boundary condition to propagate to the coast. SWAN allows one to extract wave variables from specific gridded locations in the nearshore. For False Bay, a resolution of 200 meters was modelled and output produced at both the 7 m and 15 m isobaths. A 200 m resolution was used as the False Bay computational grid was nested within a larger 1 km resolution grid. This allowed for a computational effective wave resolution of increasing resolution, from the NCEP, low resolution output to nested, high resolution coastal output.

For Table Bay and east of Cape Hangklip the resolution was 500 m and also had output at the 7 and 15 m isobaths. These contour outputs were chosen in the original study by the CSIR as most engineering run-up calculations require wave parameter information at these contour depths and were the main focus of the original study. For this study the 7 m contours were used. These data were then used to calculate over all wave power (kW/m) as this was considered the best measure of overall wave exposure. Annual wave power was plotted and categorized into different wave exposure categories which ranged from fully sheltered too extremely exposed.

2.2.4 Collection of kelp morphological characteristics

The morphological characteristics of both species are presented in Figure 2:2. *Laminaria pallida* is characterized by a single smooth blade which is divided longitudinally into sections and develops from a single meristematic region located at the junction between the blade and the stipe (Dyer, 2018). This species has a solid stipe along the south-west coast but develops a hollow stipe along the west coast northward and into Namibia (Rothman et al., 2017a). *Ecklonia maxima* consists of a single primary blade which develops above a gas-filled float and a hollow stipe below. Secondary blades are produced laterally from the primary blade from several meristematic regions along the margins of the primary blade (Dyer, 2018). Both species are held to the substrate by finger-like haptera, collectively known as the holdfast.

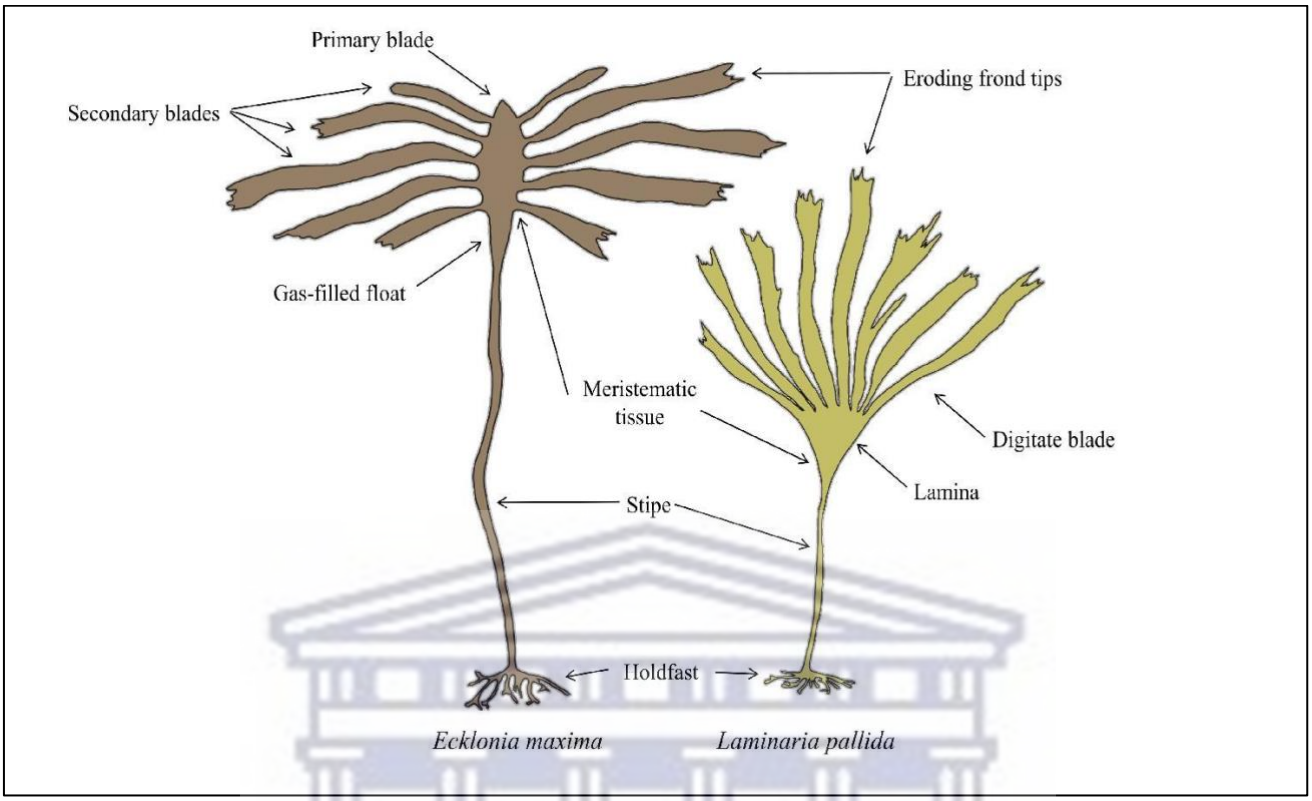

Figure 2:2 Schematic of Laminaria pallida and Ecklonia maxima morphology (Dyer, 2018).

Morphological measurements of *L. pallida* and *E. maxima* were collected at 18 sites along the Western Cape coast of South Africa between October 2014 and April 2015. AlgaeBase was used to confirm the latest taxonomic associations for each species (Guiry, 2013). Divers sampled kelp individuals by means of SCUBA for deeper populations and freediving for shallower populations. The sampled individuals were then taken ashore and the relevant morphological measurements taken. In each instance only the 13 largest individuals were sampled to ensure that only mature and fully grown sporophytes were measured. The age of *E. maxima* was determined by size, presence at the surface as well as a darker coloration of the stipe; as this occurs with age. In the case of *L. pallida*, the individuals with the longest stipe were selected which is considered a reasonable estimate of age. In each case the age of the individuals was estimated visually before the individual was sampled. In instances where one of the species was not present at a site, the

Table 2:1 A list of measured environmental variables (temperature, waves and wind) and their associated abbreviations.

Species	Morphological Characteristic	Unit Measurement
Ecklonia maxima	Frond mass	Kilograms (kg)
Ecklonia maxima	Primary length	Centimetres (cm)
Ecklonia maxima	Primary width	Centimetres (cm)
Ecklonia maxima	Frond length	Centimetres (cm)

Species	Morphological Characteristic	Unit Measurement
Ecklonia maxima	Stipe mass	Kilograms (kg)
Ecklonia maxima	Stipe length	Centimetres (cm)
Ecklonia maxima	Stipe circumference	Millimetres (mm)
Ecklonia maxima	Number of tufts	Count
Ecklonia maxima	Epiphyte length	Centimetres (cm)
Ecklonia maxima	Total length	Centimetres (cm)
Laminaria pallida	Lamina weight	Kilograms (kg)
Laminaria pallida	Lamina length	Centimetres (cm)
Laminaria pallida	Lamina thickness	Millimetres (mm)
Laminaria pallida	Stipe mass	Kilograms (kg)
Laminaria pallida	Stipe length	Centimetres (cm)
Laminaria pallida	Stipe diameter	Millimetres (mm)
Laminaria pallida	Number of digits	Count
Laminaria pallida	Thallus mass	Grams (g)
Laminaria pallida	Total length	Centimetres (cm)

nearest population of the missing species was sampled. Because the macroalgae differ in morphological features, species-specific morphological characteristics were included and are presented in Table 2:1 Table 2:1 A list of measured environmental variables (temperature, waves and wind) and their associated abbreviations.

The stipe length for *E. maxima* was considered to be the portion of the plant just below the pneumatocyst and just above the holdfast. Stipe circumference was measured just above the holdfast for both species. Between February 2017 and November 2018, morphological measurements for *E. maxima* individuals in shallow water (<1m) at seven sites along the Western Cape coast of South Africa were also collected. The same morphological characteristic measurements were taken as for the deeper *E. maxima*, and this allowed comparison between morphological characteristics between deep and shallow individuals within sites. Measurements were not collected for *L. pallida* in the shallow depths, as this species is largely absent from the shallow in this portion of the South African coastline.

2.2.5 Statistical analyses

Summary statistics were calculated for each site and region for each of the environmental variables considered in this study and are presented in Table 2:2. The associated abbreviations used are also presented in Table 2:2. In addition, annual median wave and wind direction were also calculated.

Table 2:2 A list of measured environmental variables (temperature, waves and wind) and their associated abbreviations.

Variable	Abbreviation
Maximum temperature	max_temp
Minimum temperature	min_temp
Mean temperature	mean_temp
Range in temperature	temp_range
Standard deviation in temperature	sd_temp
Mean significant wave height	hs_mean
Maximum significant wave height	hs_max
Minimum significant wave height	hs_min
Standard deviation in swell height	hs_sd
Mean wave period	tp_mean
Maximum wave period	tp_max
Minimum wave period	tp_min
Standard deviation in wave period	tp_sd
Median wave direction	dir_median
Mean wind speed	spw_mean
Standard deviation in wind speed	spw_sd
Median wind direction	dirw_median

The median was calculated for wind and wave direction, as issues arise when calculating the mean and standard deviation for compass metrics. Summary statistics for wind was not plotted and instead are discussed, as the data were course relative to the other environmental variables considered in this study. Morphological characteristics in relation to temperature and wave exposure were investigated using non-parametric statistical methods. Morphological characteristics were placed into categories according to temperature regime and wave exposure class for each species and population of kelp in this study. The appropriate category was determined by kelp's sampling location along the coastline and the according wave exposure and temperature category assigned to that species and/or population. The R software package *ggplot2* was used for graphical output and non-parametric analyses. Significant differences between temperature regimes and across wave exposure categories were tested with Wilcox tests and Kruskal-Wallis tests, respectively, and notched boxplots allowed comparison between individual categories of wave exposure. The alpha level used to define significance was $p = 0.05$. Boxplots were created using the software package *ggplot2* (Oksanen et al., 2013). In order to investigate specific drivers of morphological characteristics a distance-based redundancy analysis (db-RDA) was performed using the *rda*

function in the *vegan* software package (Oksanen et al., 2013) in R (RStudio Team 2019). The abiotic data covered all study sites for both species of kelp.

Both morphology and abiotic data (temperature, waves and wind) were standardized using the *decostand* function in the *vegan* software package; morphology data were used as response variables and the abiotic data as explanatory variables. A list of the abbreviations used and the associated metrics are presented in Table 2:2. To determine the explanatory variables that best describe patterns in the response data, a full RDA was performed using a complete set of explanatory variables. Forward selection was then used to reduce the number of explanatory variables, as well as prevent the inflation of overall Type I error. To further improve the model, pairwise coefficients and Variance Inflation Factor (VIF) were calculated to identify variables with high multicollinearity. The computation of the parsimonious RDA was followed by permutation tests of the adjusted R^2 to assess significance of constraints.

2.3 Results

2.3.1 Abiotic environment

2.3.1.1 Temperature

The mean annual coastal water temperature for the study sites located on the western side of the peninsula ranged from 14.5 ± 0.9°C (mean ± SD) at St. Helena Bay, the most northern site on the western side of the peninsula, to 14.6 ± 0.3°C at Olifantsbos, the most southern site on the western side of the peninsula (Figure 2:3A). For sites located on the

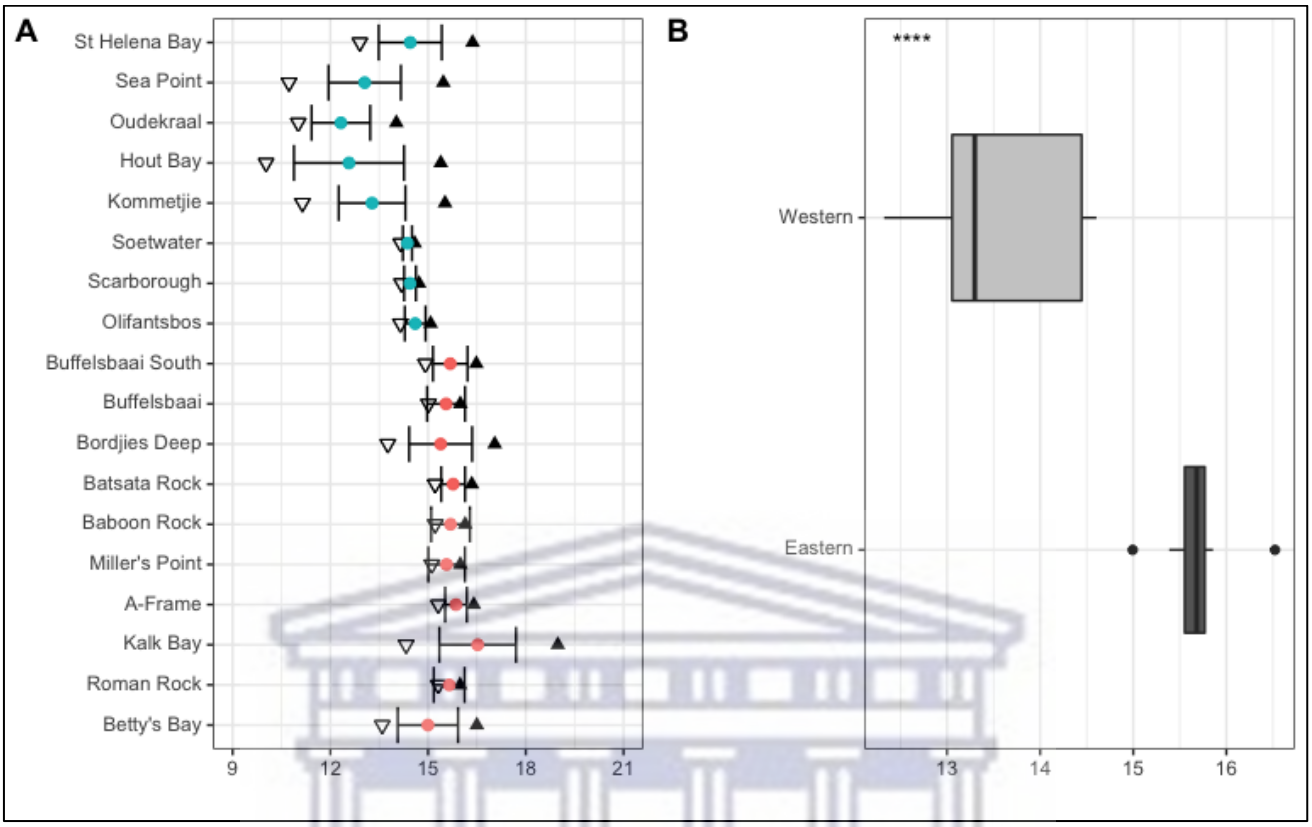

*Figure 2:3 Annual temperature variables at the collection sites around the Cape Peninsula are represented in panel (A), with sites in order from north to south. Temperature variables include minimum represented by inverted triangles, mean represented by blue and red dots which represent the western and eastern side of the peninsula, respectively, maximum by black triangles, and whiskers standard deviation. Summary of temperature data for sites grouped by region are represented in panel (B). Significance levels are as follows: * represents ≤0.05, ** represents ≤0.01, *** represents ≤0.001, **** represents ≤0.0001.*

eastern side of the peninsula (within False Bay), the annual mean coastal water temperatures ranged from 15.5 ± 0.9°C at Buffelsbaai to 15.0 ± 0.9°C at Betty's Bay, the most eastern site on the coastline in this study (Figure 2:3A). In general, the mean temperature increases for sites located within False Bay with less variation around the mean temperature compared to sites on the western side of the peninsula (Figure 2:3A). This is verified by statistical difference based on region, which shows a significantly lower ($p < 0.05$, Figure 2:3B) mean temperature and less variation in temperature for sites located on the western side of the peninsula compared to sites on the eastern side.

2.3.1.2 Wave environment

Our data show the western side of the peninsula experiences higher significant wave heights and variation in wave heights compared to the eastern side of the peninsula (Figure 2:4A). Mean significant wave height ranged from 0.5 ± 0.2 m (mean ± SD) at St. Helena Bay to 2.3 ± 0.7 m at Olifantsbos on the western side of the peninsula, and on the eastern side of the peninsula it ranged from 0.9 ± 0.4 m at Buffelsbaai to 1.9 ± 0.6 m at Betty's Bay (Figure 2:4A). The maximum significant

wave height ranged from 1.4 m at St. Helena Bay to 4.7 m at Olifantsbos on the western side of the peninsula, and on the eastern side ranged from 2.6 m at Buffelsbaai to 4.2 m at Betty's Bay. Mean peak period for sites on the western side of the peninsula ranged from 10.3 ± 3.5 s at St. Helena Bay to 11.0 ± 2.0 s at Olifantsbos and ranged from 10.6 ± 3.0 s at Buffelsbaai to 10.8 ± 2.2 s at Betty's Bay (Figure 2:4B). The data show no trend in mean peak period for the coastline. These data show that the western side of the peninsula has a lower variation (SD) compared to the eastern side, with Miller's Point showing the highest variation across timescales. Maximum peak period ranged from 18.9 s at St. Helena Bay to 18.4 s at Olifantsbos for the western side of the peninsula and ranged from 18.0 s at Buffelsbaai to 18.0 s at Betty's Bay on the eastern side of the peninsula. When wave variables were grouped by region significant differences were found for both mean significant swell height and mean peak period. The western region experiences a significantly higher mean significant swell height ($p < 0.05$; Figure 2:4C) and mean peak period ($p < 0.05$; Figure 2:4D).

Data for median wave direction showed no trend across timescales, however, the variation (SD) in wave direction is lower on the western side of the peninsula compared to the eastern side both annually and for winter. Summer data were the exception and showed lower variation for the eastern side of the peninsula (see Appendix).

In Figure 2:5A the total coastal wave exposure of the Cape Peninsula is given in terms of wave energy (kW per meter wave crest length). The classification from fully sheltered to extremely exposed is based on the total wave energy upper and lower limits (Figure 2:5B). The western periphery of the Cape Peninsula is almost continuously exposed to high wave exposures while the eastern periphery of the peninsula (western coastline of False Bay) revealed sheltered wave exposures (Figure 2:5). There the marked seasonality, with higher energy waves during winter, may be clearly observed once more. To clarify the averaged wave exposure map presented in Figure 2:5A, the propagation of a typical offshore wave spectrum as produced from a single time-step in SWAN is presented in Figure 2:5C. Tracing the wave height contours into False Bay its clear why this bay's western periphery is predominantly sheltered.

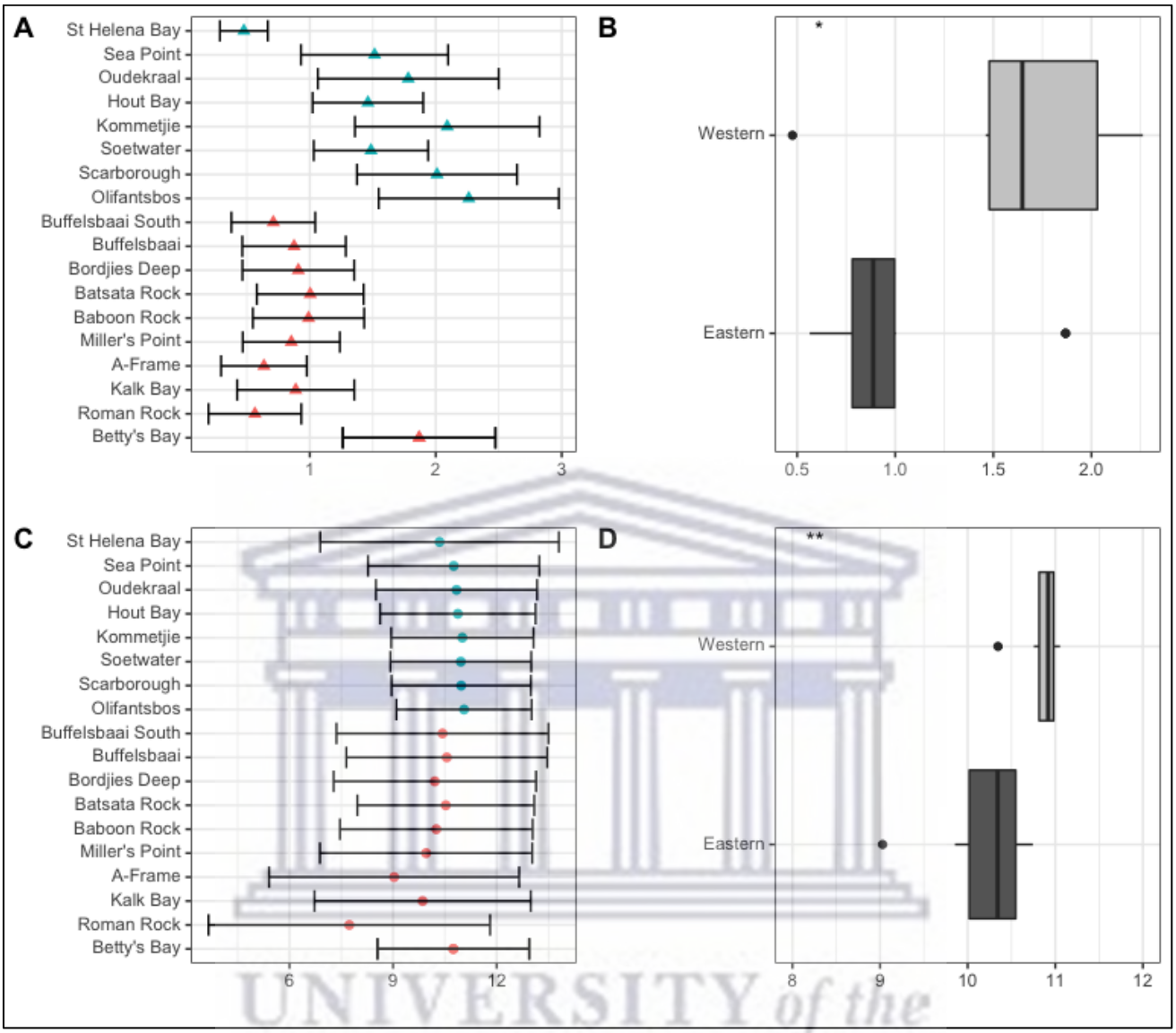

*Figure 2:4 Mean significant wave height (meters) and mean significant peak period (seconds) across sites and by region. Annual mean significant wave height across sites is presented in panel (A) and is represented by solid triangles and standard deviation by the whiskers. Differences in annual mean significant wave height between regions are presented in panel (B). Annual mean significant peak period across sites is presented in panel (C) and is represented by solid dots and standard deviation by whiskers. Differences in annual mean significant peak period between regions are presented in panel (D). Significance levels are as follows: * represents ≤0.05, ** represents ≤0.01, *** represents ≤0.001, **** represents ≤0.0001.*

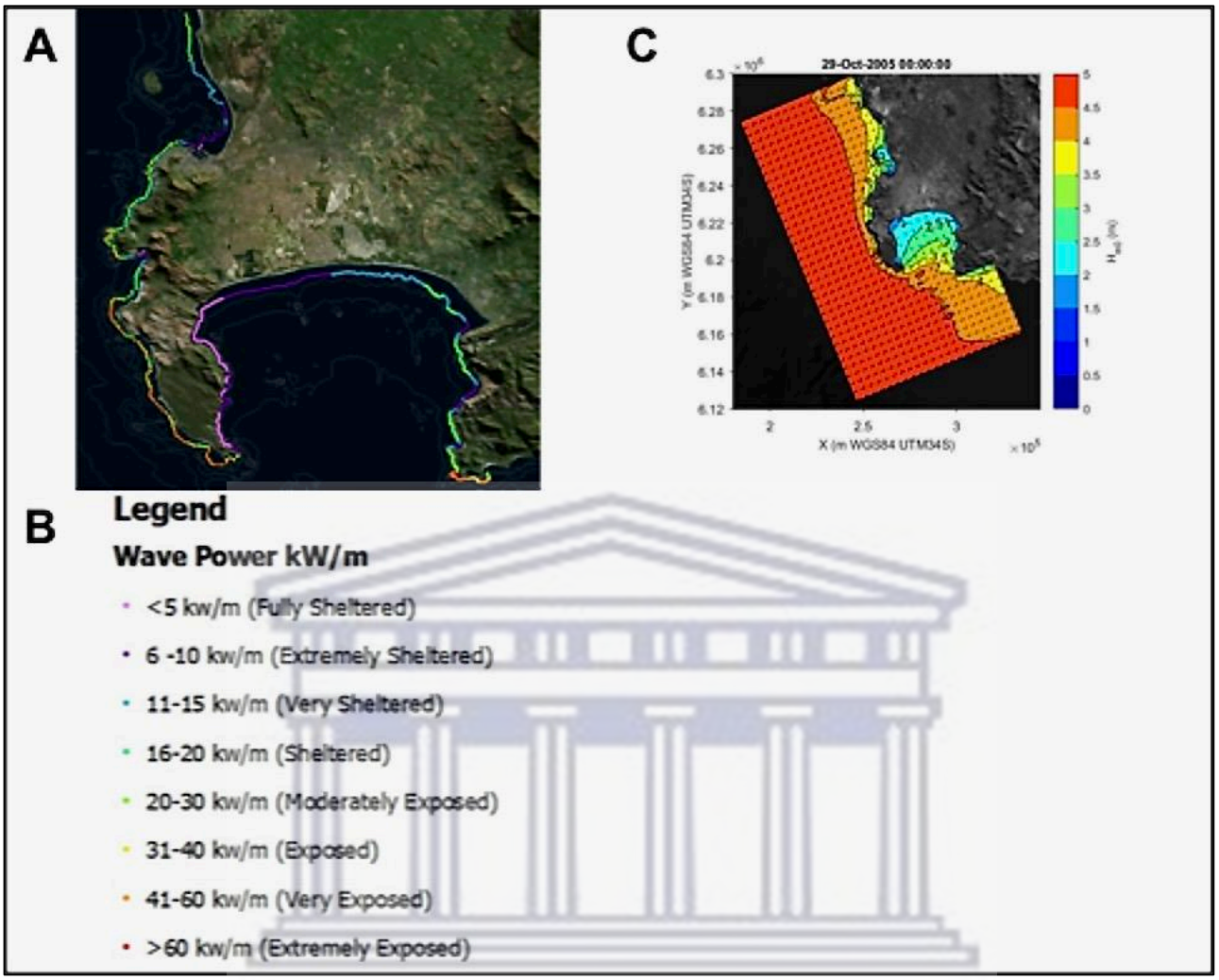

Figure 2:5 The total coastal wave exposure of the Cape Peninsula is given in terms of wave energy (kW per meter wave crest length) is presented in panel (A) and the associated legend in panel (B). The propagation of a typical offshore wave spectrum is given as produced from a single time-step in SWAN, is represented in panel (C).

2.3.1.3 Drivers of kelp morphological characteristics

Significant differences were found between cool temperate and warm temperate regimes for most *L. pallida* morphological characteristics with lamina length, number of digits and thallus mass the exceptions (Figure 2.6). Certain morphological characteristics such as stipe mass, stipe length, total length and stipe diameter had significantly higher means for kelp from the cool temperate regime when compared to kelp from the warm temperate regime ($p < 0.05$; Figure 2:6). Conversely, lamina weight and lamina thickness had significantly lower means for kelp from the cool temperate regime compared to kelp from the warm temperate regime. When *L. pallida* morphological characteristics were grouped to wave exposure categories Kruskal-Wallis tests revealed significant differences amongst categories for most morphological characteristics with lamina length, number of digits and thallus mass the exceptions (Figure 2:7). The morphological characteristics that were significantly different amongst sites exhibited similar patterns, with increasing mean values from the fully

sheltered to extremely sheltered categories and a decrease in mean values for the remainder of the categories. Two morphological characteristics, namely lamina thickness and stipe diameter, both exhibited higher variations for the exposed categories compared to other morphological characteristics.

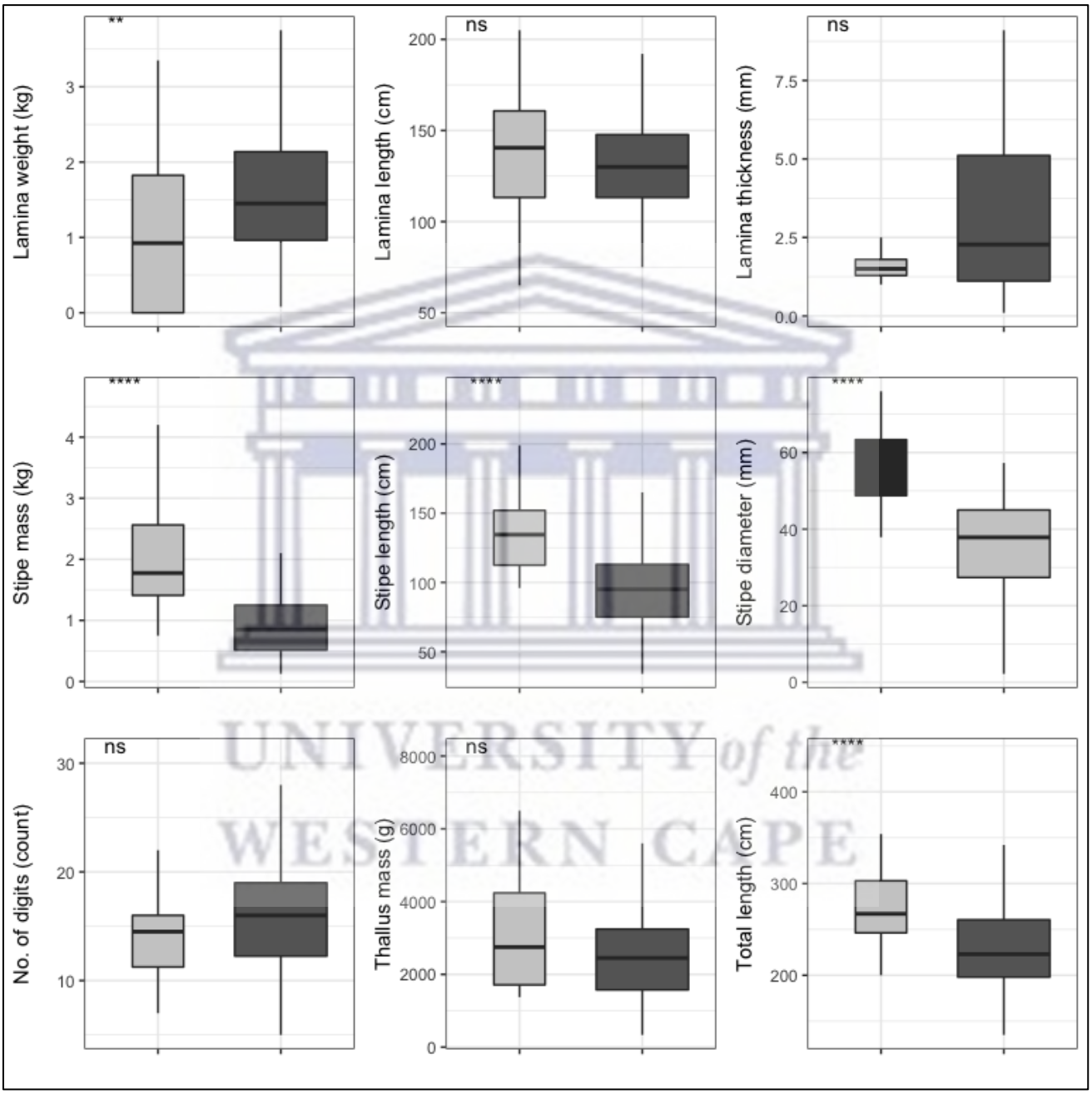

*Figure 2:6 Boxplots representing L. pallida morphological characteristics grouped by temperature regime measured around the Western Cape coastline, with the y-axis depicting the specific morphology measured, with units provided. The lower and upper "hinges" correspond to the first and third quartiles. The whiskers represent the range, solid black lines represent the median and black dots are outliers. Light grey boxes represent cool-temperate and dark grey warm-temperate. Significance levels are as follows: * represents ≤0.05, ** represents ≤0.01, *** represents ≤0.001, **** represents ≤0.0001.*

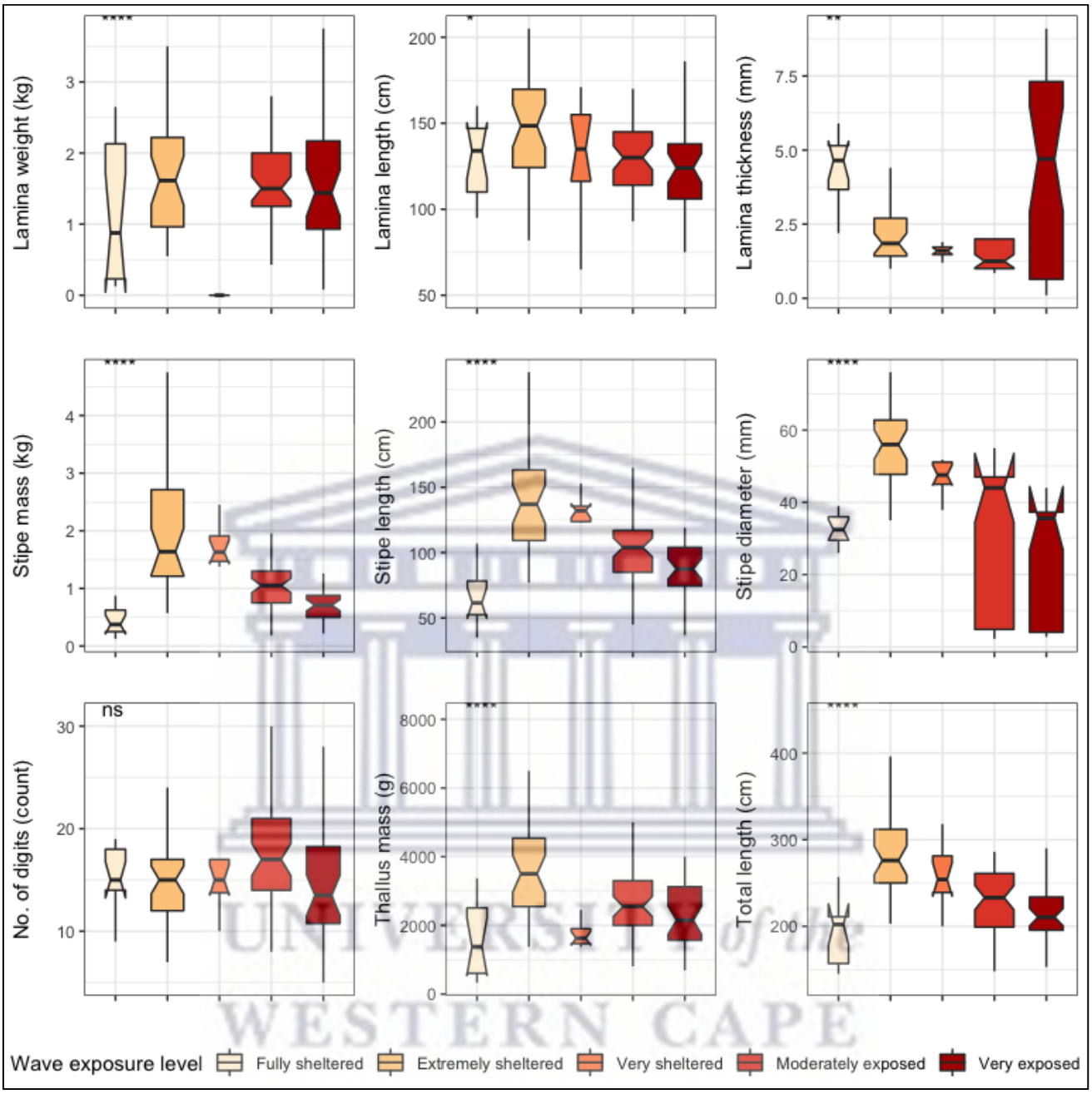

*Figure 2:7 Boxplots representing L. pallida morphological characteristics grouped by wave exposure category measured around the Western Cape coastline, with the y-axis depicting the specific morphology measured, with units provided. The lower and upper hinges correspond to the first and third quartiles. The whiskers represent the range, solid black lines represent the median and black dots are outliers. Significance levels are as follows: * represents ≤0.05, ** represents ≤0.01, *** represents ≤0.001, **** represents ≤0.0001.*

Six out of the ten deep *E. maxima* morphological characteristics showed differences between cool temperate and warm temperate regime except for frond mass, frond length, stipe mass and epiphyte length. Mean values for primary length, primary width and stipe circumference were significantly higher for kelp from the cool temperate regime than for kelp from the warm temperate regime (Figure 2:8). The remaining morphological characteristics, stipe length, number of tufts and total length had significantly lower means for kelp from cool temperate compared to kelp from the

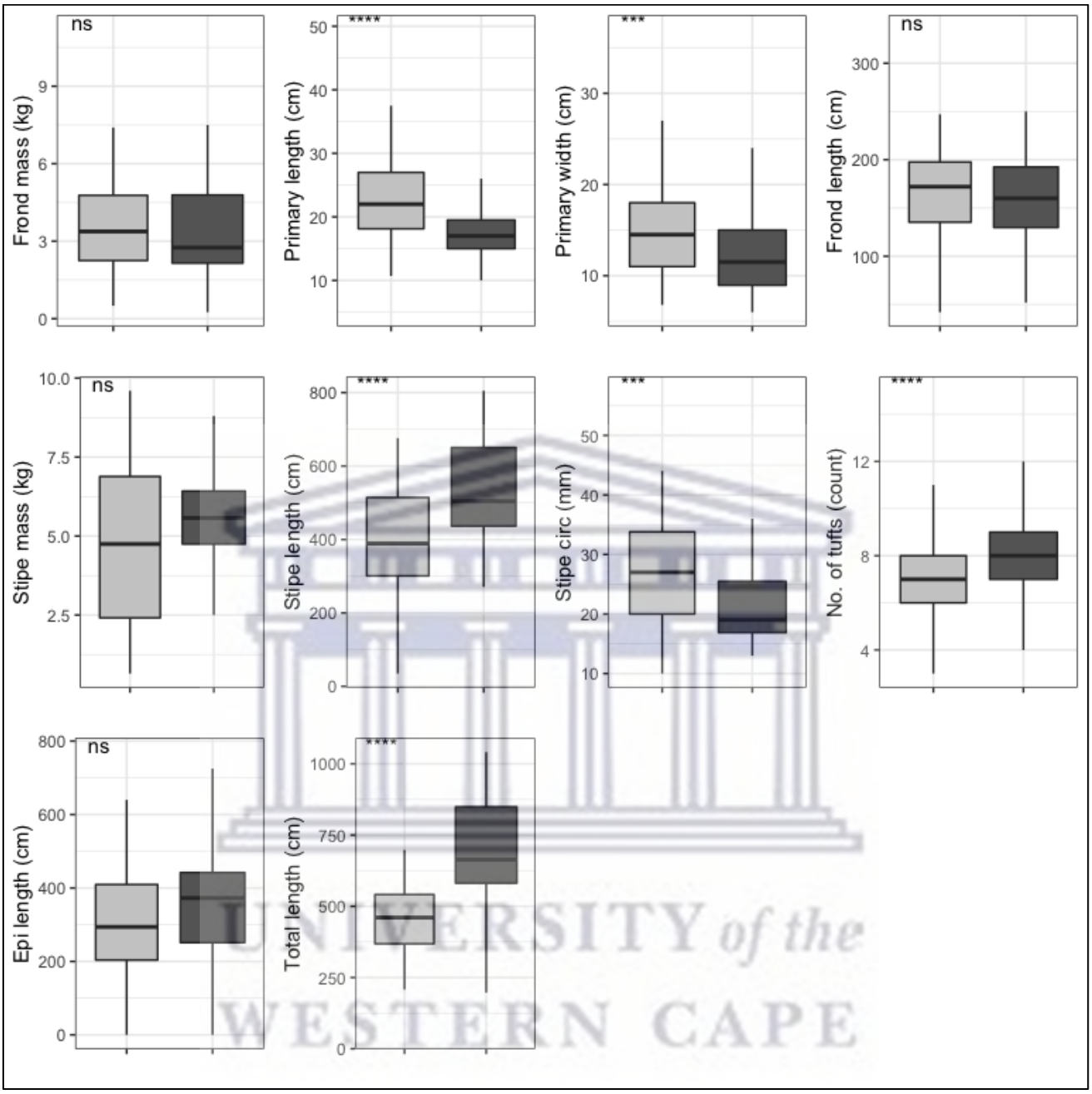

*Figure 2:8 Boxplots representing deep population E. maxima morphological characteristics grouped by temperature regime measured around the Western Cape coastline, with the y-axis depicting the specific morphology measured, with units provided. The lower and upper hinges correspond to the first and third quartiles. The whiskers represent the range, solid black lines represent the median and black dots are outliers. Light grey boxes represent cool-temperate and dark Gray warm-temperate. Significance levels are as follows: * represents ≤0.05, ** represents ≤0.01, *** represents ≤0.001, **** represents ≤0.0001.*

warm temperate regime ($p < 0.05$; Figure 2:8). Significant differences amongst wave exposure categories were found for all morphological characteristics of deep *E. maxima* populations (Figure 2:9). Certain morphological characteristics showed a gradual increase in mean value with increasing degree of wave exposure. The remaining morphological characteristics exhibited decreased means

for only the higher wave exposure categories, followed by a sharp increase in mean value for the highest wave exposure category.

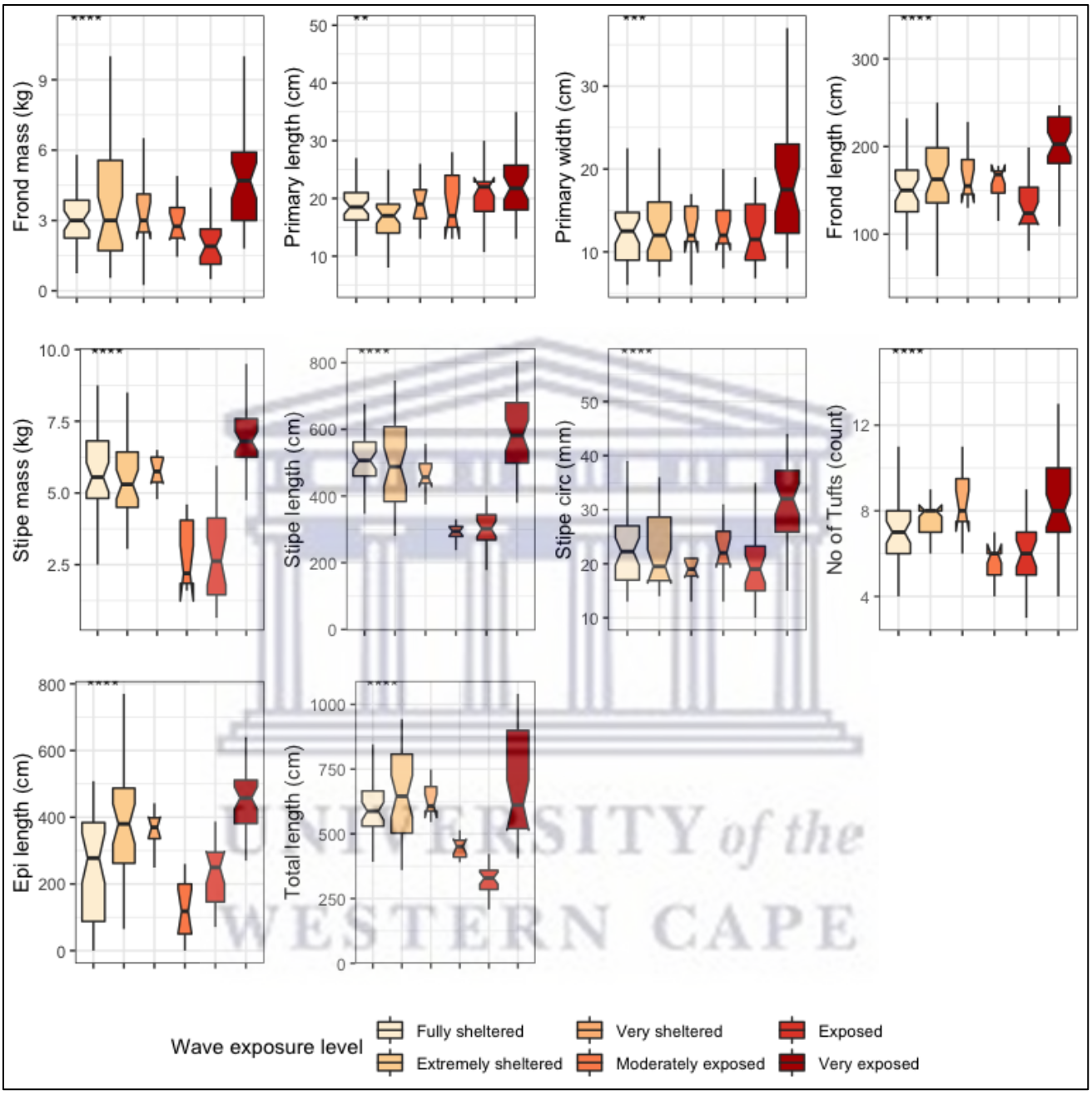

*Figure 2:9 Boxplots representing deep E. maxima morphological characteristics grouped by wave exposure category measured around the Western Cape coastline, with the y-axis depicting the specific morphology measured, with units provided. The lower and upper hinges correspond to the first and third quartiles. The whiskers represent the range, solid black lines represent the median and black dots are outliers. Significance levels are as follows: * represents ≤0.05, ** represents ≤0.01, *** represents ≤0.001, **** represents ≤0.0001.*

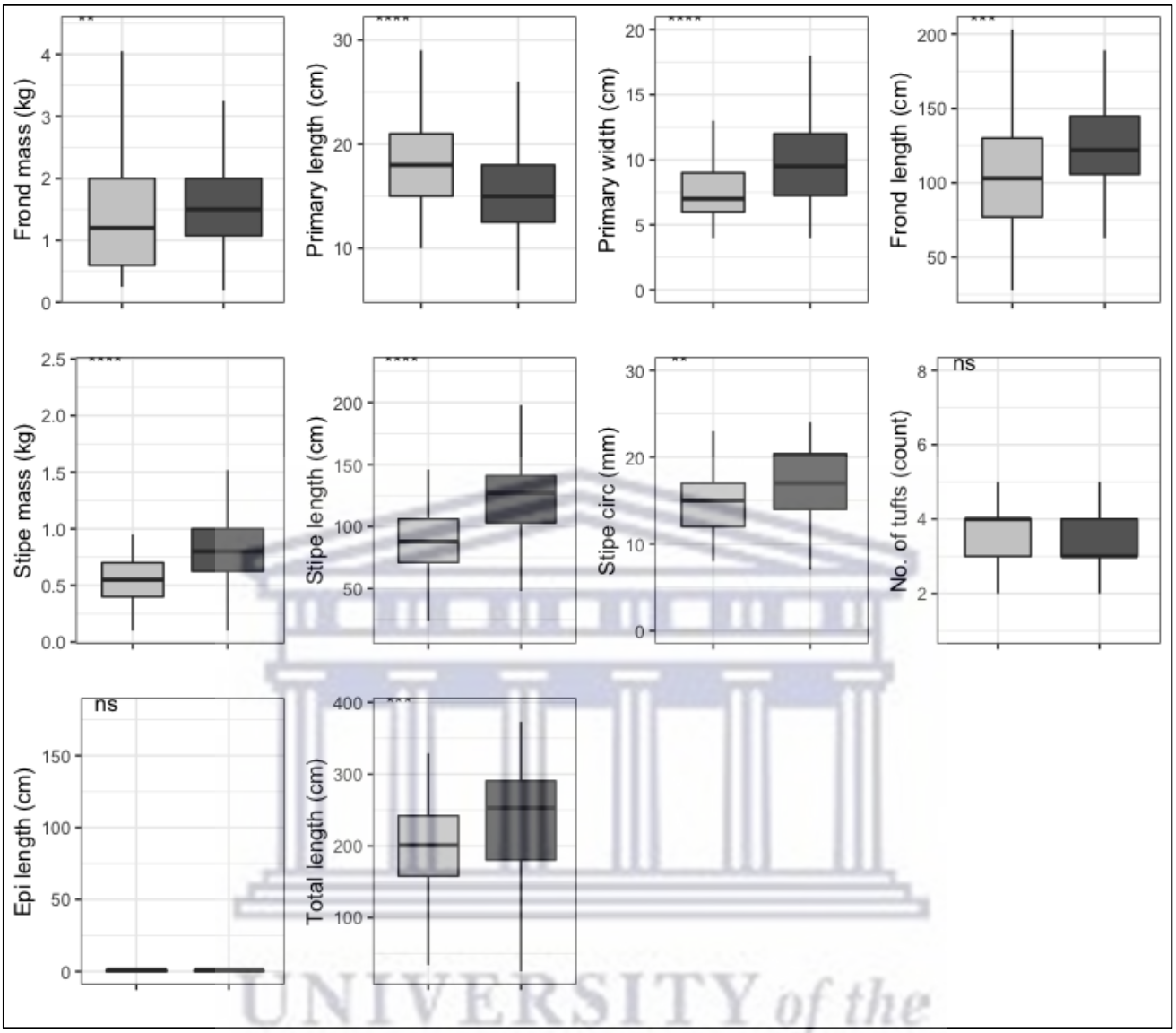

*Figure 2:10 Boxplots representing shallow E. maxima morphological characteristics grouped by temperature regime measured around the Western Cape coastline, with the y-axis depicting the specific morphology measured, with units provided. The lower and upper hinges correspond to the first and third quartiles. The whiskers represent the range, solid black lines represent the median and black dots are outliers. Light grey boxes represent cool-temperate and dark Gray warm-temperate. Significance levels are as follows: * represents ≤0.05, ** represents ≤0.01, *** represents ≤0.001, **** represents ≤0.0001.*

When grouped by temperature regime, shallow *E. maxima* exhibited significant differences between temperature regimes for frond mass, primary length, primary width, frond length, stipe mass, stipe length, stipe circumference and total length ($p < 0.05$; Figure 2:10). All of the significantly different morphological characteristics, except primary length, had lower values for the western region compared to the eastern region. When shallow *E. maxima* were grouped by wave exposure category significant difference were found for all morphological characteristics ($p < 0.05$; Figure 2:11). In general, values of the various morphological characteristics increase for the lower wave exposure categories, followed by a sharp decrease and a gradual increase in value.

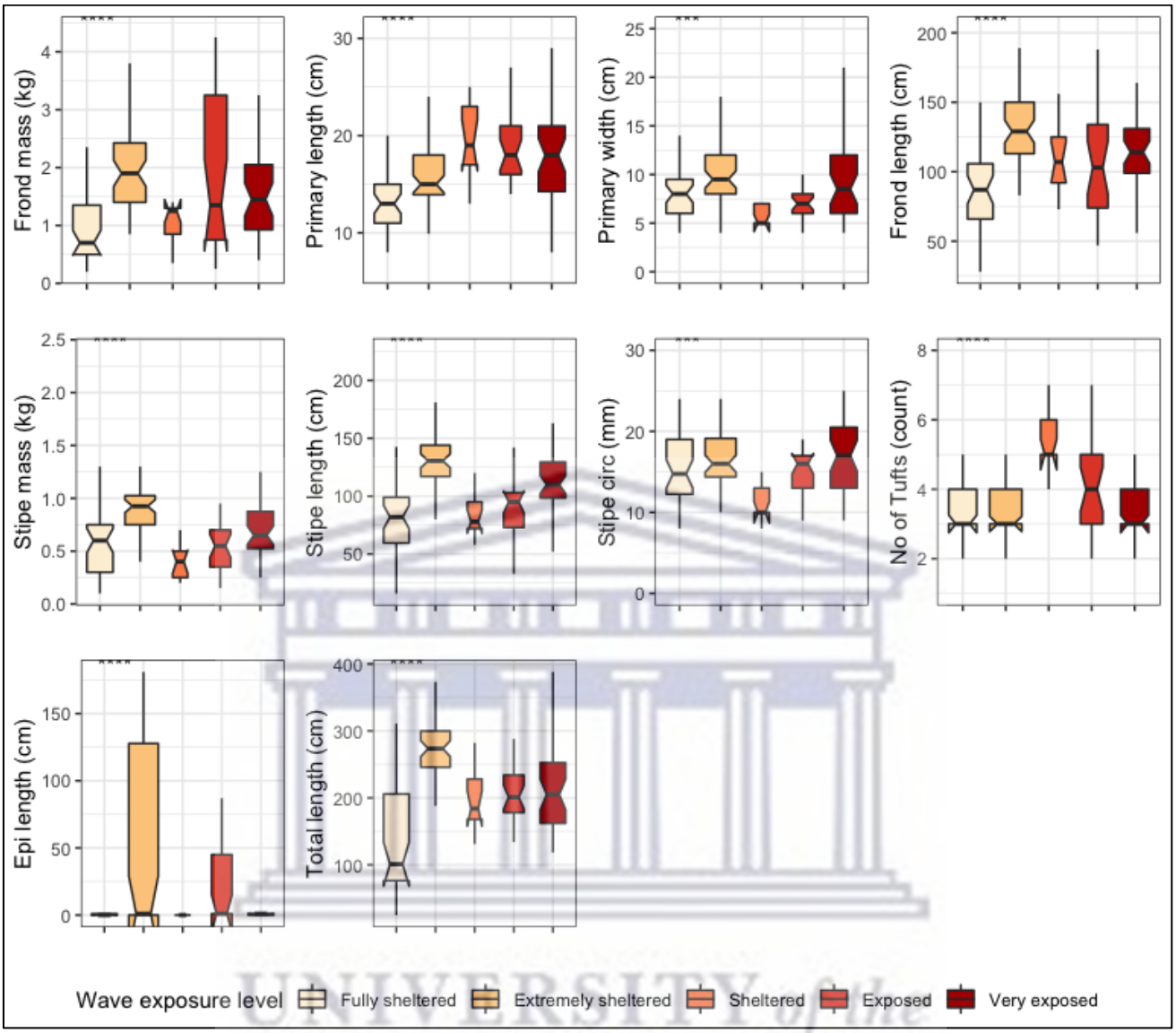

*Figure 2:11 Boxplots representing shallow E. maxima morphological characteristics grouped by wave exposure category measured around the Western Cape coastline, with the y-axis depicting the specific morphology measured, with units provided. The lower and upper hinges correspond to the first and third quartiles. The whiskers represent the range, solid black lines represent the median and black dots are outliers. Significance levels are as follows: * represents ≤0.05, ** represents ≤0.01, *** represents ≤0.001, **** represents ≤0.0001.*

2.3.2 Abiotic drivers of *L. pallida* morphological characteristics

Forward selection, assessment of VIF and an examination of pairwise Pearson correlation coefficients allowed us to retain the most parsimonious descriptors of *L. pallida* morphological characteristics with an adjusted R^2 of 0.49, explaining 72% of the variation (global permutation test on final model: d.f = 1, F = 8.51, p = 0.008; Figure 2:12A). RDA1 was the only significant axis in the model and explained 48% of the variation while RDA2 was not significant and explained 63% of the variation. Total length, stipe length, stipe diameter and stipe mass were positively influenced (i.e., increased size corresponding with the environmental driver) by mean significant wave height and median swell direction for kelp mostly from the western region and negatively influenced (i.e.,

decreased size corresponding with the environmental driver) by peak period standard deviation and mean temperature for kelp from the eastern region. Although sites from the western region did not cluster as closely as eastern region study sites, grouping according to region was still evident.

2.3.3 Abiotic drivers of *E. maxima* morphological characteristics

The same approaches to identify the descriptors for *L. pallida* were employed for both populations of *E. maxima*. Forward selection, assessment of VIF and Pearson correlation coefficients allowed us to retain as the most parsimonious descriptors of deep *E. maxima* morphological characteristics with an adjusted R^2 of 0.39, explaining 67% of the variation (global permutation test on final model: d.f = 5, F = 2.4, p = 0.026; Figure 2:12B).

RDA1 was the only significant axis in the model (p = 0.03) and explained 72% of the variation. Primary length, primary width and stipe circumference were positively influenced by mean significant wave height, mean peak period and median swell direction for kelp from the western region. The remaining morphological characteristics were positively influenced by minimum temperature and negatively influenced by peak period standard deviation for kelp from the eastern region.

Forward selection, assessment of VIF and Pearson correlation coefficients allowed us to retain the most parsimonious descriptors of shallow *E. maxima* morphological characteristics with an adjusted R^2 of 0.36, explaining 61% of the variation (global permutation test on final model: d.f = 4, F = 2.41, p = 0.013, Figure 2:12C). The model consisted of one significant axis, RDA1 (p = 0.02) explained 62% of the variation.

Stipe length, stipe mass and stipe circumference were positively influenced by maximum temperature and mean temperature along RDA1, and explained 50 and 55% of the variation, respectively. The remaining morphological characteristics were positively influenced by maximum peak period and negatively influenced by median wind direction along RDA2 and explained 86 and 94% of the variation, respectively. There was overlapping of clusters according to region with no clear patterns in sites evident.

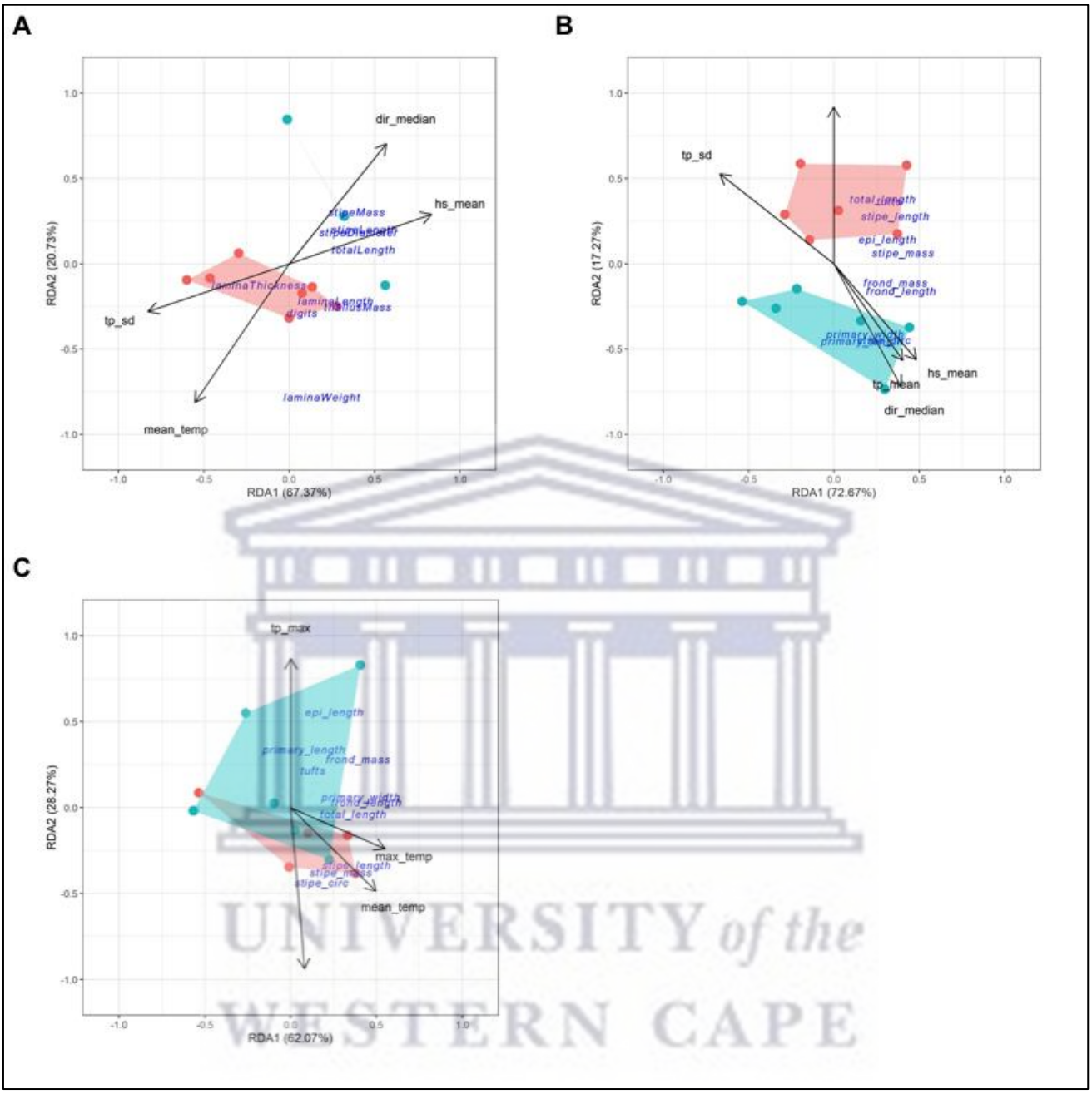

Figure 2:12 RDA output for L. pallida (A), deep E. maxima (B) and shallow E. maxima (C). The blue cluster represents sites from the western region and the red represents sites from the eastern region.

2.4 Discussion

This study considered important drivers of the morphology of *E. maxima* and *L. pallida* around the Cape Peninsula. These abiotic variables, namely temperature and wave exposure, have been identified in previous research on other brown algae species such as *E. radiata* and *Macrocystis pyrifera* (Linnaeus) C.Agardh 1820 (Thomsen et al., 2004; Fowler-Walker et al., 2005, 2006; Wernberg and Thomsen 2005; Wing et al., 2007; Stewart et al., 2009; Miller et al., 2011; Pedersen et al., 2012). The complex geomorphology of the Western Cape coastline creates an ideal natural

laboratory for studies of kelp in interaction with their environment. Unlike previous research, this study used a complex numerical model to provide the various variables of wave exposure, which is based on linear wave theory to calculate overall wave exposure. We also considered wind in addition to temperature and wave variables, since wind is an important component of wind-driven surface gravity waves (Holthuijsen, 2010). The results show that specific variables of wave exposure are the main drivers of kelp morphology with temperature playing only a minor role. The morphological adaptation was also shown to be associated with the magnitude of wave exposure which had only been inferred in previous studies. Finally, the investigation of differences in morphological characteristics between shallow and deep populations of *E. maxima* suggests that in low wave exposure environments the role of temperature as a morphological driver increases; this is particularly the case for False Bay.

There were clear patterns and clines in both the temperature and wave exposure data. The thermal and wave exposure regimes around the Cape Peninsula are driven by a complex interaction between wind, temperature and wave metrics, which do not act independently but instead influence one another. The hydrodynamic regime is modulated by the relative sheltering against the predominant south-westerly swell direction and the size of the fetch for local wave generation. The direction of the dominant swell changes to the southwest in winter, generated by strong low pressures that originate from the Southern Ocean (Reason et al., 2006), which False Bay is sheltered from (Shipley, 1964; Atkins, 1970; Dufois and Rouault et al. 2010). In summer, these swells rotate anticlockwise and are able to enter False Bay, providing an increased variability of swell height and peak period in this region. It should be noted that what is classified as sheltered around the South African coastline (a high energy coastline) might be classified as exposed in other regions of the world (Leliaert et al., 2000; Norderhaug et al., 2012). It is due to the near consistent south-westerly swell and the complex orography around the peninsula that the wave energy distribution around the Cape Peninsula varies significantly over a small geographical area.

The directional sheltering effect of the Cape Peninsula, against the dominant swell direction is clearly observed in the wave exposure maps. It should be mentioned that some of the annual winter frontal depression systems pass the Cape Peninsula from the west to east, resulting in wave propagating toward the continent from much more southerly directions. This results in positive and negative wave exposure anomalies all around the peninsula. Increased wind speed at sites along the west side of the peninsula in a southerly direction trigger upwelling events along the western side of the peninsula (Field et al., 1980; Rouault et al., 2010). In general, the western side of the peninsula is more exposed than the eastern side (False Bay) and experiences significantly higher mean significant swell height and mean significant peak period. This was also reflected in the wave exposure categories which show a trend of decreasing wave exposure (wave power) around the

peninsula and into False Bay. There are also differences between the types of waves that each side of the peninsula experiences. We provide strong support that variations in the environmental variables, particularly wave exposure variables, are driving kelp morphological characteristics around the Cape Peninsula. Morphological adaptation due to water motion may manifest in a number of ways in high wave energy environments. For instance, reduction of blade thickness, blade elongation, increase of stipe length, increase in stipe circumference and force of attachment (Friedland and Denny, 1995; Denny et al., 1997; Denny and Gaylord, 2002; Wernberg and Thomsen, 2005; Fowler-Walker et al., 2006; Bekkby et al., 2014) have been identified in previous studies. Although this study did not measure force of attachment, other morphological responses to temperature and wave variables were evident.

Species-specific responses are evident in both wave exposure and temperature. In cool temperate environments *L. pallida* tended to show increases in certain morphological characteristics (stipe mass, stipe length and stipe diameter) while in the warm-temperate environments these were significantly lower. This was also true for deep *E. maxima* populations, which had longer, thinner stipes for kelp from the warm temperate compared to kelp from the cool temperate. Reduction in certain morphological characteristics has been attributed to temperature by Serisawa et al. (2002) in the kelp *Ecklonia cava* Kjellman 1885, which was smaller and shorter in warmer sites compared to cooler sites. The reduction in size of adult may be a response to low nutrient conditions, which has been shown to reduce growth rate and overall morphology (Simonson et al., 2015).

Warmer temperatures are associated with low nutrient concentrations (Waldron and Probyn, 1992) and the low frequency of upwelling conditions in False Bay (low nutrient supply) coupled with warmer temperatures may be a contributing factor. It should be noted, however, that from these analyses that in general the cool temperate region is more exposed to waves than that of the warm-temperate region. Therefore, the significantly larger morphological characteristics for kelp from the cool temperate region may overlap with responses to wave exposure. The response of kelp morphological characteristics to wave exposure was evident and both species exhibit tactics based on the magnitude of wave exposure. Strength increasing traits were exhibited for lower exposure levels while a “go-with-the-flow” tactic for moderate levels of wave exposure. This suggests that how morphological characteristics manifest themselves is dependent on the magnitude of wave exposure. When grouped by wave exposure category, *L. pallida* characteristics showed a significant increase in length for the “extremely sheltered” category compared to the fully sheltered category, which may be a “go-with-the-flow” tactic (Denny et al., 1997; Hurd, 2000; Denny and Gaylord, 2002). Kelp are able to increase flexibility by increasing stipe length which increases the extension capabilities of kelp to a passing wave (Denny et al., 1997; Hurd, 2000; Denny and Gaylord, 2002). However, increasing stipe length is only beneficial under lower exposure levels as a long stipe

actually increases overall drag on the plant under high wave exposure (Denny et al., 1997; Hurd, 2000; Denny and Gaylord, 2002). This is reflected in the *L. pallida* morphology which shows an overall reduction of morphological characteristics suggesting a size reducing tactic to cope with higher levels of wave exposure. The results suggest that deep *E. maxima* populations exhibit a different response, as well as a higher wave exposure threshold. Unlike *L. pallida*, *E. maxima* exhibits a size reducing tactic with increasing wave exposure by decreasing stipe mass, stipe length, stipe circumference, total length and frond length. A magnitude related response has been suggested by Wernberg and Vanderklift (2010) who investigated the temporal and spatial variations of various environmental drivers of the kelp *E. radiata*. The authors identified wave exposure as the most important driver of kelp morphological characteristics and that the type of response elicited is dependent on the magnitude of wave exposure.

A size reduction tactic has been shown before (Hurd, 2000; Denny and Gaylord, 2002; Fowler-Walker et al., 2005, 2006) and is regarded as a strategy to reduce overall drag on the plant. However, *E. maxima* morphological characteristics changed significantly as wave exposure increases. When grouped to the higher wave exposure levels, *E. maxima* morphology exhibited a strength and flexibility increasing trait. Furthermore, the morphological response of *E. maxima* to wave exposure only occurs at the "Moderately exposed" level compared to *L. pallida* which exhibits a response at a lower wave exposure level. This suggests that *E. maxima* can tolerate higher exposure levels before having to exhibit a morphological response. The redundancy analysis performed confirms the patterns and responses observed as well as identifying specific temperature and wave variables as drivers of kelp morphology. Kelp morphology characteristics are largely wave driven for both species but differ in terms of specific temperature and wave metrics.

The wave metrics identified in this study are important components of determining overall wave power, which will vary seasonally in the region based on the swell direction. The differences in temperature metrics between *E. maxima* and *L. pallida* point to underlying differences in nutrient availability. Low temperatures are often associated with upwelling events which bring cool, nutrient rich water into the nearshore. False Bay has comparatively little upwelling events compared to the western side of the peninsula, and so nutrients may be a limiting factor for *E. maxima* populations within False Bay, hence the identification of minimum temperature as an influencer. Mean temperature identified as a driver for *L. pallida* may be related to diurnal temperature fluctuations in the water column. Solar heating of the water surface in combination with wind-driven transport causes fluctuations within the water column, which can occur daily or seasonally (Kaplan et al., 2003). Vertical mixing of the water column for inshore regions are driven by several abiotic processes: (1) turbulence of breaking waves inside or outside of the surf zone; (2) convective mixing through a combination of cooling and evaporation; (3) wind driven currents; and (4) tidal mixing

(Smit et al., 2013). These abiotic processes cause effective vertical mixing of surface and deeper water stratification which leads to a homogeneous thermal environment, which in this study may be interpreted as the mean temperature. Therefore, the homogeneous thermal regime of inshore regions may be a reason why mean temperature is driver of *L. pallida* morphological characteristics. The difference in canopy type between the species may be the reason why *E. maxima* is driven by multiple wave metrics compared to *L. pallida*. Since *E. maxima* are a canopy-kelp, it is exposed to all components of a wave compared to *L. pallida* which occurs deeper in the water column.

Although temperature plays an important role in distribution (Bolton, 2010; Miller et al., 2011; Rinde et al., 2014) of kelp and physiological functioning of adults and gametophytes (Gerard, 1997; Steneck et al., 2002; Bearham et al., 2013; Mohring et al., 2014; Smale and Moore, 2017), there is little evidence in this study that temperature is an important driver of morphological variation. However, we suggest that temperature plays a larger role in determining kelp morphology at sites where wave energy is low enough not to elicit a response in morphological characteristics. Temperature metrics influence stipe length and frond length in shallow *E. maxima* individuals located at sites within False Bay; which was not the case for deeper *E. maxima* individuals as well as *L. pallida* which were largely driven by wave variables. The shallow *E. maxima* individuals may not experience the same amount of wave energy as do deeper populations. This may be due to wave dampening from deeper populations of *E. maxima*, which attenuate the wave energy entering coastal environments (Jackson, 1984; Kobayashi et al., 1993; Mork, 1996).

The morphological variations in characteristics for deep *E. maxima* populations are not seen for shallow *E. maxima* populations. The lack of variation in shallow *E. maxima* populations was also found in previous research by (Rothman et al., 2017a) who identified light as a significant driver. This influence of light may suggest photosynthetic ability and nutrient uptake as important drivers in shallow environments. Wave exposure may be reduced in shallow environments due to the wave damping effect of deep kelp and seaweed populations (Jackson, 1984; Kobayashi et al., 1993; Mork, 1996) thereby reducing the need to adapt morphological characteristics to reduce drag. Furthermore, the reduction in differences between deep and shallow *E. maxima* at wave exposed sites on the western of the peninsula compared to sites in False Bay provides further evidence that wave exposure may not be an important driver of shallow *E. maxima* populations in this study. Increased temperatures corresponded with a reduction in stipe circumference, frond length, stipe length, total length and stipe mass resulting in slim or “skinny” kelp individuals, which supports findings from previous research by Mabin et al. (2013), Serisawa et al. (2002). These findings were confirmed by the redundancy analysis which showed the contribution of wave variables as a driver of kelp morphological characteristics was lower compared to temperature variables. The sites do cluster by region but almost overlap entirely; further indicating wave variables are not the main

driver. Although wave variables were not identified as an important driver, it is important to note the wave variables identified in the RDA differ to deep *E. maxima*. The identification of median wind direction suggests that surface gravity waves as a driver compared to swell waves identified for *L. pallida* and *E. maxima*.

Kelps living in warmer environments have been shown to have a lower resilience to disturbance, such as storms (Wernberg et al., 2010). The kelp in False Bay may therefore be more vulnerable to dislodgment under high wave exposure scenarios compared to kelp on the western side of the Cape Peninsula, which experiences higher wave energy on a regular basis. In South Africa, the main contributing factors to the hydrodynamic environment are the Southern Annular Node (SAM) and El Niño Southern Oscillation (ENSO), while the latter is also the main source of variability (Veitch et al., 2019). These climate systems are expected to alter storm frequency and magnitude under future climate scenarios, which may increase the overall wave power around the Cape Peninsula. The magnitude-specific response of the kelp species to wave exposure in this study suggests there is a limit to morphological adaptation in reducing the probability of dislodgement. Therefore, if this limit is reached and exceeded in future climate scenarios, kelp populations may risk being reduced over time. Furthermore, although recent studies suggest a cooling trend of coastal waters around South Africa (Rouault et al., 2010; Smit et al., 2013), the impact of marine heat waves may reduce the resilience of kelp to storms and high wave energy. Although this study identifies specific wave and temperature metrics that drive morphological adaptation and suggests a possible wave exposure threshold, it does not identify the metrics or magnitude of wave exposure required to dislodge kelp. Therefore, future studies should consider using advanced numerical methods to investigate the specific wave power needed to dislodge kelp, and ideally, given a specific set of morphological measures. These types of studies in conjunction with forecasting studies can be used to determine the vulnerability of kelp populations to future climate scenarios.

2.4.1 Conclusion

Past research shows that macroalgal morphological characteristics are largely driven by a wave exposure while others have suggested a complex interaction between various environmental variables. We confirm that wave variables are the main driver of kelp morphological characteristics in both *E. maxima* and *L. pallida* populations around the Cape Peninsula, and differences in morphological characteristics between shallow and deep populations of *E. maxima* may reflect differences in hydrodynamic and temperature regimes. This study also confirms the findings of previous research which shows morphological adaptation is dependent on the magnitude of wave exposure, but also provides quantitative, reproducible measure of wave exposure while identifying the specific wave metrics and wave energy thresholds involved. Furthermore, the current study highlights the need to understand how kelp populations, which are not exposed to high wave energy

and morphological characteristics are largely driven by temperature, are vulnerable to changes in storm frequency and magnitude. Kelp populations located in low wave energy environments, such as False Bay, may be more vulnerable to increased storm frequency and magnitude in future climate scenarios.

2.4.2 Supplementary Material

The Supplementary Material for this article can be found online at: https://www.frontiersin.org/articles/10.3389/fmars.2020.00567/full#supplementary-material

3 : Numerical experiment investigating the influence of drag on trajectory patterns of floating macroalgae

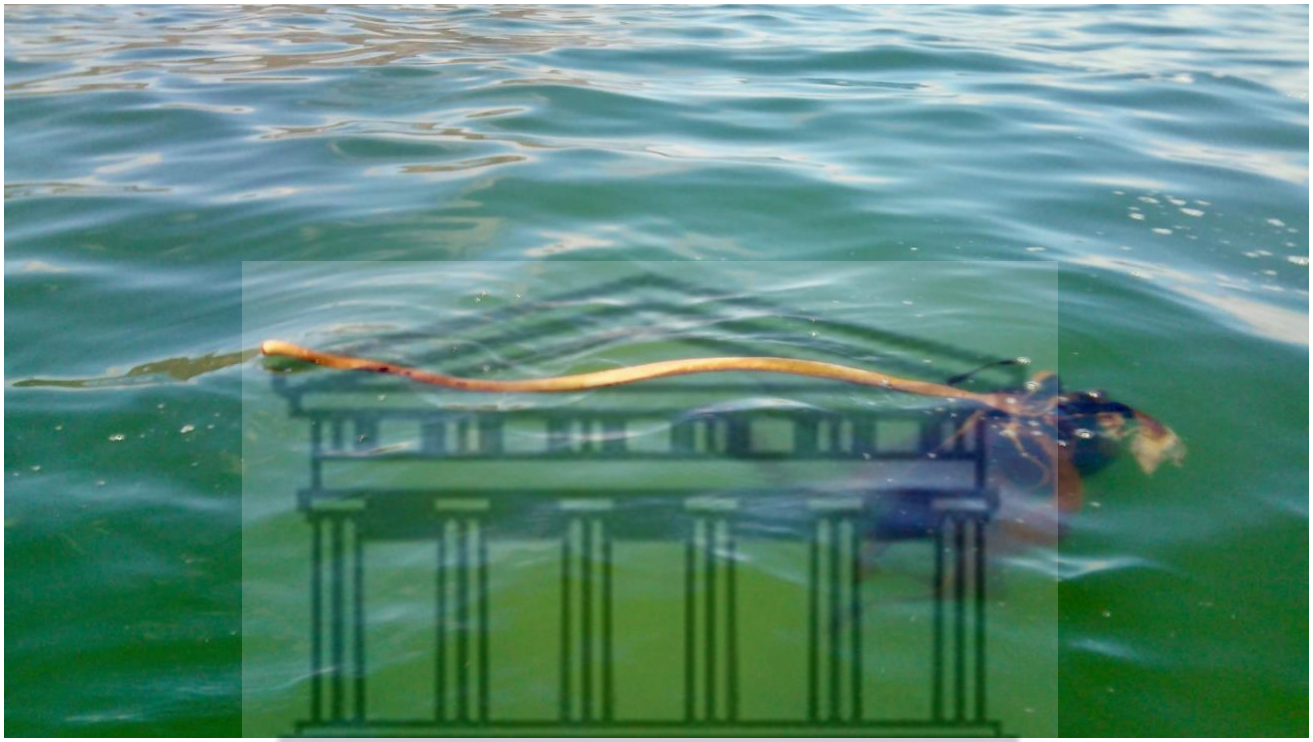

In this chapter, I aimed to use a numerical approach to shed light on the role of hydrodynamic and direct wind drag (windage) on floating *E. maxima* trajectory using Lagrangian-based trajectory simulations and site-specific kelp morphological characteristics characterised in chapter 2 (kelp morphology). Once established, would allow for further investigation into the spatial distribution patterns of floating *E. maxima* on the surface and seafloor in Chapter 4. The main findings from this chapter were:

- Solitary floating virtual *E. maxima* particles follow the prevailing surface currents.
- Inclusion of hydrodynamic drag caused the trajectories to differ greatly from that of a purely Lagrangian particle.
- Windage did not significantly alter trajectories of virtual kelp particles.
- Inclusion of both hydrodynamic and wind drag caused clustering of particles along the trajectory as well as caused particles to become entrained in eddies.
- Oceanographic processes in the study region, Benguela Jet and mesoscale processes, play a significant role in overall trajectory.
- Stokes drift did not alter trajectories.

3.1 Introduction

Passive dispersal vectors of marine taxa include a range of natural and anthropogenic objects that float in the ocean, and kelp are regarded as one of the most important of these (Edgar, 1987; Norton, 1992; Bushing, 1994; Holmquist, 1994; Helmuth et al., 1994; Smith, 2002; McCormick et al., 2008). Floating macroalgae are regarded as important transport mechanisms for marine invertebrates, which remain attached to the plant when dislodged from the substratum (Edgar, 1987; Norton, 1992; Bushing, 1994; Holmquist, 1994; Helmuth et al., 1994; Smith, 2002; McCormick et al., 2008). For example, a study by Holmquist (1994) investigated the long-distance dispersal of the bivalve *Gaimardia trapesina* Lamarck via drifting kelp. The authors used observational techniques to quantify kelp rafts along with haphazard sampling of the kelp rafts observed. Genetic samples were taken from the target species for each of the haphazardly sampled kelp rafts for comparison amongst populations. The results suggest that kelp rafting, along with the local wind patterns, most likely played a key role in the dispersal of *G. trapesina* between genetically similar but spatially disconnected populations.

Some macroalgal species are negatively buoyant and sink to the seafloor when detached from the substrate, while other species have air-filled pneumatocysts or stipes, which allow the plants to remain at the surface where light is more abundant and, in turn, cause plants to float to the surface when detached, potentially remaining alive for extended periods of time. The structure and number of pneumatocysts vary among species. For example, species belonging to the genera *Macrocystis*, *Sargassum*, *Ascophyllum*, and *Fucus* have thalli with many small pneumatocysts, while other species such as *Nereocystis luetkeana* (K.Mertens) Postels & Ruprecht, *Pelagophycus porra* (Léman) Setchell, *Ecklonia radiata* (C.Agardh) J.Agardh, and *Ecklonia maxima* (Osbeck) Papenfuss have single, large pneumatocysts (Dayton, 1985; Smith, 2002; Thiel and Gutow, 2005; Graiff et al., 2016; Batista et al., 2018). In some cases, the stipe itself may be air-filled, such as with *E. maxima* and *E. radiata*. Although there have been reports of floating species of Chlorophyta and Rhodophyta, Phaeophyceae species are the most reported forms of floating algae. This is most likely because the green and red species reported to float are not actually positively buoyant, but instead are kept at the surface by gas trapped in-between or in their thalli (Dromgoole, 1982; Bäck et al., 2000). The giant kelp *Macrocystis pyrifera* (Linnaeus) C.Agardh (Helmuth et al., 1994; Kingsford, 1995; Hobday, 2000b; Macaya et al., 2005; Graiff et al., 2016; Batista et al., 2018), the bull kelp *Durvillaea antarctica* (Chamisso) Hariot (Smith, 2002; Collins et al., 2010; Wichmann et al., 2012; Tala et al., 2013, 2017; Saunders, 2014; Batista et al., 2018), and pelagic *Sargassum* species (Brooks et al., 2018, 2019; Putman et al., 2018, 2020; Wang et al., 2019) have been the focus of much of the research regarding spatial and temporal dispersal patterns, the ecological role of rafting, marine connectivity, and raft-time.

Past research points to macroalgal trajectories being largely determined by a combination of prevailing wind conditions and surface currents (Hobday, 2000b; Thiel and Gutow, 2005; Rothäusler et al., 2011; Fraser et al., 2011). Although ocean currents are regarded as the primary influence, the relative importance of wind versus surface current is still unclear, although the role of wind has been recognised as important in several studies. For example, a study by Harrold and Lisin (1989) investigated the seasonal trajectories of radio-transmitter tagged *M. pyrifera* in nearshore Monterey Bay. The results showed that kelp rafts, with little surface area exposed to the wind, were largely driven by a combination of wind and surface currents; however, the relative importance of wind was not clear. This work also showed that the trajectories of tagged kelp were congruent with the formation of eddies during winter. Other studies have used genetic approaches to determine macroalgal raft trajectory characteristics by inferring source location from genetically similar populations. For example, a study by Nikula et al. (2013) used genetic markers (mtDNA and AFLP) of invertebrate species to show that in the sub-Antarctic latitudes, the West Wind Drift causes continuous unidirectional surface flow and is regarded as an important mechanism for dispersal of floating bull kelp *D. antarctica*. Another study by Fraser et al. (2011) on the rafting capabilities of *D. antarctica* used a combination of population genetics and relative age estimate of goose barnacles attached to kelp rafts. The presence of goose barnacles suggests a long rafting time as these species have a slow growth rate. Genetic analyses showed these species can raft up to 390 km from their local origin. The authors suggested that wind and surface currents were the primary influences of trajectory; however, this was inferred from the genetic analyses and local climatology data (Fraser et al., 2011).

Besides wind and surface currents, waves are also an important ocean feature and work by the maritime industry has shown that the size, shape, and orientation of an object determine the relative importance of waves or wind as drivers of trajectory (Grue and Biberg, 1993; Breivik et al., 2011). In general, if the length of the object is longer than the significant wave height, then waves will be the primary driver of trajectory, while the opposite is true for shorter objects where the effect of waves is regarded as negligible (Grue and Biberg, 1993; Breivik et al., 2011). Stokes drift is a wave-driven process, and previous work has identified this as an aspect that needs to be considered when investigating dispersal of macroalgal species. Stokes drift is the net drift velocity of a particle floating at the ocean surface in the direction of wave propagation due to the differences between the velocity of the fluid particle and flow field (Bremer and Breivik, 2018). More generally, the particle floating at the surface moves slightly faster in the direction of the wave as a result of the oscillatory motion of fluid particles within a wave. Stokes drift can significantly influence the trajectory of a particle or object floating at the surface of the ocean. For example, work by Fraser et al., (2018) included Stokes drift into the advection scheme for a Lagrangian model used to investigate the dispersal

potential of the southern bull kelp *D. antarctica* to reach Antarctica. The results showed that the inclusion of wave-driven Stokes drift and mesoscale eddies suggest frequent incursions into King George Island Antarctica, which the authors attributed to storm-forced surface waves, further highlighting the role of wave-driven processes in the open ocean.

Research has shown that buoyancy and drag also play a role in determining the trajectory and rate of transport for surface floating material (Furnans et al., 2008; Beron-Vera et al., 2016; Trinanes et al., 2016; D'Asaro et al., 2018; Gates et al., 2018; Onink et al., 2019; Shen et al., 2019). Therefore, to accurately determine the trajectory of kelp, both water and wind drag need to be considered. Drag is the force an object experiences when moving through a fluid which is proportional to the velocity of the object (Vogel, 2020). The fluid viscosity and the friction from the surface of the object results in the overall drag component, as well as the surface area and shape of the object (Vogel, 2020). If the object is partially submerged, as a result of buoyancy forces, then drag will be a combination of drag from the air and fluid (Vogel, 2020). The 'sail' area of an object floating at sea is the surface area exposed to the wind (air), which results in air-form drag, while the area of the object below the surface of the water is exposed to surface currents which results in hydrodynamic-form drag (Breivik et al., 2011; Griffin et al., 2017). Allen and Plourde (1999) and Breivik et al. (2011) have provided estimates of drag for various objects based on experimental work using both direct and indirect methods of the Leeway model; however, this work did not consider biological material such as macroalgae. Therefore, no drag estimates exist for macroalgae floating at the surface of the ocean, and alternative approaches should be used to account for the drag components. Although drag estimates do exist, these have been applied for kelp not detached from the substratum and are regarded as fixed-point estimates (Denny et al., 1997; Gaylord and Denny, 1997; Denny and Roberson, 2002; Denny and Gaylord, 2002).

Although various approaches have been used in the past to investigate floating macroalgal trajectories, very few studies have employed the use of Lagrangian trajectory modelling. Works by Brooks et al. (2019), Putman et al. (2018), and Putman et al. (2020) used Lagrangian approaches to investigate the effects of inertia, raft size, and windage (drag from the wind) on kelp trajectory. For example, Brooks et al. (2019) used a custom growth model to estimate changes in biomass and ultimately radial size, while a customised Hybrid Coordinate Ocean Model (HYCOM) for the trajectory simulations was used. Their results showed that the trajectory of pelagic *Sargassum* was significantly influenced by inertia and the radial size of the rafts. The inclusion of wind into studies has also been performed on an *ad-hoc* basis, where a fraction of wind velocity field is simply added to the ocean velocity field in terms of the velocity vectors (meridional and zonal); for example, 1%, 2%, 5% of the ocean velocity field has been used previously (Putman et al., 2018, 2020). Putman et al., (2020) investigated the effect of including windage in kelp trajectory simulations and showed that

including *ad-hoc* windage factors greatly improved accuracy regarding entrainment or expulsion from eddies when compared to tracked *Sargassum* mats in the ocean. Lagrangian trajectory modelling is clearly a useful tool; however, the various models available often assume the object to either be purely Lagrangian (no drag) or to be only influenced by windage (drag from the wind), which is obviously not the case for both biological and anthropogenic forms of marine debris in nature. The radial size in relation to windage included by Brooks et al. (2019) is an improvement, but this approach does not consider hydrodynamic drag. Another example is work by Zhong et al. (2012) describing *Sargassum* distribution in relation to mesoscale and submesoscale eddies by simulating passive tracers. The authors used two model configurations, one with an idealised eddy-flow and another that simulates flow in the western region Gulf of Mexico to advect passive tracers as a proxy for *Sargassum*. The authors showed that mesoscale and submesoscale features both play a role in accumulation zones for the virtual *Sargassum* and were able to explain some of the observed accumulation of *Sargassum* in the study region. Treating the virtual *Sargassum* particles as passive tracers may be the reason for the unexplained patterns during comparison of simulated and observed distributions. The authors do mention running simulations which included Stokes drift and inertia using a Maxey-Riley approach, and state that it made no significant difference to the overall results. However, the authors only used density as a parameter for calculating the relevant forces by making the particles 10% lighter than the surrounding fluid. Additionally, the authors did not consider surface area or take hydrodynamic drag and windage into account, all of which are important influencers of trajectory.

Gyres, eddies, and converging surface currents have been identified as important in the accumulation and dispersal of plastics and other marine debris (Brach et al., 2018; D'Asaro et al., 2018; Onink et al., 2019). Investigations into the dispersal of marine debris have also included the possible effects of inertia in the accumulation of ocean drifter instruments in mesoscale features. For example, Beron-Vera et al. (2016) used a modelling approach to investigate the role of Ekman transport and inertia to explain the observed behaviour of undrogued drifters in the ocean gyres. Undrogued drifter trajectory is affected by wind, unlike the drogue counterparts which makes the effects of wind negligible. The results showed that inertia, not Ekman transport, played a significant role in the observed drifter behaviour (Beron-Vera et al., 2016). These authors also noted that the presence of other flotsam, along with the undrogued drifters in ocean gyres, suggests that aspects of inertia also play a role in the accumulation of other marine debris (Beron-Vera et al., 2016). The approach by Beron-Vera et al. (2016) has also been improved upon by Beron-Vera et al. (2019) and highlights the significant role of inertia in flotsam trajectory and accumulation.

I aim to use a numerical approach to shed light on the role of hydrodynamic and direct wind drag (windage) on macroalgal drift trajectory using Lagrangian-based trajectory simulations. The

'behaviour' of surface drifting kelp is investigated with a specific focus on trajectories from a coastal environment to the open ocean. I achieved this by comparing the trajectory outputs of virtual passive particles (purely Lagrangian i.e. no drag characteristics added, as a reference) with kelp particles (drag characteristics added) with surface area exposed to the various drag components.

3.2 Methods

3.2.1 Study site

The region of interest for this study was the Cape Peninsula in the Western Cape, South Africa (Figure 3:1A). Kommetjie, located on the Atlantic side of the Cape Peninsula (Figure 3:1B), was chosen as a release site. The hydrodynamics in the study region are characterised by a complex interaction of wind, sea waves and ocean swell, and are also influenced by larger-scale regional oceanic processes. The larger processes in the region can be attributed to the Agulhas Current (AC) and the Benguela Current (BC) (Garzoli et al., 1996; Lutjeharms et al., 2000; Lutjeharms, 2007; Hutchings et al., 2009; Rubio et al., 2009). The AC is a component of the South-west Indian Ocean sub-gyre, flowing predominantly south-westward along the continental shelf edge and eventually retroreflecting eastward back into the South Indian Ocean (Lutjeharms et al., 2000; Lutjeharms, 2007).

The region where the retroflection occurs is known as the Agulhas Retroflection and consists of high levels of mesoscale variability (Garzoli et al., 1996). The variability results in shedding of rings and filaments known as the Agulhas Rings and have an average diameter of ~324km (Lutjeharms and Van Ballegooyen, 1988; Lutjeharms, 2007). Agulhas Rings are the main contributors to the Agulhas leakage, which is the transport of warm water from the Indian Ocean to the South Atlantic Ocean (Garzoli et al., 1996; Beal et al., 2015). The Agulhas leakage is also a source of mesoscale variability within the Benguela region as anticyclonic rings are shed and drift north-westward along the southern Benguela slope (Rubio et al., 2009). The Benguela region—known as the Benguela Upwelling System (BUS)—is characterised by strong coastal upwelling which is primarily driven by equatorward winds (Shannon and Nelson, 1996; Hardman-Mountford et al., 2003; Veitch and Penven, 2017; Veitch et al., 2018). The BUS starts at 27°S and extends southward to 35°S (Shannon and Nelson, 1996). The region is also characterised by large amounts of mesoscale variability in the form of eddies and filaments (Blanke et al., 2002, 2005; Rubio et al., 2009). Inshore, the BUS is dominated by a north-westward flow, known as the Benguela Jet, due to topographical steering, wind stress and interactions with passing Agulhas Rings and eddies (Stramma and Peterson, 1989; Hutchings et al., 2009; Veitch et al., 2010, 2018; Veitch and Penven, 2017). The stability of the jet varies seasonally with more stable flows in winter; in January, the jet begins to split between Cape Point and Cape Columbine (Blanke et al., 2002, 2005; Veitch et al., 2018) which

results in a weak narrow inshore branch that flows along the shelf edge and a strong flowing north-westwards offshore branch. These winds are most intense during Austral summer (December-March), which favours upwelling conditions in the region, and also act to reinforce the flow of the Benguela Jet, which favours upwelling waters contributing to the across-shore density gradient (Ragoasha et al., 2019). In Austral winter, the wind direction is reversed, which decreases upwelling favourable conditions, but the core of the Benguela Jet is maintained by the intrusion of warm Agulhas waters into the Benguela region over the shelf edge (Hutchings et al., 2009; Veitch et al., 2018; Ragoasha et al., 2019).

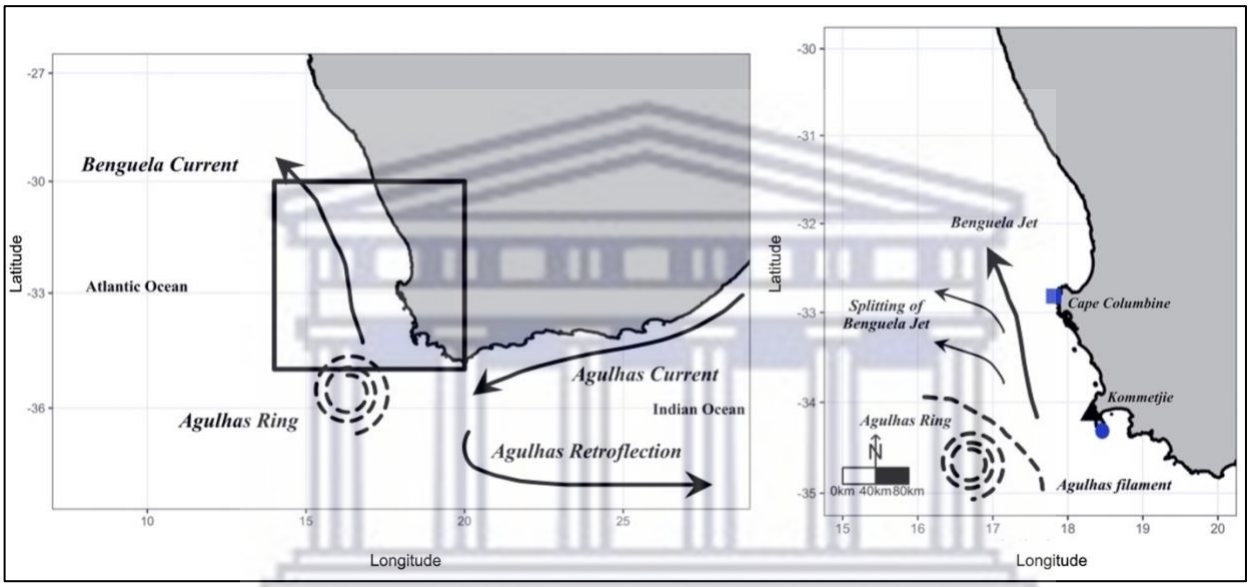

Figure 3:1 Map of the study domain and the main features pertaining to transport in the region. In panel A, the map of the western portion of the South African coastline and the main currents are presented. The resulting eddies and filaments forming from the Agulhas Retroflection are indicated, and the position of the study area is drawn in as a black rectangle. Details of the study area are given in panel B. Here the splitting of the Benguela Jet, eddy features, and the general flow within the study domain are presented. The release site of simulated kelp 'particles' is represented by a black triangle.

3.2.2 Numerical models

Virtual particles were released with no drag effects from the study site to act as a reference for comparison to simulations with varying combinations of hydrodynamic and wind drag and are referred to hereafter as 'passive particles.' All particles that have any form of drag exposure are hereafter referred to as 'kelp particles.' All simulations have the same release location. The release site, Kommetjie, is in an area of a known kelp population, which a previous study by Coppin et al., (2020) collected morphological data from. Due to the resolution of the underlying ocean model (see 'Flow-models' section), nearshore processes are not resolved well. Therefore, the release site was placed in the adjacent grid cell in order to better represent offshore transport and to avoid model limitations with regard to nearshore transport. Since the aim of this investigation was to investigate the relative surface behaviour of virtual kelp particles, only the surface layer of the underpinning ocean models was used.

The time-period used in all simulations was Austral summer, autumn, winter, and spring of 2018. These time periods were chosen based on variable mesoscale activities and stability of the Benguela Jet that occurs throughout the year. For example, the splitting of the Benguela Jet occurs in January, which also coincides with a period of higher wind intensity, upwelling along the coast and mesoscale activity, while in winter the Benguela Jet begins to stabilise until summer (Rubio et al., 2009; Ragoasha et al., 2019; Veitch et al., 2019). Simulations were executed for the duration of each season, with 3-hourly timesteps and 3-hourly outputs using a fourth order Runge-Kutta advection scheme for both passive and kelp particles. Drag components for kelp particles were incorporated by the modifiable component of the OceanParcels advection scheme (North et al., 2009; Van Sebille et al., 2018). Simulations included both single and repeated releases. For the repeated releases, the appropriate repeated release time was identified by comparing density distribution maps of 1-hour, 3-hour, 6-hour, and 12-hour release times (see Appendix; Figure A2). The appropriate repeated release time identified was every 3 hours for repeated releases.

To test the different magnitudes that hydrodynamic and wind drag might play in the overall trajectory, simulations were run with degrees of drag exposure scenarios based on personal observations of drifting kelp. This acts as a proxy for buoyancy, which determines the surface area exposed to hydrodynamic and wind drag. These estimates were expressed as percentages which were used to calculate hydrodynamics and wind drag for the applicable simulation. The scenarios used in this study were 100% and 85% for hydrodynamic and Stokes drift drag and 0% and 15% for wind. Simulations were separated into fully submerged (100% hydrodynamic drag and 0% wind drag, Figure 3.2A) and partially submerged (85% hydrodynamic drag, and 15% wind drag, Figure 3.2C-D) categories. For each of the categories, particles were advected with different combinations of flow fields (currents, currents-Stokes drift, currents-wind, currents-wind-Stokes drift). A similar approach has been used in past research investigating the role of windage in distribution of pelagic *Sargassum* rafts by Putman et al., (2018) and Putman et al., (2020) in the form of *ad-hoc* windage estimates, although the authors did not include hydrodynamic drag unlike the current study.

To determine if vortices and eddies play a role in kelp accumulation on the surface, a separate set of simulations were performed. Unlike the previous simulations, these simulations released 10 particles over the latitudinal extent of the study domain from the study site, equidistant from each other. The release sites cover a region where eddies and vortices are mostly likely to form.

3.2.3 Particle tracking model

The model is based on parameterisations that have been used for previous studies investigating the dispersal patterns of various flotsam by implementing custom parameterisations of Lagrangian trajectory models (Furnans et al., 2008; Beron-Vera et al., 2016; Hart-Davis et al., 2018; Brooks et

al., 2019; Jutzeler et al., 2020; Putman et al., 2020). Once dislodged, kelp can accumulate on the surface and become entangled to form a dense mat known as a kelp raft (Hobday, 2000a; Smith, 2002). Kelp rafts are not a common feature around the coast of the Cape Peninsula; rather, solitary kelp is (pers. obs). Therefore, the trajectory of only solitary *E. maxima* individuals was considered. All simulations in this study used the OceanParcels software package (version 2.0), which is an open-source, customisable Lagrangian Trajectory tool (Delandmeter and Van Sebille, 2019). OceanParcels calculates the advection of particle trajectory with a Lagrangian method (Delandmeter and Van Sebille, 2019), which can be described by the equation:

$$X(t + \Delta t) = X(t) + \int_{t}^{t+\Delta t} v(x, \tau) d\tau + \Delta X_b(t) \quad (3.1)$$

Here, $X(t + \Delta t)$ is the position after a timestep Δt, $v(x, t)$ is the ocean velocity field at that location, dt is the time-step and $\Delta X_b(t)$ is a change in position due to 'behaviour' or some kind of effect. To determine the new position of a particle, the integral has to be calculated. To investigate the effects of drag components of trajectory of floating macroalgae, this study incorporated drag as the custom behaviour for virtual kelp particles and zero effect for passive particles.

This study simulated two scenarios: one where the plant is fully submerged and only exposed to hydrodynamic drag and/or Stoke drift, and the other where parts of the plants are partially exposed resulting in combinations of hydrodynamic and air form drag. Drag based on spherical shape-based coefficients were used in the calculations for determining the overall kelp velocity vectors (see 'Drag components' section). The assumption made was that the mass of the kelp did not change for each virtual kelp particle over the course of the simulations. All velocity components (Hydrodynamic drag, wind drag, Stokes drift drag, and surface current-flow) are two-dimensional vector quantities and were calculated for each time step for each simulation.

3.2.4 Model inputs

3.2.4.1 Cross-sectional area and simulation scenarios

To incorporate the various forms of drag, the cross-sectional area of the kelp was first calculated. Known geometric shapes reflecting the relevant plant sections were used to estimate the surface area for various parts of the plant (Figure 3:2A). The structure of *E. maxima* consists of a single primary blade that develops above a gas-filled float and a hollow stipe below. Secondary blades

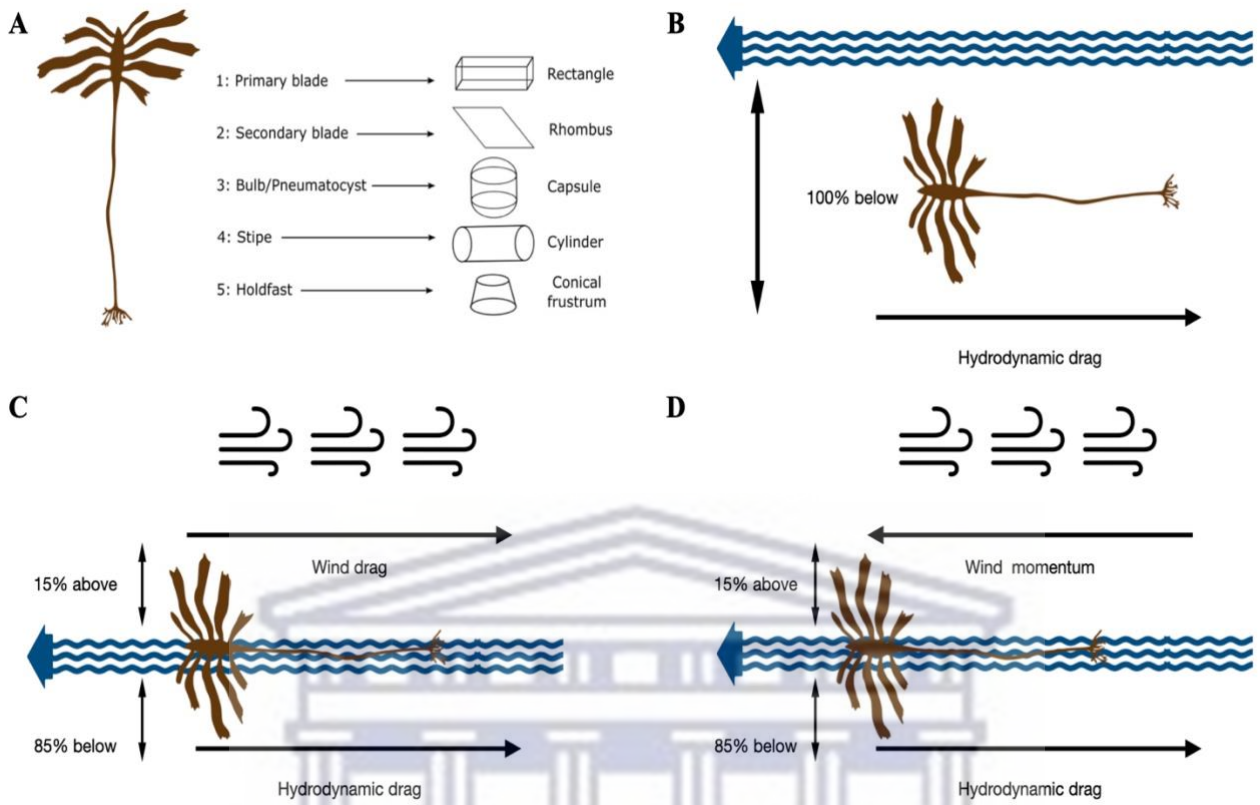

Figure 3:2 Panel A is a diagram of the E. maxima morphological characteristics considered in this study, along with the associated geometric shapes used to calculate the overall surface area of each morphological characteristic. Panel B represents the fully submerged scenario, panel C represents the combined drag scenario when kelp is partially submerged, and panel D represents a partially submerged kelp exposed to hydrodynamic drag and momentum transfer from the wind when in the same direction of the current. The kelp Schematic was adapted from Dyer, (2018).

are produced laterally from the primary blade from several meristematic regions along the margins of the primary blade and is held to the substrate by finger-like haptera known collectively as the holdfast (Dyer, 2018). For details refer to Figure 3:2.

Table 3:1 Summary of the attributes and estimates used to calculate the overall surface area of Kommetjie kelp individuals used in the various simulations. Approximate shape refers to the dimensions of the geometric shape used to represent a particular characteristic. Equations used are the equations relating to the dimensions used for the geometric shape estimate. Plant dimensions are the measurements used, collected in previous work by Coppin et al., (2020), used to calculate the associated surface areas. Ac refers to the cross-sectional area calculated. The total surface areas for each plant characteristic for each surface area type make up the remaining columns. Where applicable r is the radius, h is the height, l is the length, w is the width, and h is the height.

Plant characteristic	Approximate shape	Equation Used	Plant dimensions	Ac Minimum	Ac Mean	Ac Maximum
Secondary blade	Rectangle	Ac = 2lw + 2lh + 2wh	frond length, frond width*, frond thickness*	1,135.61	1,993.18	2,550.00
Primary blade	Rhombus	Ac = (lxb)/2	primary length, primary width	96.00	261.62	536.50

Plant characteristic	Approximate shape	Equation Used	Plant dimensions	Ac Minimum	Ac Mean	Ac Maximum
Bulb/pneomatocyst	Capsule	$Ac = 4\pi r^2 + 2\pi rh$	bulb length*, bulb base radius*	628.32	628.32	628.32
Stipe	Cylinder	$Ac = 2\pi r(r + h)$	stipe radius from stipe circumference, stipe length	9,797.27	19,338.49	34,273.35
Holdfast area	Conical frustrum	$Ac = \pi(R^2 + r^2) + \pi(R+r)\sqrt{((R-r)^2 + h^2)}$	top radius*, bottom radius*, height*	639.76	639.76	639.76
			total area (centimetres)	12,296.96	22,861.37	38,627.93
			total area (meters)	122.97	228.61	386.28
	N/A	mass (kg) = stipe mass + (frond mass x 6)	total mass (kg)	17.10	34.45	48.65

The dimensional data needed were estimated in cases where data were not available for that morphological characteristic. The bulb/pneumatocyst is a highly variable morphological feature and in some cases can appear absent; the same is true for the holdfast. Therefore, a standard cross-sectional area was used for both the bulb and holdfast, for all simulations.

The cross-sectional area calculated was site-specific and the dimensions needed were garnered from morphology data from a previous study by Coppin et al., (2020). The minimum, mean and maximum cross-sectional areas (Ac, Table 3:1) were calculated for each morphological characteristic, which were used for calculating the overall cross-sectional area needed to run the various simulations. Initially, experiments included minimum and mean surface areas, but no differences could be seen. Therefore, the minimum and mean cross-sectional areas were ignored, and simulations only considered the maximum cross-sectional area. Different combinations of flow fields were used for both passive and kelp particles, in order to determine the influence of drag (hydrodynamic, Stokes drift and wind) on macroalgal trajectory. The different combinations of flow fields and the associated drag components are hereafter referred to as 'scenarios.' A summary of the simulations executed is provided in Table 3:2

Table 3:2 Details for each simulation run for the study. Type refers to either a passive particle with no drag behaviour or a kelp particle that has been advected with any type of drag exposure. The Number column refers to the simulation number, the condition column refers to the situation under which the particle is being advected, the advection column refers to the underlying velocity field or combination thereof, the simulation column refers to the type of particle (passive or kelp), and

the season refers to the seasonal time period of the simulation. The run-time for summer simulations was 89, autumn 91, winter 91 and spring 91. The simulation output for all simulations was 3 hours and advected with a Runge-Kutta fourth order advection scheme. Particles were released every 3 hours for simulations which executed repeated releases

No.	Condition	Advection	Simulation	Season
1	Passive particle, Single	Currents	No drag, purely Lagrangian	Summer
2				Autumn
3				Winter
4				Spring
5	Passive particle, Single	Currents and Stokes	No drag, purely Lagrangian	Summer
6				Autumn
7				Winter
8				Spring
9	Passive particle, Single	Currents and wind	No drag, purely Lagrangian	Summer
10				Autumn
11				Winter
12				Spring
13	Passive particle, Single	Currents, wind and Stokes	No drag, purely Lagrangian	Summer
14				Autumn
15				Winter
16				Spring
17	Kelp fully submerged, Single	Currents	Hydrodynamic drag only	Summer
18				Autumn
19				Winter
20				Spring
21	Kelp fully submerged, Single	Currents and Stokes	Hydrodynamic and Stokes drag	Summer
22				Autumn
23				Winter
24				Spring
25	Kelp partially submerged, Single	Currents and wind	Hydrodynamic and wind drag	Summer
26				Autumn
27				Winter
28				Spring
29	Kelp partially submerged, Single	Currents, wind and Stokes	Hydrodynamic, wind and Stokes drag	Summer
30				Autumn
31				Winter
32				Spring
33	Passive particle, Repeated release	Currents	No drag, purely Lagrangian	Summer
34				Autumn
35				Winter
36				Spring

No.	Condition	Advection	Simulation	Season
37	Passive particle, Repeated release	Currents and Stokes	No drag, purely Lagrangian	Summer
38				Autumn
39				Winter
40				Spring
41	Passive particle, Repeated release	Currents and wind	No drag, purely Lagrangian	Summer
42				Autumn
43				Winter
44				Spring
45	Passive particle, Repeated release	Currents, wind and Stokes	No drag, purely Lagrangian	Summer
46				Autumn
47				Winter
48				Spring
49	Kelp fully submerged, Repeated release	Currents	Hydrodynamic drag only	Summer
50				Autumn
51				Winter
52				Spring
53	Kelp fully submerged, Repeated release	Currents and Stokes	Hydrodynamic and Stokes drag	Summer
54				Autumn
55				Winter
56				Spring
57	Kelp partially submerged, Repeated release	Currents and wind	Hydrodynamic and wind drag	Summer
58				Autumn
59				Winter
60				Spring
61	Kelp partially submerged, Repeated release	Currents, wind and Stokes	Hydrodynamic, wind and Stokes drag	Summer
62				Autumn
63				Winter
64				Spring
65	Passive particle, Line experiment, Single	Currents	No drag, purely Lagrangian	Summer
66				Autumn
67				Winter
68				Spring
69	Passive particle, Line experiment, Single	Currents and Stokes	No drag, purely Lagrangian	Summer
70				Autumn
71				Winter
72				Spring
73	Passive particle, Line experiment, Single	Currents and wind	No drag, purely Lagrangian	Summer
74				Autumn
75				Winter
76				Spring

No.	Condition	Advection	Simulation	Season
77	Passive particle, Line experiment, Single	Currents, wind and Stokes	No drag, purely Lagrangian	Summer
78				Autumn
79				Winter
80				Spring
81	Kelp fully submerged, Line experiment, Single	Currents	Hydrodynamic drag only	Summer
82				Autumn
83				Winter
84				Spring
85	Kelp fully submerged, Line experiment, Single	Currents and Stokes	Hydrodynamic and Stokes drag	Summer
86				Autumn
87				Winter
88				Spring
89	Kelp partially submerged, Line experiment, Single	Currents and wind	Hydrodynamic and wind drag	Summer
90				Autumn
91				Winter
92				Spring
93	Kelp partially submerged, Line experiment, Single	Currents, wind and Stokes	Hydrodynamic, wind and Stokes drag	Summer
94				Autumn
95				Winter
96				Spring

Drag components

Drag components calculated were incorporated into simulations by means of the modifiable custom behaviour component of the underling OceanParcels advection scheme. The drag coefficient for a spherical particle was used in the calculation of hydrodynamic drag, as the trajectory model assumes the particles are spherical. Although this may be considered a limitation, this study uses a spherical drag coefficient regardless, as no experimental based drag coefficients have been established for macroalgae floating on the surface. The drag equation used was:

$$F_d = (0.5\rho A_c C_d U^2)/m, \quad (3.2)$$

where ρ is the density of seawater or air, A_c is the cross-sectional area exposed to the relevant drag component, C_d is the drag coefficient for a spherical particle, m is the total mass of the plant, and U is the surface velocity vector of the flow-/wind- field. Dividing the calculated force by the mass of the plant transforms it to the appropriate units (m/s) for use in the trajectory modelling script. Hydrodynamic, wind drag, and Stokes drift components were calculated separately for both the meridional and zonal velocity vectors (Furnans et al., 2008; Putman et al., 2018, 2020). The same

equation and approach used to calculate hydrodynamic drag, was also used to calculate drag resulting from wind and Stokes drift components. Since drag force is dependent on the velocity vectors, which vary with time, the meridional and zonal velocities were interpolated and used in the drag force calculation for each time step. The velocity of the resultant drag component is then added to the particle velocity, which is based on the underlying Euerlian flow field and determines the overall velocity of the particle and grid node position.

3.2.4.2 Flow models

Both passive and kelp particles were simulated around the South African coastline within hindcast outputs from the Copernicus Marine Environment Monitoring Service (Copernicus, http://marine.copernicus.com). The Copernicus model is based on the modelling framework known as Nucleus for European Modelling of the Ocean (NEMO). The Copernicus outputs used in this study contain 3D daily current information from the surface layer to the bottom (Global Analysis Forecast PHY_001_030). The model has a spatial resolution of 0.08 geographical degrees and is interpolated on a rectangular grid. To incorporate the effects of direct wind drag within the simulations, the Copernicus Marine Environment Monitoring Service global wind product was used (Global Ocean Wind L4_NRT_012_006). The outputs from the model are composed of 6-hourly averaged fields of surface 10 m wind velocity vectors with a spatial resolution of 0.25 geographical degrees. Finally, to test the direct effects of Stokes-drift, the Copernicus Marine Environment Monitoring Service global wave product was used (Global Analysis Forecast WAVE_001_027), composed of 3-hourly instantaneous velocity vectors on a standard grid at 0.08 geographical degrees. Averaged ocean current, wind, and Stokes drift data are stored as meridional and zonal velocity vectors. Important to note, velocity vectors for both the ocean and wind models cover portions of land near the coast and, in the case of the wind model, significant portions of land. In order to prevent particles crossing over onto land, a landmask was incorporated into simulations which removes the particle from the simulation if it makes contact with land.

3.2.5 Analysis

To compare trajectories between scenarios and seasons, trajectories were plotted, and density distribution maps were produced. Single trajectories allow comparison of pathways between scenarios, and density distribution maps are an effective method for assessing pathways and ocean connectivity (Van Sebille et al., 2018). The distance that particles travelled was also measured and used to produce boxplots. Distance travelled from the release site can help reveal topographic steering and momentum energy transfer from the wind field to kelp particles (Van Sebille et al., 2018). If the wind direction is in the same direction as the current the virtual particles will cover larger distances due to an increase in the velocity because of momentum energy transfer (Putman

et al., 2018, 2020; Van Sebille et al., 2018). Topographic steering occurs when ocean currents make contact with underlying bathymetry features, such as sea mounts and ridges. Under topographic steering, currents will tend to follow lines of constant potential vorticity (Davis, 1991; Van Sebille et al., 2018).

3.3 Results

Overall, the results showed that the inclusion of drag parameters influenced trajectory patterns and entrainment patterns of virtual kelp particles. Single trajectories for each of the scenarios will be presented, followed by the comparison of density distributions and distance travelled by particles. Finally, the results from the separate set of experiments advecting single particles across the study domain will be presented.

3.3.1 Trajectory comparison

The trajectories of the virtual kelp under different drag scenarios during Austral summer show no differences with those of passive particles advected by currents but do differ with passive particles advected by the different combinations of currents, Stokes drift and wind fields (Austral summer; Figure 3:3A). Any passive scenario which included wind made contact with land almost immediately after release (Figure 3:3A). The results from the simulations of virtual kelp particles show no differences between scenarios. Any passive particles advected with Stokes drift travelled further than those that did not, while the combination of wind and currents for passive particles travelled the least distance compared to the other simulations for the same time period (Figure 3:3A). In all simulations for Austral summer, particles flowed north-westward except for the currents and wind combination for passive particles, which initially travelled shoreward.

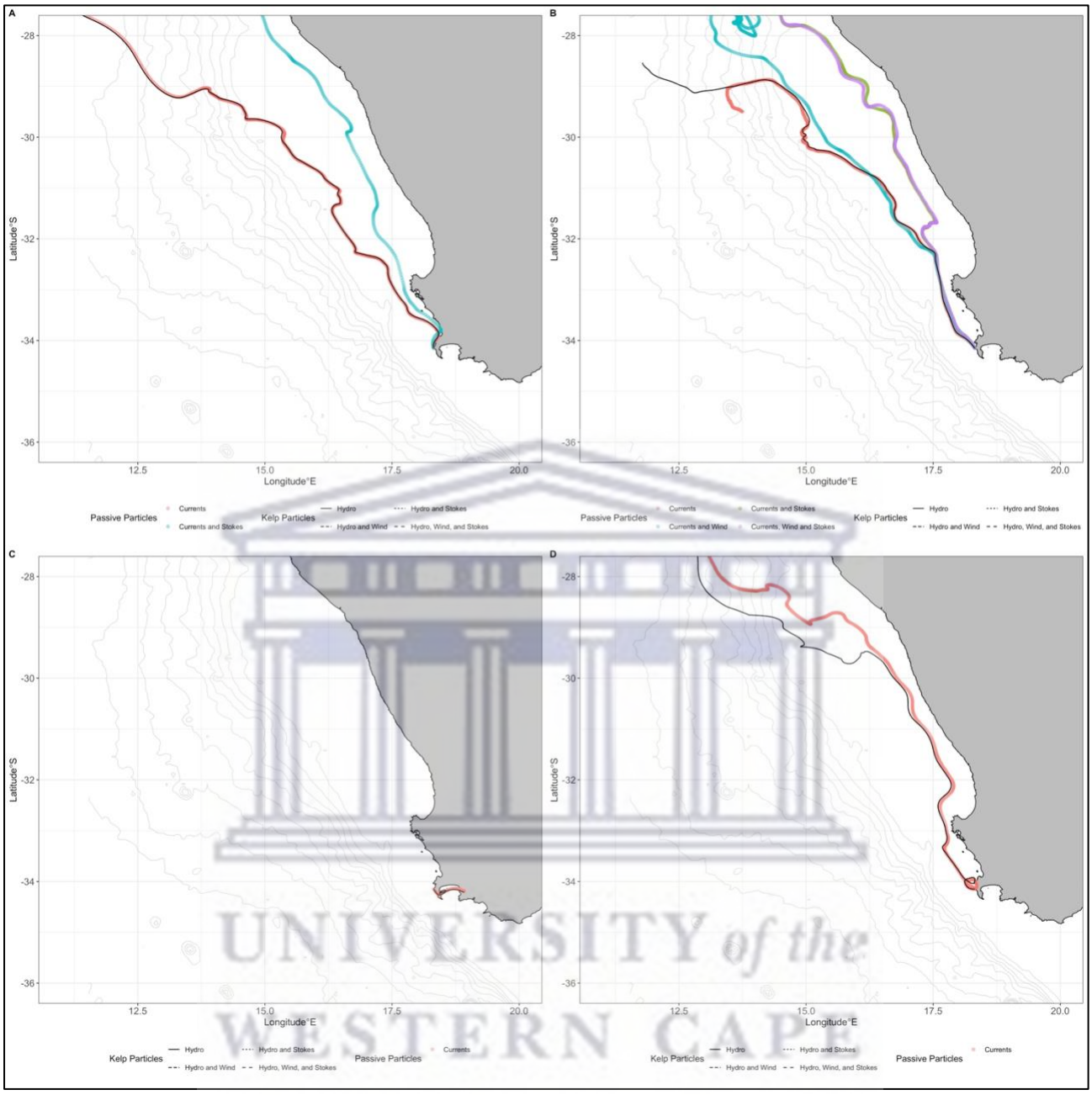

Figure 3:3 Comparison of single trajectories. Simulations 1, 5, 9, 13, 17, 21, 25, 29 are represented in panel A (Austral summer simulations), 2, 6, 10, 14, 18, 22, 26, 30 in panel B (Austal autumn simulations), 3, 7, 11, 15, 19, 23, 27, 31 in panel C (Austral winter simulations), and 4, 8, 12, 16, 20, 24, 28, 32 in panel D (Austral spring simulations). Overlapping of line types will be represented by a solid black line for kelp particles. Faint grey lines represent the various bathymetry layers.

The trajectories of kelp particles across all drag scenarios showed no difference with passive particles advected by currents, but differences between the other passive scenarios were evident for Austral autumn (Figure 3:3B). When comparing passive particles, only slight variations were evident for any simulation including Stokes drift, while currents and currents-wind showed slight variations between each other; with passive particles advected by currents travelling further offshore. The results from the simulations show that any scenario, including Stokes drift for the passive particles,

results in the trajectories flowing closer to shore (Figure 3:3B). Particles flowed in a north-westward direction and then slightly eastward near the end of the simulation run, across all simulations for both passive and kelp particles.

No differences were evident across drag scenarios between kelp particles and between passive particles advected by currents for Austral winter (Figure 3:3C). All other passive scenarios made contact with land almost immediately after release. Unlike the previous time periods, the overall direction for both passive and kelp particles was shoreward (eastwards) and then south along the eastern part of the coastline. In Austral spring, no differences between kelp particles with different drag scenarios were evident, and variation was evident between kelp particle scenarios and passive particles advected by currents (Figure 3:3D). When comparing passive particles, only particles advected by currents did not immediately make contact with land after release.

Particles travelled north-westward across all scenarios for both passive and kelp particles. Overall, all kelp particles, regardless of the drag scenario, followed a similar trajectory as passive particles advected by currents across all seasons.

3.3.2 Comparison of density distributions

Density distributions summarising the conclusion of simulating all passive and kelp scenarios (Table 3:2) are presented in below. Across all simulations for Austral summer, particles flow in a north-westward direction. The only passive particle scenario that resulted in entrainment were particles advected by currents with particles concentrated on the boundary of the mesoscale feature (Figure 3.4A). The passive particles that were advected with Stokes drift resulted in particles concentrating closer to shore, and less dispersion of particles off the continental shelf (Figure 3:4A). Passive particles advected by currents-wind showed greater dispersion over the continental shelf and closer to shore compared to the other passive particle scenarios. The density plots that considered any form of drag showed entrainment patterns, with kelp particles towards the centre of the mesoscale feature (Figure 3:4B). No differences were evident between different drag scenarios for kelp particles.

In Austral autumn (Figure 3:4C-D), across all simulations, particles flowed in a north-westward direction. Passive particles advected by currents showed similar density distribution to kelp particles,

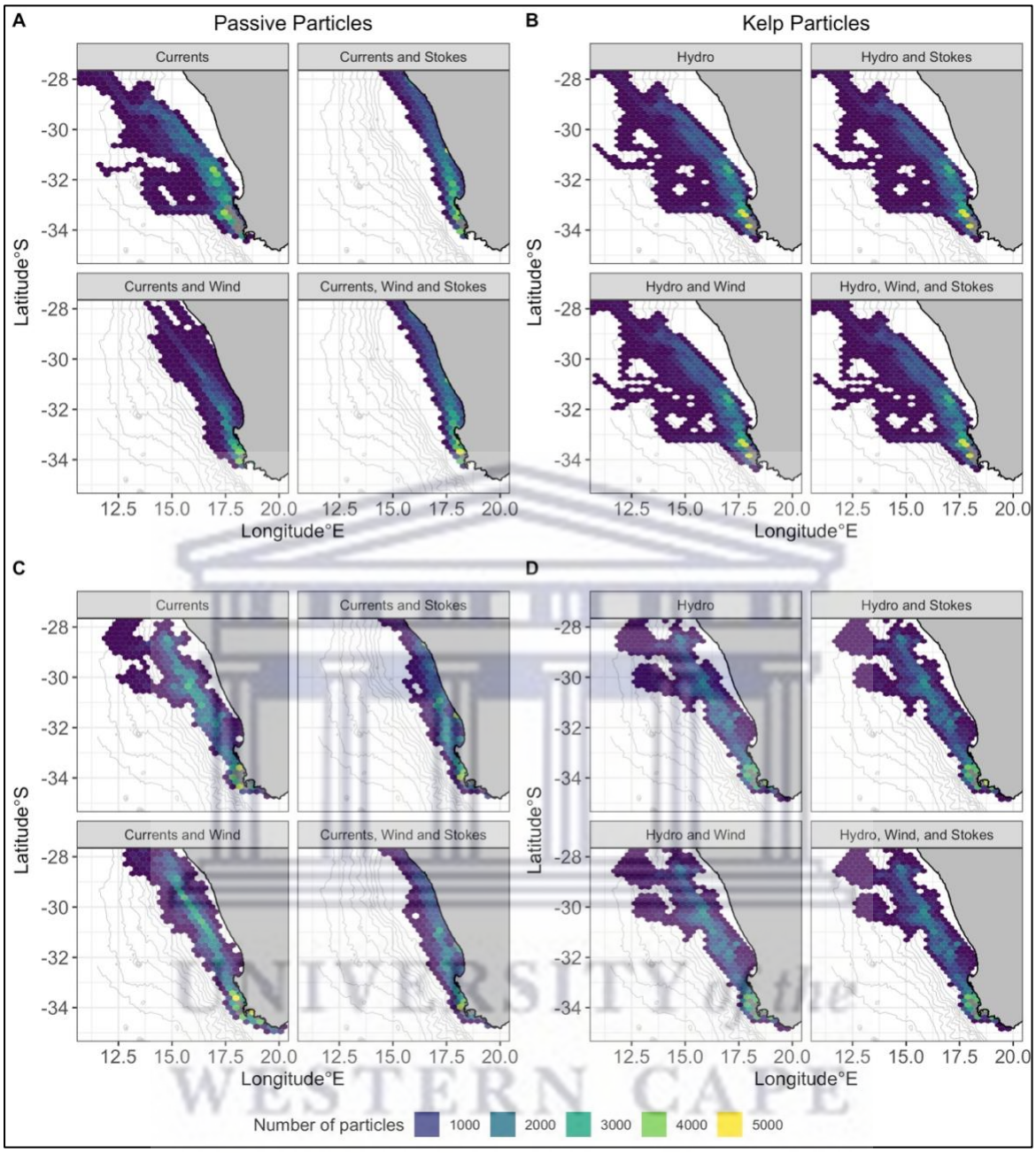

Figure 3:4 Comparison of density plots at the end-run time for both passive and kelp scenarios, for Austral summer (panel A - B) and autumn (panel C-D). Simulations 33, 37, 41, 45 are represented in panel A, 49, 53, 57, 61 are represented in panel B, simulations 34, 38, 42, 46 are represented in panel C, and simulations 50, 54, 58, 62 are represented in panel D. The plots are regular hexagons within which the density of particles were calculated. The reader is referred to Tables 1 and 2 for details pertaining to each simulation. Faint grey lines represent the various bathymetry layers.

but other passive particles scenarios showed no entrainment patterns (Figure 3:4C). The density plots for kelp particles with any drag scenario show slight entrainment patterns with no differences in density evident between kelp particle drag scenarios (Figure 3:4D). When comparing kelp particles to passive particles, clear differences in density were evident. Kelp particles are less concentrated along the overall trajectory compared to passive particles, which show a higher concentration of particles.

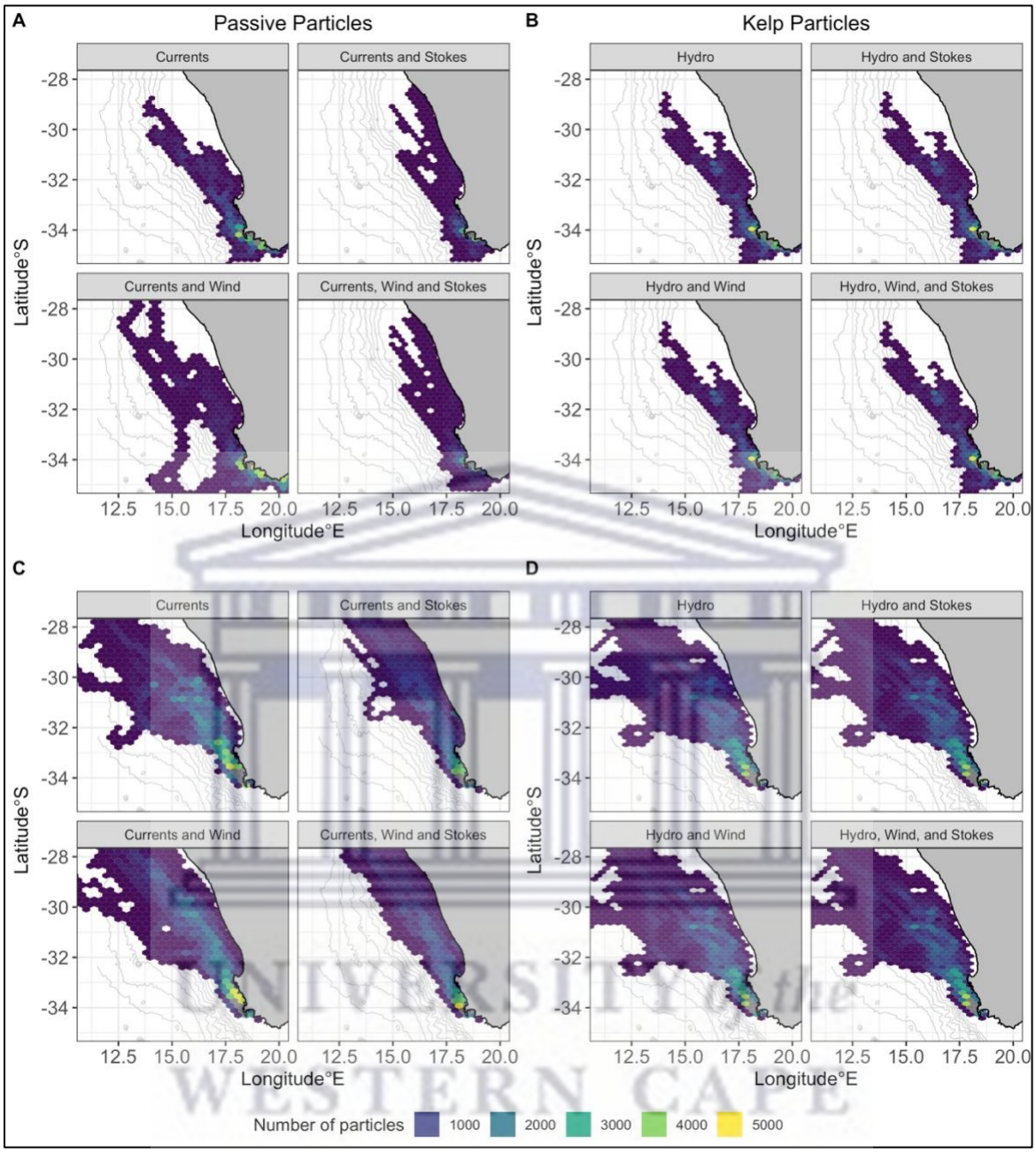

Figure 3:5 Comparison of density plots at the end-run time for both passive and kelp scenarios, for Austral winter (panel A-B) and spring (panel C-D). Simulations 35, 39, 43, 47 are represented in panel A, 51, 55, 59, 63 are represented in panel B, simulations 36,40,44,48 are represented in panel C, and simulations 52, 56, 60, 64 are represented in panel D. The plots are regular hexagons within which the density of particles were calculated. The reader is referred to Tables 1 and 2 for details pertaining to each simulation. Faint grey lines represent the various bathymetry layers.

Simulations for Austral winter (Figure 3:5A-B) showed that the flow was also north-westward with only slight variation in density distribution for kelp particles and clear differences between passive particle scenarios. Clear differences are evident between passive particle scenarios (Figure 3:5A). Passive particles advected by currents show a similar density distribution to that of kelp particles for the same time period (Austral Winter, Figure 3:5A-B). Passive particles advected with Stokes drag showed distribution of particles closer to shore compared to the other passive scenarios. No

differences or variation was evident when comparing kelp particle drag scenarios, with all scenarios showing slight entrainment patterns in the north-westward portion of the study domain (Figure 3:5B). The currents-wind scenario differed from all the kelp and passive scenarios for the same time-period (Austral winter, Figure 3:5B) and showed large spread of particles over the study domain and surrounding mesoscale features offshore.

Simulations executed for Austral spring (Figure 3:5C-D) showed no differences in density distribution between kelp particles. Passive particles for the same time-period (Austral spring, Figure 3:5C) are concentrated along the overall trajectory and are less spread out. Passive particles that are close to mesoscale activity follow the boundary of the feature and do not spread out or become entrained (Figure 3:5C). Passive particles advected with Stokes drift are less distributed offshore and are instead concentrated along the overall trajectory and towards shore. Across all drag scenarios for kelp particles, entrainment patterns were evident, and particles were spread westwards across the study domain Figure 3:5B and Figure 3:5D).

3.3.3 Comparison of distances

The results for the comparison of distance travelled by passive and kelp particles across all scenarios and seasons are presented in Figure 3:6. There were no significant differences (Figure 3:6; $p > 0.05$) for distance travelled across all kelp particles drag scenarios and seasons. Kelp particles travelled the least distance in Austral winter (Figure 3:6C) compared to other seasons and across passive particle scenarios. With regards to passive particles, clear differences and variation in the mean distance travelled were evident.

For Austral summer, the currents-wind scenario for passive particles travelled significantly less distance compared to the other scenarios (currents, currents-Stokes drift, currents-wind-Stokes drift, Figure 3:6B). There were no significant differences in distance travelled between all passive scenarios for Austral autumn ($p > 0.05$; Figure 3:6D). For Austral winter, all passive particle scenarios with Stokes drift included travelled significantly less distance compared to other passive particle scenarios ($p < 0.05$; Figure 3:6F). The same was true for Austal spring, which also showed that passive particles with Stokes drift flow travelled significantly less distance compared to other passive particle scenarios ($p < 0.05$; Figure 3:6H).

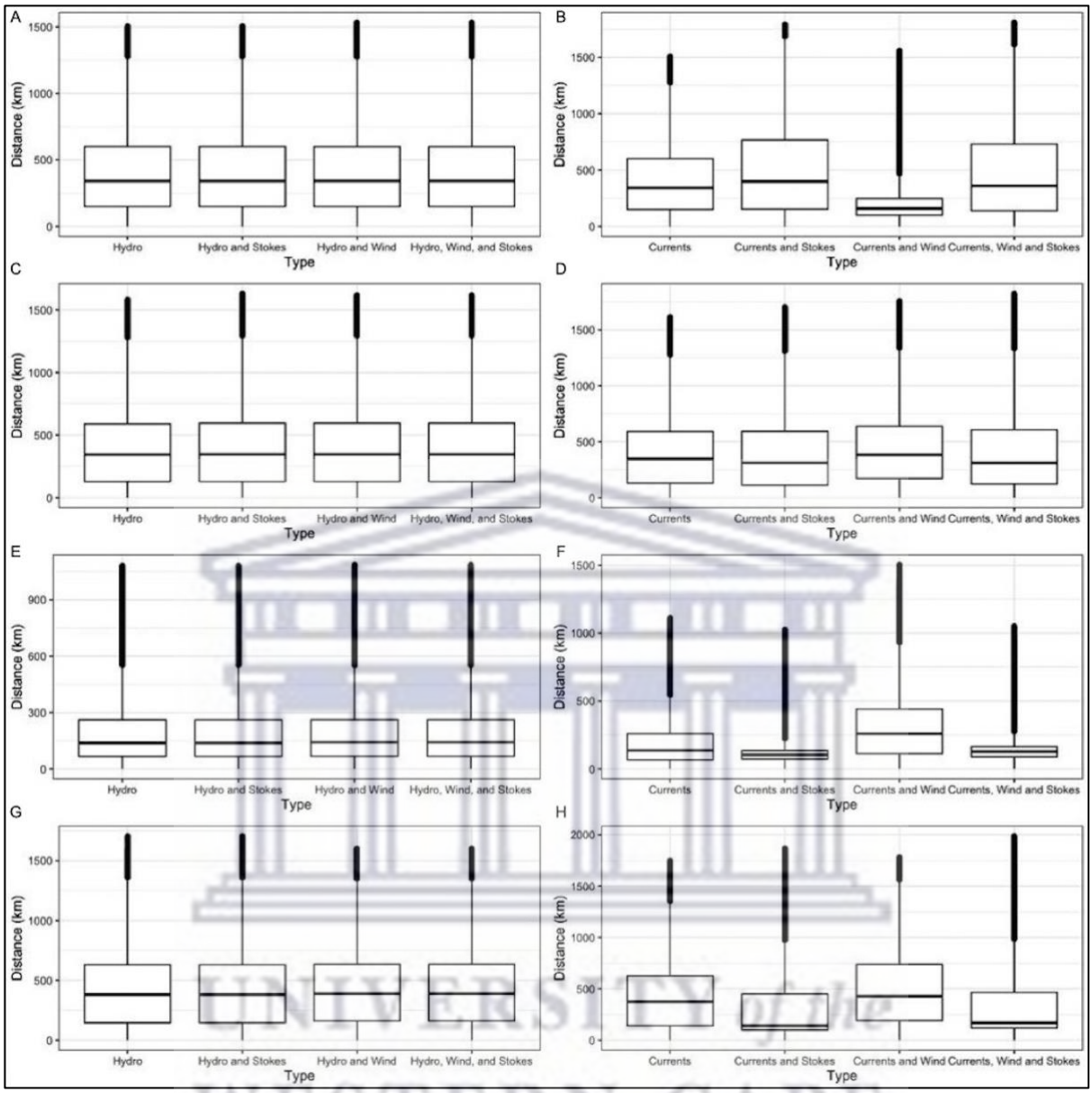

Figure 3:6 Boxplots of total distance travelled by all particles from the release site over the course of the simulations for scenarios 1-64. The x-axis represents the scenario number, and the y-axis is the distance travelled in kilometres. The lower and upper hinges correspond to the first and third quartiles. The whiskers represent the range, solid black vertical lines represent the median, and black dots are outliers. The reader is referred to Tables 1 and 2 for details pertaining to each scenario.

3.3.4 Line experiment

The results from simulations which released single particles along the longitudinal extend of the study domain are presented in Figure 3:7 and Figure 3:8. When comparing kelp particles with different drag scenarios, no differences or even variation in the trajectory of single particles were evident from the results. Across all seasons and drag scenarios, kelp particles located from the edge

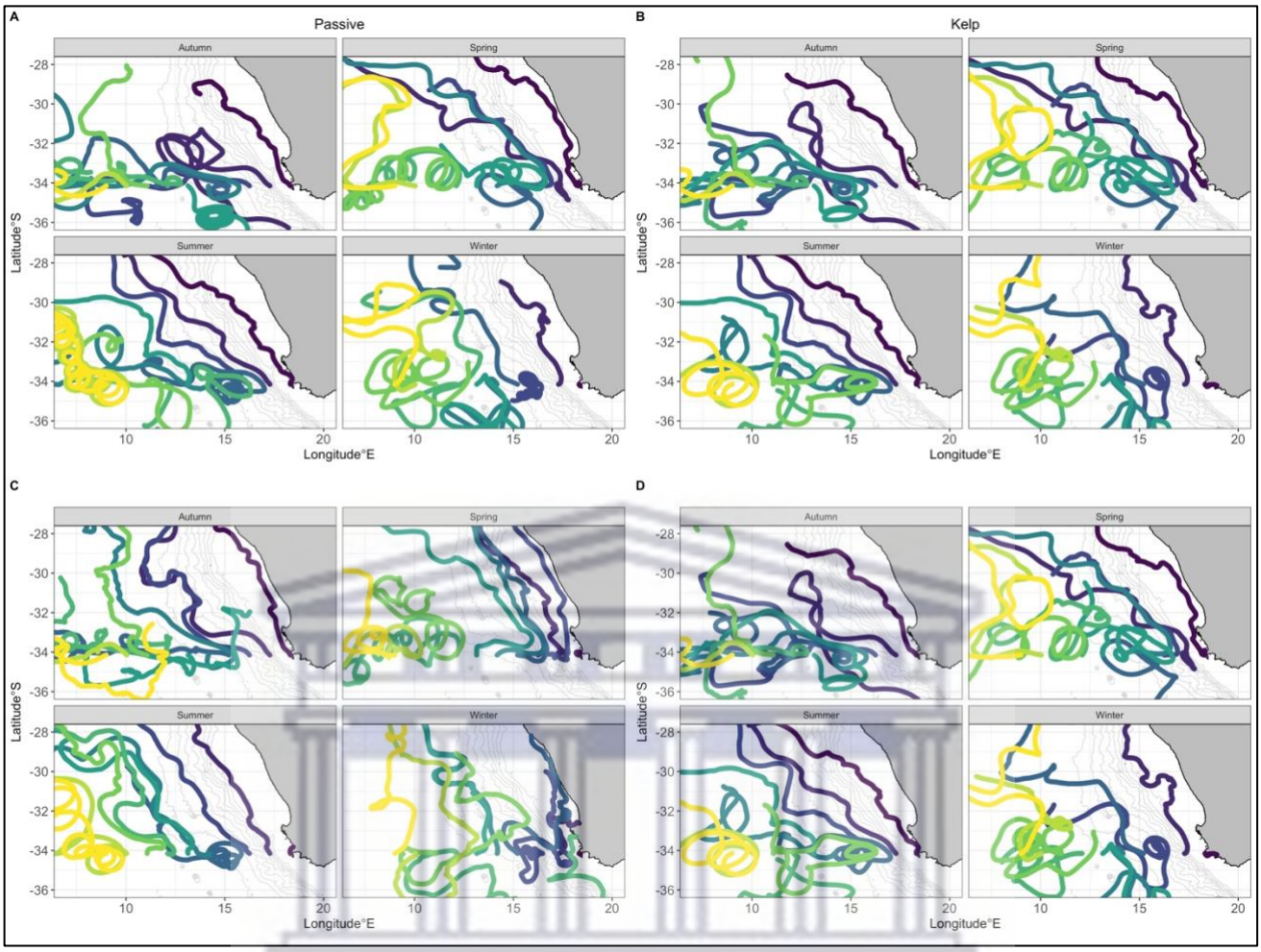

Figure 3:7 Comparison of single kelp and passive particle trajectories for all seasons released along a line from the study site (Kommetjie), equidistant apart. Colours represent the different trajectories executed within that scenario. Simulations 65-68 are represented in panel A, 81-84 are represented in panel B, 69-72 are represented in panel C, and 85-88 in panel D. Faint grey lines represent the various bathymetry layers. Particles that travelled slow will have very little distance between points and will be represented by a solid line, while distance between particles suggests a faster travel time. Each colour represents an individual particle trajectory.

of the continental shelf towards the eastern part of the study domain showed entrainment patterns and/or flowed northward. Kelp particles released from the study site (Kommetjie) did not show any entrainment patterns and flowed north-westward. When comparing passive particles advected with no drag but by the same combination of flow fields as kelp particles, differences and variation was evident. Passive particle trajectories across all advection scenarios generally flowed north-westward and/or flowed on the boundary of mesoscale features (Figure 3:7A&C and Figure 3:8A&C).

Additionally, any passive scenario which included wind, hit land almost immediately or shortly after release (Figure 3:8A&C). Passive particles released further offshore travelled northward and showed no visible entrainment patterns, and the distances between points plotted suggests that

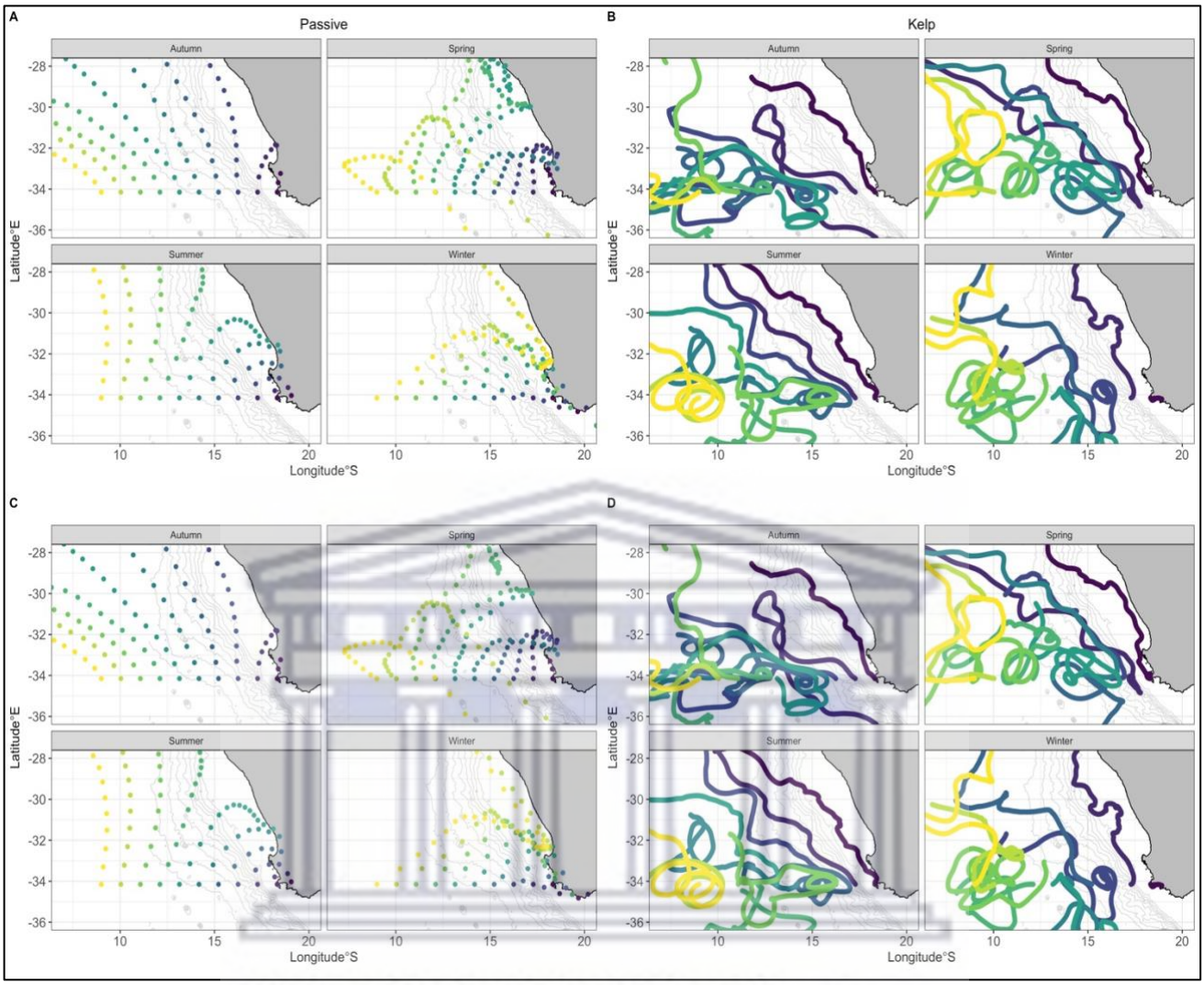

Figure 3:8 Comparison of single kelp and passive particle trajectories for all seasons released along a line from the study site (Kommetjie), equidistant apart. Simulations 73-76 are represented in panel A, 89-92 are represented in panel B, 77-80 are represented in panel C, and 93-96 in panel D. Faint grey lines represent the various bathymetry layers. Particles that travelled slow will have very little distance between points and will be represented by a solid line, while distance between particles suggests a faster travel time.

passive particle travelled faster compared to other passive scenarios, as well as kelp scenarios (Figure 3:8B&D).

3.4 Discussion

The findings from this study broaden our understanding of detached macroalgal trajectory patterns and behaviour in the ocean. In particular, the results show that consideration of drag and surface area are important when investigating macroalgal trajectory patterns. The treatment of drifting kelp as purely Lagrangian does not accurately determine patterns of passive dispersal, such as entrainment in eddies or vortices (Fossette et al., 2012; Miron et al., 2020). Although past research has shown the inclusion of inertia and windage greatly increase observed kelp trajectory and

entrainment characteristics (Brooks et al., 2018, 2019; Putman et al., 2018, 2020), it has focused on large macroalgal rafts, which can vary greatly in size and surface area. None of the extant research has taken advantage of the advancement in numerical ocean models and Lagrangian trajectory modelling to investigate how aspects of drag (hydrodynamic and wind) affect the trajectory patterns of solitary drifting kelp. This study compared particle trajectories with simulations that included no forms of drag with simulations that included various forms of drag. Kelp transport trajectory deviated from the passive trajectory when including varying levels of hydrodynamic and wind drag scenarios. The results from this study show the inclusion of hydrodynamic drag results in observable entrainment patterns and broaden our understanding of how surface area plays a role in solitary drifting kelp trajectory, in this case that of *E. maxima*.

Past research has inferred from direct and indirect techniques that drifting macroalgae tend to follow the prevailing surface currents (Hobday 2000b; Thiel and Gutow, 2005; Rothäusler et al., 2011; Fraser et al., 2011). The results from this numerical experiment confirm that drifting macroalgae do follow the surface currents in the study region when considering only hydrodynamic drag. In addition, not only are the trajectories similar, but so are the endpoints at the end of simulation. Interestingly, when *ad-hoc* wind drag (windage) is considered in combination with hydrodynamic drag the end locations do not differ either. It was expected that the inclusion of wind drag would cause kelp particles to flow further away from the coast and with a greater distance travelled from the release location. Wind drag adds to the influence of current when the wind direction and current direction are opposite to each other. However, when the wind direction is in the same or similar direction to that of the current, momentum energy from the wind is transferred to the object (Hackett et al., 2006; Putman et al., 2020). This causes objects to travel further as well as become exposed to different time-varying flows. Past studies have shown this when including windage as a function of inertia (Putman et al., 2018, 2020; Brooks et al., 2019). A study by Putman et al. (2020) used ad-hoc windage factors that were based on the surface current velocity to assess the approach for improving transport predictions of pelagic *Sargassum* sp. The results showed that including ad-hoc windage factors improved virtual trajectories compared to tracked *Sargassum* sp. mats. This was partly due to the inclusion of momentum energy transfer from the wind. The results from this study suggest that when considering solitary floating kelp, the effect of wind in the form of momentum energy transfer is negligible and does not influence the overall trajectory. The previously mentioned studies, including wind drag, focused on rafts which would have a significantly larger surface area exposed to the wind compared to a solitary individual. Therefore, in this study, the surface area of kelp particles exposed to wind drag was not enough to influence the overall trajectory. A similar result was found by Le Gouvello et al. (2020), who investigated the effects of swimming behaviour on sea turtle hatchling dispersal in the Agulhas region. The results suggested that the hatchling

trajectories were mostly influenced by the ocean currents in the first year of hatching, as juveniles do not swim fast enough to alter their overall trajectory. Another possible reason considered was the resolution of the ocean model used.

The resolution of the underlying ocean model is an important aspect of Lagrangian ocean modelling and must be able to resolve sub-grid scale ocean processes for finer scale applications. A study by Hart-Davis et al. (2018) assessed the inclusion of stochastic motion, wind, and currents in forecasting for search and rescue using the same ocean model used in this study. The authors found that the inclusion of Brownian motion greatly increased the accuracy in representing sub-grid scale processes and that the inclusion of wind, currents, and stochastic motion greatly improved forecasting applications. In this study, an eddy-resolving model was used, which greatly increases the sub-grid scale processes. Therefore, I argue that the lack of dissimilarity between trajectories of kelp particles is not a result of the ocean model used. Important to note is that the crossing of trajectories onto land resulted from the wind field. This would have resulted in the beaching of kelp; however, since this study focused on the transport of kelp in the open ocean, this was not considered a concern. Instead, the results highlight the role that wind plays in the beaching, which should be investigated and considered for future studies.

The different trajectory patterns between seasons reflect the underlying seasonal variation in regional oceanography. Transport in the study region is driven by a combination of variation of alongshore jets and wind-induced Ekman transport of surface water (Rubio et al., 2009; Ragoasha et al., 2019; Veitch et al., 2019). Ragoasha et al. (2019) investigated the success of Lagrangian particles reaching St. Helena Bay from Cape Point using Lagrangian trajectory modelling and the inclusion of regional oceanographic processes. The authors showed that transport success was higher in spring due to the single coherent Benguela Jet, which is most intense over the 300 m isobath (Ragoasha et al., 2019). During the upwelling season (December-March) transport success was less efficient as particles tend to flow offshore. The move offshore was a result of the bifurcation of the Benguela Jet, which splits because of shoaling and causes particles to be exposed to higher amounts of mesoscale activity. In the winter months, the Benguela Jet was still split, but the flow weakened, which resulted in lower transport success (Ragoasha et al., 2019). Similar patterns were found in this study, suggesting that the difference in seasonal patterns reflects the regional oceanographic features, particularly the Benguela Jet. The addition of drag forces caused the kelp particles to cluster together compared to the passive particles, which were more evenly dispersed. This was most likely due to the shared drag characteristics among the kelp particles, which included the plants' mass and surface area in the calculation. Other studies investigating flotsam trajectory characteristics have found similar results (Breivik et al., 2011; Miron et al., 2020; Olascoaga et al., 2020). A study by Miron et al., (2020) conducted field experiments using a range of objects such as

spheres, cubes, and cuboids to investigate the effect of inertia on particle dynamics. The results from the study showed that objects tended to cluster according to the shape of the object, which the authors attributed to shared characteristics of inertia. Although drag force and not inertia were used in this study, the same conclusion applies—drag is, therefore, an important characteristic to consider when investigating or predicting solitary drifting macroalgal trajectories.

The similarities between the different combined drag scenarios suggest that wind exposure did not significantly alter trajectories. Instead, the results from this study suggest that the inclusion of drag forces (both hydrodynamic and wind) in simulating macroalgal trajectory may result in improving the accuracy of modelling entrainment patterns. All the simulations that included any form of drag resulted in a high density of particles entrained in an eddy. The entrainment and expulsion from eddies and vortices are essential characteristics of floating kelp. Accuracy in predicting entrainment and expulsion of kelp rafts from eddies has been investigated previously by Putman et al., (2018, 2020), who showed that including windage greatly improved entrainment patterns when comparing virtual and real *Sargassum* rafts. However, these studies investigated large rafts and not floating individuals. Inertia was based on the size/mass of the raft, while hydrodynamic and wind drag was based on current velocity and surface area. Therefore, the role of inertia may be negligible for a solitary individual, and instead, other forms of drag, such as in this study, should be considered. The results from this study suggest that the inclusion of hydrodynamic and/or wind drag was an important component when simulating virtual kelp particles and greatly increased the accuracy of entrainment and expulsion from sub-grid mesoscale oceanographic features, such as eddies and vortices.

These results clearly show that the inclusion of drag greatly increases the number of particles entrained in mesoscale features within the study domain. Eddies may act as accumulation zones for kelp where the formation of rafts may occur, or the kelp is entrained for long enough to eventually sink in an area below the eddy. A study by Woodborne et al. (1989) references a site offshore approximately 120 km from Cape Columbine where dredged kelp was found, which coincides with the region where virtual kelp was entrained by an eddy. Finally, the inclusion of Stokes drift within the simulations had no effect on overall trajectory or entrainment patterns of virtual kelp particles, which suggests that the influence of waves is negligible with regards to solitary floating *E. maxima*. Past research has shown that the length of a floating object in relation to the significant wave height determines the influence of waves on the overall trajectory. Trajectories of objects with lengths shorter than the significant wave height will not be influenced by wave-related processes, in this case, Stokes drift (Allen and Plourde, 1999; Breivik et al., 2011; Griffin et al., 2017).

3.4.1 Conclusion

Most of the past research has focused on large kelp rafts, which can vary greatly in size and shape; however, prior to our study, no research existed to clarify the drifting characteristics of solitary kelp. Understanding how to accurately model the distribution of solitary kelp will lead to a better understanding of accumulation zones and sinks and, ultimately, the ecological links pertaining to those processes. The ecological links characterised will highlight ecosystems that are tightly dependent on kelp for proper ecological functioning. These areas might also have unique biodiversity compared to surrounding areas where less detrital input is present. The findings from this study indicated that solitary floating virtual *E. maxima* particles tended to follow the prevailing surface currents and the inclusion of hydrodynamic drag caused the trajectories to differ greatly from that of a purely Lagrangian particle. Furthermore, the inclusion of both hydrodynamic and wind drag caused clustering of particles along the trajectory as well as caused particles to become entrained in eddies. Finally, Stokes drift drag did not influence trajectory and dispersal patterns of virtual kelp particles, suggesting that the effect of waves can be ignored when modelling solitary floating kelp. Overall, the inclusion of drag forces is a vital aspect to consider when investigating the dispersal patterns of solitary kelp, while differences in cross-sectional areas are not. This study also provided an approach which can be adapted to model any floating solitary kelp, provided the surface area can be estimated accurately. Our results further highlight the importance of regional oceanographic processes to better understand how kelp flotsam is dispersed in the ocean. In particular, I highlight the role of the Benguela Jet and mesoscale processes, which ultimately determine the transport success around the coast. Gaps in the research exist when considering what oceanographic processes play a role in solitary macroalgal dispersal. The identification of biological and physical factors that play a role in accumulation zones is also needed, as well as estimates for kelp sinking rates which would aid in describing the spatial distribution on the seafloor.

4 : Individual-based numerical experiment to describe the distribution of floating kelp within the Southern Benguela Upwelling System

In this chapter, I use the findings from chapter 3 with additional site-specific parameters (buoyancy and sinking) and multiple sites to characterise the spatial distribution of virtual *E. maxima* on the surface, sub-surface, and sink locations.

- Solitary floating virtual *E. maxima* are prone to entrainment in mesoscale features and associated filaments.
- Solitary floating *E. maxima* remained entrained in mesoscale features while sinking.
- Mesoscale features, such as eddies, act as accumulation zones and barriers to further offshore transport.
- Spatial distribution of virtual kelp has a seasonal component.
- Characterisation of sink locations of *E. maxima* within the Benguela Upwelling System.
- Results shed light on the role of the sunken kelp regarding organic subsidy and Blue Carbon contribution.

4.1 Introduction

The role of drag has been well established in studies investigating ocean flotsam; however, no research has attempted to investigate the role of wind on solitary drifting kelp, nor has any consideration been given to the role of hydrodynamic drag. Instead, the focus has been on kelp rafts and the role of windage (wind drag) on floating macroalgae distribution patterns (Brooks et al., 2019; Putman et al., 2018, 2020). In the previous chapter (see Chapter 3), results highlighted the role of hydrodynamic drag in influencing virtual kelp trajectories, as well as the direct effect of wind in influencing entrainment and beaching patterns. Since this has now been established, the overall distribution patterns of solitary floating *Ecklonia maxima* (Osbeck) Papenfuss can now be investigated. This will require releases from multiple sites within the study domain, using the site-specific morphology approach, which would allow for a deeper numerical investigation into the role of underlying mesoscale ocean processes, such as eddies. Mesoscale features have been shown to act as important accumulation zones of marine flotsam (Brach et al., 2008; Beron-Vera et al., 2019; Miron et al., 2020), as well as acting as a potential barrier to offshore transport (Bracco et al., 2000). In addition, oceanographic processes may influence the location of sinking debris on the seafloor. This is of particular interest from an ecological standpoint as this would suggest a coupling of organic subsidy between near – and offshore areas. Macroalgae are conspicuous organisms along temperate shorelines and investigating the contribution of these organisms is essential to broadening our understanding of kelp forests' ecological contribution in terms of organic subsidy.

The rocky inter- to sub-tidal habitats of temperate shorelines are usually dominated by numerous species of macroalgae, specifically brown seaweeds of the order Laminariales, commonly referred to as kelp (Steneck et al., 2002; Schiel and Foster, 2015). Kelps are highly productive organisms (Mann, 1973; Dayton et al., 1998; Miller et al., 2011; Krumhansl and Scheibling, 2012; Pedersen et al., 2012) which provide a 3-dimensional habitat for various fauna and flora (Anderson et al., 1997; Leliaert et al., 2000; Steneck et al., 2002; Norderhaug et al., 2012; Krumhansl et al., 2016). Kelps are also capable of altering the local wave and light environment by wave dampening (Mork, 1996; Ma et al., 2013; Monismith et al., 2022) and shading the understorey habitat (Duggins et al., 1990; Watanabe et al., 1992; Clark et al., 2004), as well as providing important organic subsidy through erosion of fronds and fragmentation of plant structures (Krumhansl and Scheibling, 2012; De Bettignies et al., 2013; Simonson et al., 2015; Filbee-Dexter et al., 2018; Ramirez-Llodra et al., 2021). Due to kelps' ecological role in the nearshore, they are regarded as ecological engineers as well as important influencers of biodiversity along temperate shorelines (Graham, 2004; Fowler-Walker et al., 2005; Wing et al., 2007; Wernberg and Goldberg, 2008; Harley et al., 2012; Smale and Moore, 2017). Kelps are also important from a socio-economic perspective, as they provide habitats for economically important species such as abalone and rock lobster (Vásquez et al., 2014;

Blamey and Bolton, 2018) and are harvested for various uses, ranging from feed for the aquaculture sector (Troell et al., 2006) to pharmaceuticals (Smit 2004).

Kelps' ecological and socio-economic contributions are not limited to their local environment. During times of high wave energy, kelp can become dislodged from the substrate (Seymour et al., 1989; Thomsen et al., 2004) and are transported via ocean currents, eventually deposited on beaches or offshore areas (Hobday, 2000a). The kelp deposited on beaches provides important organic subsidies for coastal invertebrate communities (Griffiths et al., 1983; Michaud et al., 2019; Gilson et al., 2021), as well as a resource which can be harvested for economic purposes (Kirkman and Kendrick, 1997; Troell et al., 2006; Holden et al., 2018). Along with the organic input are 'hitchhikers,' which are organisms that remain attached during offshore transport once dislodged (Highsmith, 1985; Holmquist, 1994; Thiel and Gutow, 2005; Macaya et al., 2016). The transport of other organisms attached to kelp is regarded as important regarding invasive species intrusion (Lewis et al., 2005; McCormick et al., 2008; Nikula et al., 2010; Batista et al., 2018) and marine connectivity (Ingólfsson 1995). Kelps which are transported offshore can become entangled to form a kelp raft, providing habitat complexity in the pelagic environment for various fish species (Kingsford, 1992; Kingsford, 1995). However, there is no clear mechanism for kelp raft formation. The structural integrity of individual kelp or rafts will degrade over time through a combination of biotic and abiotic factors, which ultimately results in sinking (Smith, 2002; Thiel and Gutow, 2005; Graiff et al., 2016; Macaya et al., 2016). Once settled on the seafloor, the kelp will degrade further over time resulting in organic input into offshore areas, which may be transported back towards the coast through upwelling processes (Krumhansl and Scheibling, 2012; Dyer et al., 2019).

Understanding the distribution patterns of macroalgae in the ocean and the underlying oceanographic processes influencing trajectory has received much attention in the literature. Approaches such as radio-tagged kelp rafts (Harrold and Lisin, 1989), geological forms in holdfasts (Waters et al., 2018), genetic approaches (Nikula et al., 2013; Waters et al., 2018; Craw and Waters, 2018), the presence of region-specific epibionts on beach-cast kelp (Fraser et al., 2011), and Lagrangian approaches (Putman et al., 2018, 2020; Brooks et al., 2019) have helped to shed light on the processes involved in macroalgal transport. Ocean currents are the main influencer of trajectory as well as drag and windage, which is the direct effect of wind on a floating object (Furnans et al., 2008; Beron-Vera et al., 2016; Trinanes et al., 2016; D'Asaro et al., 2018; Gates et al., 2018; Onink et al., 2019; Shen et al., 2019). The previous chapter (see Chapter 3) has numerically established the importance of both hydrodynamic and wind drag in entrainment patterns within oceanographic mesoscale processes, more specifically eddies.

Although the past research concerning the transport of kelp has greatly improved our understanding of such processes, limitations and gaps still exist. For example, kelps are highly morphologically

diverse, which may influence buoyancy and overall drag characteristics. Morphological characteristics, sea surface temperatures, and light also influence the time kelp remains afloat at the surface (known as raft-time). Macroalgal rafts also vary significantly in size, and studies investigating a specific raft size limit our understanding of that scenario as the findings cannot be inferred for other sizes of kelp rafts. Finally, it has been well established that morphological characteristics of macroalgae are influenced by local abiotic factors, which can vary greatly along coastlines. Although factors such as light, turbidity, and nutrients have been shown to influence macroalgae morphology; temperature and waves are regarded as the prominent influencers (Hurd, 2000; Denny and Gaylord, 2002; Thomsen et al., 2004; Fowler-Walker et al., 2005; Wernberg and Thomsen, 2005; Mabin et al., 2013; Coppin et al., 2020; Bekkby et al., 2014). How the variable response in morphological characteristics influences sink rates, buoyancy, and drag is also yet to be established. There is also no current work where rafts may form on the surface. It is most likely that eddies might play a role in this regard, as they have been shown to cause the collection of other types of flotsams at the surface via entrainment (D'Asaro et al., 2018; Brach et al., 2018; Onink et al., 2019). For example, a study by Beron-Vera et al. (2019) showed that the inclusion of inertia in numerical experiments resulted in entrainment patterns of flotsam in eddies which are more closely reflected in observational data.

A better understanding of the distribution of floating kelp and the ocean processes involved will aid in understanding the broader ecological role that kelp plays in the marine environment but will also be useful for coastal management and harvesting activities. My aims are to shed light on the distribution patterns of floating kelp by a series of Lagrangian individual particle tracking numerical experiments. This approach will allow for the morphological characteristics that vary with the local temperature and wave environment to be accounted for. In addition, since individual kelp has a higher probability of dislodgement compared to kelp in which holdfasts are clustered together, an individual-based approach will reflect real-world scenarios (Thomsen et al., 2004). The approach of including hydrodynamic and wind drag based on site-specific morphological characteristics in Chapter 3 will be used and the current work will build on this approach by the inclusion of morphological-specific buoyancy and sinking rates. In the current chapter I will also seek to investigate the role of mesoscale features as accumulation areas on the surface, which may act as 'kelp raft formation zones' in the open ocean, as well as the role of mesoscale features as barriers to offshore transport.

4.2 Methods

4.2.1 Study site

The same study region used in chapter 3 was used for the current chapter. The reader is referred to section Chapter 3, Methods, Study site section 3.2.1 in the previous chapter for a detailed overview of the regional oceanographic processes. The extent of the study domain and release site locations are presented in Figure 4:1.

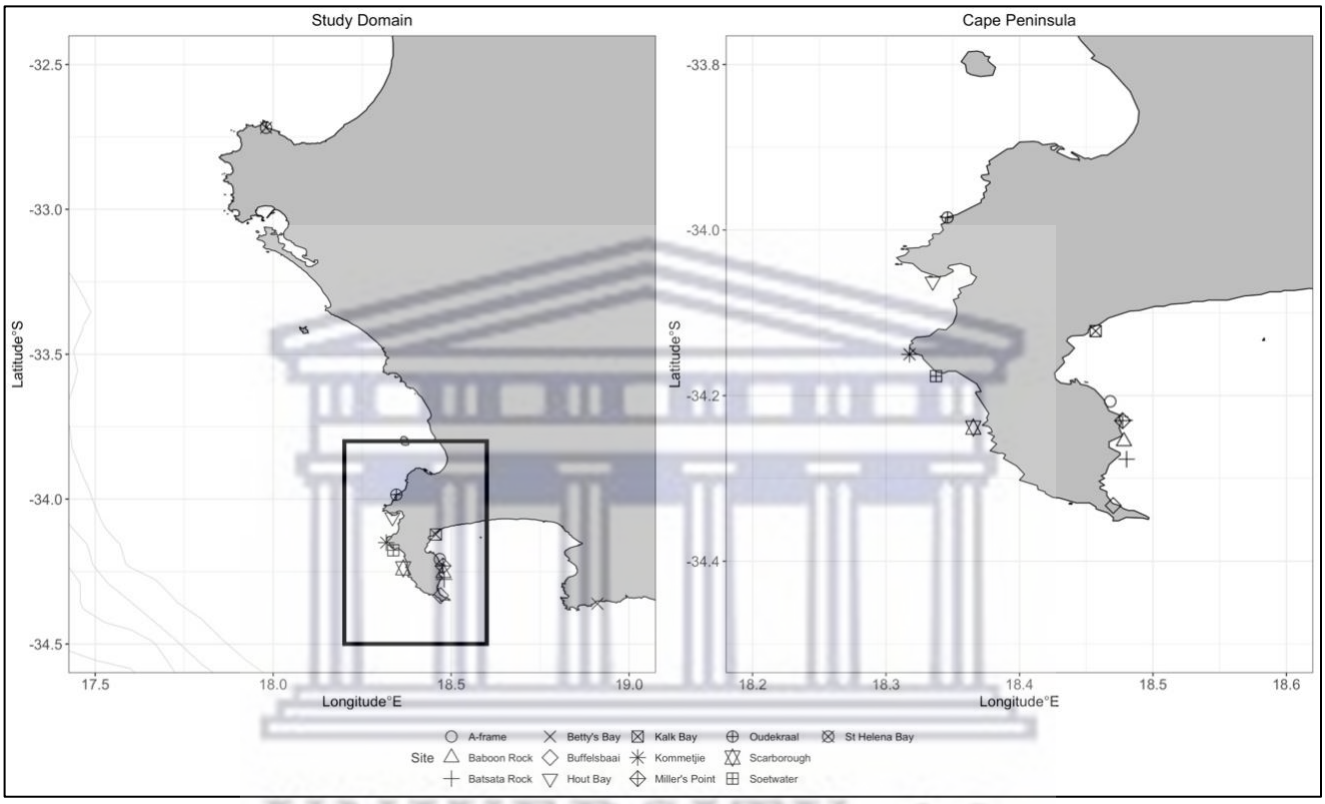

Figure 4:1 Map of the study domain and location of release sites to act as a reference for the reader. The map on the left covers the extent of the study domain and the right image covers the Cape Peninsula. Different shapes have been used to represent the various release sites. Faint grey lines represent the various bathymetry layers.

4.2.2 Simulations

Simulations used daily outputs of velocity vectors (meridional and zonal) and salinity (*psu*) for varying depths for the study region. The reader is referred to the 'Flow models' of Chapter 3 section 3.2.4.2 for details pertaining to underlying ocean and wind models used. To account for the role of morphological characteristics in influencing drift trajectory in terms of hydrodynamic and wind drag, as identified in Chapter 3, simulations were run separately for each site per season. Morphological characteristics of macroalgae have been shown to be based on the local wave and temperature environment, hence the need for site-specific parameters with regards to morphological characteristics. Running simulations per season allowed incorporation of seasonal raft-times identified in previous work Graiff et al. (2013). The outputs from each simulation (site) were pooled based on season. Passive simulations (purely Lagrangian) were executed for the same time-periods

with sinking and beaching parameters and are provided in the Appendix for comparison (Figures A3 & A4).

Simulations were run using the OceanParcels software (available from https://oceanparcels.org/). All simulations were run using a Runge-Kutta fourth order advection scheme, while custom kernels simulated the effects of hydrodynamic and wind drag on overall trajectory, seasonal raft-times, sinking and settling on seafloor of virtual kelp particles—i.e., all important processes in the determination of surface accumulation and bottom sinks. The simulations were run for two years, which were divided into the relevant seasons. For incorporating drag, the site-specific buoyancy calculations were used to determine the magnitude of hydrodynamic (portion below surface) and wind (portion above the surface) while virtual kelp particles were on the surface and then converted to full hydrodynamic drag exposure (100%) once the virtual kelp started sinking, as wind would no longer act as a direct influencer of trajectory once below the ocean surface.

Although OceanParcels is a robust and flexible tool, it does have some limitations when combining mixed fields of wind and ocean vectors. Essentially, problems arise when including wind fields with ocean vector fields when simulations include sinking. This creates limitations when running simulations and requires the approach to be adapted. It was decided to incorporate a similar approach used in previous work by Putman et al. (2018, 2020) and Jutzeler et al. (2020) who used a percentage of the wind field as an estimate for windage. Although estimating windage directly from the wind field is not possible in this instance, a general estimate of windage based on 50% of the surface current vector field was used, which has been used in previous work investigating trajectory patterns of pumice flotsam (Bryan et al., 2004). Therefore, the total potential wind was estimated as 50% of the current speed to attain the velocity vectors for the estimated wind field, which was then used to calculate the total effect of windage based on buoyancy characteristics (magnitude of surface area exposed to wind and hydrodynamic drag respectively).

Kelp floating on the surface of the ocean will begin to sink once the structural integrity of air-filled structures of the plants fails and become flooded. It is also possible for sinking to begin due to an increase in epibiont biomass which overwhelms the buoyancy of kelp; however, this is beyond the scope of this study. The target species of this study, *Ecklonia maxima* (Osbeck) Papenfuss, contains a hollow stipe and a single air-filled pneumatocyst which acts to keep the plant upright in the water

Table 4:1 Summary of the simulations run for the study. Simulations were run for each site over the course of 2 years and then pooled based on season for each year. The start of each year was the beginning of Austral summer.

Site	Lon	Lat	Season	Year	Start date	End date	Runtime	Ac (m^2)	Mass (kg)	Volume (m^3)
Soetwater	18,33	-34,17	Summer	Year 1	2017-12-01	2018-02-28	89	16,657	7,68	5,568,850
Soetwater	18,33	-34,17	Autumn	Year 1	2018-03-01	2018-05-31	91			
Soetwater	18,33	-34,17	Winter	Year 1	2018-06-01	2018-08-31	91			

Soetwater	18,33	-34,17	Spring	Year 1	2018-09-01	2018-11-30	91			
Soetwater	18,33	-34,17	Summer	Year 2	2018-12-01	2019-02-28	89			
Soetwater	18,33	-34,17	Autumn	Year 2	2019-03-01	2019-05-31	91			
Soetwater	18,33	-34,17	Winter	Year 2	2019-06-01	2019-08-31	91			
Soetwater	18,33	-34,17	Spring	Year 2	2019-09-01	2019-11-30	91			
St Helena Bay	17.98	-32,71	Summer	Year 1	2017-12-01	2018-02-28	89	2,411	1,835	878,191
St Helena Bay	17.98	-32,71	Autumn	Year 1	2018-03-01	2018-05-31	91			
St Helena Bay	17.98	-32,71	Winter	Year 1	2018-06-01	2018-08-31	91			
St Helena Bay	17.98	-32,71	Spring	Year 1	2018-09-01	2018-11-30	91			
St Helena Bay	17.98	-32,71	Summer	Year 2	2018-12-01	2019-02-28	89			
St Helena Bay	17.98	-32,71	Autumn	Year 2	2019-03-01	2019-05-31	91			
St Helena Bay	17.98	-32,71	Winter	Year 2	2019-06-01	2019-08-31	91			
St Helena Bay	17.98	-32,71	Spring	Year 2	2019-09-01	2019-11-30	91			
Kommetjie	18.31	-34,15	Summer	Year 1	2017-12-01	2018-02-28	89	31,055	4,865	10,382,923
Kommetjie	18.31	-34,15	Autumn	Year 1	2018-03-01	2018-05-31	91			
Kommetjie	18.31	-34,15	Winter	Year 1	2018-06-01	2018-08-31	91			
Kommetjie	18.31	-34,15	Spring	Year 1	2018-09-01	2018-11-30	91			
Kommetjie	18.31	-34,15	Summer	Year 2	2018-12-01	2019-02-28	89			
Kommetjie	18.31	-34,15	Autumn	Year 2	2019-03-01	2019-05-31	91			
Kommetjie	18.31	-34,15	Winter	Year 2	2019-06-01	2019-08-31	91			
Kommetjie	18.31	-34,15	Spring	Year 2	2019-09-01	2019-11-30	91			
Hout Bay	18.33	-34,06	Summer	Year 1	2017-12-01	2018-02-28	89	14,499	5,105	4,880,537
Hout Bay	18.33	-34,06	Autumn	Year 1	2018-03-01	2018-05-31	91			
Hout Bay	18.33	-34,06	Winter	Year 1	2018-06-01	2018-08-31	91			
Hout Bay	18.33	-34,06	Spring	Year 1	2018-09-01	2018-11-30	91			
Hout Bay	18.33	-34,06	Summer	Year 2	2018-12-01	2019-02-28	89			
Hout Bay	18.33	-34,06	Autumn	Year 2	2019-03-01	2019-05-31	91			
Hout Bay	18.33	-34,06	Winter	Year 2	2019-06-01	2019-08-31	91			
Hout Bay	18.33	-34,06	Spring	Year 2	2019-09-01	2019-11-30	91			
Scarborough	18.36	-34,23	Summer	Year 1	2017-12-01	2018-02-28	89	8,9	3,55	3,016,072
Scarborough	18.36	-34,23	Autumn	Year 1	2018-03-01	2018-05-31	91			
Scarborough	18.36	-34,23	Winter	Year 1	2018-06-01	2018-08-31	91			
Scarborough	18.36	-34,23	Summer	Year 2	2018-12-01	2019-02-28	89			
Scarborough	18.36	-34,23	Autumn	Year 2	2019-03-01	2019-05-31	91			
Scarborough	18.36	-34,23	Winter	Year 2	2019-06-01	2019-08-31	91			
Scarborough	18.36	-34,23	Spring	Year 2	2019-09-01	2019-11-30	91			
Scarborough	18.36	-34,23	Spring	Year 1	2018-09-01	2018-11-30	91			
Oudekraal	18.34	-33,98	Summer	Year 1	2017-12-01	2018-02-28	89	5,175	340	1,783,155
Oudekraal	18.34	-33,98	Autumn	Year 1	2018-03-01	2018-05-31	91			
Oudekraal	18.34	-33,98	Winter	Year 1	2018-06-01	2018-08-31	91			
Oudekraal	18.34	-33,98	Spring	Year 1	2018-09-01	2018-11-30	91			
Oudekraal	18.34	-33,98	Summer	Year 2	2018-12-01	2019-02-28	89			
Oudekraal	18.34	-33,98	Autumn	Year 2	2019-03-01	2019-05-31	91			
Oudekraal	18.34	-33,98	Winter	Year 2	2019-06-01	2019-08-31	91			
Oudekraal	18.34	-33,98	Spring	Year 2	2019-09-01	2019-11-30	91			
Betty's Bay	18.91	-34,36	Summer	Year 1	2017-12-01	2018-02-28	89	20,636	470	6,918,617
Betty's Bay	18.91	-34,36	Autumn	Year 1	2018-03-01	2018-05-31	91			
Betty's Bay	18.91	-34,36	Winter	Year 1	2018-06-01	2018-08-31	91			
Betty's Bay	18.91	-34,36	Spring	Year 1	2018-09-01	2018-11-30	91			
Betty's Bay	18.91	-34,36	Summer	Year 2	2018-12-01	2019-02-28	89			
Betty's Bay	18.91	-34,36	Autumn	Year 2	2019-03-01	2019-05-31	91			
Betty's Bay	18.91	-34,36	Winter	Year 2	2019-06-01	2019-08-31	91			

Betty's Bay	18.91	-34,36	Spring	Year 2	2019-09-01	2019-11-30	91			
Kalk Bay	18.45	-34,12	Summer	Year 1	2017-12-01	2018-02-28	89	9,074	3,875	3,092,212
Kalk Bay	18.45	-34,12	Autumn	Year 1	2018-03-01	2018-05-31	91			
Kalk Bay	18.45	-34,12	Winter	Year 1	2018-06-01	2018-08-31	91			
Kalk Bay	18.45	-34,12	Spring	Year 1	2018-09-01	2018-11-30	91			
Kalk Bay	18.45	-34,12	Summer	Year 2	2018-12-01	2019-02-28	89			
Kalk Bay	18.45	-34,12	Autumn	Year 2	2019-03-01	2019-05-31	91			
Kalk Bay	18.45	-34,12	Winter	Year 2	2019-06-01	2019-08-31	91			
Kalk Bay	18.45	-34,12	Spring	Year 2	2019-09-01	2019-11-30	91			
A-frame	18,46	-34,20	Summer	Year 1	2017-12-01	2018-02-28	89	7,83	3,875	2,674,925
A-frame	18,46	-34,20	Autumn	Year 1	2018-03-01	2018-05-31	91			
A-frame	18,46	-34,20	Winter	Year 1	2018-06-01	2018-08-31	91			
A-frame	18,46	-34,20	Spring	Year 1	2018-09-01	2018-11-30	91			
A-frame	18,46	-34,20	Summer	Year 2	2018-12-01	2019-02-28	89			
A-frame	18,46	-34,20	Autumn	Year 2	2019-03-01	2019-05-31	91			
A-frame	18,46	-34,20	Winter	Year 2	2019-06-01	2019-08-31	91			
A-frame	18,46	-34,20	Spring	Year 2	2019-09-01	2019-11-30	91			
Miller's Point	18.47	-34,23	Summer	Year 1	2017-12-01	2018-02-28	89	8,327	3,845	2,835,901
Miller's Point	18.47	-34,23	Autumn	Year 1	2018-03-01	2018-05-31	91			
Miller's Point	18.47	-34,23	Winter	Year 1	2018-06-01	2018-08-31	91			
Miller's Point	18.47	-34,23	Spring	Year 1	2018-09-01	2018-11-30	91			
Miller's Point	18.47	-34,23	Summer	Year 2	2018-12-01	2019-02-28	89			
Miller's Point	18.47	-34,23	Autumn	Year 2	2019-03-01	2019-05-31	91			
Miller's Point	18.47	-34,23	Winter	Year 2	2019-06-01	2019-08-31	91			
Miller's Point	18.47	-34,23	Spring	Year 2	2019-09-01	2019-11-30	91			
Buffelsbaai	18.47	-34,33	Summer	Year 1	2017-12-01	2018-02-28	89	4,361	2,97	1,523,592
Buffelsbaai	18.47	-34,33	Autumn	Year 1	2018-03-01	2018-05-31	91			
Buffelsbaai	18.47	-34,33	Winter	Year 1	2018-06-01	2018-08-31	91			
Buffelsbaai	18.47	-34,33	Spring	Year 1	2018-09-01	2018-11-30	91			
Buffelsbaai	18.47	-34,33	Summer	Year 2	2018-12-01	2019-02-28	89			
Buffelsbaai	18.47	-34,33	Autumn	Year 2	2019-03-01	2019-05-31	91			
Buffelsbaai	18.47	-34,33	Winter	Year 2	2019-06-01	2019-08-31	91			
Buffelsbaai	18.47	-34,33	Spring	Year 2	2019-09-01	2019-11-30	91			
Batsata Rock	18.48	-34,27	Summer	Year 1	2017-12-01	2018-02-28	89	15,546	6,85	5,224,027
Batsata Rock	18.48	-34,27	Autumn	Year 1	2018-03-01	2018-05-31	91			
Batsata Rock	18.48	-34,27	Winter	Year 1	2018-06-01	2018-08-31	91			
Batsata Rock	18.48	-34,27	Spring	Year 1	2018-09-01	2018-11-30	91			
Batsata Rock	18.48	-34,27	Summer	Year 2	2018-12-01	2019-02-28	89			
Batsata Rock	18.48	-34,27	Autumn	Year 2	2019-03-01	2019-05-31	91			
Batsata Rock	18.48	-34,27	Winter	Year 2	2019-06-01	2019-08-31	91			
Batsata Rock	18.48	-34,27	Spring	Year 2	2019-09-01	2019-11-30	91			
Baboon Rock	18.47	-34,25	Summer	Year 1	2017-12-01	2018-02-28	89	7,612	5,15	3,844,252
Baboon Rock	18.47	-34,25	Autumn	Year 1	2018-03-01	2018-05-31	91			
Baboon Rock	18.47	-34,25	Winter	Year 1	2018-06-01	2018-08-31	91			
Baboon Rock	18.47	-34,25	Spring	Year 1	2018-09-01	2018-11-30	91			
Baboon Rock	18.47	-34,25	Summer	Year 2	2018-12-01	2019-02-28	89			
Baboon Rock	18.47	-34,25	Autumn	Year 2	2019-03-01	2019-05-31	91			
Baboon Rock	18.47	-34,25	Winter	Year 2	2019-06-01	2019-08-31	91			
Baboon Rock	18.47	-34,25	Spring	Year 2	2019-09-01	2019-11-30	91			

column, allowing the light-saturated surface waters to be reached. These structures also cause the plant to float if dislodged and therefore were considered when calculating the overall volume of the

plant; this, in turn, was used to calculate other important parameters (buoyancy, drag, and sink rate). Details about the simulations executed are presented in Table 4:1.

4.2.3 Morphological characteristics

Morphological characteristics of kelp are influenced by local wave and temperature conditions, which in turn will influence buoyancy, drag, and sinking parameters. Kelp morphological data were garnered from a previous study by Coppin et al. (2020). The assumption made is that the largest kelp (largest surface area) was the most likely to be dislodged from the substrate, therefore only maximum surface areas were garnered from the data. In instances where the morphological data needed were not available, reasonable estimates were used based on previous studies and experience.

The hollowness of *E. maxima* has been investigated as a part of a previously by Rothman et al. (2017a) who showed that the relative hollowness did not significantly differ among sites, with 86-90% of the total stipe length containing air. Therefore, based on these results, it is assumed that *E. maxima* individuals will exbibit the same degree of hollowness amongst populations along South African coastline.

An estimate of stipe thickness of the hollow sections was used in conjunction with the 90% of the stipe length shown by Rothman et al. (2017a) to calculate a reasonable estimate for the volume of air in the stipe. This is an important aspect as it directly effects the buoyancy of an individual floating kelp which ultimately determines the magnitude of exposure to hydrodynamic and wind drag. To calculate the surface area and volume for kelp from each site, geometric shapes were used which most closely matched the shape of the relevant kelp morphological characteristics as per Chapter 3. Unlike in Chapter 3, additional parameters were included, which were buoyancy and sinking rate. The total surface area used for each of the virtual kelps from release sites are presented in Table 4:2.

Table 4:2 Table of morphological attributes used.

Site	Frond mass (kg)	Primary blade length (cm)	Primary blade width (cm)	Frond length (cm)	Stipe mass (kg)	Stipe length (cm)	Stipe circumference (mm)
A-Frame	5.00	22.5	20.0	181	8.75	541	30
Baboon Rock	7.50	26.0	17.0	228	6.50	645	27
Batsata Rock	10.00	29.0	22.5	250	8.50	746	36
Betty's Bay	6.25	21.0	24.0	239	9.50	805	40
Buffelsbaai	3.90	21.0	9.0	170	6.30	676	20

Hout Bay	7.10	32.0	22.5	232	8.45	593	39
Kalk Bay	5.25	19.0	19.0	165	7.25	490	34
Kommetjie	6.80	29.0	37.0	245	7.85	587	57
Miller's Point	5.20	25.0	22.0	200	7.25	574	30
Oudekraal	4.90	28.0	20.0	220	4.60	330	31
Scarborough	4.90	27.0	16.0	241	5.95	402	37
Soetwater	11.20	49.5	25.0	335	9.60	676	39
St Helena Bay	2.65	30.0	19.0	164	2.45	333	21
Site	**No. of Tufts**	**Epiphyte length (cm)**	**Total length (cm)**	**Stipe radius (cm)**	**Frond width (cm)**	**Frond thickness (cm)**	**Bulb length (cm)**
A-Frame	10	508	668.0	4.77	5	0.2	10
Baboon Rock	11	639	873.0	4.30	5	0.2	10
Batsata Rock	10	770	944.0	5.73	5	0.2	10
Betty's Bay	15	725	1 041.0	6.36	5	0.2	10
Buffelsbaai	11	157	846.0	3.18	5	0.2	10
Hout Bay	9	473	614.0	6.21	5	0.2	10
Kalk Bay	9	442	638.0	5.41	5	0.2	10
Kommetjie	11	527	616.0	9.15	5	0.2	10
Miller's Point	10	500	745.0	4.77	5	0.2	10
Oudekraal	7	260	514.0	4.93	5	0.2	10
Scarborough	9	387	422.0	5.88	5	0.2	10
Soetwater	15	640	697.5	6.21	5	0.2	10
St Helena Bay	7	306	353.5	3.34	5	0.2	10
Site	**Bulb base radius (cm)**	**Top radius (cm)**	**Bottom radius (cm)**	**Hollow radius (cm)**	**Hollow length (cm)**	**Height (cm)**	**Hollow Volume (cm^3)**
A-Frame	5	3	10	2.91	486.9	5	12 975
Baboon Rock	5	3	10	2.62	580.5	5	12 530
Batsata Rock	5	3	10	3.50	671.4	5	25 765
Betty's Bay	5	3	10	3.88	724.5	5	34 324
Buffelsbaai	5	3	10	1.94	608.4	5	7 206
Hout Bay	5	3	10	3.79	533.7	5	24 036
Kalk Bay	5	3	10	3.30	441.0	5	15 095
Kommetjie	5	3	10	5.58	528.3	5	51 720
Miller's Point	5	3	10	2.91	516.6	5	13 767
Oudekraal	5	3	10	3.01	297.0	5	8 451
Scarborough	5	3	10	3.59	361.8	5	14 666
Soetwater	5	3	10	3.78	608.4	5	27 401
St Helena Bay	5	3	10	2.04	299.7	5	3 913

Site	Total Ac (m^2)	Total mass (kg)	Total volume (m^3)	Kelp Volume (m^3)	Kelp density (kg/m^3)		
A-Frame	78	38.75	39724.99	26749	0.001		
Baboon Rock	76	51.50	38442.52	25911	0.002		
Batsata Rock	155	68.50	78005.63	52240	0.001		
Betty's Bay	206	47.00	103510.98	69186.17	0.001		
Buffelsbaai	43	29.70	22442.00	15235.92	0.002		
Hout Bay	144	51.05	72842.11	48805.33	0.001		
Kalk Bay	90	38.75	46017.57	30922.11	0.001		
Kommetjie	310	48.65	155550.14	103829.23	0.001		
Miller's Point	83	38.45	42126.24	28359.00	0.001		
Oudekraal	51	34.00	26282.97	17831.55	0.002		
Scarborough	89	35.35	44827.07	30160.72	0.001		
Soetwater	166	76.80	83089.62	55688.50	0.001		
St Helena Bay	24	18.35	12685.63	8772.04	0.002		

Buoyancy

To effectively model the trajectory of a floating object, buoyancy needs to be calculated. The buoyancy will determine the amount of exposure to, and ultimately magnitude of, hydrodynamic and wind drag which in turn influences the trajectory of the object to the variable current and wind fields (Dietrich, 1982; Kooi et al., 2017; Lobelle et al., 2021). The portion of an object above and below the surface of the water is determined by the net effect of forces acting on the object, namely buoyancy force (BF) and the mass of the object (Dietrich, 1982; Kooi et al., 2017; Lobelle et al., 2021). The BF is the force pushing the object out of the water and the mass is the force pulling the object down. In order to calculate the buoyancy force (BF) the density and volume of the object must be known, such that:

$$BF = p_f V_s g \qquad (4.1)$$

where p_f is the density of the liquid, V_s is the volume of the object submerged, and g is the gravitational acceleration (m/s^2).

The force resulting from the weight of an object can be calculated by $W_f = p_o V_o g$. Substitution of mass for density and volume alters the equation to:

$$W_f = p_o V_o g$$

(4.2)

where p_o is the density of the object, V_o is the total volume of the object and g is gravitational acceleration. An object will only float if the forces acting on it (BF and W_f) are equal, such that:

$$BF = W_f$$

(4.3)

then substituting density and volume results in:

$$p_f V_s g = p_o V_o g$$

(4.4)

which can also be further expressed as:

$$V_s / V_o = p_o / p_f$$

(4.5)

The solution of equation (4.5) results in a unitless fraction that can be expressed as a percentage of the relevant portion submerged. This in turn can be used to calculate the percentage of the object above the surface of the water (exposed to wind). The percentage of the object below and above the water surface was used in the calculation of hydrodynamic and wind drag when the virtual kelp is at the surface, while only hydrodynamic drag is considered for transport when sinking. Since morphological characteristics are influenced by the local wave and temperature environment, the buoyancy of virtual kelp particles may vary from site to site.

4.2.4 Sink rate

The force responsible for the kelp to begin to sink once the structural integrity has been compromised is the mass of the overall plant. The calculation of the force resulting from the mass was based on previous work by Dietrich (1982), Kooi et al., (2017), and Lobelle et al., (2021) such that

$$F_w = (p_s - p_l) g V$$

(4.6)

Where p_s is the density of the particle, p_l the density of the medium, g is the gravitational acceleration constant, and V is the total volume of the particle. To accurately calculate the density of virtual kelp based on volume and mass, the volume of the hollow section of the stipe was subtracted from the overall volume. The target species used for this experiment (*E. maxima*) has an air-filled stipe and therefore the hollowness needs to be accounted for when calculating the overall volume of the stipe. The volume of the kelp is:

$$Volume = V_t - V_h$$

(4.7)

where V_t is the total volume of the stipe if no hollowness is considered and V_h is the hollowness volume of the stipe. The other component of the vertical velocity is the drag force in the opposite direction to the downward force of the weight. The vertical drag component is calculated by the same equation for drag in the horizontal, such that:

$$F_d = 1/2pv^2C_DA_c$$

(4.8)

where p is the density of the medium, v is the velocity at a particular time-step, C_d is the shape drag-coefficient, and A_c is the cross-sectional area of the object. However, unlike surface drag where the velocity is interpolated from the underlying ocean model, the velocity component for the vertical drag force is calculated from the same equation used for hydrodynamic and wind drag. The approach for modelling the 'behaviour' of kelp was used in this paper allows for the incorporation of site-specific morphological characteristics regarding sinking characteristics.

4.2.5 Raft-time

Raft-time, sometimes referred to as raft-longevity, is the time a macroalgal raft remains afloat at the surface of the ocean after detachment before sinking. Raft-time is determined by epibiont load, macroalgal growth rate and the loss of kelp biomass over time through fragmentation. Epibiont load consists of epiphytic and bryozoan species which tend to grow more rapidly in higher light and temperature environments, such as the ocean surface (Smith, 2002; Thiel and Gutow, 2005; Graiff et al., 2013, 2016). The increase in epibiont load reduces the buoyancy of floating macroalgal rafts over time eventually causing them to sink to the seafloor, while also potentially increasing drag (Hobday, 2000b; Tala et al., 2013; Craw and Waters, 2018). Fragmentation of kelp biomass over time may also reduce raft-times further, while growth may counteract the effects of epibiont load and fragmentation provided the environmental conditions are favourable (Graiff et al., 2013, 2016; Macaya et al., 2016). For instance, a study by Rothäusler et al., (2011) investigated the abiotic and biotic factors influencing raft-time and dispersal potential of the giant kelp *Macrocystis pyrifera* (Linnaeus) C. Agardh by a combination of tethering experiments and field surveys. The results showed the physiological performance of kelp declined with increasing epiphyte biomass and that higher temperatures increased the growth rate of epibionts and fragmentation of kelp. The authors concluded from the results of both the experiments and field surveys that *M. pyrifera* dispersal is dependent on low temperature and moderate irradiance conditions, with high temperatures and higher irradiance reducing overall raft-time and hence dispersal potential (Rothäusler et al., 2011). Raft-time was estimated from the results of past studies by Graiff et al., (2016) and Graiff et al.,

(2013) for each season. For summer, the raft-time was 22 days, autumn was 41 days, winter was 38 days, and spring was 33 days.

4.2.6 Analysis

To compare virtual kelp trajectories between sites, trajectories were plotted, and density distribution maps were produced for each phase of the virtual kelp life cycle (surface, subsurface, beached and sunk). Density distribution maps are an effective method for assessing pathways and ocean connectivity (Van Sebille et al., 2018). To aid in seasonal comparison of trajectories, the proportions of each kelp phase at the end of each simulation run was calculated and compared. The different phases were surface, subsurface, beached, sunk and out of bounds.

In addition to the above analyses, the distance particles travelled was also measured and used to produce boxplots to aid in discerning patterns and distributions from the density distribution maps. Distance travelled from the release site can help reveal topographic steering and momentum energy transfer from the wind field to kelp particles (Van Sebille et al., 2018). If the wind direction is in the same direction as the current the virtual particles will cover larger distances due to an increase in the velocity because of momentum energy transfer (Putman et al., 2018, 2020; Van Sebille et al., 2018).

4.3 Results

Overall, the results show that the predominate trajectory of simulated virtual kelp flow north-westward, with the exception of winter months when particles flowed southward or towards the coast. In terms of entrainment patterns, clear accumulation in mesoscale features was evident and also played a role in determining where virtual kelp settles on the seafloor. The results also shed light on the role of mesoscale features may play as barriers to offshore transport outside the study domain, due to the weakening of dynamics on the eastern side of mesoscale features.

4.3.1 Surface distribution

The general direction of particles was north-westward with the exception of winter where direction changed to predominately southward for both years (Figure 4:2). Entrainment within eddies was evident during times of high mesoscale activity, which was summer and winter (Figure 4:2).

The overall particle direction during summer for both years was north-westward. The only visible differences between years 1 and 2 was entrainment of particles in an eddy in year 1, as well as a higher concentration of particles closer to the coast (Figure 4:2). The concentration of particles in the north-westward direction was lower during year 1 of autumn compared to year 2 entrainment patterns (Figure 4:2). During spring of year 1 there was a high concentration of particles flowing in the north-westward direction, and no signs of entrainment (Figure 4:2). During spring of year 2, the

particles were almost evenly spread across the southern portion of the study domain (Figure 4:2). There were also two visible concentrations of particles flowing offshore (Figure 4:2). The first starts at approximately 18°32.8” E and the other at 18°34” E (Figure 4:2).

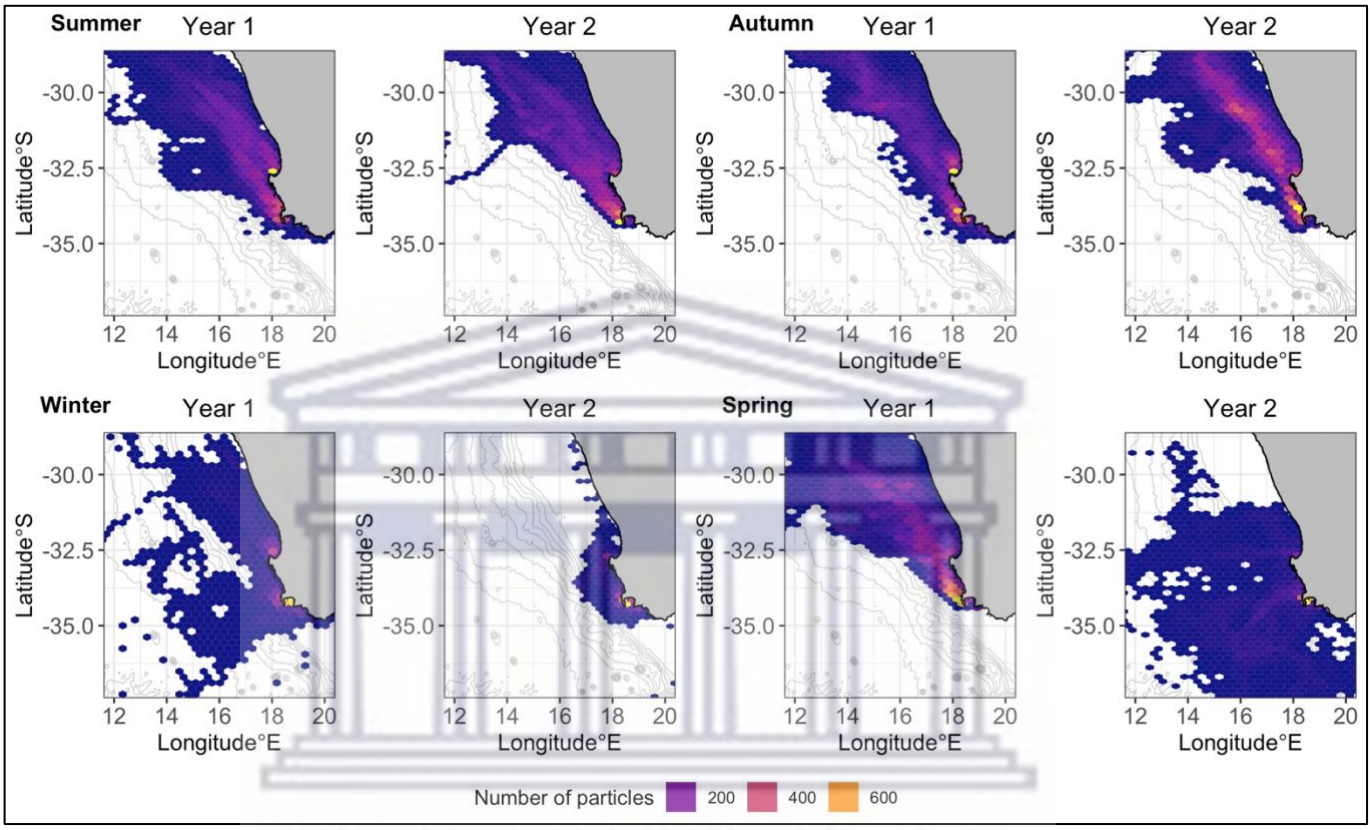

Figure 4:2 Hexagonal heatmaps for all virtual surface kelp for both years and all seasons. The plane has been divided into regular hexagons and then are filled according to the number of particles within each hexagon. Faint grey lines represent the various bathymetry layers.

4.3.2 Subsurface distribution

Differences in concentration patterns for both years and across seasons were evident when comparing subsurface virtual kelp particle distributions (Figure 4:3). In general, particles were located near the north-western part of the study domain with only slight variation across seasons and between years, with the exception of winter and autumn of year 2 where particles were located in the highest concentrations in the south-western portion of the study domain (Figure 4:3).

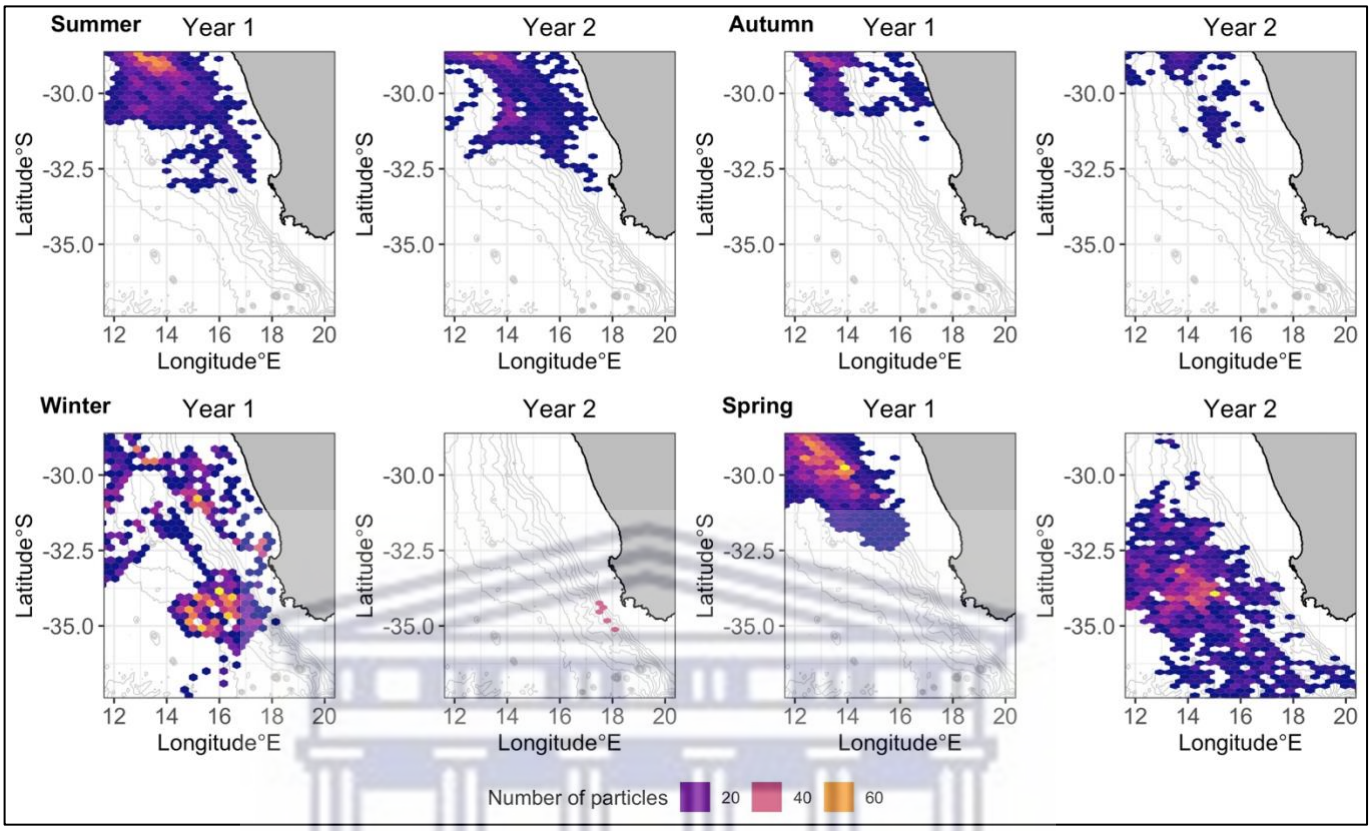

Figure 4:3 Hexagonal heatmaps for all virtual sub-surface kelp for both years and all seasons. The plane has been divided into regular hexagons and then are filled according to the number of particles within each hexagon. Faint grey lines represent the various bathymetry layers.

During the summer of year 1, particles were located between the coast and where the continental shelf edge ends, while in year 2 particles were located further west of the shelf edge and closer to the coast (Figure 4:3). Clear entrainment of particles was visible in year 1, with reduced entrainment during the summer of year 2 (Figure 4:3). No differences in particle concentrations were evident for autumn of both years, with only slight variation in the spread of particles. During autumn of year 1, particles were located close to the coast and spread eastwards with an even distribution (Figure 4:3). In autumn of year 2, particles were located further from the coast compared to year 1 and limited to a narrow band of particles (Figure 4:3). The overall direction of particles and entrainment patterns were different for winter of both years and compared to other seasons, with particle direction towards the south-west of the study domain (Figure 4:3). During winter of year 1, particles were initially concentrated in the north-western and south-western portions of the study domain, the latter with higher concentrations (Figure 4:3). The high concentration of particles in the south-western portion also reflected eddy entrainment patterns (Figure 4:3). The concentration of particles which exited the eddy on the northern side spread evenly (Figure 4:3). For winter of year 2, particles were located south of the peninsula in highly concentrated, limited patches (Figure 4:3).

There were clear differences between particle distribution patterns between years for spring (Figure 4:3). For spring of year 1, particles flowed in a north-westward direction evenly and concentrated in the most north-western portion of the study domain (Figure 4:3). The even distribution occurred over the wider portion of the underlying bathymetry (Figure 4:3). In year 2, particles were highly concentrated in the most southern portion of the study domain (Figure 4:3).

4.3.3 Sunken distribution

Differences in sink locations and concentration of particles were evident between years and across seasons (Figure 4:4). For summer of year 1, particles sank along the seafloor in a north-westward direction, while in year 2 particles were concentrated to a patch in the most northern part of the study domain (Figure 4:4). During autumn of year 1, particles sunk close to the coastline with the

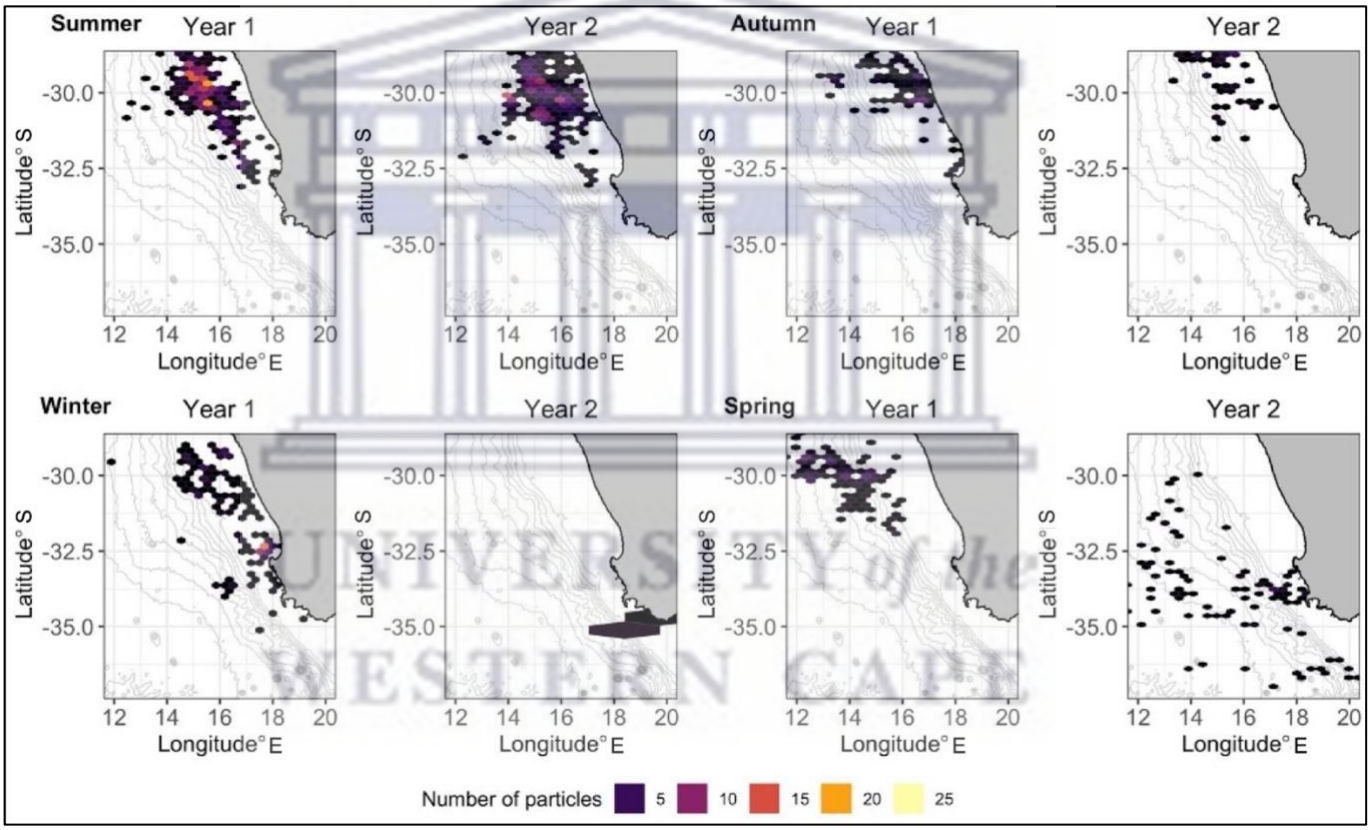

Figure 4:4 Hexagonal heatmaps for all virtual sunken kelp for both years and all seasons. The plane has been divided into regular hexagons and then are filled according to the number of particles within each hexagon. Faint grey lines represent the various bathymetry layers.

highest concentration to the north of the study domain (Figure 4:4). For autumn of year 2, particles were located further offshore with lower concentrations to the north of the study domain (Figure 4:4). For winter of year 1, particles sank close to the coast in the northern part of the study domain with a lower concentration of particles extending southwards along the coast (Figure 4:4). For winter of year 2, particles were concentrated along the eastern part of the coastline and the study domain (Figure 4:4). Particles sunk in the most north-western part of the study domain for Spring of year 1

(Figure 4:4). For year 2, particles were spread out to the south-western portion of the study domain, with no clear differences in concentrations evident (Figure 4:4).

4.3.4 Beached distribution

No clear differences, only variation, were evident for beaching locations and concentrations across all seasons and years, with the exception of winter (Figure 4:5). There was only slight variation between the summer of year 1 and year 2, where fewer concentrations of particles located to the north of St. Helena Bay (Figure 4:5).

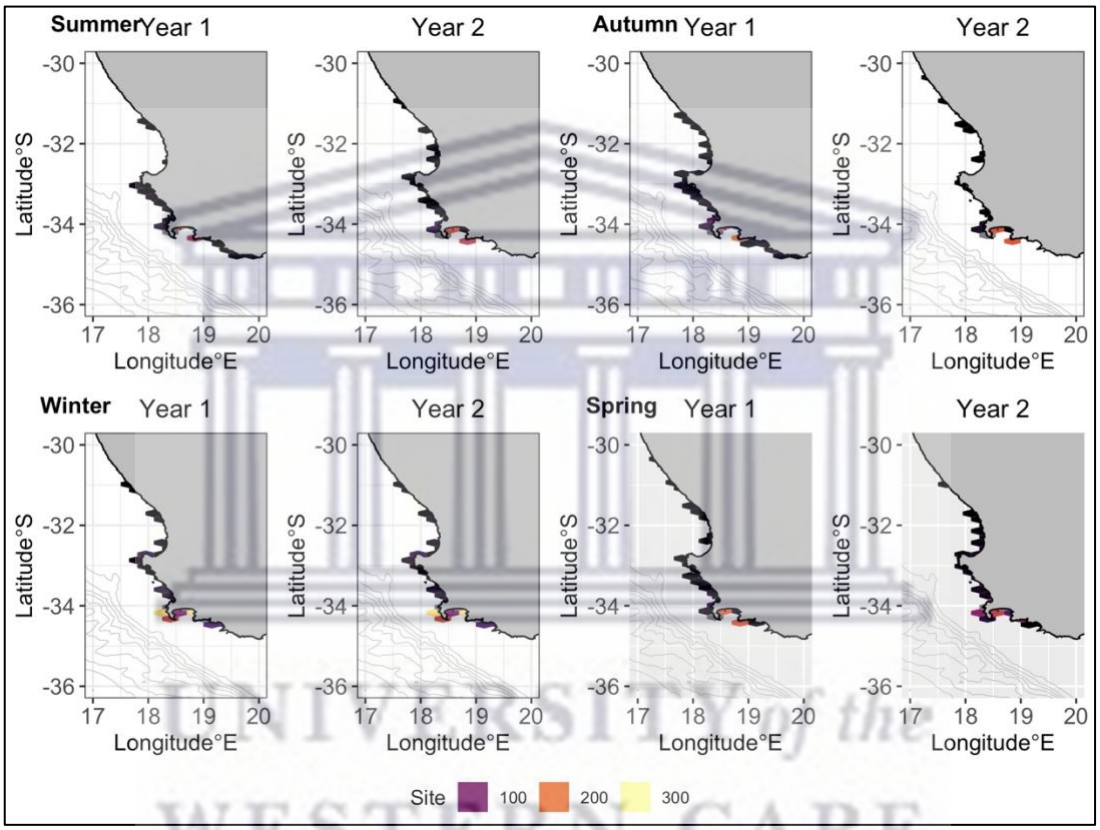

Figure 4:5 Hexagonal heatmaps for all virtual beached kelp for both years and all seasons. The plane has been divided into regular hexagons and then are filled according to the number of particles within each hexagon. Faint grey lines represent the various bathymetry layers.

In year 2, a higher concentration of particles was located north of St. Helena Bay compared to year 1 (Figure 4:5). For winter, no differences were evident in distributions between years, with the highest concentration of particles located around the southern tip of the Cape Peninsula and within False Bay (Figure 4:5).

4.3.5 Surface and sink convergence

In both years and across seasons, site particle trajectories were all directed north-westward with the exception of winter (Figure 4:6). In winter for both years, the general direction of site trajectories was south-eastwards and closer to the Caper Peninsula (Figure 4:6). For both years and across

seasons, the trajectory for particles released from St. Helena Bay flowed separately and did not overlap with the other site trajectories (Figure 4:6). With the exception of Buffelsbaai and Batsata Rock, particles released from sites within False Bay did not tend to travel outside of False Bay (Figure 4:6). Instead, these particles generally beached near release locations, except for during winter when particles travelled and beached on the eastern side of False Bay (Figure 4:6). During summer for both years, particle trajectories were more evenly spread out in the north-western direction, with little overlap between trajectories (Figure 4.6). In autumn and spring for both years, trajectories were concentrated along a narrow band that starts approximately at -34°S (Figure 4:6).

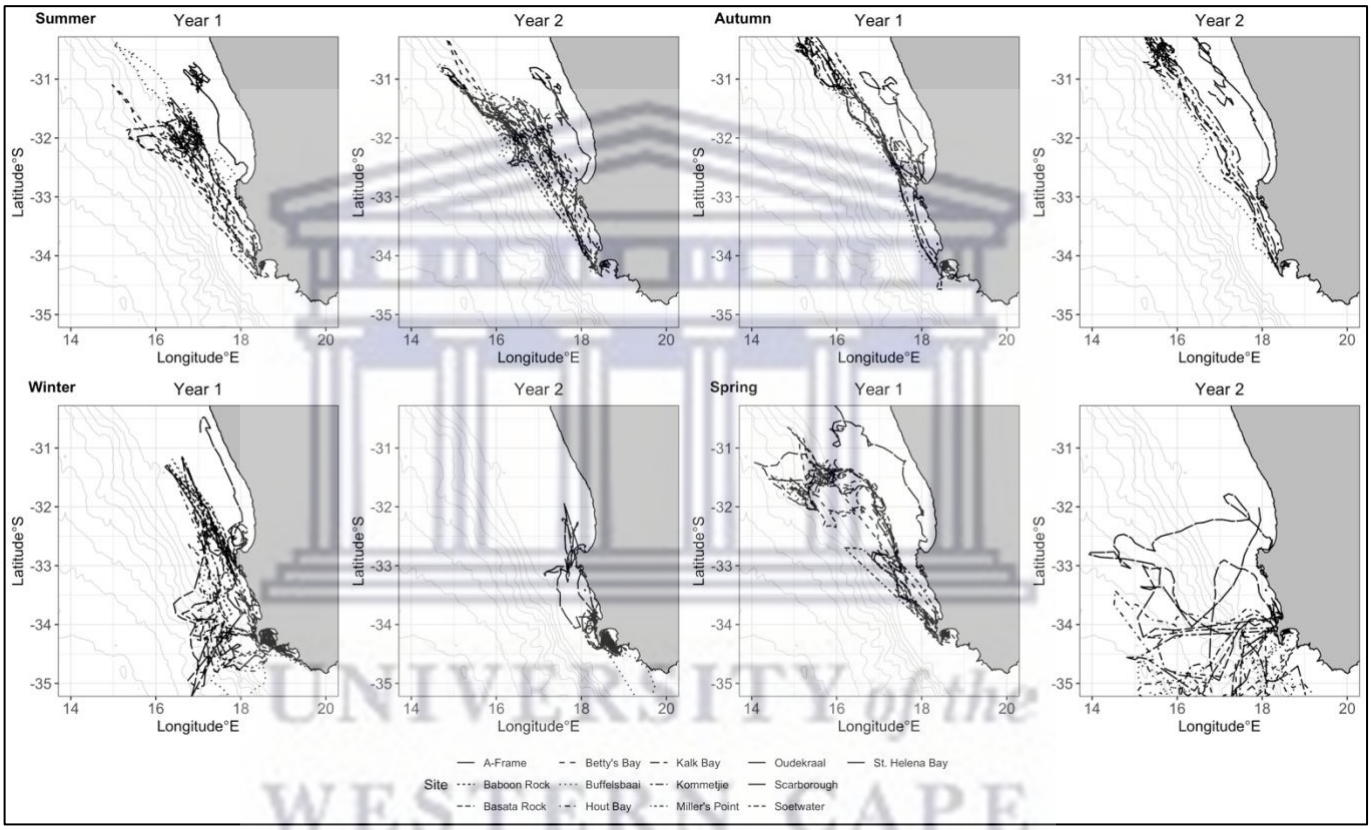

Figure 4:6 The trajectories of all surface virtual kelp for both years and all seasons. The trajectory and the associated release site are represented by the various line types. Faint grey lines represent the various bathymetry layers.

The most overlap of particles occurred during winter for both years, where the flow of trajectories was chaotic and directed towards the south-western portion of the study domain and eastwards along the coastline towards Betty's Bay (Figure 4:6). The distribution and overlap of sites for surface and sunken virtual kelp particles differ across seasons and varies between years (Figure 4:7). For all seasons and years particles released from the various sites generally sank in the same location, with autumn of year 2 the exception as particles were dispersed over the south-western portion of the continental shelf. Some sites from False Bay (Baboon rock, Miller's point, A-frame and Kalk Bay) were absent from sink locations (Figure 4:7).

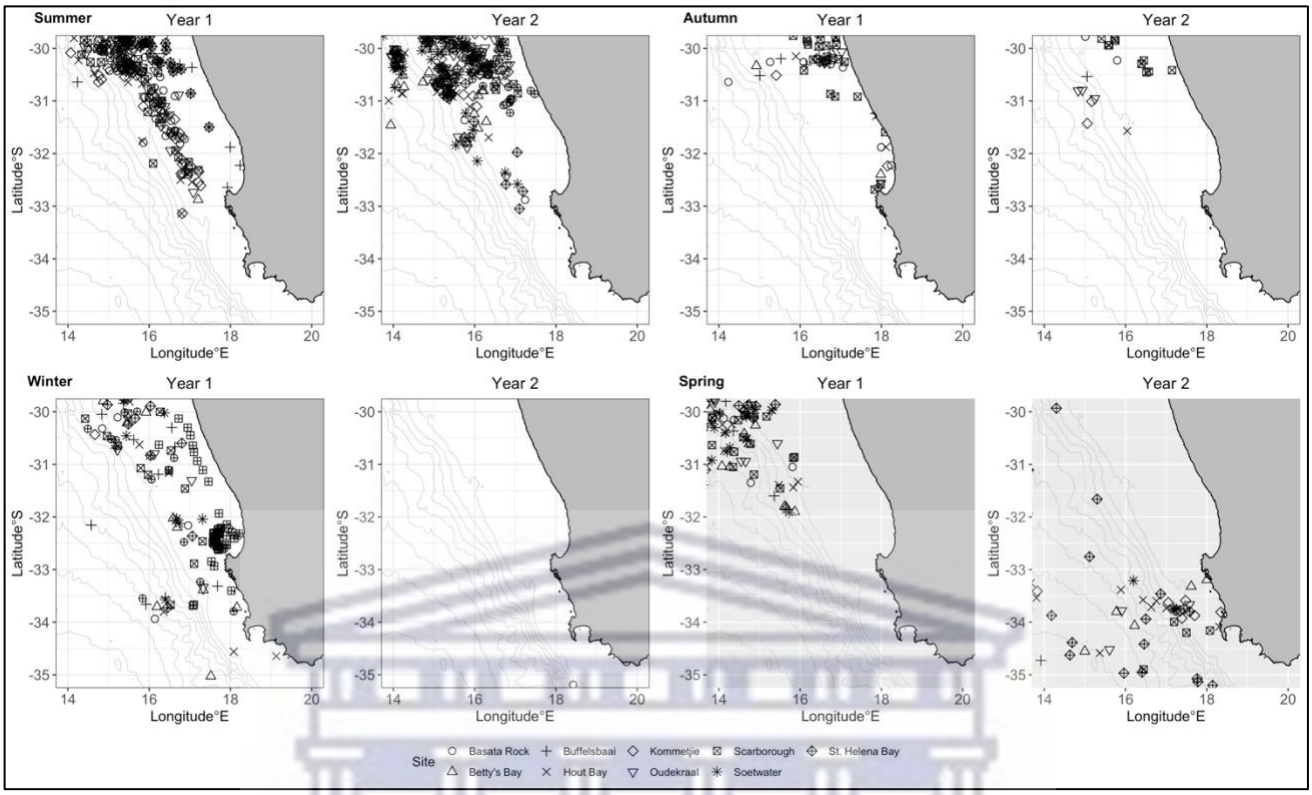

Figure 4:7 The mean point distribution for depth of all surface virtual kelp for both years and all seasons. The surface kelp distributions are grouped per site and are represented by varying shapes. Faint grey lines represent the various bathymetry layers.

Comparison of summer between years shows no differences in sink sites, with the sites mostly located along the north-western part of the study domain; some variation visible (Figure 4:7). In summer of year 1, particles sank in a narrow band east of the continental shelf with more sites converging further north (Figure 4:7). In year 2, particles were concentrated further northward near the end of the study domain and less concentrated along the continental shelf edge. In both years for summer, virtual kelp released from Buffelsbaai settle near St. Helena and close to the coast (Figure 4:7). Variation in sink sites was also evident for autumn between years. In autumn of year 1, most sank in similar locations in a narrow band close to most northern part of the coastline in the study domain (Figure 4:7).

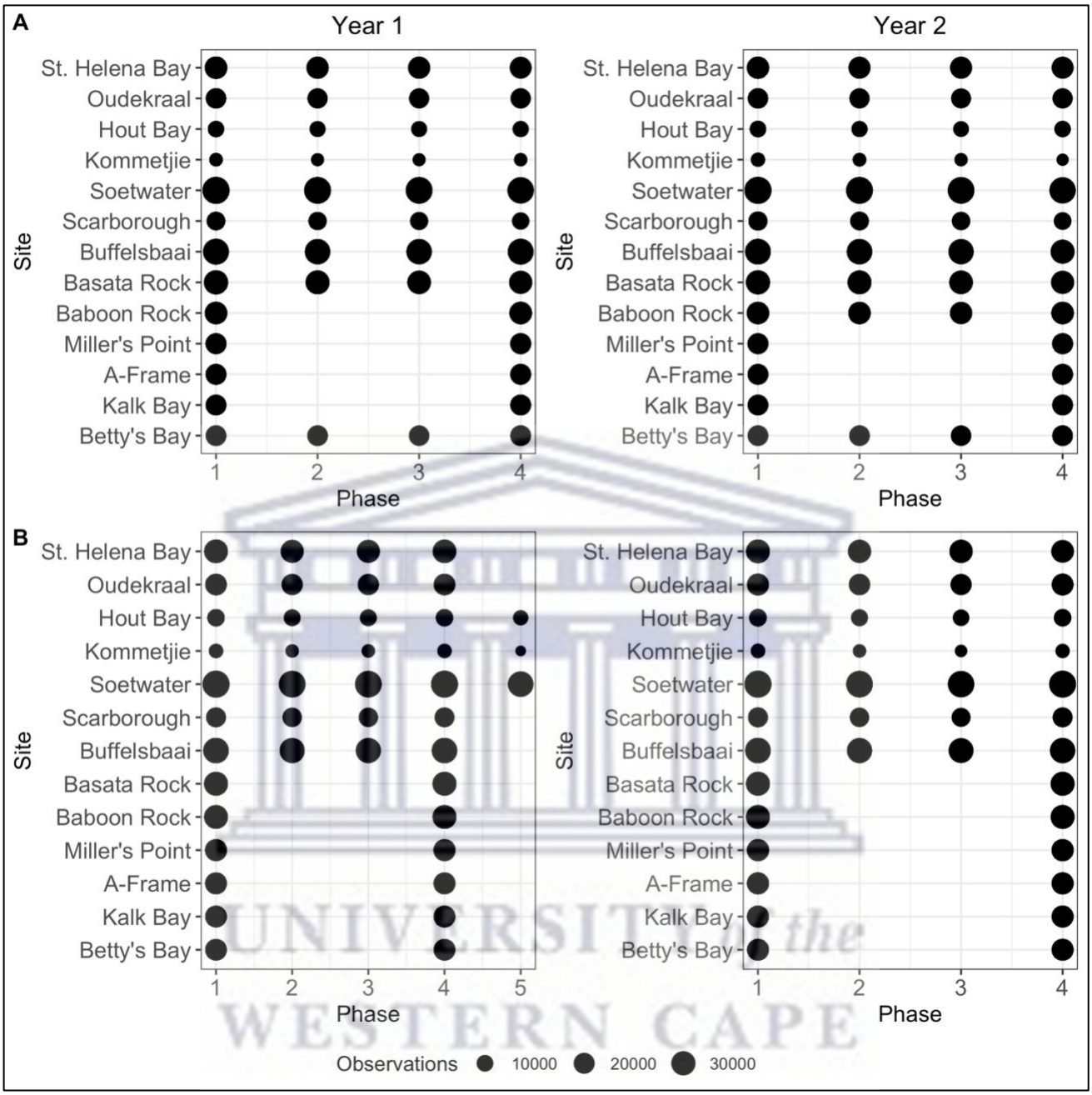

Figure 4:8 Proportion of particles for each phase at the end of the simulation run for Austral summer (row A) and autumn (row B) for each respective year. The size of the point is related to the number of particles within that life cycle phase at the end of each simulation run.

In year 2, particles were still located in the northern domain and were spread to the east of the coastline (Figure 4:7). In winter of year 1 particles sank towards the north-western part of the study domain (Figure 4:7). The virtual kelp from St. Helena Bay sank to the north and separated from the

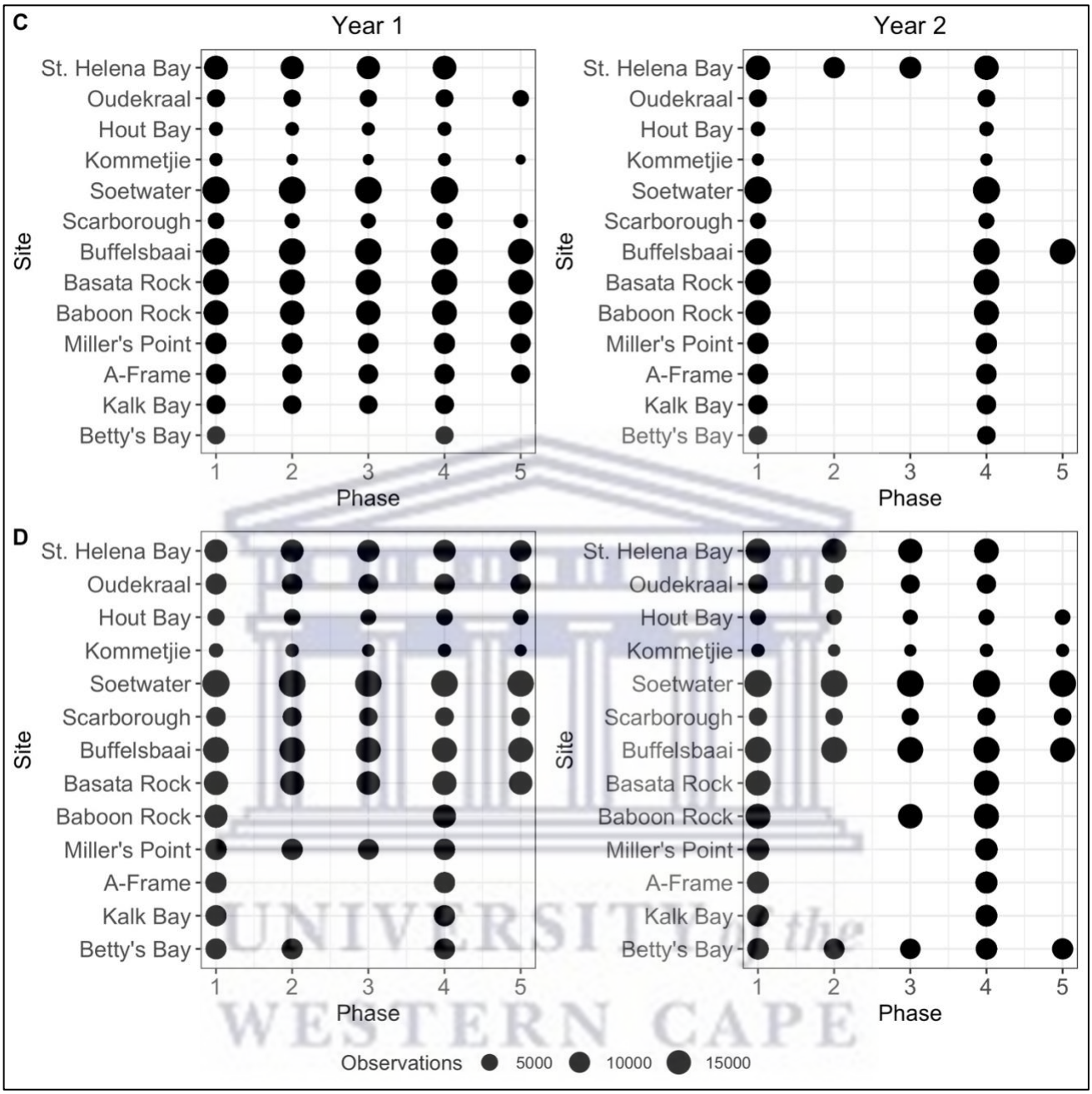

Figure 4:9 Proportion of particles for each phase at the end of the simulation run for Austral winter (row C) and spring (row D) for each respective year. The size of the point is related to the number of particles within that life cycle phase at the end of each simulation run.

other sites. During winter of year 1, kelp from the majority of release sites were present at the sink locations (Figure 4:7). In winter of year 2, the only kelp that sank in the study domain were released from St. Helena Bay, with all other sites absent. In spring of year 1, kelp sunk further north-westward compared to summer (Figure 4:7). Kelp from release sites were clustered together in the most north-western part of the study domain. Release sites in False Bay, such as Baboon rock, Miller's point, Kalk Bay, and A-Frame, did not feature as sink locations (Figure 4:7). In Autumn of year 2, kelp from the release sites spread across the south-western portion of the study domain (Figure 4:7). The

sunken virtual kelp, depending on release site, occasionally sank in the same location. For example, St. Helena Bay towards the most eastern portion of the study domain, and Hout Bay near the continental shelf edge (Figure 4:7).

There are clear differences between the amount of kelp that eventually sank, beached or travelled outside the study domain, between seasons with variation between years (Figure 4:8 and Figure 4:9). During summer months, no particles travelled outside the study domain (Figure 4:8). The highest proportion of particles that travelled outside the domain occurred during spring months and to a lesser magnitude during autumn and winter months (Figure 4:9). The highest proportion of kelp particles that beached occurred during winter months, in particular year 2, where almost all the particles beached (Figure 4.9). Kelps released from Buffelsbaai were the only material to travel outside of False Bay during all times of the year, while the remaining sites (Baboon rock, Bachata rock, Miller's point, and Kalk Bay) only travelled outside of False Bay during winter of year 2 (Figure 4.9). Kelps released from Betty's Bay (southern site extreme) usually became beached, while kelp from St. Helena Bay (northern extreme) had similar proportions of beached and sunken kelp across seasons and years (Figure 4:9).

4.4 Discussion

The findings from this study aid our understanding of the role mesoscale features play in influencing solitary macroalgal trajectory patterns and distribution. The importance of including drag components in relation to the surface area of passive solitary kelp shown in Chapter 3 was confirmed; however, the study did not find that the site-specific morphological characteristics influenced the trajectory of virtual kelp particles. Instead, the inclusion of site-specific morphological characteristics was important in describing entrainment patterns of virtual kelp particles. In addition, the simulation study supports the justification of the site-specific approach used, which I argue should be incorporated into future studies on the subject.

Previous work investigating drifting macroalgal trajectory patterns shows that macroalgae tend to follow the ocean currents (see Chapter 3) and indicated that the kelp's drag components are important for characterising entrainment patterns within mesoscale oceanographic features (Beron-Vera et al., 2016, 2019; Brooks et al., 2019; Coppin et al., 2020; Putman et al., 2020). This was evident from the analysis of surface and subsurface kelp distributions, which shows high concentrations of virtual kelp particles within mesoscale features during times of high activity (Austral summer and winter). Eddies have been identified as important surface accumulation zones for other types of flotsams (Brach et al., 2018; D'Asaro et al., 2018, 2020; Onink et al., 2019). For example, Beron-Vera et al. (2016) used a Maxey-Riley approach to include the effects of inertia on accumulation patterns. The authors found that the effects of inertia were responsible for

accumulation patterns within mesoscale features and noted the presence of other flotsam within these features during field validation work. Other work by Brooks et al. (2019) investigated the distribution of *Sargassum* rafts in relation to radial size and windage. The authors found that eddies were important surface accumulation zones and that the inclusion of windage based on radial raft size greatly increased the accuracy of numerical simulations. Improvement between observed and modelled trajectories by including ad-hoc windage was also reported by Putman et al., (2018, 2020) when investigating dispersal patterns of *Sargassum*, but the trajectories did not match completely. The discrepancy between observed and modelled trajectories and entrainment could be further reduced by including hydrodynamic drag, which Brooks et al. (2019) and Putman et al. (2018, 2020) did not consider. However, this may be difficult due to the highly variable nature of kelp raft size. I argue that the results from this study not only provide evidence for including hydrodynamic drag along with windage but also for the site-specific approach, which would allow raft-size variability to be taken into account.

Virtual kelp particles remain entrained when sinking, which was a result of the incorporated drag components. In Chapter 3 I found that purely Lagrangian particles remained on the boundary of mesoscale features with very little evidence of entrainment, while virtual kelp exhibited high entrainment patterns and focused toward the centre. Ocean eddies have a 'centre,' which acts as an important surface accumulation zone for flotsam (Brach et al., 2018) as well as the vertical transport of heat, salinity, nutrients (Jayne and Marotzke, 2002) mostly through the centres. This is due to the upwelling and downwelling characteristics of both cyclonic and anti-cyclonic eddies (Bakun and Nelson 1991; Bakun, 2006). This is dependent on whether the eddy is "spinning-up" due to frictional forcing from adjacent flow patterns, or "spinning-down" when the eddy moves away from the formation source and begins to decay (Bakun, 2006). This trend has been reported in previous work by Beron-Vera et al. (2019) and Miron et al. (2020). For example, Pichel et al. (2012) used a combination of satellite and aircraft observations to detect and describe 'ghost gear' distribution within the Gulf of Alaska. The authors found that eddies, particularly in the central cores, can collect and retain ghost gear and highlighted the role eddies play in flotsam accumulation on the surface.

The extant research on macroalgae dispersal patterns makes no effort to describe the subsurface dispersal patterns, which this study does. As well as acting as accumulation zones, eddies also disperse the kelp particles over the study domain and towards the coastline when 'leaking' of virtual kelp from an eddy occurred. Some of the entrained virtual kelp particles frequently exit on the eastern side of mesoscale features. This resulted in kelp particles becoming entrained within the Benguela Jet to travel northwest or to become entrained in other passing mesoscale activity, and or eventually beaching. Although the 'leaking' of particles was less common than continued entrainment, particle leakage from mesoscale features was an influencer of virtual kelp particle

dispersal over the study domain. The leaking of particles is most likely a result of the underlying bathymetry. A study by Rubio et al. (2009), which aimed to characterise and validate mesoscale activity in the Southern Benguela Upwelling region, found similar trends regarding volume transport of nutrients. The authors showed that eddies (which extend vertically through the water column) interacted with the underlying bathymetry on the coastal side of the feature which results in weaker dynamics. These weaker dynamics on one side of the mesoscale feature resulted in volumes of seawater particles exiting on the weaker dynamic side. Although Rubio et al. (2009) investigated fluid parcels of water and not biological flotsam, the mechanism of weaker dynamics could explain the leaking of virtual kelp particles from mesoscale features within the study domain. The mechanism of leakage and transport towards the coast may also be a form of barrier to offshore transport (Bracco et al., 2000), preventing further offshore transport and redirecting movement of virtual kelp particles toward the coast.

Eddies have also been shown to act as dynamic upwelling and downwelling of volume transport in the open ocean. Downwelling occurs on the periphery of mesoscale features in a cyclonic eddy. Flow patterns and upwelling-downwelling characteristics also differ between the centre and the interior flow patterns (Bakun 2006; Pegliasco et al., 2015). Ocean eddies which exhibit interiors of upwelling and divergent flow are associated with convergent flow and downwelling near the edges (Bakun 2006; Morrow and Le Traon, 2012; Pegliasco et al., 2015). In contrast, eddies with interiors of downwelling and divergent flow are associated with upwelling and convergent flow on the outer edges. These dynamic ocean features are regarded as important mechanisms of volume transport. For example, eddies are considered the main mechanism of transport of heat for the Antarctic Circumpolar Current (ACC) (Karsten et al., 2002a;b). Similar relationships between virtual kelp particles and mesoscale features were evident from the analyses of surface and subsurface patterns and distributions within the study domain. Virtual kelp particles located towards the centre of an eddy continue to remain entrained while sinking. Since eddies are structured vertically through the water column, this aided in the vertical transport and distribution towards the seafloor. McGillicuddy Jr et al. (2003) used an eddy-resolving model to investigate the role of mesoscale features as sources and sinks of nutrients in the North Atlantic. The authors showed that the mesoscale features have a significant influence of nutrients within the euphotic zone. In fact, the downwelling of mesoscale features is of such high magnitudes that it can counter-balance Ekman-driven upwelling in the subpolar gyre. Although biological flotsam is considered in this study, similar patterns are seen in the results for the sub-surface and sunken kelp particles. High concentrations of kelp particles are located in areas on the seafloor, which coincide with subsurface mesoscale entrainment patterns. Generally, kelp particles settle on the seafloor in the northern part of the study domain inshore of the continental shelf; the exception being spring of year 2. The distribution of

sunken virtual kelp coincides with an area where kelp has been found previously. Woodborne et al. (1989) characterised kelp rafted geological clasts along the West Coast citing previous work by Gentle (1987) who described a possible kelp sink location. Gentle (1987) describes kelp rafted clasts that were recovered from dredging an area approximately 120 km northwest of Cape Columbine at an approximate depth of 350 m. The dredged samples consisted of sand and pebbles held together by a loose mat of seaweed. Unfortunately, Gentle (1987) did not describe the species of seaweed but simply called it 'kelp;' however, based on the most common species of kelp in South Africa, the species could be *E. maxima*, *Ecklonia radiata* (C.Agardh) J.Agardh, *Laminaria pallida* Greville and *M. pyrifera* (Linnaeus) C.Agardh.

Mesoscale features within the study domain also influence the proportions of virtual kelp particles which beach by acting as barriers to offshore transport (Keith et al., 2011). Eddy filaments which originated offshore and occasionally travel shoreward entrain nearby kelp particles trajectories become largely influenced by the eddy filament. The development of filaments is due to the convergent and divergent flow patterns associated with ocean eddies (Jayne and Marotzke, 2002; Bakun, 2006; Morrow and Le Traon, 2012; Pegliasco et al., 2015). For example, an anti-cyclonic eddy that is spinning-up will be characterised by convergent flow patterns on the surface. The surface convergent flow patterns can occasionally develop into convergent frontal structures, which move within the interior of the eddy (Bakun, 2006; Morrow and Le Traon, 2012). The opposite is true for spinning-up cyclonic eddies, which are characterised by divergent horizontal flow patterns (Spall, 1995; Bakun, 2006). The divergent flow patterns on the surface can develop into submesoscale eddies and filaments through frictional and shear forces of adjacent flow patterns (Bakun, 2006; Morrow and Le Traon, 2012).

The trajectory of the kelp particle is therefore determined by the trajectory of the eddy-filament which was either north-westward or shoreward causing higher proportions of beaching during the winter months of both years. Distributions of sunken virtual kelp tend to be along the shelf edge or continental shelf, patterns that are similar to those observed in natural conditions. A study by Filbee-Dexter and Scheibling (2016) aimed to identify predictors and describe spatial patterns of drift algae. The results showed that bathymetry, distance to coast, and slope were the best predictors of the spatial distributions observed during surveys. Drift algae were often found in depressions or flats. The authors attributed the spatial patterns to flow regimes, which are slower on flats than on slopes, and also noted high accumulations on slopes and ledges close to shore. Similar spatial distributions are observed in the current study. Although sunken virtual kelp did accumulate along steep bathymetry lines, most accumulated along the continental shelf. The continental shelf's flat covers a larger area compared to deeper offshore areas within the study domain. Currents in flat areas tend

to travel slower which may explain the spatial patterns in this study, as slower currents aid in the accumulation of drift kelp or in this case virtual kelp (Filbee-Dexter and Scheibling, 2016).

The findings from this study provide insight into some important ecological questions. Although the potential of kelp as an organic subsidy has been shown through various methods (Filbee-Dexter and Scheibling, 2014; Filbee-Dexter and Scheibling, 2016; Filbee-Dexter et al., 2018; Dyer et al., 2019), these studies have only been able to infer the potential spatial extent. These results provide numerical evidence for kelps' role as an inorganic subsidy to near- and offshore ecosystems while characterising the spatial extent. In addition, these findings offer a potential method to assess kelps' contribution to Blue Carbon. Challenges exist in identifying the pathways of organic subsidy, which is vital for developing Blue Carbon policy (Howard et al., 2017; Smale et al., 2018; Filbee-Dexter and Wernberg, 2020. These results provide numerical evidence for kelps' potential role in mitigating climate change by acting as a carbon sink thorough characterising the spatial distribution and identifying the influencers of floating kelp trajectory. Populations of the target species for this study, *E. maxima*, have expanded eastward along the coast in recent years (Bolton et al., 2012). The specific mechanism that enabled populations to expand eastwards has not been identified; however, the findings from this study provide insight. Although the general flow of particles was north-westward for most of the year, virtual kelp particles moved eastwards along the coast into False Bay and further during the winter months. The eastward movement during the winter months of virtual kelp particles coupled with the release of spores while floating (Joska and Bolton, 1987) provides evidence for the potential role of ocean currents in the expansion of kelp populations around the South African coastline.

4.4.1 Conclusion

Macroalgae are prone to entrainment within mesoscale features, such as eddies and the associated eddy-filaments, if present but otherwise follow the ocean currents. The inclusion of site-specific morphological characteristics allowed for a quantitative approach to estimating windage, hydrodynamic drag, buoyancy and sink rates, all of which are important parameters for accurately characterising the distribution of macroalgae in the ocean. In this experiment, the results verify findings from other studies investigating eddies as convergence zones for flotsam but highlight a possible barrier to macroalgal transport that eddy-associated filaments and fronts may pose. Furthermore, the current work highlights the role of kelp in the overall carbon/nutrient cycle within the oceans by identifying possible 'kelp sinks' in the north-western and south-western areas of the Benguela Upwelling System. The findings from this study provide insight into some essential ecological knowledge gaps regarding kelps' spatial extent of organic subsidy, potential role in mitigating climate change, and the expansion of *E. maxima* along the South African coastline.

5 : General Discussion

5.1 General discussion

The range of numerical tools available to marine researchers is primarily driven by the oceanographic fields of study and underpinned by our current understanding of physical processes in the ocean (North et al., 2009; Van Sebille et al., 2020). The development of open-source tools from the oceanography scientific community has in recent years become a popular tool outside the fields of oceanography. One of those fields is ecology, having been used in various manners, enabling scientists to study ecological processes through a quantitative and empirical lens. An example of such a tool is Lagrangian Trajectory modelling which has advanced the study of various gaps in our ecological understanding of the effect of physical ocean processes on the dispersal of various marine taxa (North et al., 2009; Van Sebille et al., 2020). For purposes of this dissertation, advances in hydrodynamic and trajectory modelling were used to investigate the influencers of morphological characteristics and dispersal patterns of dislodged, floating kelp.

Kelp forests and their ecological contributions are a popular area of research, and their importance as ecological engineers and drivers of biodiversity is well established (Graham, 2004; Fowler-Walker et al., 2005; Wing et al., 2007; Wernberg and Goldberg, 2008; Harley et al., 2012; Smale and Moore, 2017). Kelp forests also provided an important organic subsidy into near- and offshore areas via ocean currents in the form of whole plants and plant debris (Mann, 1973; Dayton et al., 1998; Miller et al., 2011; Krumhansl and Scheibling, 2012; Pedersen et al., 2012). This has been demonstrated by studies using isotope-based approaches (Dyer et al., 2019) and field-based experiments (Filbee-Dexter et al., 2018). In terms of whole kelp (individuals dislodged during times of high wave energy), the focus has been on understanding the transport of kelp rafts (Hobday, 2000a; Thiel and Gutow, 2005; Brooks et al., 2019; Putman 2018, 2020).

The mechanism under which kelp-formation occurs is not currently known and assumed this likely occurs in times of intense wave energy, such as storms. The definition of a kelp raft is also not clear, as existing studies use context-specific definitions. For example, Harrold and Lisin (1989) used an artificial kelp raft, defined as an entanglement of mixed kelp species with a specific size. Others focus on a particular genus or species whose sizes (extent of surface area on the ocean surface) are highly variable (Brooks et al., 2019; Putman et al., 2018, 2020). In addition, the methods used cannot be replicated for other species due to the context-specific approach and the high morphological complexity seaweeds, macroalgae, and kelps are known for.

Although context-specific, the previous work on the subject has provided many important insights into the underlying transport mechanisms. Ocean currents and the indirect effect of wind have been inferred. Examples of studies that have taken advantage of the advanced tools mentioned previously have shown that wind plays a direct role in the form of windage (Brooks et al., 2019;

Putman 2018, 2020). Although drag resulting from the ocean current (hydrodynamic drag) has been identified as an important mechanism for other flotsam, none of the extant research on kelp rafts considers such aspects. Besides previous work identifying windage as an important influencer of trajectory, mesoscale ocean features were shown to be an important influence trajectory of kelp rafts; albeit with the same context-specific limitations (Brooks et al., 2019; Putman 2018, 2020). However, gaps still exist in their potential role as accumulation zones, associated seasonal components, acting as barriers to transport, and mesoscale processes' role in determining the sink-location of floating kelp.

The mix of previous context-specific approaches, high morphological diversity and complexity of target species, gaps in important ocean transport mechanisms, and the role of physical ocean features provides a unique opportunity to develop a general approach which can be applied across species while taking the surface-area of the kelps' complicated morphological characteristics into account, using Lagrangian based methods. The importance of understanding such processes cuts across different spheres. In terms of floating kelp's ecological role, being able to quantify the organic subsidy to the near- and offshore, contribution to habitat complexity offshore, and the role floating kelps play in the transport of other species which remain attached while afloat. Kelps' contribution or mechanism for combating climate change is by acting as a 'carbon sink' and via 'carbon-sequestration' is also paramount. However, this will require a deeper understanding of the dispersal patterns of kelp floating on the ocean surface. This is also true for the socio-economic aspects.

Kelps are harvested *in situ* or collected from beaches and rocky shorelines in the form of "beach-cast" or "kelp-wrack" (Griffiths et al., 1983; Michaud et al., 2019; Gilson et al., 2021). In some countries, the harvesting of seaweed is a highly controlled resource. For example, in South Africa, the coastline is divided into 'concession areas.' The biomass of the harvested species within these concession areas is monitored to ensure sustainable harvesting (Troell et al., 2006). In addition, the rights-holders for concession areas are expected to not over harvest and abide by the biomass restrictions. In addition, the awarding of concession areas to previously disadvantaged South African citizens acts as an essential economic empowerment mechanism (Troell et al., 2006). Significant beaching events of macroalgae, usually associated with storm activity, can also act as a nuisance for the public. The decaying process of kelp releases a foul odour and attracts invertebrate species, creating an environment that is unpleasant for the public, particularly in dense metropolitan coastal areas. No current method exists for forecasting kelp-wrack as too little is known about the processes involved. A hindcast/forecast model would aid ecological studies as well as the government agencies responsible for the management of coastal areas, particularly beaches.

An additional layer of complexity to the site-specific approach proposed is that kelp morphological characteristics are driven by the local temperature and wave environment, which vary considerably

along coastlines. Also, the extant research investigating morphological characteristics had not applied quantitative, high resolution, and empirical measures of wave exposure and/or temperature. Therefore, to gain the data needed for a site-specific approach, influences of waves and temperature on morphological characteristics were first investigated and described. The investigation of morphological characteristics has added to the current understanding and improved upon it by using Linear Wave Theory, high-resolution temperature data of the nearshore, and numerical descriptions of abiotic influencers, which were lacking in the literature. The current work has shed light on the gaps that exist in macroalgal trajectory by using a morphologically site-specific, solitary approach to investigate trajectory patterns. Leveraging these advancements allowed the identification of quantitative wave and temperature metrics, and morphological characteristics were described, which were used to investigate the role of size, shape and buoyancy and the ocean processes involved in macroalgal trajectory. Finally, once the important aspects and ocean processes were identified, a numerical description of macroalgal distribution within the study region was developed and described.

In chapter 2, the investigation of morphological characteristics added to the current understanding as well as improved upon it by using Linear Wave Theory, high-resolution temperature data of the nearshore, and numerical descriptions of abiotic influencers. The results from chapter 2 confirmed that the local wave environment is the main influencer of *Laminaria pallida* Greville and both populations (shallow and deep) of *Ecklonia maxima* (Osbeck) Papenfuss. The study was also able to identify the specific wave metrics involved, which can be further tested in future studies and allowed us to better understand the effects of climate change on kelp. Although kelps are highly resilient, there is a threshold to the wave environment which also comes with a cost. The reduction in drag reduces the available surface area of the plant to capture light and limits photosynthesis, while strength-increasing traits may incur a significant physiological cost. Ultimately, increasing wave energy in the nearshore environment may reduce the resilience of kelp forests over time increasing dislodgement rates, particularly during storms.

Temperature also directly influences morphological characteristics by increasing metabolisms which limits the growth and surface area of the plant. Not only does increased temperature reduces resilience to the physiological cost of a warmer environment, but there is also a loss of habitat for other marine taxa that kelps provide via morphological structure. Other stochastic events such as Marine Heat Waves would only push kelp forests further, resulting in a thinning out over time. However, in environments where kelp forests are expanding such as South Africa where climate change effects have resulted in increased upwelling around the coast, the expansion of kelp may buffer dislodgement rates. One of the target species of this dissertation, *E. maxima*, has expanded further eastward along the coast (Bolton et al., 2012), with reports of increased biomass in other

areas, such as Dyer Island Reserve located in Gansbaai (Pers comm. Smit). There has been no recent assessment of the kelp biomass around the coast of South Africa. The results also provided evidence for species leveraging different strategies for adaptation, such as drag-reducing or strength-increasing traits. Future studies should replicate the approach to identify the specific wave and temperature metrics which influences different species of kelps.

In chapter 3, the focus was on identifying the important physical ocean processes and drag parameters needed to model macroalgal trajectory patterns, in this case, that of *E. maxima*. Ocean currents act as an important dispersal mechanism of material on the ocean surface, both natural and anthropogenic. The extant research on the subject focused on windage, kelp- or macroalgal-rafts, and did not take the complex morphological characteristics of kelps into account. The results from this study confirmed that solitary drifting kelp dispersal in the ocean is influenced by surface currents and that the inclusion of hydrodynamic drag into simulations caused virtual kelp particle trajectories to differ from that of purely Lagrangian particles.

Although the current work was purely numerical, results showing solitary floating kelp should not be treated as purely Lagrangian is an important finding. Interestingly, results showed windage was not an influencer of offshore transport which was unexpected. The role of windage and the associated momentum energy have been shown to influence the trajectories of *Sargassum* rafts (Brooks et al., 2019; Putman 2018, 2020). Instead, simulations which included wind drag (windage) drifted closer to shore, suggesting that windage plays a role in beaching. This has been identified by Miron et al., (2020) who showed that wind was an important component when considering beaching scenarios, particularly wind direction. If the wind blows towards the shoreline, then the likelihood of beaching increases.

Additionally, the study initially used the minimum, mean, and maximum surface areas, but no differences were seen for minimum and mean surface areas. These preliminary findings suggest the range of surface area available is not necessarily important in influencing trajectory but that the maximum surface area scenario should be considered a minimum requirement in future studies. This differs from previous work which shows that small differences in velocity can result in vastly different trajectory outcomes. The resolution of the ocean model used may have limited the study in this regard, as a higher ocean model is required when investigating the variation in surface area of kelp and the potential to influence trajectory. The differences between minimum and mean surface areas may not have been significant enough to be resolved based on the current resolution of the ocean model available. Future studies should consider the varying surface area of morphological characteristics of the same species while employing high-resolution ocean models. The development of high-resolution models and resolving mesoscale ocean processes are active areas of study, it will not be long before these findings can be tested further with higher resolution models,

both temporarily and spatially, and with improved representation of ocean processes becomes available. Although not the focus of the study, the findings also highlighted the role of mesoscale processes, such as eddies, in influencing the trajectory of solitary floating *E. maxima*; as well as the importance of hydrodynamic drag increasing the potential to become entrained. Chapter 3 is the first study on the subject which provides quantitative evidence that hydrodynamic drag is an important component to consider when modelling the trajectory of solitary kelp, and a form of windage would aid in reflecting beaching events.

In chapter 4, the concepts developed in chapter 3 were employed on a larger scale with additional parameterisations to reflect natural conditions such as sinking and buoyancy. Unlike previous studies which considered different sizes of kelp rafts, this study used the site-specific approach for multiple sites around the coastline to characterise the dispersal of solitary floating kelp. Storms are often associated with large quantities of kelp-wrack and kelp rafts but dislodged solitary kelps are a more common occurrence around the coastline. The site-specific approach offers a more general description of kelps' role as an organic subsidy to offshore areas. In addition, no studies have used Lagrangian-based techniques to investigate solitary floating kelp beaching patterns.

The ability to use real-world measurements offered an opportunity to investigate the role of mesoscale features in macroalgal trajectory and identify any site-specific kelp morphological characteristics that may influence trajectory, and accumulation areas (surface and sink). Due to the limitations of using mixed fields (ocean and wind) when simulating sinking with OceanParcels, windage estimates based on the current speed were used. The compromise made for windage was not ideal however, since the direct role of wind was largely insignificant in the overall transport, coarse estimates used were considered suitable for a general description of beaching patterns. The underlying ocean processes which increase or induce beaching with marine flotsam has been investigated previously (Bakun, 2006; Beron-Vera et al., 2016; Brach et al., 2018; Onink et al., 2019; Putman et al., 2020). Studies investigating beaching phenomena of flotsam require a different set of numerical requirements and is a nuance subject. Therefore, although the results highlighted the seasonal patterns of beaching around the coastline, more studies are needed which focus on the underlying ocean processes, which is not within the scope of this dissertation. Unlike the previous chapter, more realistic measures of buoyancy were used, which in turn was used to calculate the effects of hydrodynamic and wind drag. Buoyancy was calculated using the data from chapter 2, opposed to using different scenarios of windage and the size. The technique has been used by Putman et al., (2018, 2020) to provide insights for the role of mesoscale ocean features trajectory of pelagic Sargassum and is an accepted technique. However, the site-specific approach was also applied to calculating buoyancy and sink rates, as these parameters may differ enough to alter dispersal patterns of virtual kelp between sites. The addition of sinking as a parameter allowed for

investigation of sunken distributions of kelp with the study domain, the Southern Benguela Upwelling Region. The results from showed that macroalgae, in this case *E. maxima,* are particularly prone to entrainment in mesoscale features such as fronts and eddies. Furthermore, mesoscale features in the region act as a transport barrier to offshore transport. There were no clear differences when comparing trajectories and surface accumulation areas between sites, showing that the site-specific approach may not be needed to model the trajectory of floating kelp.

Although these findings suggest that site-specific morphological characteristics did not influence overall trajectories, it would be interesting if future studies incorporated the approach with high-resolution ocean models. This was the first study which attempted to numerically characterise solitary kelp distribution on the seafloor. The results also showed possible accumulation areas on the seafloor that reflected patterns characterised in a previous study (Woodborne et al., 1989). Mesoscale eddies were also shown to play a role in the subsurface transport of kelp to the seafloor, which the extant research on the subject has not investigated. This study is also the first to use numerical simulations to characterise the solitary kelp distribution on the seafloor. Overall, mesoscale features play a fundamental role in influencing solitary kelp trajectory. Studies investigating the role of kelp as an important organic subsidy to offshore areas in the ocean have performed stable isotope approaches and field-based experiments.

The overall findings provide insight into the knowledge gaps limiting investigations of kelp as a Blue Carbon component. One of the key challenges in investigating kelp as a potential carbon sequestration mechanism is the lack of any known approach to characterise input into blue carbon ecosystems. Kelp detritus can be buried under sediments and possibly indirectly included in the blue carbon contribution of tidal marshes, mangrove forests, beaches, and seagrass beds (Howard et al., 2017; Smale et al., 2018; Filbee-Dexter and Wernberg, 2020). Additionally, the proportions of kelp sequestered in deep ocean environments are considered rudimentary. For kelp to be considered in current and future blue carbon policies, the sources and sinks within regions of interest need to be established (Howard et al., 2017; Smale et al., 2018; Filbee-Dexter and Wernberg, 2020). The results from chapters 3 and 4 provide insight, albeit numerically, into the spatial extent of floating kelp on the surface and seafloor. Identification of mesoscale ocean features as influencers of sink sites, surface accumulation, and barriers to offshore transport is also significant, as climate change causes these processes to change in various complex ways. Although not a comprehensive characterisation, the findings from this dissertation provide numerical-based evidence for the distant transport into the offshore area of floating solitary *E. maxima* and, ultimately, organic input. Proportions of kelp deposited offshore and on land (beaches and rocky shorelines) are an identified need in the study of kelp and blue carbon, which was successfully performed in this dissertation. Also, proportions of the different virtual kelp phases (floating, sinking, sunk, beached, and out of

bounds) varied seasonally, suggesting a seasonal component of kelps' ability to sequester carbon in offshore areas. I commonly criticise previous work for the context-specific findings and approaches within this dissertation. Although it could be argued it is the same for this dissertation, I provide reproducible methods that can be altered to suit the target species in question or replicated entirely on the same approach.

I also provide insight into the expansion of *E. maxima* eastwards along the South African coastline. Waters around the South African coastline are cooling due to the effects of increased upwelling (Smit et al., 2013), making larger areas of the coastline suitable for *E. maxima*. However, it has only been inferred that floating *E. maxima* most likely follow the ocean currents to expand into new areas. Kelp remains alive after dislodgement and releases spores as an ecological response to physiological shock afloat, making them a highly effective dispersal mechanism (Joska and Bolton, 1987). The expansion of *E. maxima* populations could have occurred during the winter months, as shown with virtual kelp trajectories in this study. If a kelp individual is able to reach distant shores along the coast while still releasing spores, it may be possible for recruits to establish themselves and exploit new habitats. Additionally, if the cooling trend along the South African coastline continues, it is possible that *E. maxima* and the associated biota will move further eastwards. Further expansion of kelp populations could have significant impacts on those coastal communities (Bolton et al., 2012).

Conclusion

The study shows the importance of including drag, buoyancy and sink rate components based on morphological characteristics. Individual-based numerical experiments confirm results from previous studies regarding macroalgal trajectory patterns, identifying surface currents as the primary influencer. Unlike previous studies, the current work showed the importance of including hydrodynamic drag, along with windage, as a critical parameterisation concerning simulating macroalgal dispersal patterns in the open ocean. The results show that hydrodynamic drag is an important influencer of trajectory on both the surface and subsurface, as well as entrainment in mesoscale features. The study sheds light on the seasonal component of macroalgal trajectory, which is related to the seasonality of the Benguela Jet and mesoscale oceanographic features within the study region. The surface and seafloor accumulation zones identified in numerical simulations provide evidence for the suggested resource organic resource coupling between deep and nearshore ocean environments from drifting macroalgae. Also, the current work provides an alternative individual-based approach for investigating and simulating macroalgal dispersal in the open ocean, which can be applied to any macroalgal species. The approach also offers a method

for investigating the formation of kelp rafts in the open ocean. I provide numerical evidence which sheds light in the role of kelps role in terms of organic subsidy and Blue Carbon contribution.

Limitations

The current study was limited by the resolution of the oceanographic and wind models (both spatially and temporarily), which do not resolve finer scale processes such as sub-mesoscale features. Since macroalgal distribution patterns are influenced by the underlying oceanographic conditions, patterns which emerge in nature may not be reflected in numerical simulations (McGillicuddy Jr et al., 2003; Zhong et al., 2012; Van Sebille et al., 2018). For example, it has been observed that Sargassum species tend to form long lines on the surface as a result of submesoscale geostrophic processes, which the models used in this study do not resolve (Zhong et al., 2012). Therefore, although mesoscale dispersal patterns can be simulated, the finer scale processes cannot be accurately resolved (Zhong et al., 2012). In addition, the current work focused on open-ocean processes as the investigation of nearshore transport is nuanced and beyond the scope of this study which limits the findings to open-ocean transport only. The software used made using mixed fields when simulation sinking particles impossible, and wind estimates were used based on surface current speed (the ocean model is forced by wind), which may not accurately reflect the effects of windage on both drag and momentum energy transfer.

5.2 Recommendations for further research

Future research should aim to simulate virtual kelp particles using a finer scale resolution in both the spatial and temporal sense. This would allow for the investigation of finer scale submesoscale processes to be resolved as well as the associated dispersal patterns of macroalgae. Nearshore dispersal patterns of macroalgae fell out of the scope of the study, which future work should consider. Understanding transport patterns on the nearshore would be highly beneficial to coastal management agencies and commercial entities which harvest beach-cast kelp. Future work on the subject should also consider using custom-made drifters, which would validate the findings, as well as fieldwork campaigns to identify accumulation zones on the seafloor. Also, experimental work should be performed to identify the appropriate drag characteristics and shape coefficients to be used for simulating drifting macroalgae, which may improve the accuracy of overall distribution patterns. The ability to combine mixed fields (ocean and wind fields) in Lagrangian software would be able to negate the use of wind estimates and instead interpolate from a separate wind field, which would better reflect aspects of windage.

The method used in this dissertation provides an opportunity to use such an approach to investigate the role of kelp in carbon sequestration and characterising the reliance of offshore marine

organisms. Future numerical studies should be coupled with field-based experiments to aid in validating findings which could aid in investigating these important topics. The ability to forecast beach-wrack biomass and dislodgement of kelp could be beneficial to management and harvesting agencies, to determine threats to the resource or time of high biomass of kelp raft and being a nuisance to beachgoers. Finally, future studies should build on the individual-based approach to investigate the mechanisms and conditions under which kelp rafts form.

References

Allen, A. and J. Plourde., 1999. Review of leeway: Field experiments and Implementation. US coast guard rep.

Altamirano, M., Murakami, A. and Kawai, H., 2004. High light stress in the kelp *Ecklonia cava*. *Aquatic Botany*, *79*(2), pp.125-135.

Anderson, R.J., Carrick, P., Levitt, G.J. and Share, A., 1997. Holdfasts of adult kelp *Ecklonia maxima* provide refuges from grazing for recruitment of juvenile kelps. *Marine Ecology Progress Series*, *159*, pp.265-273.

Anderson, M.J., Diebel, C.E., Blom, W.M. and Landers, T.J., 2005. Consistency and variation in kelp holdfast assemblages: spatial patterns of biodiversity for the major phyla at different taxonomic resolutions. *Journal of experimental marine biology and ecology*, *320*(1), pp.35-56.

Anderson, R.J., Rand, A., Rothman, M.D., Share, A. and Bolton, J.J., 2007. Mapping and quantifying the South African kelp resource. *African Journal of Marine Science*, *29*(3), pp.369-378.

Anderson, R.J., Rothman, M.D., Share, A. and Drummond, H., 2006. Harvesting of the kelp *Ecklonia maxima* in South Africa affects its three obligate, red algal epiphytes. In *Eighteenth International Seaweed Symposium* (pp. 117-123). Springer, Dordrecht.

Andrews, W.R.H. and Hutchings, L., 1980. Upwelling in the southern Benguela Current. *Progress in Oceanography*, *9*(1), pp.1-81.

Atkins, G.R., 1970. Winds and current patterns in False Bay. *Transactions of the Royal Society of South Africa*, *39*(2), pp.139-148.

Baba, J. and Komar, P.D., 1981. Measurements and analysis of setting velocities of natural quartz sand grains. *Journal of Sedimentary Research*, *51*(2), pp.631-640.

Bakun, A., 2006. Fronts and eddies as key structures in the habitat of marine fish larvae: opportunity, adaptive response and competitive advantage. *Scientia Marina*, *70*(S2), pp.105-122.

Bakun, A. and Nelson, C.S., 1991. The seasonal cycle of wind-stress curl in subtropical eastern boundary current regions. *Journal of Physical Oceanography*, *21*(12), pp.1815-1834.

Bäck, S., Lehvo, A. and Blomster, J., 2000, January. Mass occurrence of unattached *Enteromorpha intestinalis* on the Finnish Baltic Sea coast. In *Annales Botanici Fennici* (pp. 155-161). Finnish Zoological and Botanical Publishing Board.

Bayley, D., Brickle, P., Brewin, P., Golding, N. and Pelembe, T., 2021. Valuation of kelp forest ecosystem services in the Falkland Islands: A case study integrating blue carbon sequestration potential. *One Ecosystem*, *6*.

Bayley, D., Marengo, I. and Pelembe, T., 2017. Giant kelp 'Blue carbon' storage and sequestration value in the Falkland Islands. *Stanley: South Atlantic Environment Institute. doi*, *10*.

Beal, L.M., Elipot, S., Houk, A. and Leber, G.M., 2015. Capturing the transport variability of a western boundary jet: Results from the Agulhas Current Time-Series Experiment (ACT). *Journal of Physical Oceanography*, *45*(5), pp.1302-1324.

Bearham, D., Vanderklift, M.A. and Gunson, J.R., 2013. Temperature and light explain spatial variation in growth and productivity of the kelp Ecklonia radiata. *Marine Ecology Progress Series*, *476*, pp.59-70.

Bekkby, T., Rinde, E., Gundersen, H., Norderhaug, K.M., Gitmark, J.K. and Christie, H., 2014. Length, strength and water flow: relative importance of wave and current exposure on morphology in kelp *Laminaria hyperborea*. *Marine Ecology Progress Series*, *506*, pp.61-70.

Bennett, A., 2006. *Lagrangian fluid dynamics*. Cambridge University Press.

Bernardes Batista, M., Batista Anderson, A., Franzan Sanches, P., Simionatto Polito, P., Cesar Lima Silveira, T., Velez-Rubio, G.M., Scarabino, F., Camacho, O., Schmitz, C., Martinez, A. and Ortega, L., 2018. Kelps' long-distance dispersal: role of ecological/oceanographic processes and implications to marine forest conservation. *Diversity*, *10*(1), p.11.

Bernard, M.S., Strittmatter, M., Murúa, P., Heesch, S., Cho, G.Y., Leblanc, C. and Peters, A.F., 2019. Diversity, biogeography and host specificity of kelp endophytes with a focus on the genera *Laminarionema* and *Laminariocolax* (Ectocarpales, Phaeophyceae). *European Journal of Phycology*, *54*(1), pp.39-51.

Beron-Vera, F.J., Olascoaga, M.J. and Lumpkin, R., 2016. Inertia-induced accumulation of flotsam in the subtropical gyres. *Geophysical Research Letters*, *43*(23), pp.12-228.

Beron-Vera, F.J., Olascoaga, M.J. and Miron, P., 2019. Building a Maxey–Riley framework for surface ocean inertial particle dynamics. *Physics of Fluids*, *31*(9), p.096602.

Biskup, S., Bertocci, I., Arenas, F. and Tuya, F., 2014. Functional responses of juvenile kelps, *Laminaria ochroleuca* and *Saccorhiza polyschides*, to increasing temperatures. *Aquatic botany*, *113*, pp.117-122.

Blamey, L.K. and Bolton, J.J., 2018. The economic value of South African kelp forests and temperate reefs: past, present and future. *Journal of Marine Systems*, *188*, pp.172-181.

Blamey, L.K. and Branch, G.M., 2012. Regime shift of a kelp-forest benthic community induced by an 'invasion'of the rock lobster *Jasus lalandii*. *Journal of Experimental Marine Biology and Ecology*, *420*, pp.33-47.

Blamey, L.K., Shannon, L.J., Bolton, J.J., Crawford, R.J., Dufois, F., Evers-King, H., Griffiths, C.L., Hutchings, L., Jarre, A., Rouault, M. and Watermeyer, K.E., 2015. Ecosystem change in the southern Benguela and the underlying processes. *Journal of Marine Systems*, *144*, pp.9-29.

Blanke, B., Roy, C., Penven, P., Speich, S., McWilliams, J. and Nelson, G., 2002. Linking wind and interannual upwelling variability in a regional model of the southern Benguela. *Geophysical Research Letters*, *29*(24), pp.41-1.

Blanke, B., Speich, S., Bentamy, A., Roy, C. and Sow, B., 2005. Modeling the structure and variability of the southern Benguela upwelling using QuikSCAT wind forcing. *Journal of Geophysical Research: Oceans*, *110*(C7).

Bolton, J.J. and Anderson, R.J., 1987. Temperature tolerances of two southern African *Ecklonia* species (Alariaceae: Laminariales) and of hybrids between them. *Marine Biology*, *96*(2), pp.293-297.

Bolton, J.J., Anderson, R.J., Smit, A.J. and Rothman, M.D., 2012. South African kelp moving eastwards: the discovery of *Ecklonia maxima* (Osbeck) Papenfuss at De Hoop Nature Reserve on the south coast of South Africa. *African Journal of Marine Science*, *34*(1), pp.147-151.

Bolton, J.J., 2010. The biogeography of kelps (Laminariales, Phaeophyceae): a global analysis with new insights from recent advances in molecular phylogenetics. *Helgoland Marine Research*, *64*(4), pp.263-279.

Bolton, J.J. and Levitt, G.J., 1985. Light and temperature requirements for growth and reproduction in gametophytes of *Ecklonia maxima* (Alariaceae: Laminariales). *Marine Biology*, *87*(2), pp.131-135.

Booij, N., Holthuijsen, L.H. and Ris, R.C., 1996. The" SWAN" wave model for shallow water. *Coastal Engineering Proceedings*, (25).

Booij, N., Ris, R.C. and Holthuijsen, L.H., 1999. A third-generation wave model for coastal regions: 1. Model description and validation. *Journal of geophysical research: Oceans*, *104*(C4), pp.7649-7666.

Bracco, A., Provenzale, A. and Scheuring, I., 2000. Mesoscale vortices and the paradox of the plankton. *Proceedings of the Royal Society of London. Series B: Biological Sciences*, *267*(1454), pp.1795-1800.

Brach, L., Deixonne, P., Bernard, M.F., Durand, E., Desjean, M.C., Perez, E., van Sebille, E. and Ter Halle, A., 2018. Anticyclonic eddies increase accumulation of microplastic in the North Atlantic subtropical gyre. *Marine pollution bulletin*, *126*, pp.191-196.

Breivik, Ø., Allen, A.A., Maisondieu, C. and Roth, J.C., 2011. Wind-induced drift of objects at sea: The leeway field method. *Applied Ocean Research*, *33*(2), pp.100-109.

van den Bremer, T.S. and Breivik, Ø., 2018. Stokes drift. *Philosophical Transactions of the Royal Society A: Mathematical, Physical and Engineering Sciences*, *376*(2111), p.20170104.

Bressan, A. and Constantin, A., 2019. The deflection angle of surface ocean currents from the wind direction. *Journal of Geophysical Research: Oceans*, *124*(11), pp.7412-7420.

Brooks, M.T., Coles, V.J. and Coles, W.C., 2019. Inertia influences pelagic *Sargassum* advection and distribution. *Geophysical Research Letters*, *46*(5), pp.2610-2618.

Brooks, M.T., Coles, V.J., Hood, R.R. and Gower, J.F., 2018. Factors controlling the seasonal distribution of pelagic *Sargassum*. *Marine Ecology Progress Series*, *599*, pp.1-18.

Bruhn, J. and Gerard, V.A., 1996. Photoinhibition and recovery of the kelp Laminaria saccharina at optimal and superoptimal temperatures. *Marine Biology*, *125*(4), pp.639-648.

Bryan, S.E., Cook, A., Evans, J.P., Colls, P.W., Wells, M.G., Lawrence, M.G., Jell, J.S., Greig, A. and Leslie, R., 2004. Pumice rafting and faunal dispersion during 2001–2002 in the Southwest Pacific: record of a dacitic submarine explosive eruption from Tonga. *Earth and Planetary Science Letters*, *227*(1-2), pp.135-154.

Brzezinski, M.A., Reed, D.C., Harrer, S., Rassweiler, A., Melack, J.M., Goodridge, B.M. and Dugan, J.E., 2013. Multiple sources and forms of nitrogen sustain year-round kelp growth: on the Inner Continental Shelf of the Santa Barbara Channel. *Oceanography*, *26*(3), pp.114-123.

Burrows, M.T., Schoeman, D.S., Buckley, L.B., Moore, P., Poloczanska, E.S., Brander, K.M., Brown, C., Bruno, J.F., Duarte, C.M., Halpern, B.S. and Holding, J., 2011. The pace of shifting climate in marine and terrestrial ecosystems. *Science*, *334*(6056), pp.652-655.

Bushing, W.W., 1994, March. Biogeographic and ecological implications of kelp rafting as a dispersal vector for marine invertebrates. In *Proceedings of the Fourth California Islands Symposium: Update on the Status of Resources, March* (Vol. 22).

Bustamante, R.H., Branch, G.M. and Eekhout, S., 1995. Maintenance of an exceptional intertidal grazer biomass in South Africa: subsidy by subtidal kelps. *Ecology*, *76*(7), pp.2314-2329.

Bustamante, R.H. and Branch, G.M., 1996. The dependence of intertidal consumers on kelp-derived organic matter on the west coast of South Africa. *Journal of Experimental Marine Biology and Ecology*, *196*(1-2), pp.1-28.

Byrnes, J.E., Reed, D.C., Cardinale, B.J., Cavanaugh, K.C., Holbrook, S.J. and Schmitt, R.J., 2011. Climate-driven increases in storm frequency simplify kelp forest food webs. *Global Change Biology*, *17*(8), pp.2513-2524.

Callaghan, D.P., Leon, J.X. and Saunders, M.I., 2015. Wave modelling as a proxy for seagrass ecological modelling: Comparing fetch and process-based predictions for a bay and reef lagoon. *Estuarine, Coastal and Shelf Science*, *153*, pp.108-120.

Cardoso, C. and Caldeira, R.M., 2021. Modeling the exposure of the Macaronesia islands (NE Atlantic) to marine plastic pollution. *Frontiers in Marine Science*, *8*, p.653502.

Cavanaugh, K.C., Siegel, D.A., Reed, D.C. and Dennison, P.E., 2011. Environmental controls of giant-kelp biomass in the Santa Barbara Channel, California. *Marine Ecology Progress Series*, *429*, pp.1-17.

Cheng, A., Wang, H. and Wang, K., 2015. A Eulerian–Lagrangian control volume method for solute transport with anomalous diffusion. *Numerical Methods for Partial Differential Equations*, *31*(1), pp.253-267.

Chenillat, F., Blanke, B., Grima, N., Franks, P.J., Capet, X. and Rivière, P., 2015. Quantifying tracer dynamics in moving fluids: a combined Eulerian-Lagrangian approach. *Frontiers in Environmental Science*, *3*, p.43.

Clark, R.P., Edwards, M.S. and Foster, M.S., 2004. Effects of shade from multiple kelp canopies on an understory algal assemblage. *Marine Ecology Progress Series*, *267*, pp.107-119.

Claustre, H., Kerhervé, P., Marty, J.C., Prieur, L., Videau, C. and Hecq, J.H., 1994. Phytoplankton dynamics associated with a geostrophic front: ecological and biogeochemical implications. *Journal of Marine Research*, *52*(4), pp.711-742.

Collins, C.J., Fraser, C.I., Ashcroft, A. and Waters, J.M., 2010. Asymmetric dispersal of southern bull-kelp (*Durvillaea antarctica*) adults in coastal New Zealand: testing an oceanographic hypothesis. *Molecular Ecology*, *19*(20), pp.4572-4580.

Constantin, A., 2021. Frictional effects in wind-driven ocean currents. *Geophysical & Astrophysical Fluid Dynamics*, *115*(1), pp.1-14.

Coppin, R., Rautenbach, C., Ponton, T.J. and Smit, A.J., 2020. Investigating waves and temperature as drivers of kelp morphology. *Frontiers in Marine Science*, *7*, p.567.

Corey, A.T., 1949. *Influence of shape on the fall velocity of sand grains* (Doctoral dissertation, Colorado A & M College).

Cousens, R., 1982. The effect of exposure to wave action on the morphology and pigmentation of *Ascophyllum nodosum* (L.) Le Jolis in south-eastern Canada.

Cram, D.L., 1970. A suggested origin for the cold surface water in central False Bay. *Transactions of the Royal Society of South Africa*, *39*(2), pp.129-137.

Craw, D. and Waters, J., 2018. Long distance kelp-rafting of rocks around southern New Zealand. *New Zealand Journal of Geology and Geophysics*, *61*(4), pp.428-443.

D'Asaro, E.A., Shcherbina, A.Y., Klymak, J.M., Molemaker, J., Novelli, G., Guigand, C.M., Haza, A.C., Haus, B.K., Ryan, E.H., Jacobs, G.A. and Huntley, H.S., 2018. Ocean convergence and the dispersion of flotsam. *Proceedings of the National Academy of Sciences*, *115*(6), pp.1162-1167.

d'Ovidio, F., Della Penna, A., Trull, T.W., Nencioli, F., Pujol, M.I., Rio, M.H., Park, Y.H., Cotté, C., Zhou, M. and Blain, S., 2015. The biogeochemical structuring role of horizontal stirring: Lagrangian perspectives on iron delivery downstream of the Kerguelen Plateau. *Biogeosciences*, *12*(19), pp.5567-5581.

Davis, R.E., 1991. Observing the general circulation with floats. *Deep Sea Research Part A. Oceanographic Research Papers*, *38*, pp.S531-S571.

Dayton, P.K., 1985. Ecology of kelp communities. *Annual review of ecology and systematics*, pp.215-245.

Dayton, P.K., Tegner, M.J., Parnell, P.E. and Edwards, P.B., 1992. Temporal and spatial patterns of disturbance and recovery in a kelp forest community. *Ecological Monographs*, *62*(3), pp.421-445.

Dayton, P.K., Tegner, M.J., Edwards, P.B. and Riser, K.L., 1998. Sliding baselines, ghosts, and reduced expectations in kelp forest communities. *Ecological Applications*, *8*(2), pp.309-322.

Dayton, P.K., Tegner, M.J., Edwards, P.B. and Riser, K.L., 1999. Temporal and spatial scales of kelp demography: the role of oceanographic climate. *Ecological Monographs*, *69*(2), pp.219-250.

De Bettignies, T., Wernberg, T., Lavery, P.S., Vanderklift, M.A. and Mohring, M.B., 2013. Contrasting mechanisms of dislodgement and erosion contribute to production of kelp detritus. *Limnology and Oceanography*, *58*(5), pp.1680-1688.

Delandmeter, P. and Van Sebille, E., 2019. The Parcels v2. 0 Lagrangian framework: new field interpolation schemes. *Geoscientific Model Development*, *12*(8), pp.3571-3584.

Delft3D-WAVE, A. 2000. User manual, version 2.00. WL | *Delft Hydraulics*.

Dellatorre, F.G., Pisoni, J.P., Barón, P.J. and Rivas, A.L., 2012. Tide and wind forced nearshore dynamics in Nuevo Gulf (Northern Patagonia, Argentina): Potential implications for cross-shore transport. *Journal of Marine Systems*, *96*, pp.82-89.

Deltares, D., 2013. Delft3D-FLOW user manual. *Deltares Delft, The Netherlands*, *330*.

Demes, K.W., Pruitt, J.N., Harley, C.D. and Carrington, E., 2013. Survival of the weakest: increased frond mechanical strength in a wave-swept kelp inhibits self-pruning and increases whole-plant mortality. *Functional Ecology*, *27*(2), pp.439-445.

Denny, M. and Gaylord, B., 2002. The mechanics of wave-swept algae. *Journal of Experimental Biology*, *205*(10), pp.1355-1362.

Denny, M. and Roberson, L., 2002. Blade motion and nutrient flux to the kelp, *Eisenia arborea*. *The Biological Bulletin*, *203*(1), pp.1-13.

Deysher, L. and Norton, T.A., 1981. Dispersal and colonization in Sargassum muticum (Yendo) Fensholt. *Journal of experimental marine biology and ecology*, *56*(2-3), pp.179-195.

Dietrich, W.E., 1982. Settling velocity of natural particles. *Water resources research*, *18*(6), pp.1615-1626.

Doney, S.C., Ruckelshaus, M., Emmett Duffy, J., Barry, J.P., Chan, F., English, C.A., Galindo, H.M., Grebmeier, J.M., Hollowed, A.B., Knowlton, N. and Polovina, J., 2012. Climate change impacts on marine ecosystems. *Annual review of marine science*, *4*, pp.11-37.

Döös, K., Kjellsson, J. and Jönsson, B., 2013. TRACMASS—A Lagrangian trajectory model. In *Preventive methods for coastal protection* (pp. 225-249). Springer, Heidelberg.

Dromgoole, F.I., 1982. The buoyant properties of *Codium*. Botanica Marina 25: 391–398.

Dubi, A. and Torum, A., 1994. Wave damping by kelp vegetation. *Coastal Engineering Proceedings*, (24).

Dufois, F. and Rouault, M., 2012. Sea surface temperature in False Bay (South Africa): Towards a better understanding of its seasonal and inter-annual variability. *Continental Shelf Research*, *43*, pp.24-35.

Duggins, D.O., Eckman, J.E. and Sewell, A.T., 1990. Ecology of understory kelp environments. II. Effects of kelps on recruitment of benthic invertebrates. *Journal of Experimental Marine Biology and Ecology*, *143*(1-2), pp.27-45.

Duggins, D.O., Eckman, J.E., Siddon, C.E. and Klinger, T., 2003. Population, morphometric and biomechanical studies of three understory kelps along a hydrodynamic gradient. *Marine Ecology Progress Series*, *265*, pp.57-76.

Dunne, R. and Brown, B., 2001. The influence of solar radiation on bleaching of shallow water reef corals in the Andaman Sea, 1993–1998. *Coral Reefs*, *20*(3), pp.201-210.

Durgadoo, J.V., Biastoch, A., New, A.L., Rühs, S., Nurser, A.J., Drillet, Y. and Bidlot, J.R., 2021. Strategies for simulating the drift of marine debris. *Journal of operational Oceanography*, *14*(1), pp.1-12.

Dyer, D. C. 2018. Stable Isotope Ecology of South African Kelp Forests J. Bolton, R. Anderson, and A.J. Smit [eds.].

Dyer, D.C., Butler, M.J., Smit, A.J., Anderson, R.J. and Bolton, J.J., 2019. Kelp forest POM during upwelling and downwelling conditions: using stable isotopes to differentiate between detritus and phytoplankton. *Marine Ecology Progress Series*, *619*, pp.17-34.

Edgar, G.J., 1987. Dispersal of faunal and floral propagules associated with drifting *Macrocystis pyrifera* plants. *Marine Biology*, *95*(4), pp.599-610.

Eggert, A., Peters, A.F. and Küpper, F.C., 2010. The potential impact of climate change on endophyte infections in kelp sporophytes. In *Seaweeds and their role in globally changing environments* (pp. 139-154). Springer, Dordrecht.

Elliott Smith, E.A. and Fox, M.D., 2022. Characterizing energy flow in kelp forest food webs: a geochemical review and call for additional research. *Ecography*, *2022*(6), p.e05566.

Elliott Smith, E.A., Harrod, C. and Newsome, S.D., 2018. The importance of kelp to an intertidal ecosystem varies by trophic level: Insights from amino acid δ13C analysis. *Ecosphere*, *9*(11), p.e02516.

El-Nabulsi, R.A., 2019. Geostrophic flow and wind-driven ocean currents depending on the spatial dimensionality of the medium. *Pure and Applied Geophysics*, *176*(6), pp.2739-2750.

Field, J.G., Griffiths, C.L., Linley, E.A., Carter, R.A. and Zoutendyk, P., 1980. Upwelling in a nearshore marine ecosystem and its biological implications. *Estuarine and Coastal Marine Science*, *11*(2), pp.133-150.

Filbee-Dexter, K. and Scheibling, R.E., 2014. Detrital kelp subsidy supports high reproductive condition of deep-living sea urchins in a sedimentary basin. *Aquatic Biology*, *23*(1), pp.71-86.

Filbee-Dexter, K. and Scheibling, R.E., 2016. Spatial patterns and predictors of drift algal subsidy in deep subtidal environments. *Estuaries and Coasts*, *39*(6), pp.1724-1734.

Filbee-Dexter, K., Wernberg, T., Norderhaug, K.M., Ramirez-Llodra, E. and Pedersen, M.F., 2018. Movement of pulsed resource subsidies from kelp forests to deep fjords. *Oecologia*, *187*(1), pp.291-304.

Filbee-Dexter, K. and Wernberg, T., 2020. Substantial blue carbon in overlooked Australian kelp forests. *Scientific Reports*, *10*(1), pp.1-6.

Fossette, S., Putman, N.F., Lohmann, K.J., Marsh, R. and Hays, G.C., 2012. A biologist's guide to assessing ocean currents: a review. *Marine Ecology Progress Series*, *457*, pp.285-301.

Fowler-Walker, M.J., Connell, S.D. and Gillanders, B.M., 2005. To what extent do geographic and associated environmental variables correlate with kelp morphology across temperate Australia?. *Marine and freshwater research*, *56*(6), pp.877-887.

Fowler-Walker, M.J., Wernberg, T. and Connell, S.D., 2006. Differences in kelp morphology between wave sheltered and exposed localities: morphologically plastic or fixed traits?. *Marine Biology*, *148*(4), pp.755-767.

Fram, J.P., Stewart, H.L., Brzezinski, M.A., Gaylord, B., Reed, D.C., Williams, S.L. and MacIntyre, S., 2008. Physical pathways and utilization of nitrate supply to the giant kelp, *Macrocystis pyrifera*. *Limnology and Oceanography*, *53*(4), pp.1589-1603.

Fraser, C.I., Morrison, A.K., Hogg, A.M., Macaya, E.C., van Sebille, E., Ryan, P.G., Padovan, A., Jack, C., Valdivia, N. and Waters, J.M., 2018. Antarctica's ecological isolation will be broken by storm-driven dispersal and warming. *Nature climate change*, *8*(8), pp.704-708.

Fraser, C.I., Nikula, R. and Waters, J.M., 2011. Oceanic rafting by a coastal community. *Proceedings of the Royal Society B: Biological Sciences*, *278*(1706), pp.649-655.

Friedland, M.T. and Denny, M.W., 1995. Surviving hydrodynamic forces in a wave-swept environment: consequences of morphology in the feather boa kelp, *Egregia menziesii* (Turner). *Journal of Experimental Marine Biology and Ecology*, *190*(1), pp.109-133.

Furnans, J., Imberger, J. and Hodges, B.R., 2008. Including drag and inertia in drifter modelling. *Environmental Modelling & Software*, *23*(6), pp.714-728.

Gaines, S.D. and Roughgarden, J., 1987. Fish in offshore kelp forests affect recruitment to intertidal barnacle populations. *Science*, *235*(4787), pp.479-481.

Gao, X., Endo, H., Taniguchi, K. and Agatsuma, Y., 2013. Combined effects of seawater temperature and nutrient condition on growth and survival of juvenile sporophytes of the kelp *Undaria pinnatifida* (Laminariales; Phaeophyta) cultivated in northern Honshu, Japan. *Journal of applied phycology*, *25*(1), pp.269-275.

Garzoli, S.L., Gordon, A.L., Kamenkovich, V., Pillsbury, D. and Duncombe-Rae, C., 1996. Variability and sources of the southeastern Atlantic circulation. *Journal of Marine Research*, *54*(6), pp.1039-1071.

Gates, D.C., Margolina, T., Collins, C.A. and Rago, T.A., 2018. Observation and prediction of flotsam trajectories in the California Current System based on surface drift of RAFOS floats. *Deep Sea Research Part II: Topical Studies in Oceanography*, *151*, pp.102-114.

Gaylord, B., Nickols, K.J. and Jurgens, L., 2012. Roles of transport and mixing processes in kelp forest ecology. *Journal of Experimental Biology*, *215*(6), pp.997-1007.

Gentle, R.I., 1987. The geology of the inner continental shelf and Agulhas Arch: Cape Town to Port Elizabeth.

Gerard, V.A., 1982. In situ rates of nitrate uptake by giant kelp, *Macrocystis pyrifera* (L.) C. Agardh: tissue differences, environmental effects, and predictions of nitrogen-limited growth. *Journal of Experimental Marine Biology and Ecology*, *62*(3), pp.211-224.

Gerard, V.A., 1984. The light environment in a giant kelp forest: influence of *Macrocystis pyrifera* on spatial and temporal variability. *Marine Biology*, *84*(2), pp.189-195.

Gerard, V. A. 1997. The role of nitrogen nutrition in high-temperature tolerance of the kelp, *Laminaria saccharina* (Chlorophyta). *Journal of Phycology*, *33*(5), pp.800-810.

Gill, A.E. and Clarke, A.J., 1974, May. Wind-induced upwelling, coastal currents and sea-level changes. In *Deep Sea Research and Oceanographic Abstracts* (Vol. 21, No. 5, pp. 325-345). Elsevier.

Gilson, A.R., Smale, D.A., Burrows, M.T. and Connor, N.E., 2021. Spatio-temporal variability in the deposition of beach-cast kelp (wrack) and inter-specific differences in degradation rates. *Marine Ecology Progress Series*, *674*, pp.89-102.

Gorman, D., Bajjouk, T., Populus, J., Vasquez, M. and Ehrhold, A., 2013. Modeling kelp forest distribution and biomass along temperate rocky coastlines. *Marine Biology*, *160*(2), pp.309-325.

Graham, M.H., 2004. Effects of local deforestation on the diversity and structure of southern California giant kelp forest food webs. *Ecosystems*, *7*(4), pp.341-357.

Graiff, A., Karsten, U., Meyer, S., Pfender, D., Tala, F. and Thiel, M., 2013. Seasonal variation in floating persistence of detached *Durvillaea antarctica* (Chamisso) Hariot thalli. *Botanica Marina*, *56*(1), pp.3-14.

Graiff, A., Pantoja, J.F., Tala, F. and Thiel, M., 2016. Epibiont load causes sinking of viable kelp rafts: seasonal variation in floating persistence of giant kelp *Macrocystis pyrifera*. *Marine biology*, *163*(9), pp.1-14.

Griffin, D.A., Oke, P.R. and Jones, E.M., 2017. *The search for MH370 and ocean surface drift*. Commonwealth Scientific and Industrial Research Organisation.

Griffiths, C.L., Stenton-Dozey, J.M.E. and Koop, K., 1983. Kelp wrack and the flow of energy through a sandy beach ecosystem. In *Sandy beaches as ecosystems* (pp. 547-556). Springer, Dordrecht.

Group, T.W., 1988. The WAM model—A third generation ocean wave prediction model. *Journal of Physical Oceanography*, *18*(12), pp.1775-1810.

Grue, J. and Biberg, D., 1993. Wave forces on marine structures with small speed in water of restricted depth. *Applied Ocean Research*, *15*(3), pp.121-135.

de Guimaraens, M.A. and Coutinho, R., 1996. Spatial and temporal variation of benthic marine algae at the Cabo Frio upwelling region, Rio de Janeiro, Brazil. *Aquatic Botany*, *52*(4), pp.283-299.

Guiry, M.D., 2013. AlgaeBase. World-wide electronic publication. *http://www. algaebase. org*.

Hackett, B., Breivik, Ø. and Wettre, C., 2006. Forecasting the drift of objects and substances in the ocean. In *Ocean weather forecasting* (pp. 507-523). Springer, Dordrecht.

Haine, T.W. and Williams, P.D., 2002. The role of nonhydrostatic dynamics in controlling development of a surface ocean front. *Ocean Modelling*, *4*(2), pp.121-135.

Halliwell Jr, G.R., Ro, Y.J. and Cornillon, P., 1991. Westward-propagating SST anomalies and baroclinic eddies in the Sargasso Sea. *Journal of physical oceanography*, *21*(11), pp.1664-1680.

Hardman-Mountford, N.J., Richardson, A.J., Agenbag, J.J., Hagen, E., Nykjaer, L., Shillington, F.A. and Villacastin, C., 2003. Ocean climate of the South East Atlantic observed from satellite data and wind models. *Progress in Oceanography*, *59*(2-3), pp.181-221.

Harley, C.D., Anderson, K.M., Demes, K.W., Jorve, J.P., Kordas, R.L., Coyle, T.A. and Graham, M.H., 2012. Effects of climate change on global seaweed communities. *Journal of Phycology*, *48*(5), pp.1064-1078.

Harley, C.D., Randall Hughes, A., Hultgren, K.M., Miner, B.G., Sorte, C.J., Thornber, C.S., Rodriguez, L.F., Tomanek, L. and Williams, S.L., 2006. The impacts of climate change in coastal marine systems. *Ecology letters*, *9*(2), pp.228-241.

Harrold, C. and Lisin, S., 1989. Radio-tracking rafts of giant kelp: local production and regional transport. *Journal of Experimental Marine Biology and Ecology*, *130*(3), pp.237-251.

Hart-Davis, M., Backeberg, B. and Bakhoday-Paskyabi, M., 2018. An assessment of the importance of combining wind, ocean currents and stochastic motions in a particle trajectory model for search and rescue applications. *South African Society for Atmospheric Sciences, 34*, pp.157-160.

Hauser, A., Attrill, M.J. and Cotton, P.A., 2006. Effects of habitat complexity on the diversity and abundance of macrofauna colonising artificial kelp holdfasts. *Marine Ecology Progress Series*, *325*, pp.93-100.

Helmuth, B., Veit, R.R. and Holberton, R., 1994. Long-distance dispersal of a subantarctic brooding bivalve (*Gaimardia trapesina*) by kelp-rafting. *Marine biology*, *120*(3), pp.421-426.

Hepburn, C.D., Holborow, J.D., Wing, S.R., Frew, R.D. and Hurd, C.L., 2007. Exposure to waves enhances the growth rate and nitrogen status of the giant kelp *Macrocystis pyrifera*. *Marine Ecology Progress Series*, *339*, pp.99-108

Highsmith, R.C., 1985. Floating and algal rafting as potential dispersal mechanisms in brooding invertebrates. *Marine ecology progress series. Oldendorf*, *25*(2), pp.169-179.

Hill, N.A., Pepper, A.R., Puotinen, M.L., Hughes, M.G., Edgar, G.J., Barrett, N.S., Stuart-Smith, R.D. and Leaper, R., 2010. Quantifying wave exposure in shallow temperate reef systems: applicability of fetch models for predicting algal biodiversity. *Marine Ecology Progress Series*, *417*, pp.83-95.

Hobday, A.J., 2000a. Abundance and dispersal of drifting kelp *Macrocystis pyrifera* rafts in the Southern California Bight. *Marine Ecology Progress Series*, *195*, pp.101-116.

Hobday, A.J., 2000b. Age of drifting *Macrocystis pyrifera* (L.) C. Agardh rafts in the Southern California Bight. *Journal of Experimental Marine Biology and Ecology*, *253*(1), pp.97-114.

Holden, J.J., Kingzett, B.C., MacNeill, S., Smith, W., Juanes, F. and Dudas, S.E., 2018. Beach-cast biomass and commercial harvesting of a non-indigenous seaweed, *Mazzaella japonica*, on the east coast of Vancouver Island, British Columbia. *Journal of Applied Phycology*, *30*(2), pp.1175-1184.

Holland, W.R. and Rhines, P.B., 1980. An example of eddy-induced ocean circulation. *Journal of Physical Oceanography*, *10*(7), pp.1010-1031.

Holmquist, J.G., 1994. Benthic macroalgae as a dispersal mechanism for fauna: influence of a marine tumbleweed. *Journal of Experimental Marine Biology and Ecology*, *180*(2), pp.235-251.

Holthuijsen, L.H., 2010. *Waves in oceanic and coastal waters*. Cambridge University Press.

Howard, J., Sutton-Grier, A., Herr, D., Kleypas, J., Landis, E., Mcleod, E., Pidgeon, E. and Simpson, S., 2017. Clarifying the role of coastal and marine systems in climate mitigation. *Frontiers in Ecology and the Environment*, *15*(1), pp.42-50.

Hurd, C.L., 2000. Water motion, marine macroalgal physiology, and production. *Journal of Phycology*, *36*(3), pp.453-472.

Hutchings, L., Van der Lingen, C.D., Shannon, L.J., Crawford, R.J.M., Verheye, H.M.S., Bartholomae, C.H., Van der Plas, A.K., Louw, D., Kreiner, A., Ostrowski, M. and Fidel, Q., 2009. The Benguela Current: An ecosystem of four components. *Progress in Oceanography*, *83*(1-4), pp.15-32.

Ingólfsson, A., 1995. Floating clumps of seaweed around Iceland: natural microcosms and a means of dispersal for shore fauna. *Marine Biology*, *122*(1), pp.13-21.

Isaeus, M., 2004. A GIS-based wave exposure model calibrated and validated from vertical distribution of littoral lichens.

Jackson, G.A., 1977. Nutrients and production of giant kelp, *Macrocystis pyrifera*, off southern California. *Limnology and Oceanography*, *22*(6), pp.979-995.

Jackson, G.A., 1984. Internal wave attenuation by coastal kelp stands. *Journal of Physical Oceanography*, *14*(8), pp.1300-1306.

Jackson, S.T. and Sax, D.F., 2010. Balancing biodiversity in a changing environment: extinction debt, immigration credit and species turnover. *Trends in ecology & evolution*, *25*(3), pp.153-160.

Jalón-Rojas, I., Wang, X.H. and Fredj, E., 2019. On the importance of a three-dimensional approach for modelling the transport of neustic microplastics. *Ocean Science*, *15*(3), pp.717-724.
Jayne, S.R. and Marotzke, J., 2002. The oceanic eddy heat transport. *Journal of Physical Oceanography*, *32*(12), pp.3328-3345.

Jennings, S. and Brander, K., 2010. Predicting the effects of climate change on marine communities and the consequences for fisheries. *Journal of Marine Systems*, *79*(3-4), pp.418-426.

Johnson, C.R., Banks, S.C., Barrett, N.S., Cazassus, F., Dunstan, P.K., Edgar, G.J., Frusher, S.D., Gardner, C., Haddon, M., Helidoniotis, F. and Hill, K.L., 2011. Climate change cascades: Shifts in oceanography, species' ranges and subtidal marine community dynamics in eastern Tasmania. *Journal of Experimental Marine Biology and Ecology*, *400*(1-2), pp.17-32.

Jönsson, B.F., Salisbury, J.E. and Mahadevan, A., 2011. Large variability in continental shelf production of phytoplankton carbon revealed by satellite. *Biogeosciences*, *8*(5), pp.1213-1223.

Joska, M.A.P. and Bolton, J.J., 1987. In situ measurement of zoospore release and seasonality of reproduction in *Ecklonia maxima* (Alariaceae, Laminariales). *British Phycological Journal*, *22*(2), pp.209-214.

Jury, M.R., 1980. *Characteristics of summer wind fields and air-sea interactions over the Cape Peninsula upwelling region*(Doctoral dissertation, University of Cape Town).

Jury, M.R., Kamstra, F. and Taunton-Clark, J., 1985. Synoptic summer wind cycles and upwelling off the southern portion of the Cape Peninsula. *South African Journal of Marine Science*, *3*(1), pp.33-42.

Jutzeler, M., Marsh, R., van Sebille, E., Mittal, T., Carey, R.J., Fauria, K.E., Manga, M. and McPhie, J., 2020. Ongoing dispersal of the 7 August 2019 pumice raft from the Tonga arc in the southwestern Pacific Ocean. *Geophysical Research Letters*, *47*(5), p.e1701121.

Kaplan, D.M., Largier, J.L., Navarrete, S., Guiñez, R. and Castilla, J.C., 2003. Large diurnal temperature fluctuations in the nearshore water column. *Estuarine, Coastal and Shelf Science*, *57*(3), pp.385-398.

Karsten, R.H. and Marshall, J., 2002a. Constructing the residual circulation of the ACC from observations. *Journal of physical oceanography*, *32*(12), pp.3315-3327.

Karsten, R., Jones, H. and Marshall, J., 2002b. The role of eddy transfer in setting the stratification and transport of a circumpolar current. *Journal of Physical Oceanography*, *32*(1), pp.39-54.

Kawamata, S., 2001. Adaptive mechanical tolerance and dislodgement velocity of the kelp *Laminaria japonica* in wave-induced water motion. *Marine Ecology Progress Series*, *211*, pp.89-104.

Keith, S.A., Herbert, R.J., Norton, P.A., Hawkins, S.J. and Newton, A.C., 2011. Individualistic species limitations of climate-induced range expansions generated by meso-scale dispersal barriers. *Diversity and Distributions*, *17*(2), pp.275-286.

Kingsford, M.J., 1992. Drift algae and small fish in coastal waters of northeastern New Zealand. *Marine Ecology Progress Series*, pp.41-55.

Kingsford, M.J., 1995. Drift algae: a contribution to near-shore habitat complexity in the pelagic environment and an attractant for fish. *Marine ecology progress series. Oldendorf*, *116*(1), pp.297-301.

Kirkman, H. and Kendrick, G.A., 1997. Ecological significance and commercial harvesting of drifting and beach-cast macro-algae and seagrasses in Australia: a review. *Journal of Applied Phycology*, *9*(4), pp.311-326.

Klocker, A., Ferrari, R., LaCasce, J.H. and Merrifield, S.T., 2012. Reconciling float-based and tracer-based estimates of lateral diffusivities. *Journal of Marine Research*, *70*(4), pp.569-602.

Kobayashi, N., Raichle, A.W. and Asano, T., 1993. Wave attenuation by vegetation. *Journal of Waterway, Port, Coastal, and Ocean Engineering*, *119*(1), pp.30-48.

Koehl, M.A.R., Silk, W.K., Liang, H. and Mahadevan, L., 2008. How kelp produce blade shapes suited to different flow regimes: a new wrinkle. *Integrative and Comparative Biology*, *48*(6), pp.834-851.

Kooi, M., Nes, E.H.V., Scheffer, M. and Koelmans, A.A., 2017. Ups and downs in the ocean: effects of biofouling on vertical transport of microplastics. *Environmental science & technology*, *51*(14), pp.7963-7971.

Krumhansl, K.A., Okamoto, D.K., Rassweiler, A., Novak, M., Bolton, J.J., Cavanaugh, K.C., Connell, S.D., Johnson, C.R., Konar, B., Ling, S.D. and Micheli, F., 2016. Global patterns of kelp forest change over the past half-century. *Proceedings of the National Academy of Sciences*, *113*(48), pp.13785-13790.

Krumhansl, K.A. and Scheibling, R.E., 2012. Production and fate of kelp detritus. *Marine Ecology Progress Series*, *467*, pp.281-302.

Le Gouvello, D.Z., Hart-Davis, M.G., Backeberg, B.C. and Nel, R., 2020. Effects of swimming behaviour and oceanography on sea turtle hatchling dispersal at the intersection of two ocean current systems. *Ecological Modelling*, *431*, p.109130.

Lebreton, L.M., Greer, S.D. and Borrero, J.C., 2012. Numerical modelling of floating debris in the world's oceans. *Marine pollution bulletin*, *64*(3), pp.653-661.

Leliaert, F., Anderson, R.J., Bolton, J.J. and Coppejans, E., 2000. Subtidal understorey algal community structure in kelp beds around the Cape Peninsula (Western Cape, South Africa).

León, L.F., Lam, D.C., McCrimmon, C. and Swayne, D.A., 2003. Watershed management modelling in Malawi: application and technology transfer. *Environmental Modelling & Software*, *18*(6), pp.531-539.

Levin, P.S., 1994. Fine-scale temporal variation in recruitment of a temperate demersal fish: the importance of settlement versus post-settlement loss. *Oecologia*, *97*(1), pp.124-133.

Levitt, G.J., Anderson, R.J., Boothroyd, C.J.T. and Kemp, F.A., 2002. The effects of kelp harvesting on its regrowth and the understorey benthic community at Danger Point, South Africa, and a new method of harvesting kelp fronds. *African Journal of Marine Science*, *24*, pp.71-85.

Lewis, P.N., Riddle, M.J. and Smith, S.D., 2005. Assisted passage or passive drift: a comparison of alternative transport mechanisms for non-indigenous coastal species into the Southern Ocean. *Antarctic Science*, *17*(2), pp.183-191.

Li, Y., Zhang, H. and Tang, C., 2020. A review of possible pathways of marine microplastics transport in the ocean. *Anthropocene Coasts*, *3*(1), pp.6-13.

Lindegarth, M. and Gamfeldt, L., 2005. Comparing categorical and continuous ecological analyses: effects of "wave exposure" on rocky shores. *Ecology*, *86*(5), pp.1346-1357.

Lobelle, D., Kooi, M., Koelmans, A.A., Laufkötter, C., Jongedijk, C.E., Kehl, C. and van Sebille, E., 2021. Global modeled sinking characteristics of biofouled microplastic. *Journal of Geophysical Research: Oceans*, *126*(4), p.e2020JC017098.

Long, M., Moriceau, B., Gallinari, M., Lambert, C., Huvet, A., Raffray, J. and Soudant, P., 2015. Interactions between microplastics and phytoplankton aggregates: impact on their respective fates. *Marine Chemistry*, *175*, pp.39-46.

Lutjeharms, J.R.E., 2007. Three decades of research on the greater Agulhas Current. *Ocean Science*, *3*(1), pp.129-147.

Lutjeharms, J.R.E., Cooper, J. and Roberts, M., 2000. Upwelling at the inshore edge of the Agulhas Current. *Continental Shelf Research*, *20*(7), pp.737-761.

Lutjeharms, J.R.E. and Van Ballegooyen, R.C., 1988. The retroflection of the Agulhas Current. *Journal of Physical Oceanography*, *18*(11), pp.1570-1583.

Lutjeharms, J.R.E., Walters, N.M. and Allanson, B.R., 1985. Oceanic frontal systems and biological enhancement. In *Antarctic nutrient cycles and food webs* (pp. 11-21). Springer, Berlin, Heidelberg.

Ma, G., Kirby, J.T., Su, S.F., Figlus, J. and Shi, F., 2013. Numerical study of turbulence and wave damping induced by vegetation canopies. *Coastal Engineering*, *80*, pp.68-78.

Mabin, C.J., Gribben, P.E., Fischer, A. and Wright, J.T., 2013. Variation in the morphology, reproduction and development of the habitat-forming kelp *Ecklonia radiata* with changing temperature and nutrients. *Marine Ecology Progress Series*, *483*, pp.117-131.

MacArthur, R.H. and Wilson, E.O., 2001. The Theory of Island Biogeography, reprint edn.

Macaya, E.C., Boltana, S., Hinojosa, I.A., Macchiavello, J.E., Valdivia, N.A., Vasquez, N.R., Buschmann, A.H., Vasquez, J.A., Alonso Vega, J.M. and Thiel, M., 2005. Presence of Sporophylls in Floating Kelp Rafts of *Macrocystis* Spp. (Phaeophyceae) Along the Chilean Pacific Coast. *Journal of Phycology*, *41*(5), pp.913-922

Macaya, E.C., López, B., Tala, F., Tellier, F. and Thiel, M., 2016. Float and raft: role of buoyant seaweeds in the phylogeography and genetic structure of non-buoyant associated flora. In *Seaweed phylogeography* (pp. 97-130). Springer, Dordrecht.

Mackas, D.L., Denman, K.L. and Abbott, M.R., 1985. Plankton patchiness: biology in the physical vernacular. *Bulletin of Marine Science*, *37*(2), pp.652-674.

Mann, K.H., 1973. Seaweeds: Their Productivity and Strategy for Growth: The role of large marine algae in coastal productivity is far more important than has been suspected. *Science*, *182*(4116), pp.975-981.

McCormick, T.B., Buckley, L.M., Brogan, J. and Perry, L.M., 2008. Drift macroalgae as a potential dispersal mechanism for the white abalone *Haliotis sorenseni*. *Marine Ecology Progress Series*, *362*, pp.225-232.

McGillicuddy Jr, D.J., Anderson, L.A., Doney, S.C. and Maltrud, M.E., 2003. Eddy-driven sources and sinks of nutrients in the upper ocean: Results from a 0.1 resolution model of the North Atlantic. *Global Biogeochemical Cycles*, *17*(2).

McGowan, J.A., Cayan, D.R. and Dorman, L.M., 1998. Climate-ocean variability and ecosystem response in the Northeast Pacific. *Science*, *281*(5374), pp.210-217.

Michaud, K.M., Emery, K.A., Dugan, J.E., Hubbard, D.M. and Miller, R.J., 2019. Wrack resource use by intertidal consumers on sandy beaches. *Estuarine, Coastal and Shelf Science*, *221*, pp.66-71.

Miller, R.J., Lafferty, K.D., Lamy, T., Kui, L., Rassweiler, A. and Reed, D.C., 2018. Giant kelp, *Macrocystis pyrifera*, increases faunal diversity through physical engineering. *Proceedings of the Royal Society B: Biological Sciences*, *285*(1874), p.20172571.

Miller, S.M., Hurd, C.L. and Wing, S.R., 2011. Variations in growth, erosion, productivity, and morphology of *Ecklonia radiata* (Alariaceae; Laminariales) along a fjord in southern New Zealand. *Journal of Phycology*, *47*(3), pp.505-516.

Miron, P., Olascoaga, M.J., Beron-Vera, F.J., Putman, N.F., Triñanes, J., Lumpkin, R. and Goni, G.J., 2020. Clustering of marine-debris-and *Sargassum*-like drifters explained by inertial particle dynamics. *Geophysical research letters*, *47*(19), p.e2020GL089874.

Mohring, M.B., Wernberg, T., Wright, J.T., Connell, S.D. and Russell, B.D., 2014. Biogeographic variation in temperature drives performance of kelp gametophytes during warming. *Marine Ecology Progress Series*, *513*, pp.85-96.

Molloy, F.J. and Bolton, J.J., 1996. The effects of wave exposure and depth on the morphology of inshore populations of the Namibian kelp, *Laminaria schinzii* Foslie. Walter de Gruyter, 39, pp.525-531.

Monismith, S.G., Alnajjar, M.W., Woodson, C.B., Boch, C.A., Hernandez, A., Vazquez-Vera, L., Bell, T.W. and Micheli, F., 2022. Influence of kelp forest biomass on nearshore currents. *Journal of Geophysical Research: Oceans*, *127*(7), p.e2021JC018333

Mork, M., 1996. The effect of kelp in wave damping. *Sarsia*, *80*(4), pp.323-327.

Morrow, R. and Le Traon, P.Y., 2012. Recent advances in observing mesoscale ocean dynamics with satellite altimetry. *Advances in Space Research*, *50*(8), pp.1062-1076.

Moss, B.L., 1950. Studies in the Genus Fucus II. The Anatomical Structure and Chemical Composition of Receptacles of *Fucus vesiculosus* from Three Contrasting Habitats. *Annals of Botany*, *14*(55), pp.395-410.

Nardelli, B.B., Santoleri, R. and Sparnocchia, S., 2001. Small mesoscale features at a meandering upper-ocean front in the Western Ionian Sea (Mediterranean Sea): Vertical motion and potential vorticity analysis. *Journal of physical oceanography*, *31*(8), pp.2227-2250.

Nikula, R., Fraser, C.I., Spencer, H.G. and Waters, J.M., 2010. Circumpolar dispersal by rafting in two subantarctic kelp-dwelling crustaceans. *Marine Ecology Progress Series*, *405*, pp.221-230.

Nikula, R., Spencer, H.G. and Waters, J.M., 2013. Passive rafting is a powerful driver of transoceanic gene flow. *Biology Letters*, *9*(1), p.20120821.

Norderhaug, K.M., Christie, H., Andersen, G.S. and Bekkby, T., 2012. Does the diversity of kelp forest macrofauna increase with wave exposure?. *Journal of Sea Research*, *69*, pp.36-42.

North, E.W., Gallego, A. and Petitgas, P., 2009. Manual of recommended practices for modelling physical–biological interactions during fish early life. *ICES Cooperative Research Report*, (295).

Norton, T.A., 1992. Dispersal by macroalgae. *British Phycological Journal*, *27*(3), pp.293-301.

Oksanen, J., Blanchet, F.G., Kindt, R., Legendre, P., Minchin, P.R., O'hara, R.B., Simpson, G.L., Solymos, P., Stevens, M.H.H., Wagner, H. and Oksanen, M.J., 2013. Package 'vegan'. *Community ecology package, version*, *2*(9), pp.1-295.

Olascoaga, M.J., Beron-Vera, F.J., Miron, P., Triñanes, J., Putman, N.F., Lumpkin, R. and Goni, G.J., 2020. Observation and quantification of inertial effects on the drift of floating objects at the ocean surface. *Physics of Fluids*, *32*(2), p.026601.

Onink, V., Wichmann, D., Delandmeter, P. and van Sebille, E., 2019. The role of Ekman currents, geostrophy, and Stokes drift in the accumulation of floating microplastic. *Journal of Geophysical Research: Oceans*, *124*(3), pp.1474-1490.

Page, H.M., Reed, D.C., Brzezinski, M.A., Melack, J.M. and Dugan, J.E., 2008. Assessing the importance of land and marine sources of organic matter to kelp forest food webs. *Marine Ecology Progress Series*, *360*, pp.47-62.

Paul, A.X. and Steneck, R., 1993. Kelp beds as habitat for American lobster *Homarus americanus*. *Marine Ecological Progress Series*, *100*, p.127.

Pedersen, M.F., Nejrup, L.B., Fredriksen, S., Christie, H. and Norderhaug, K.M., 2012. Effects of wave exposure on population structure, demography, biomass and productivity of the kelp *Laminaria hyperborea*. *Marine Ecology Progress Series*, *451*, pp.45-60.

Pegliasco, C., Chaigneau, A. and Morrow, R., 2015. Main eddy vertical structures observed in the four major Eastern Boundary Upwelling Systems. *Journal of Geophysical Research: Oceans*, *120*(9), pp.6008-6033.

Phillips, J.S., Gupta, A.S., Senina, I., van Sebille, E., Lange, M., Lehodey, P., Hampton, J. and Nicol, S., 2018. An individual-based model of skipjack tuna (*Katsuwonus pelamis*) movement in the tropical Pacific ocean. *Progress in Oceanography*, *164*, pp.63-74.

Pichel, W.G., Veenstra, T.S., Churnside, J.H., Arabini, E., Friedman, K.S., Foley, D.G., Brainard, R.E., Kiefer, D., Ogle, S., Clemente-Colón, P. and Li, X., 2012. GhostNet marine debris survey in the Gulf of Alaska–Satellite guidance and aircraft observations. *Marine pollution bulletin*, *65*(1-3), pp.28-41.

Polovina, J.J., 2005. Climate variation, regime shifts, and implications for sustainable fisheries. *Bulletin of Marine Science*, *76*(2), pp.233-244.

Price, J.F., Weller, R.A. and Schudlich, R.R., 1987. Wind-driven ocean currents and Ekman transport. *Science*, *238*(4833), pp.1534-1538.

Probyn, T.A. and McQuaid, C.D., 1985. In-situ measurements of nitrogenous nutrient uptake by kelp (*Ecklonia maxima*) and phytoplankton in a nitrate-rich upwelling environment. *Marine Biology*, *88*(2), pp.149-154.

Pujolar, J.M., Schiavina, M., Di Franco, A., Melià, P., Guidetti, P., Gatto, M., De Leo, G.A. and Zane, L., 2013. Understanding the effectiveness of marine protected areas using genetic connectivity patterns and Lagrangian simulations. *Diversity and Distributions*, *19*(12), pp.1531-1542.

Putman, N.F., Goni, G.J., Gramer, L.J., Hu, C., Johns, E.M., Trinanes, J. and Wang, M., 2018. Simulating transport pathways of pelagic Sargassum from the Equatorial Atlantic into the Caribbean Sea. *Progress in Oceanography*, *165*, pp.205-214.

Putman, N.F., Lumpkin, R., Olascoaga, M.J., Trinanes, J. and Goni, G.J., 2020. Improving transport predictions of pelagic *Sargassum*. *Journal of Experimental Marine Biology and Ecology*, *529*, p.151398.

Qiu, Z., Coleman, M.A., Provost, E., Campbell, A.H., Kelaher, B.P., Dalton, S.J., Thomas, T., Steinberg, P.D. and Marzinelli, E.M., 2019. Future climate change is predicted to affect the microbiome and condition of habitat-forming kelp. *Proceedings of the Royal Society B*, *286*(1896), p.20181887.

Ragoasha, N., Herbette, S., Cambon, G., Veitch, J., Reason, C. and Roy, C., 2019. Lagrangian pathways in the southern Benguela upwelling system. *Journal of Marine Systems*, *195*, pp.50-66.

Ramirez-Llodra, E., Pedersen, T., Dexter, K.F., Hauquier, F., Guilini, K., Mikkelsen, N., Borgersen, G., Van Gyseghem, M., Vanreusel, A. and Vilas, D., 2021. Community structure of deep fjord and shelf benthic fauna receiving different detrital kelp inputs in northern Norway. *Deep Sea Research Part I: Oceanographic Research Papers*, *168*, p.103433.

Rautenbach, C., 2015. Southern African coastal vulnerability assessment.

Reason, C.J.C., Landman, W. and Tennant, W., 2006. Seasonal to decadal prediction of southern African climate and its links with variability of the Atlantic Ocean. *Bulletin of the American Meteorological Society*, *87*(7), pp.941-956.

Reed, D.C. and Foster, M.S., 1984. The effects of canopy shadings on algal recruitment and growth in a giant kelp forest. *Ecology*, *65*(3), pp.937-948.

Reed, D., Washburn, L., Rassweiler, A., Miller, R., Bell, T. and Harrer, S., 2016. Extreme warming challenges sentinel status of kelp forests as indicators of climate change. *Nature Communications*, *7*(1), pp.1-7.

Reguero, B.G., Losada, I.J. and Méndez, F.J., 2019. A recent increase in global wave power as a consequence of oceanic warming. *Nature Communications*, *10*(1), pp.1-14.

Rinde, E., Christie, H., Fagerli, C.W., Bekkby, T., Gundersen, H., Norderhaug, K.M. and Hjermann, D.Ø., 2014. The influence of physical factors on kelp and sea urchin distribution in previously and still grazed areas in the NE Atlantic. *PLoS One*, *9*(6), p.e100222.

Rinde, E., Sloreid, S.E., Bakkestuen, V., Bekkby, T., Erikstad, L. and Longva, O., 2004. Modelling of some selected marine nature types and EUNIS classes. Two projects within the national programme for mapping and monitoring of biological diversity. *NINA Oppdragsmelding*, *807*, pp.1-33.

Rose, T.H., Smale, D.A. and Botting, G., 2012. The 2011 marine heat wave in Cockburn Sound, southwest Australia. *Ocean Science*, *8*(4), pp.545-550.

Rossby, C.G. and Montgomery, R.B., 1935. The layer of frictional influence in wind and ocean currents. Papers in Physical Oceanography and Meteorology 3 (3). Cambridge, MA: Massachusetts Institute of Technology and Woods Hole Oceanographic Institution

Rossi, V., Ser-Giacomi, E., López, C. and Hernández-García, E., 2014. Hydrodynamic provinces and oceanic connectivity from a transport network help designing marine reserves. *Geophysical Research Letters*, *41*(8), pp.2883-2891.

Rothäusler, E., Gómez, I., Hinojosa, I.A., Karsten, U., Miranda, L., Tala, F. and Thiel, M., 2011. Kelp rafts in the Humboldt Current: interplay of abiotic and biotic factors limit their floating persistence and dispersal potential. *Limnology and oceanography*, *56*(5), pp.1751-1763.

Rothman, M.D., 2006. *Investigations into the harvesting ecology of the South African kelp Ecklonia maxima (Alariaceae, Laminariales)* (Master's thesis, University of Cape Town).

Rothman, M.D., Bolton, J.J., Stekoll, M.S., Boothroyd, C.J., Kemp, F.A. and Anderson, R.J., 2017. Geographical variation in morphology of the two dominant kelp species, *Ecklonia maxima* and *Laminaria pallida* (Phaeophyceae, Laminariales), on the west coast of Southern Africa. *Journal of Applied Phycology*, *29*(5), pp.2627-2639.

Rothman, M.D., Anderson, R.J. and Smit, A.J., 2006. The effects of harvesting of the South African kelp (*Ecklonia maxima*) on kelp population structure, growth rate and recruitment. In *Eighteenth International Seaweed Symposium*(pp. 109-115). Springer, Dordrecht.

Rouault, M., Pohl, B. and Penven, P., 2010. Coastal oceanic climate change and variability from 1982 to 2009 around South Africa. *African Journal of Marine Science*, *32*(2), pp.237-246.

Rothman, M.D., Mattio, L., Anderson, R.J. and Bolton, J.J., 2017b. A phylogeographic investigation of the kelp genus *Laminaria* (Laminariales, Phaeophyceae), with emphasis on the South Atlantic Ocean. *Journal of Phycology*, *53*(4), pp.778-789.

Team, R., 2019. RStudio: Integrated Development Environment for R. Boston, MA: RStudio, Inc; 2016.

Rubio, A., Blanke, B., Speich, S., Grima, N. and Roy, C., 2009. Mesoscale eddy activity in the southern Benguela upwelling system from satellite altimetry and model data. *Progress in Oceanography*, *83*(1-4), pp.288-295.

Rummukainen, M., 2012. Changes in climate and weather extremes in the 21st century. *Wiley Interdisciplinary Reviews: Climate Change*, *3*(2), pp.115-129.

Russo, S., Dosio, A., Graversen, R.G., Sillmann, J., Carrao, H., Dunbar, M.B., Singleton, A., Montagna, P., Barbola, P. and Vogt, J.V., 2014. Magnitude of extreme heat waves in present climate and their projection in a warming world. *Journal of Geophysical Research: Atmospheres*, *119*(22), pp.12-500.

Ryan, J.P., Harvey, J.B.J., Zhang, Y. and Woodson, C.B., 2014. Distributions of invertebrate larvae and phytoplankton in a coastal upwelling system retention zone and peripheral front. *Journal of Experimental Marine Biology and Ecology*, *459*, pp.51-60.

Salmon, R., 1998. *Lectures on geophysical fluid dynamics*. Oxford University Press.

Saltzman, B. and Tang, C.M., 1975. Formation of meanders, fronts, and cutoff thermal pools in a baroclinic ocean current. *Journal of Physical Oceanography*, *5*(1), pp.86-92.

Saunders, G.W., 2014. Long distance kelp rafting impacts seaweed biogeography in the Northeast Pacific: the kelp conveyor hypothesis. *Journal of phycology*, *50*(6), pp.968-974.

Schiel, D.R. and Foster, M.S., 2006. The population biology of large brown seaweeds: ecological consequences of multiphase life histories in dynamic coastal environments. *Annual review of ecology, evolution, and systematics*, pp.343-372.

Schiel, D.R. and Foster, M.S., 2015. *The Biology and Ecology of Giant Kelp Forests*. Univeristy of California Press.

Serisawa, Y., Akino, H., Matsuyama, K., Ohno, M., Tanaka, J. and Yokohama, Y., 2002. Morphometric study of *Ecklonia cava* (Laminariales, Phaeophyta) sporophytes in two localities with different temperature conditions. *Phycological Research*, *50*(3), pp.193-199.

Seymour, R.J., Tegner, M.J., Dayton, P.K. and Parnell, P.E., 1989. Storm wave induced mortality of giant kelp, *Macrocystis pyrifera*, in southern California. *Estuarine, Coastal and Shelf Science*, *28*(3), pp.277-292.

Shannon, L.V. and Nelson, G., 1996. The Benguela: large scale features and processes and system variability. In *The south Atlantic* (pp. 163-210). Springer, Berlin, Heidelberg.

Shen, H., Perrie, W. and Wu, Y., 2019. Wind drag in oil spilled ocean surface and its impact on wind-driven circulation. *Anthropocene Coasts*, *2*(1), pp.244-260.

Shipley, A.M., 1964. Some aspects of wave refraction in False Bay. *South African Journal of Science*, *60*(4), pp.115-120.

Siegel, D.A., Kinlan, B.P., Gaylord, B. and Gaines, S.D., 2003. Lagrangian descriptions of marine larval dispersion. *Marine Ecology Progress Series*, *260*, pp.83-96.

Simonson, E.J., Scheibling, R.E. and Metaxas, A., 2015. Kelp in hot water: I. Warming seawater temperature induces weakening and loss of kelp tissue. *Marine Ecology Progress Series*, *537*, pp.89-104.

Smale, D.A., Burrows, M.T., Moore, P., O'Connor, N. and Hawkins, S.J., 2013. Threats and knowledge gaps for ecosystem services provided by kelp forests: a northeast Atlantic perspective. *Ecology and evolution*, *3*(11), pp.4016-4038.

Smale, D.A. and Moore, P.J., 2017. Variability in kelp forest structure along a latitudinal gradient in ocean temperature. *Journal of Experimental Marine Biology and Ecology*, *486*, pp.255-264.

Smale, D.A., Moore, P.J., Queirós, A.M., Higgs, S. and Burrows, M.T., 2018. Appreciating interconnectivity between habitats is key to blue carbon management. *Frontiers in Ecology and the Environment*, *16*(2), pp.71-73.

Smale, D.A., 2020. Impacts of ocean warming on kelp forest ecosystems. *New Phytologist*, *225*(4), pp.1447-1454.

Smale, D.A., Pessarrodona, A., King, N. and Moore, P.J., 2022. Examining the production, export, and immediate fate of kelp detritus on open-coast subtidal reefs in the Northeast Atlantic. Limnology and Oceanography, 67, pp.S36-S49.

Smit, A.J., 2004. Medicinal and pharmaceutical uses of seaweed natural products: A review. *Journal of applied phycology*, *16*(4), pp.245-262.

Smit, A.J., Bolton, J.J. and Anderson, R.J., 2017. Seaweeds in two oceans: beta-diversity. *Frontiers in Marine Science*, *4*, p.404.

Smit, A.J., Roberts, M., Anderson, R.J., Dufois, F., Dudley, S.F., Bornman, T.G., Olbers, J. and Bolton, J.J., 2013. A coastal seawater temperature dataset for biogeographical studies: large biases between in situ and remotely-sensed data sets around the coast of South Africa. *PLoS One*, *8*(12), p.e81944.

Smith, J.M., Sherlock, A.R. and Resio, D.T., 2001. *STWAVE: Steady-state spectral wave model user's manual for STWAVE, Version 3.0. Engineer Research and Development Center Vicksburg MS Coastal and Hydraulicslab.*

Smith, S.D., 2002. Kelp rafts in the Southern Ocean. *Global Ecology and Biogeography*, *11*(1), pp.67-69.

Spall, M.A., 1995. Frontogenesis, subduction, and cross-front exchange at upper ocean fronts. *Journal of Geophysical Research: Oceans*, *100*(C2), pp.2543-2557.

Stegenga, H., 1997. Seaweeds of the South African west coast. *Control Bolus Herbarium*, *18*.

Steneck, R.S., Graham, M.H., Bourque, B.J., Corbett, D., Erlandson, J.M., Estes, J.A. and Tegner, M.J., 2002. Kelp forest ecosystems: biodiversity, stability, resilience and future. *Environmental conservation*, *29*(4), pp.436-459.

Stewart, H.L., Fram, J.P., Reed, D.C., Williams, S.L., Brzezinski, M.A., MacIntyre, S. and Gaylord, B., 2009. Differences in growth, morphology and tissue carbon and nitrogen of *Macrocystis pyrifera* within and at the outer edge of a giant kelp forest in California, USA. *Marine Ecology Progress Series*, *375*, pp.101-112.

Stommel, H., 1948. The westward intensification of wind-driven ocean currents. *Eos, Transactions American Geophysical Union*, *29*(2), pp.202-206.

Stramma, L. and Peterson, R.G., 1989. Geostrophic transport in the Benguela Current region. *Journal of Physical Oceanography*, *19*(10), pp.1440-1448.

Sundblad, G., Bekkby, T., Isæus, M., Nikolopoulos, A., Norderhaug, K.M. and Rinde, E., 2014. Comparing the ecological relevance of four wave exposure models. *Estuarine, Coastal and Shelf Science*, *140*, pp.7-13.

Supratya, V.P., Coleman, L.J. and Martone, P.T., 2020. Elevated temperature affects phenotypic plasticity in the bull kelp (*Nereocystis luetkeana*, Phaeophyceae). *Journal of phycology*, *56*(6), pp.1534-1541.

Tala, F., Gómez, I., Luna-Jorquera, G. and Thiel, M., 2013. Morphological, physiological and reproductive conditions of rafting bull kelp (*Durvillaea antarctica*) in northern-central Chile (30 S). *Marine biology*, *160*(6), pp.1339-1351.

Tala, F., Penna-Díaz, M.A., Luna-Jorquera, G., Rothäusler, E. and Thiel, M., 2017. Daily and seasonal changes of photobiological responses in floating bull kelp *Durvillaea antarctica* (Chamisso) Hariot (Fucales: Phaeophyceae). *Phycologia*, *56*(3), pp.271-283.

Tallis, H., 2009. Kelp and rivers subsidize rocky intertidal communities in the Pacific Northwest (USA). *Marine Ecology Progress Series*, *389*, pp.85-96.

Taylor, D.I. and Schiel, D.R., 2003. Wave-related mortality in zygotes of habitat-forming algae from different exposures in southern New Zealand: the importance of 'stickability'. *Journal of Experimental Marine Biology and Ecology*, *290*(2), pp.229-245.

Taylor, J.R., 2018. Accumulation and subduction of buoyant material at submesoscale fronts. *Journal of Physical Oceanography*, *48*(6), pp.1233-1241.

Taylor, J.R. and Ferrari, R., 2011. Ocean fronts trigger high latitude phytoplankton blooms. *Geophysical Research Letters*, *38*(23).

Teagle, H., Hawkins, S.J., Moore, P.J. and Smale, D.A., 2017. The role of kelp species as biogenic habitat formers in coastal marine ecosystems. *Journal of Experimental Marine Biology and Ecology*, *492*, pp.81-98.

Tegner, M.J., Dayton, P.K., Edwards, P.B. and Riser, K.L., 1996. Is there evidence for long-term climatic change in southern California kelp forests?. *California Cooperative Oceanic Fisheries Investigations Report*, pp.111-126.

Thiel, M. and Gutow, L., 2005. The ecology of rafting in the marine environment. II. The rafting organisms and community. In *Oceanography and Marine Biology* (pp. 289-428). CRC Press.

Thomsen, M.S., Wernberg, T. and Kendrick, G.A., 2004. The effect of thallus size, life stage, aggregation, wave exposure and substratum conditions on the forces required to break or dislodge the small kelp *Ecklonia radiata*. Botanica Marina, 47, pp. 454-460.

Trinanes, J.A., Olascoaga, M.J., Goni, G.J., Maximenko, N.A., Griffin, D.A. and Hafner, J., 2016. Analysis of flight MH370 potential debris trajectories using ocean observations and numerical model results. *Journal of Operational Oceanography*, *9*(2), pp.126-138.

Troell, M., Robertson-Andersson, D., Anderson, R.J., Bolton, J.J., Maneveldt, G., Halling, C. and Probyn, T., 2006. Abalone farming in South Africa: an overview with perspectives on kelp resources, abalone feed, potential for on-farm seaweed production and socio-economic importance. *Aquaculture*, *257*(1-4), pp.266-281.

Tzetlin, A.B., Mokievsky, V.O., Melnikov, A.N., Saphonov, M.V., Simdyanov, T.G. and Ivanov, I.E., 1997. Fauna associated with detached kelp in different types of subtidal habitats of the White Sea. *Hydrobiologia*, *355*(1), pp.91-100.

Ullman, D.S., O'Donnell, J., Kohut, J., Fake, T. and Allen, A., 2006. Trajectory prediction using HF radar surface currents: Monte Carlo simulations of prediction uncertainties. *Journal of Geophysical Research: Oceans*, *111*(C12).

Utter, B. and Denny, M., 1996. Wave-induced forces on the giant kelp *Macrocystis pyrifera* (Agardh): field test of a computational model. *The Journal of experimental biology*, *199*(12), pp.2645-2654.

Van Sebille, E., Aliani, S., Law, K.L., Maximenko, N., Alsina, J.M., Bagaev, A., Bergmann, M., Chapron, B., Chubarenko, I., Cózar, A. and Delandmeter, P., 2020. The physical oceanography of the transport of floating marine debris. *Environmental Research Letters*, *15*(2), p.023003.

Van Sebille, E., Griffies, S.M., Abernathey, R., Adams, T.P., Berloff, P., Biastoch, A., Blanke, B., Chassignet, E.P., Cheng, Y., Cotter, C.J. and Deleersnijder, E., 2018. Lagrangian ocean analysis: Fundamentals and practices. *Ocean Modelling*, *121*, pp.49-75.

Vásquez, J.A., Zuñiga, S., Tala, F., Piaget, N., Rodríguez, D.C. and Vega, J.M., 2014. Economic valuation of kelp forests in northern Chile: values of goods and services of the ecosystem. *Journal of Applied Phycology*, *26*(2), pp.1081-1088.

Veitch, J.A. and Penven, P., 2017. The role of the A gulhas in the B enguela current system: A numerical modeling approach. *Journal of Geophysical Research: Oceans*, *122*(4), pp.3375-3393.

Veitch, J., Hermes, J., Lamont, T., Penven, P. and Dufois, F., 2018. Shelf-edge jet currents in the southern Benguela: A modelling approach. *Journal of Marine Systems*, *188*, pp.27-38.

Veitch, J., Penven, P. and Shillington, F., 2010. Modeling equilibrium dynamics of the Benguela Current System. *Journal of Physical Oceanography*, *40*(9), pp.1942-1964.

Veitch, J., Rautenbach, C., Hermes, J. and Reason, C., 2019. The Cape Point wave record, extreme events and the role of large-scale modes of climate variability. *Journal of Marine Systems*, *198*, p.103185.

Velimirov, B., Field, J.G., Griffiths, C.L. and Zoutendyk, P., 1977. The ecology of kelp bed communities in the Benguela upwelling system. *Helgoländer wissenschaftliche Meeresuntersuchungen*, *30*(1), pp.495-518.

Vergés, A., Steinberg, P.D., Hay, M.E., Poore, A.G., Campbell, A.H., Ballesteros, E., Heck Jr, K.L., Booth, D.J., Coleman, M.A., Feary, D.A. and Figueira, W., 2014. The tropicalization of temperate marine ecosystems:

climate-mediated changes in herbivory and community phase shifts. *Proceedings of the Royal Society B: Biological Sciences*, *281*(1789), p.20140846.

Vergés, A., Doropoulos, C., Malcolm, H.A., Skye, M., Garcia-Pizá, M., Marzinelli, E.M., Campbell, A.H., Ballesteros, E., Hoey, A.S., Vila-Concejo, A. and Bozec, Y.M., 2016. Long-term empirical evidence of ocean warming leading to tropicalization of fish communities, increased herbivory, and loss of kelp. *Proceedings of the National Academy of Sciences*, *113*(48), pp.13791-13796.

Vogel, S., 2020. *Life in Moving Fluids: The Physical Biology of Flow-Revised and Expanded Second Edition*. Princeton university press.

Waldron, H.N. and Probyn, T.A., 1992. Nitrate supply and potential new production in the Benguela upwelling system. *South African Journal of Marine Science*, *12*(1), pp.29-39.

Wang, M., Hu, C., Barnes, B.B., Mitchum, G., Lapointe, B. and Montoya, J.P., 2019. The great Atlantic *Sargassum* belt. *Science*, *365*(6448), pp.83-87.

Wang, Y. and Xia, Z., 2009. Assessing spawning ground hydraulic suitability for Chinese sturgeon (*Acipenser sinensis*) from horizontal mean vorticity in Yangtze River. *Ecological Modelling*, *220*(11), pp.1443-1448.

Watanabe, J.M., Phillips, R.E., Allen, N.H. and Anderson, W.A., 1992. Physiological response of the stipitate understory kelp, *Pterygophora californica* Ruprecht, to shading by the giant kelp, *Macrocystis pyrifera* C. Agardh. *Journal of Experimental Marine Biology and Ecology*, *159*(2), pp.237-252.

Waters, J.M., King, T.M., Fraser, C.I. and Craw, D., 2018. Crossing the front: contrasting storm-forced dispersal dynamics revealed by biological, geological and genetic analysis of beach-cast kelp. *Journal of the Royal Society Interface*, *15*(140), p.20180046.

Wegman, T., 2020. Spreading of floating marine microplastics. Student Report. Delft University of Technology

Weisse, R., 2010. *Marine climate and climate change: storms, wind waves and storm surges*. Springer Science & Business Media.

Wernberg, T., Coleman, M., Fairhead, A., Miller, S. and Thomsen, M., 2003. Morphology of *Ecklonia radiata* (Phaeophyta: Laminarales) along its geographic distribution in south-western Australia and Australasia. *Marine Biology*, *143*(1), pp.47-55.

Wernberg, T. and Goldberg, N., 2008. Short-term temporal dynamics of algal species in a subtidal kelp bed in relation to changes in environmental conditions and canopy biomass. *Estuarine, Coastal and Shelf Science*, *76*(2), pp.265-272.

Wernberg, T., Russell, B.D., Moore, P.J., Ling, S.D., Smale, D.A., Campbell, A., Coleman, M.A., Steinberg, P.D., Kendrick, G.A. and Connell, S.D., 2011. Impacts of climate change in a global hotspot for temperate marine biodiversity and ocean warming. *Journal of Experimental Marine Biology and Ecology*, *400*(1-2), pp.7-16.

Wernberg, T. and Thomsen, M.S., 2005. The effect of wave exposure on the morphology of *Ecklonia radiata*. *Aquatic Botany*, *83*(1), pp.61-70.

Wernberg, T., Thomsen, M.S., Tuya, F., Kendrick, G.A., Staehr, P.A. and Toohey, B.D., 2010. Decreasing resilience of kelp beds along a latitudinal temperature gradient: potential implications for a warmer future. *Ecology Letters*, *13*(6), pp.685-694.

Wernberg, T. and Vanderklift, M.A., 2010. Contribution Of Temporal And Spatial Components To Morphological Variation In The Kelp *Ecklonia* (Laminariales) 1. *Journal of Phycology*, *46*(1), pp.153-161.

Wichmann, C.S., Hinojosa, I.A. and Thiel, M., 2012. Floating kelps in Patagonian Fjords: an important vehicle for rafting invertebrates and its relevance for biogeography. *Marine Biology*, *159*(9), pp.2035-2049.

Willis, T.J. and Anderson, M.J., 2003. Structure of cryptic reef fish assemblages: relationships with habitat characteristics and predator density. *Marine Ecology Progress Series*, *257*, pp.209-221.

Wing, S.R., Leichter, J.J. and Denny, M.W., 1993. A dynamic model for wave-induced light fluctuations in a kelp forest. *Limnology and Oceanography*, *38*(2), pp.396-407.

Wing, S.R., Leichter, J.J., Perrin, C., Rutger, S.M., Bowman, M.H. and Cornelisen, C.D., 2007. Topographic shading and wave exposure influence morphology and ecophysiology of *Ecklonia radiata* (C. Agardh 1817) in Fiordland, New Zealand. *Limnology and Oceanography*, *52*(5), pp.1853-1864.

Wong, L., Jamal, M.H.B. and Kasiman, E.H.B., 2021, June. A Short Review on Numerical Simulation of Floating Debris Migration. In *Proceedings of the International Conference on Civil, Offshore and Environmental Engineering* (pp. 310-317). Springer, Singapore.

Wood, W.F., 1987. Effect of solar ultra-violet radiation on the kelp *Ecklonia radiata*. *Marine Biology*, *96*(1), pp.143-150.

Woodborne, M.W., Rogers, J. and Jarman, N., 1989. The geological significance of kelp-rafted rock along the west coast of South Africa. *Geo-Marine Letters*, *9*(2), pp.109-118.

Zakas, C., Binford, J., Navarrete, S.A. and Wares, J.P., 2009. Restricted gene flow in Chilean barnacles reflects an oceanographic and biogeographic transition zone. *Marine Ecology Progress Series*, *394*, pp.165-177.

Zhong, Y., Bracco, A. and Villareal, T.A., 2012. Pattern formation at the ocean surface: *Sargassum* distribution and the role of the eddy field. *Limnology and Oceanography: Fluids and Environments*, *2*(1), pp.12-27.

Zimmerman, R.C. and Kremer, J.N., 1986. In situ growth and chemical composition of the giant kelp, *Macrocystis pyrifera*: response to temporal changes in ambient nutrient availability. *Marine Ecology Progress Series*, *27*(2), pp.277-285.

5.3 Appendix

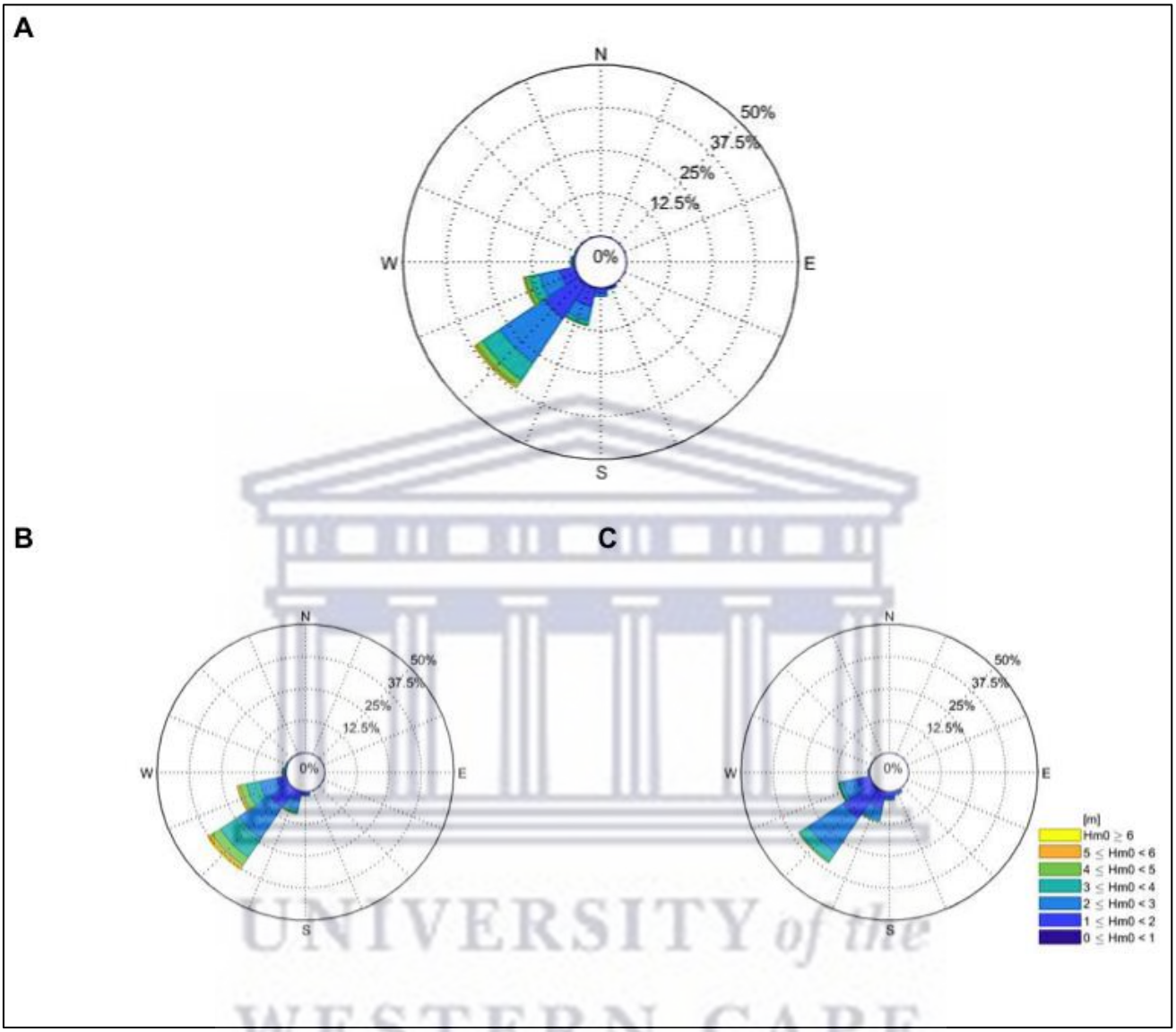

Figure A1: The total and seasonal wave roses of the directional wave buoy just offshore from Cape Town is given for years 2000 till end of 2017 (the period for which the directional wave spectra was available). The total (A), Austral winter (B), and Austral summer (C) are presented, respectively.

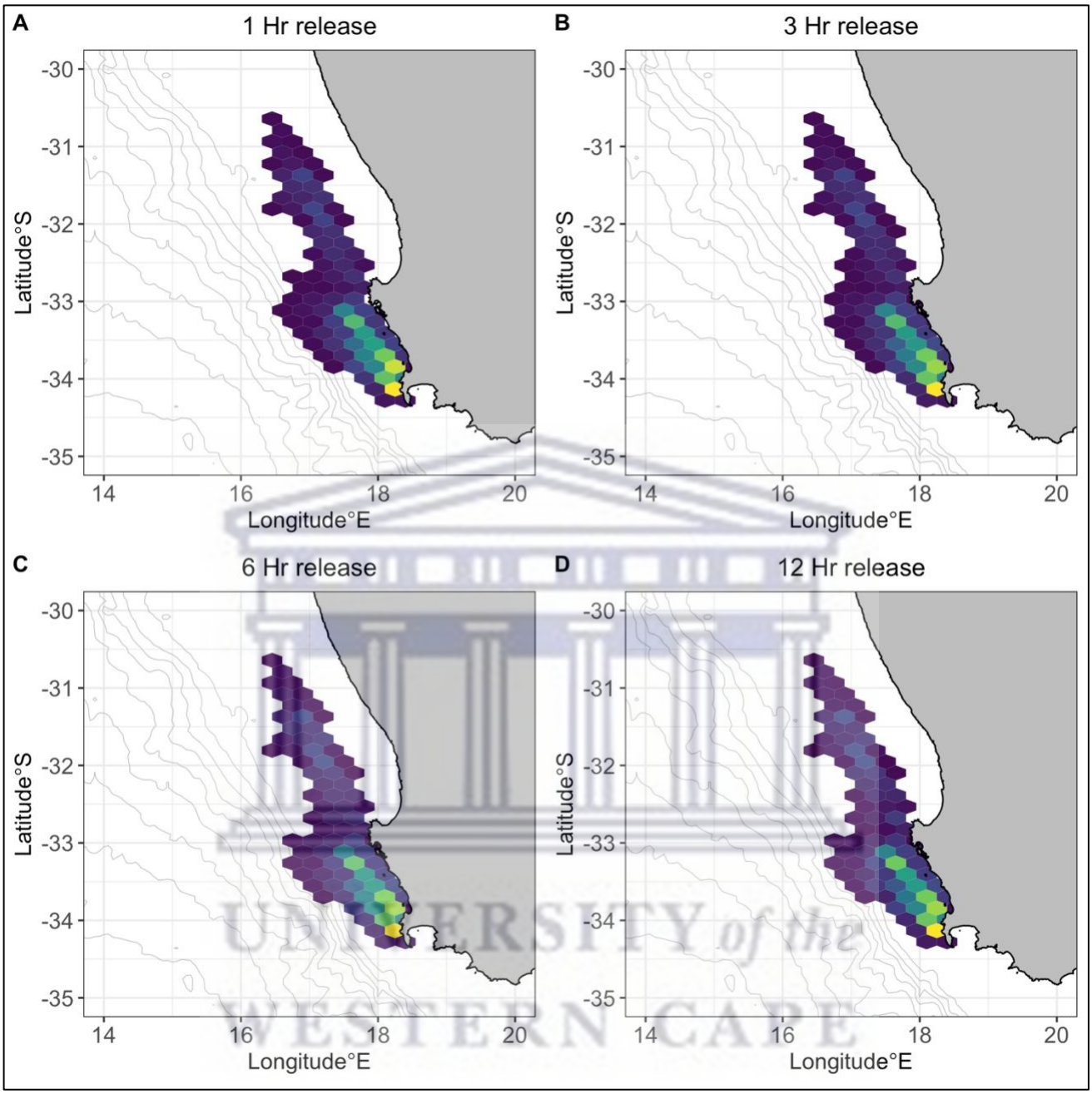

Figure A2: Heatmaps comparing densities and patterns across time-release options. The plots are regular hexagons within which the density of particles were calculated. Faint grey lines represent the various bathymetry layers.

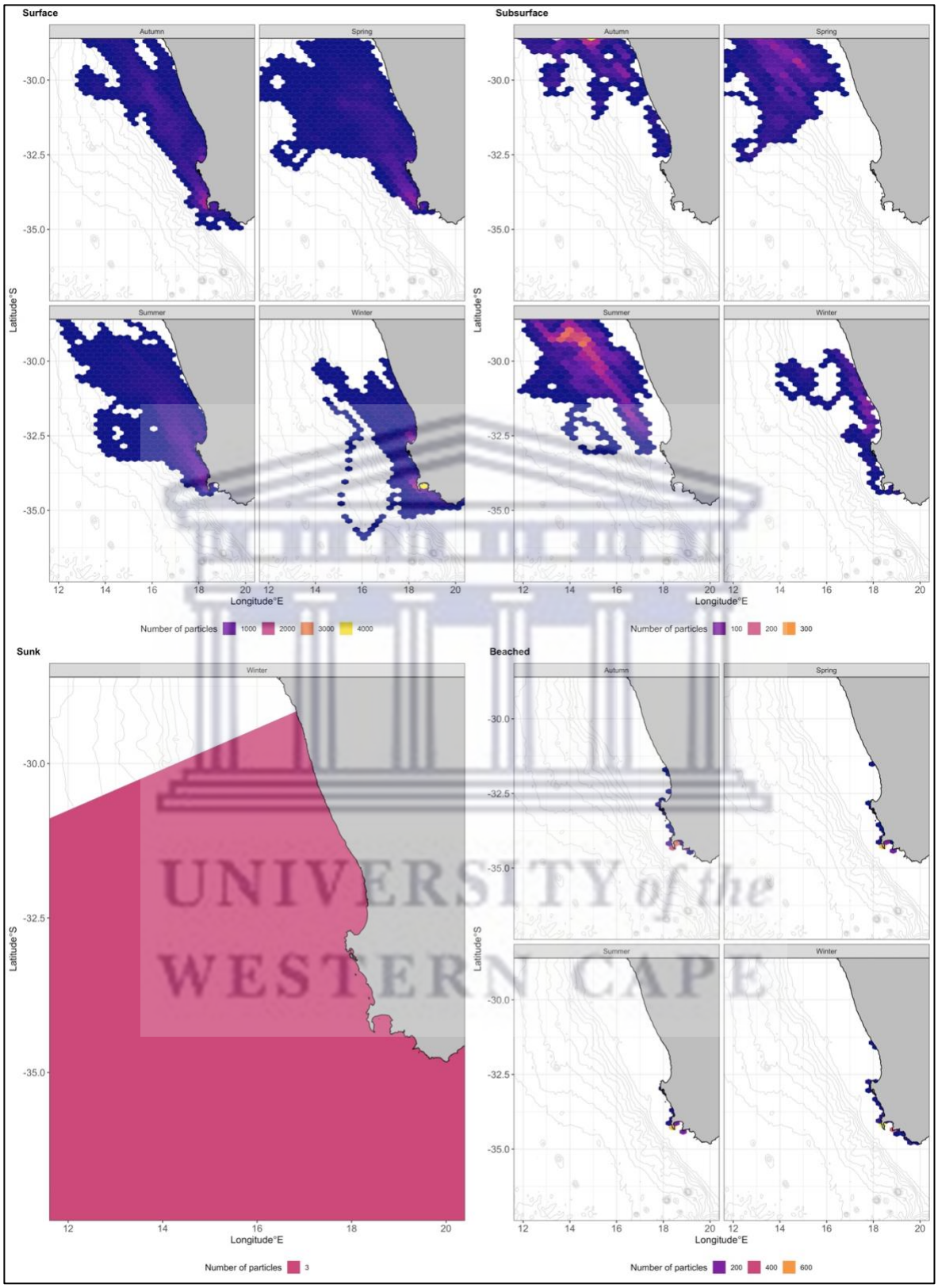

Figure A3: Hexagonal heatmaps for all passive surface particles for year 1 and all seasons. The plane has been divided into regular hexagons and then are filled according to the number of particles within each hexagon. Faint grey lines represent the various bathymetry layers.

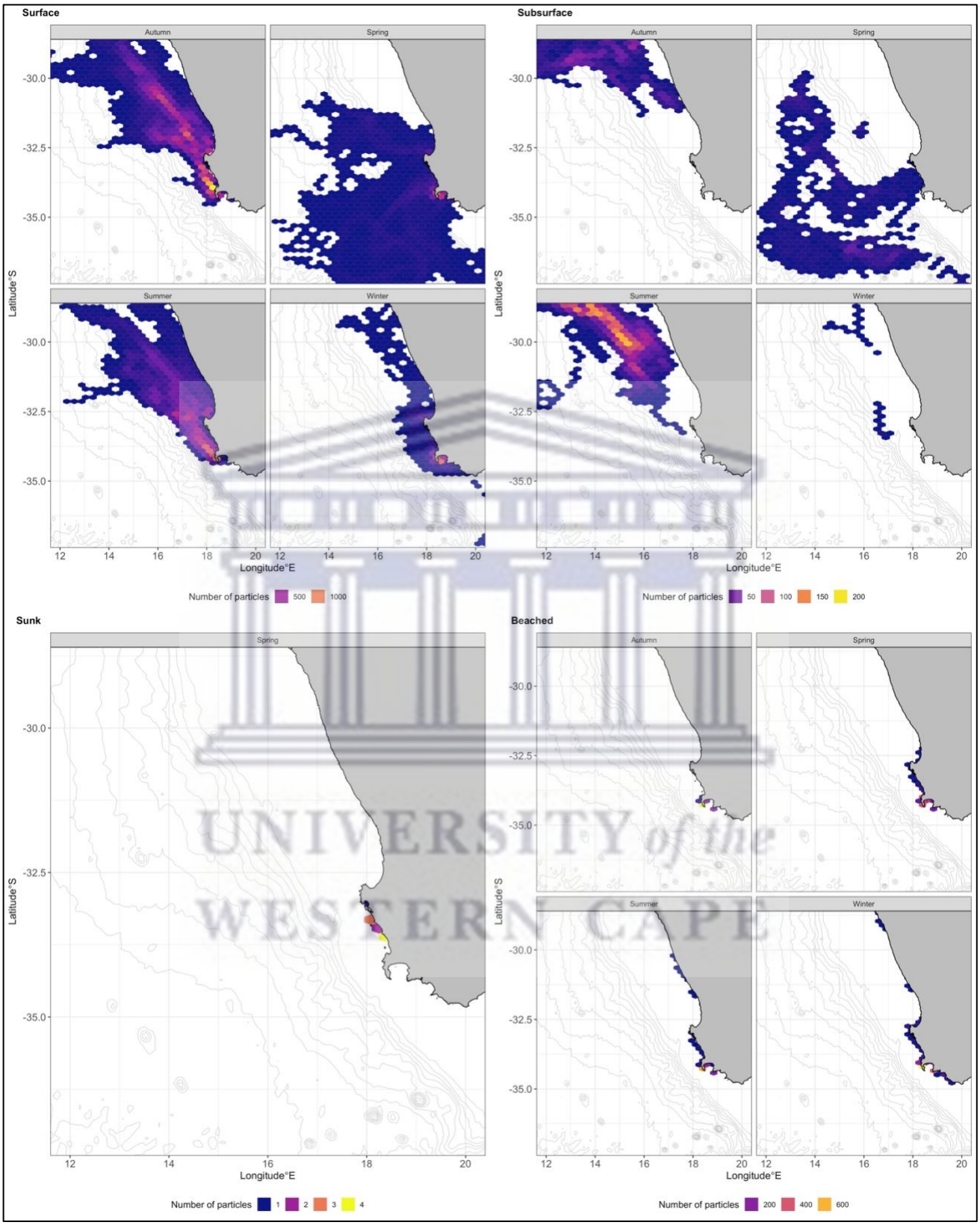

Figure A4: Hexagonal heatmaps for all phases passive surface particles for year 2 and all seasons. The plane has been divided into regular hexagons and then are filled according to the number of particles within each hexagon. Faint grey lines represent the various bathymetry layers.